The Role of Activated Platelets in the Regulation of a Pro-Atherogenic Monocyte Phenotype

Thesis submitted for the degree of

Doctor of Philosophy

by

Dr Sameer Ahamed Kurmani MA, MBBChir, MRCP

Department of Cardiovascular Sciences

University of Leicester

2018

1.1   <u>Abstract</u>

Platelets are circulating megakaryocytic fragments that have a well-established role in athero-thrombosis. Monocytes are circulating leucocytes which migrate to sites of endothelial damage, infiltrate a nascent plaque and avidly accumulate lipids to become foam cells. Evidence is provided to show that activated platelets accelerate this process by promoting a pro-atherogenic phenotype in monocytes and monocyte-derived monocytes (MDMs).

A cross-linked collagen peptide mimetic (CRP-XL) was used to specifically activate platelets and monocytes were subsequently isolated and cultured using a methodology developed to minimise platelet contamination and iatrogenic activation. Activated platelets were shown to induce the formation of CD16^{pos} monocytes from the previously CD16^{neg} classical subset. This was accompanied by surface integrin (ICAM1, CD11b) and chemokine receptor expression (CXCR1, CXCR6) consistent with a pro-inflammatory phenotype. Platelets also induced the formation of intracellular lipid droplets in circulating monocytes and subsequently increased foam cells in MDMs which was dependent on the formation of monocyte-platelet aggregates (MPAs). This was shown to be as a result of both dysregulated cholesterol metabolism in MDMs and increased ingestion of platelets by monocytes.

The *in-vivo* relevance of these findings were assessed in the FOAMI study, an observation, laboratory-based study of patients with non ST-elevation Myocardial Infarction (NSTEMI). Many of the *in-vitro* findings were recapitulated in patients within the first 24hrs of an MI, with increased intracellular lipid droplets, increased pro-inflammatory CD16^{pos} monocyte subset and increased formation of foam cells above that seen in age-matched controls (AMC).

Novel evidence is therefore provided to show that platelets induce a pro-atherogenic phenotype in monocytes and promote foam cell formation in MDMs. This has potentially important implications in the management of coronary artery disease (CAD) and might provide new therapeutic insights.

1.2 <u>Acknowledgements</u>

<div align="center">

بِسۡـــمِ اللّٰهِ الرَّحۡمٰنِ الرَّحِیۡمِ

</div>

importance of education, hard work and perseverance for which I am grateful. I hope I have made them proud.

I would also like to say thank you to my mother and father in-law who have always been there to support me, my daughter and my wife through this demanding time. I would like to particularly mention my wife's nani (grandmother) who lived with us briefly to support me and my wife. She sadly passed, and I will miss seeing her playing with my daughter and cutting vegetables on the kitchen table... may her soul rest in peace.

Saving the best till last, I would like to acknowledge the two main people in my life, namely my daughter Sophia and my wife Sana. Doing this PhD has meant that my roles as a father and husband have taken a back seat which has been difficult on us all. Sophia has always found a way to cheer me up and my wife continues to be a wonderful mother, work as a doctor, give me a kick up the backside whenever I needed it as well as do the million non-glamorous tasks any family requires. None of this would have been possible without her help and support, she has and continues to be an inspiration and my best friend. 'I love you' isn't enough to describe my gratitude and affection.

I dedicate this thesis to my Sophia.

1.3 <u>Table of Contents</u>

1.4 <u>Table of Figures</u>

Chapter 2: Introduction

Chapter 3: Materials & Methods

Chapter 4: Development of Core Methods

Chapter 5: Platelets Promote a Pro-Atherogenic Phenotype in Monocytes and Monocyte-Derived Macrophages

Chapter 6: Monocyte Subset Switching in Response to Platelet Activation

Chapter 7: Foam Cell Formation in Myocardial Infarction (The FOAMI Study)

Chapter 8: General Discussion

1.5 <u>Table of Tables</u>

1.6   <u>Publications & Presentation Arising From Thesis</u>

Activated platelets promote foam cell generation in monocytes
Kurmani SA, Krishnan U, Erridge C, Goodall AH. Atherosclerosis 2016. 244(e1-e12)

Comparison of the release of microRNAs and extracellular vesicles from platelets in response to different agonists
Ambrose AR, Alsahli MA, Kurmani SA, Goodall AH. Platelets 2017: Jul 20;1-9

Platelets induce de-novo expression of CD16 on CD16 negative circulating monocytes
Kurmani SA, Ambrose AR, Goodall AH. British Atherosclerosis Society 2016, Cambridge UK

Isolation of monocytes from human blood: minimising platelet contamination
Turnbull RE, Kurmani SA, Goodall AH
East Midlands Flow Cytometry Conference 2015, Nottingham, UK

Platelets Induce CD16^{pos}CCR2^{dim}Slan1^{neg} Monocytes and Differential Expression of Surface Chemokine Receptors
Kurmani SA, Krishnan U, Hamby S, Ambrose AR, Goodall AH. British Atherosclerosis Society 2017, Cambridge UK

1.7 **Abbreviations**

AA	Arachidonic Acid
ACS	Acute Coronary Syndrome
ADP	Adenosine Diphosphate
AMI	Acute Myocardial Infarction
ANOVA	Analysis of Variance
BHF	British Heart Foundation
CABG	Coronary Artery Bypass Grafting
CD	Cluster of Differentiation
CE	Cholesterol Esters
COX	Cyclo-Oxygenase
CRF	Case Record File
CRP-XL	Cross-linked Collagen-related peptide
CVD	Cardiovascular Disease
DAMP	Damage-Associated Molecular Pattern
DAPT	Dual Anti-Platelet Therapy
dim	Diminished
DNA	Deoxyribonucleic Acid
DoH	Department of Health
DoH	Department of Health
ECG	Electrocardiogram
ECM	Extracellular Matrix
EDTA	Ethylene-Diamine-Tetraacetic Acid
eNOS	Endothelial Nitric Oxide
EV	Extracellular Vesicles
FBC	Full Blood Count
FC	Free Cholesterol
GPCR	G-protein Coupled Receptors
GPI	Glycophosphatidyl Inositol
GTN	Glycerine Trinitrate
HBS	Hepes-buffered Saline
HRA	Health Research Authority
HSCP	Haematopoietic stem cell progenitors
HTA	Human Tissue Authority
HTA	Human Tissue Authority
HUVEC	Human Umbilical Vein Endothelial Cell
INF	Interferon
iNOS	Inducible Nitric Oxide
IRAS	Integrated Research Application System
LOX	Lipooxygenase
LPS	Lipopolysaccharide
mAbs	Monoclonal Antibodies
MDM	Monocyte-Derived Macrophage
MHC	Major Histocompatibility Complex
MI	Myocardial Infarction
MP	Microparticles

MPA	Monocyte-Platelet Aggregates
MPO	Myeloperoxidase
neg	Negative
NIHR	National Institutes of Health Research
NIHR	National Institute of Health Research
NO	Nitric Oxide
NOS	Nitric Oxide Synthase
NR	Nile Red
NSAID	Non-Steroidal Anti-Inflammatory Drug
NSTEMI	Non ST-elevation Myocardial Infarction
OMT	Optimum Medical Therapy
PAMP	Pathogen-Associated Molecular Pattern
PCI	Percutaneous Coronary Intervention
PFA	Paraformaldehyde
PGE	Prostaglandin E
PMA	Phorbiol Myristic Acid
PMP	Platelet-Derived Microparticles
pos	Positive
PPP	Platelet-Poor Plasma
PRP	Platelet-Rich Plasma
PVD	Peripheral Vascular Disease
RBBB	Right Bundle Branch Block
REC	Research Ethics Committee
RM-ANOVA	Repeated Measures Analysis of Variance
RNA	Ribonucleic Acid
ROS	Reactive Oxygen Species
SD	Standard Deviation
STEMI	ST-Elevation Myocardial Infarction
TnI	Troponin I
TPO	Thrombopoetin
TRALI	Transfusion-Related Acute Lung Injury
TRAP	Thrombin Receptor Associated Peptide
TWI	T-wave Inversion
UHL	University Hospitals of Leicester
UoL	University of Leicester
VLDL	Very Low-Density Lipoprotein
WB	Whole Blood
WGA	Wheat Germ Agglutinin
Wt	Wild-Type

Chapter 2: Introduction

2.1 <u>Burden of Cardiovascular Disease</u>

Cardiovascular Disease (CVD) is a broad term encompassing a range of clinical conditions affecting the heart and circulatory system. It continues to be an important cause of morbidity and mortality worldwide and although initially considered to be a disease of 'westernised societies', its impact is also rapidly increasing in the developing world. Whilst the overall pattern of disease affecting the world has shifted over the last 20 years the threat to health posed by CVD remains constant (**Lozano *et al.* 2013**). The World Health Organisation (WHO) in 2017 concluded that CVD is the single biggest cause of death worldwide with an estimated 17.7 million people dying from the sequelae of CVD, representing 31% of all global deaths[1]. The British Heart Foundation (BHF) published a similar figure for the United Kingdom in which CVD accounts for approximately 30% of all deaths[2]. By the year 2030, CVD is likely to cause over 8 million deaths per year and remain the leading cause of global mortality accounting for 1 in 6 deaths worldwide (**Mathers and Loncar** *2006*). In addition to mortality, the long-term morbidity associated with CVD is considerable and costs the UK approximately £7 billion pounds a year (**Allender *et al.* 2008**) and resulting losses in production exceeding £3.9 billion per annum.

Although the management and prevention of CVD has improved, these statistics serve as a reminder that it continues to be a significant health problem. One of the ways in which further improvements are to be made, is to develop a better understanding of the underlying pathological processes.

CVD can be broadly divided into atherosclerotic and non-atherosclerotic disease. The latter includes inflammatory conditions affecting the heart and circulation such as systemic lupus and the seronegative vasculitides as well as non-inflammatory conditions such as systemic hypertension. The overwhelming majority of CVD is attributable to atherosclerosis and therefore, by convention, when one refers to CVD and its substrates, one refers, *de facto*, to the clinical sequelae of atherosclerosis.

---

[1] Comprehensive data is published by the World Health Organisation (http://www.int/cardiovascular_diseases/en/)

[2] Available on the BHF website (https://www.bhf.org/what-we-do/our-research/heart-statistics/heart-statistics-publications/cardiovascular-disease statistics-2018)

2.2 <u>Overview of Atherosclerosis</u>

For much of the last century, most people considered atherosclerosis to be a cholesterol storage disease characterised by the accumulation of cholesterol and thrombotic debris within the arterial wall. The modern era of cell biology focussed on the proliferation of smooth muscle cells as the nidus for atherosclerotic plaques (**Ross and Glomset** *1976*). As the understanding of this disease process has evolved over the past 25 years, the concept of inflammation has gained ascendancy despite this being a feature within the literature for more than a century[3]. The advent of robust microscopy, allowed for a raft of observers in the 19th century to describe the diapedesis of leucocytes from the blood into tissues. Virchow in the middle of the 19th century recognised the inflammatory nature of atherosclerosis as an active process of tissue reaction rather than mere encrustation of thrombus and fatty material. The birth of modern immunology allowed for a more detailed understanding of this process including the description of antibody-antigen complexes and phagocytosis (**Karnovsky** *1981*), yet the application of these concepts to atherosclerosis lagged by almost a century.

Today, atherosclerosis is understood to be a chronic inflammatory condition affecting the vascular endothelium at sites of predilection with disturbed laminar flow. There is a wealth of data from both post-mortem studies and animal models that highlight the complex nature of this disease (**Lusis** *2000*). The histological progression of this disease is expounded in the arterial wall where the earliest observable feature is the appearance of the 'fatty streak' often seen from the first decade of human life (**Figure 2.1**). It is initiated by the sub-endothelial retention of apolipoprotein B (apoB)-containing lipoproteins in focal areas of arteries at sites of turbulent flow (**Williams and Tabas** *1995*).

---

[3] Virchow R, Cellular Pathology. London: John Churchill; 1858
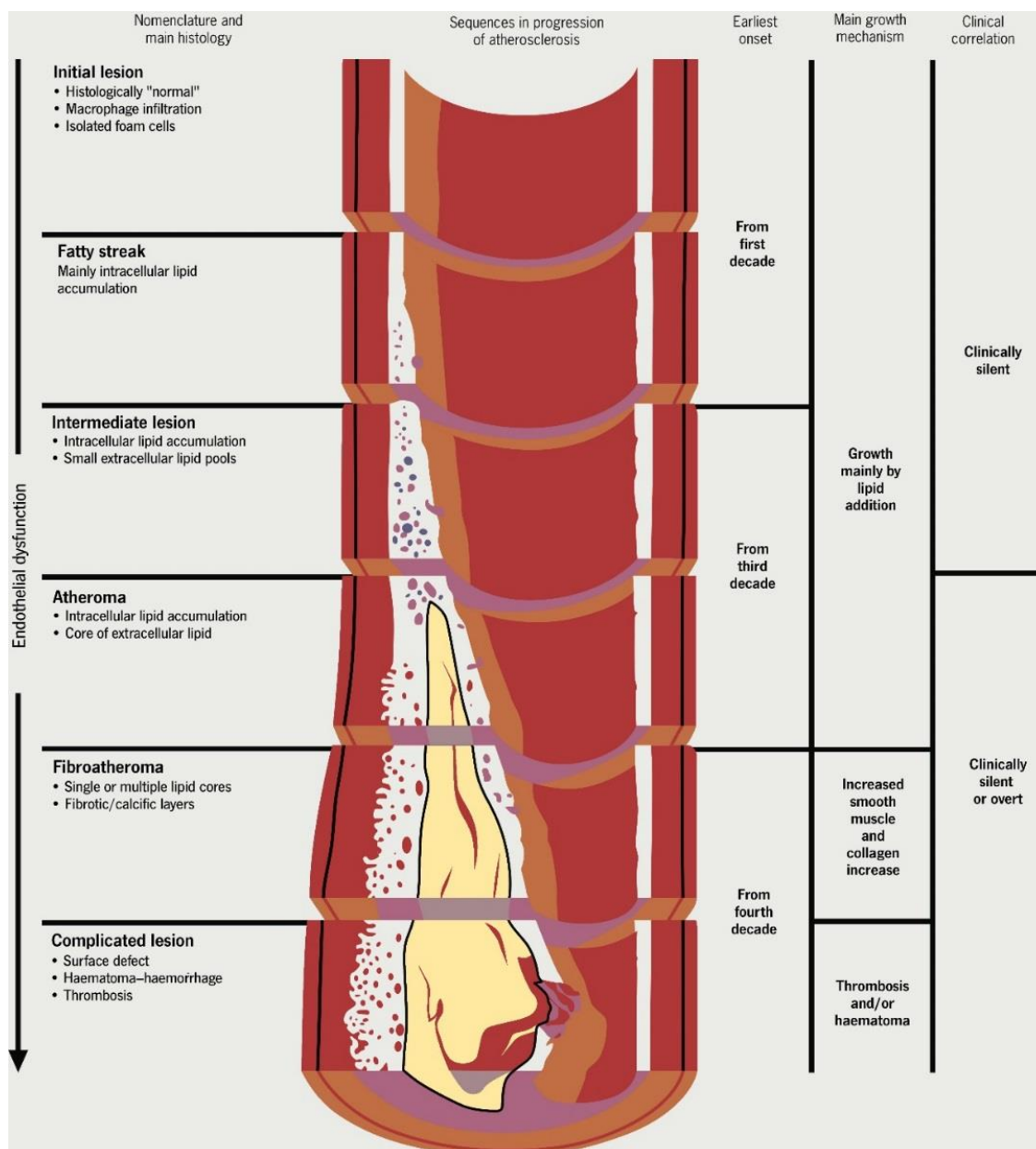
Figure 2.1: Schematic Overview of Atherosclerosis within a Coronary Artery. Diagram shows the progression of atherosclerosis from normal vessel at the top to advanced ulcerated plaque at the bottom. Also given on concomitant timelines are the age of onset, the main mechanism of growth and an indication of when these pathological lesions become clinically manifest. Overall, there is progressive endothelial dysfunction as the lesion matures[4].

---

[4] Image taken from British Journal of Cardiology Lipid Module I, 2015

This is accompanied by physiological changes within the arterial wall, notably a decreased production of nitric oxide (NO) from the endothelium. NO is synthesised from L-arginine by means of the enzyme nitric oxide synthase (eNOS) and is released in response to shear stress (**Zhao** *et al. 2015*). It has important anti-inflammatory, anti-thrombotic and anti-proliferative properties which means that its decreased production leads to progressive endothelial dysfunction. In athero-prone areas, the combination of reduced eNOS and oxidative damage leads to accumulation and retention of ApoB and Very Low-Density Lipoproteins (VLDL) remnants, which are then oxidatively-modified, thus promoting further endothelial dysfunction through exerting oxidative stress on the endothelium.

The combination of these factors act as a potent signal for the recruitment of monocyte occurring through a cascading process from rolling, firm adhesion and activation with eventual transendothelial migration (**Figure 2.2**). The anchors of this cascade are the adhesion molecules comprising the integrins and selectins. The selectins (CD62) are single-chain transmembrane glycoproteins belonging to a family of cell adhesion molecules that bind sugar moieties and therefore considered to be a type of lectin. All known three members (L-, E- and P-selectin) share a similar cassette structure with variable transmembrane and cytoplasmic tails leading to their different targeting affinities (**McEver** *2015*). This group of proteins, and especially P-selectin, mediates the initial rolling interaction of monocytes with the endothelium. Upon activation, the vascular endothelium also expresses a range of integrins, an evolutionarily conserved family composed of 24 αβ heterodimeric membranes that mediate attachment of cells to the extracellular matrix (ECM) but also take part in specialised cell-cell interactions (**Barczyk** *et al. 2010*). Electron microscopy has demonstrated that the quiescent form exists in a 'bent' shape which then undergo a conformational change when activated and mediate bi-directional signalling and act as mechanical links between the ECM and the cytoskeleton. In the example of atherosclerosis, the cell integrins Vascular Cell Adhesion Protein 1 (VCAM1) and Intercellular Adhesion Molecule 1 (ICAM1) are examples that mediate the firm tethering of monocytes (slowed by selectins) onto the endothelium. Chemokines are a family of small cytokines classified into four main subfamilies (CXC, CC, CX3C and XC), all approximately 8-10kDa and sharing four cysteine residues[5], whose name derives from their ability to attract nearby responsive cells. All members of this group of **chemo**tactic cyto**kines** signal through G-protein Couples Receptors (GPCRs), known as the chemokine receptors, found selectively on their target cell (**Griffith** *et al. 2014*). Potent chemoattractant factors such as MCP-1 (CCL2) and IL-8,

---

[5] These cysteine residues are in conserved locations and are key to forming their tertiary structure

produced from a variety of cells including endothelial and monocytic cells, further induce the migration of monocytes into the sub-endothelial space to become lesional macrophages (a more comprehensive list of chemokines is detailed in **Table 9.1**). Although these intimal macrophages are the main cells involved in the growth of the plaque, other cells contribute to the development of these early lesions including dendritic cells, mast cells and T-cells.

T helper cells[6] (T_H cells) in particular are involved in the vicarious regulation of other leucocytes including maturation of B-cells, activation of cytotoxic T-cells and have been shown to regulate the phenotype of macrophages (**Tabas and Lichtman** *2017*). T_H cells exist in several functional phenotypes are can change in response to environmental cues (such as hypercholesterolaemia, epigenetic changes and gut biome metabolites) thereby altering their relative ability to function as regulator or inflammatory cells. Macrophages have also been shown to respond to a variety of environmental stimuli such as modified lipids, cytokines and senescent erythrocytes which can all modify their functional phenotype (**Chinetti-Gbaguidi** *et al.* *2015*). Only M1 proinflammatory and M2 anti-inflammatory macrophages have been described *in-vitro* although a wide spectrum of intermediate phenotypes have been identified in *in-vivo* studies (summarised in **Table 2.1**). T_H1 cells promote a M1 pro-inflammatory macrophage phenotype through the production of INFγ. In contrast, T_H2 cells promote an anti-inflammatory M2 macrophage phenotype mediated through TGF-β and IL-10. The growth, morphology and, importantly, the stability of an atherosclerotic plaque is likely mediated by the balance of these phenotypes (**Yla-Herttuala** *et al.* *2013*).

Monocyte-Derived Macrophages (MDMs) then internalise apoB-containing lipoproteins which are degraded within their lysosomes and trafficked to the endoplasmic reticulum (ER) before being packaged into cytoplasmic lipid droplets (**Chistiakov** *et al.* *2017*). The progressive accumulation of these cytosolic lipid droplets leads to the classic appearance of 'foam cells' which allow for the fatty core characteristic of an advanced plaque. Important in this process are the Scavenger Receptors (SR) which are a superfamily of membrane-bound receptors known to bind a variety of ligands including endogenous proteins, pathogens and modified low-density lipoproteins (LDL). They comprise a diverse array of integral membrane proteins and soluble secreted extracellular domain isoforms but united by their ability to recognise common ligands including lipoproteins, apoptotic cells, cholesterol ester, phospholipids, proteoglycans, ferritin

---

[6] T_H cells differentiate into several subtypes including T_H1, T_H2, T_H3, T_H17, T_H9 and T_{FH} which all secrete differing profiles of cytokines. Signalling from antigen-presenting cells (APCs) direct T-cells into particular subtypes thereby augmenting the immune response

and carbohydrates (**Zani** *et al.* *2015*). This group of receptors were originally identified on their ability to recognise and bind different forms of LDL. The modification of apoB lipoproteins occurs via oxidation and glycation, as a result of oxidative stress and hyperglycaemia, which enhances their uptake into macrophages through a number of scavenger receptors including CD36 and the lectin-like superfamily and thereby promoting foam cell formation. The increased formation of foam cells within a growing plaque, combined with increased oxidative damage from modified lipoproteins, act as a precursor to advanced lesion formation.

Vascular Smooth Muscle Cells (VSMCs) also play an important role in the formation of an atherosclerotic plaque (**Bennett** *et al.* *2016*). These smooth muscle cells are the primary cell type in the pre-atherosclerotic intima, a state known as diffuse intimal thickening, and occurs in all stages of plaque development (**Dubland and Francis** *2016*). These VSMC are not terminally differentiated and can change their phenotype in response to environmental cues. Amongst these cues are the growth factors; Platelet-derived growth factor (PDGF), Matrix Metalloproteinases (MMP) and Fibroblast growth factor (FGF) which are released from platelets and the vascular media. A subset of VSMCs also express VLDL (**Swertfeger** *et al.* *2002*) and various scavenger receptors although there is a paucity of data to demonstrate that these cells are able to accumulate lipids as efficiently as macrophages. The VSMCs do however, produce a complex extracellular matrix composed of collagen, proteoglycan and elastin to form a fibrous cap over a core comprised of foam cells. The collagen, vital to the formation of the fibrous cap, is released from these cells in abundance and is stimulated by macrophage-derived TGF-β (**Kubota** *et al.* *2003*).

The formation of the fibrous cap is accompanied by progressive increases in the necrotic lipid core characteristic of an advanced atherosclerotic lesion. This results from a combination of mechanisms including impaired efferocytosis and accelerated macrophage death. Increased oxidative and ER stress are likely important mechanisms with simultaneous suppression of survival pathways such as pAkt and NF-κB (**Zhang** *et al.* *2015*). Apoptotic cells undergo secondary necrotic death if they are not internalised by phagocyte efferocytosis receptors and necrotic death leads to the leakage of intracellular oxidative and inflammatory components which in turn propagate more inflammation, oxidative stress and death in neighbouring tissue.

Components of the necrotic core then promote thinning of the fibrous capsule as a result of uncontrolled VSMC death with impaired production of TGF-β by phagocytes leading to reduced collagen production by healthy smooth muscle cells. The fibrous cap is also degraded by macrophage-derived MMPs, elastases and cathepsins (**Newby and Zaltsman** *1999*) which all

lead to a friable plaque and a lesion prone to plaque rupture and the subsequent sequelae of thrombosis.

It is the result of the unique anatomy of the coronary vasculature that render them susceptible to the vicissitudes of athero-progression. Oxygenated blood is supplied to the myocardium by the coronary arteries and given their tortuous course and turbulent flow, these vessels are prone to the development of atherosclerotic lesions, often termed coronary artery disease (CAD). CAD is a broad term, encompassing conditions such as coronary artery dissection and coronary ectasia, however the overwhelming majority of CAD is due to the build-up of fibro-fatty atheromatous plaque and therefore the two are often synonymous. With progressive coronary stenosis, blood flow rates are often not commensurate with myocardial demand. Considering that the internal diameter of these vessel range from 2.5-4.5mm (**Dodge *et al. 1992***) and that flow is proportional to the 4th power of coronary radius[7], these vessel are exquisitely sensitive to stenosis by atherosclerotic plaque. The acute coronary syndromes (ACS) represent unstable presentations of CAD, usually with an underlying plaque rupture event. This syndrome is diagnosed from a combination of history, the recording of a surface electrocardiogram (ECG) and biochemical markers of myocardial necrosis. MI is characterised biochemically by a rise in cardiac enzymes (most commonly Troponin) above a 99th centile value and reflects either progressive ischaemia or a sudden plaque rupture event with superimposed thrombus leading to a reduction in myocardial oxygen supply resulting in necrosis of tissue. Myocardial Infarction presents with either with or without ST segment elevation on the ECG. The reason for this distinction is that patients with ST segment elevation Myocardial Infarction (STEMI) often have (sub)total occlusion of one or more coronary arteries wherein prompt revascularisation or thrombolytic therapy is associated with an overall improved prognosis. Non-ST-elevation Myocardial Infarction (NSTEMI) often presents with a more insidious onset, with subtotal occlusion of one or more coronary arteries.

---

[7] Derived from the Hagen-Poiseuille equation

2.3   <u>The Canonical Role of Monocytes in Atherosclerosis</u>

Monocytes are circulating leucocytes, amoeboid in appearance and possessing a granulated cytoplasm with a distinct unilobar, kidney-shaped nucleus. They comprise 2-10% of all leucocytes within the human body and arise from myelo-monocytic stem cells within the bone marrow. They are formed from the division of promonocytes and remain within the circulation for less than 24hrs before they egress into the marginating pool or are sequestered within the spleen; a location that accounts for 50% of all monocytes in the body. Their canonical role is in inflammation and innate immunity where their function is to phagocytose, present antigen to augment the immune response and to produce a wide range of cytokines. However, it is their role in atherosclerosis which is of particular importance.

2.3.1   *Mobilisation from Bone Marrow*

In adult life, monocytes are formed solely in the bone marrow of which the most immature cell of the mononuclear phagocyte cell line is the monoblast. They arise from proliferating and differentiating haematopoietic stem and progenitor cells (HPSC) within the bone marrow and become increasingly committed until finally restricted to the monocyte progenitor cell (**Hettinger** *et al.* *2013*). Division of the monoblast gives rise to two promonocytes from which their two daughter cells are monocytes. Therefore, the progression of monoblasts to monocytes is tantamount to a four-fold increase in cell numbers. In the steady-state, constitutive production of monocytes amounts to 0.62×10^5 cells per hour (**Van Furth** *et al.* *1973*) and is regulated by various cytokines. IL-3, GM-CSF and M-CSF all act to stimulate the mitotic activity of monocyte precursors whereas Prostaglandin E (PGE), INFα and INFβ all inhibit the division of these cells. Additionally, bone marrow also contains a number of resident macrophages found in close association with diving haematopoetic cells suggesting that they also play a role in controlling their proliferation.

In a range of inflammatory contexts, there is increased production and mobilisation of BM HPSCs to peripheral tissues above and beyond that seen with constitutive monocyte release from BM (**Shi and Pamer** *2011*). The process of atherosclerosis is, at its core, pro-inflammatory and this state is reflected by high levels of inflammatory cytokines and adhesion molecules which promote the mobilisation of monocytes to the sites of atherosclerotic lesions. In experimental models of atherosclerosis, extramedullary monopoiesis is driven by HPSC mobilisation (**Robbins** *et al.* *2012*) from the BM. In the context of MI, there is increased mobilisation of monocytes from the bone marrow as a result of β_3-adrenergic receptor signalling and downregulation of the HPSC homing and retention factor CXCL12, more commonly known as fractalkine (**Dutta** *et*

al. 2012). In addition to adrenergic drive, the mobilisation of monocytes is also regulated by chemokine-chemokine receptor interactions. CCR2 blockade in murine models of atherogenesis has been shown to impair the egress of monocytes from the bone marrow and is associated with significantly reduced atherosclerotic burden (**Boring *et al.* 1998**). This is consistent with a mouse model of myocardial infarction where the increased production of MCP-3/CCL7 (another ligand of CCR2) by lymphocytes, in turn, regulates the mobilisation of monocytes from bone marrow into ischaemic myocardium (**Zouggari *et al.* 2013**). This phenomenon of accelerated monopoiesis is a consistent feature in both acute stress such as myocardial infarction and in states of chronic stress with hypercortisolaemia where monopoiesis is similarly regulated by the sympathetic nervous system (**Heidt *et al.* 2014**).

2.3.2 Response to Endothelial Dysfunction

Endothelial dysfunction is one of the earliest features in the pathogenesis of an atherosclerotic lesion (**Virmani *et al.* 2000**) and is a trigger for the activation and recruitment of circulating monocytes. Endothelial cells undergo a dramatic modulation in their functional phenotype in response to a range of stimuli including bacteria and other Pathogen-associated molecular patterns (PAMPs) as well as modified lipid species and other Damage-associated molecular patterns (DAMPs). The hallmark of this form of endothelial response is the activation of pleiotropic transcriptions factors, such as NF-κB, resulting in the expression of various effector proteins with important pathophysiological implications. Downstream effectors of NF-κB signalling include components of the major histocompatibility antigens and procoagulant molecules such as tissue factor (TF) accompanied by the downregulation of anti-coagulant factors such as Thrombomodulin (TM) and Nitric Oxide (NO) (**Pahl *1999***) thereby contributing to a hypercoagulable state. Additionally, activated endothelium also secrete the potent monocyte chemoattractants IL-8 and MCP-1 (summarised in **Table 9.1**). One such integrin, upregulated by NF-κB, is VCAM1 which is known to bind to its counter-receptor, Very Late Antigen 4 (VLA-4 also known as Integrin $\alpha_4\beta_1$), found on mononuclear leucocytes and lymphocytes and thus mediating selective adhesion (**Osborn *et al.* 1989**). Importantly, VCAM1 expression, both in human coronary atherosclerotic plaques and animal models of hypercholesterolaemia, is localised to intact endothelium overlying atherosclerotic lesions and actually precedes the earliest recruitment of mononuclear leukocytes (**O'Brien *et al.* 1993**). Further studies implicate the components of oxidized lipoproteins such as lysophosphatydylcholine as a potent stimulus for the expression of VLA-4 on mononuclear cells and thus represents a further mechanism linking VLA-4 to the atherogenic process (**Kume *et al.* 1992**).

The primary function of monocytes is the non-specific host protection against foreign pathogens. This occurs through the Pattern-Recognition Receptors (PRRs) which play a crucial role in the innate immune system. The PRRs are germline encoded host proteins, typically expressed by cells of the innate immune system that detect molecules typically expressed following a foreign insult. This group of receptors recognise both pathogen-associated molecular patterns (PAMPs), which are typically associated with microbial pathogens, and damage-associated molecular patterns (DAMPs), which are host components released through cell damage and death. Members of the PRR family are include the scavenger receptors (see section 2.2) and the Toll-Like Receptors (TLRs) (**Janeway and Medzhitov** *2002*) which detect highly conserved membrane constituents (e.g. lipopolysaccharides) of various pathogens and initiate a pro-inflammatory downstream signalling cascade. The most widely studied of these groups are the TLRs which are highly conserved from *Drosophila* to humans and even share functional similarities such as their ability to interact with different classes of PRRs and promote reciprocal augmentation of function (**Park** *et al. 2009*).

The TLR4 receptor is most closely associated with atherosclerosis and is functionally linked to the lipopolysaccharide receptor CD14 (see section 2.4.1) such that mutations in the TLR4 gene has been associated with differences in responsiveness to lipopolysaccharides (**Poltorak** *et al. 1998*). TLR4 is involved across the spectrum of atherosclerosis from the initiation of early lesions to late, advanced plaques. There is a prominent reduction in atherosclerotic burden in TLR knockout mice bred on an ApoE$^{-/-}$ background indicating that it serves to initiate and propagate atherogenesis (**Michelsen** *et al. 2004*). Furthermore, TLR4 expression was found to be increased on circulating monocytes and at sites of atherosclerotic lesions in patients with Acute Coronary Syndromes (ACS) as compared to patients with stable angina, indicating that this mechanism is also important in the evolution of a mature plaque (**Methe** *et al. 2005*). The activation of the TLRs, and other receptors involved in the innate response, on monocytes results in the upregulation of a variety of inflammatory factors and most notably the transcription of NF-κB (**Frangogiannis** *2008*). NF-κB is located in the cell cytoplasm, where it is inhibited by association with the inhibitor of κB (IκB). Stimulation of TLRs triggers activation of the IκB kinase that phosphorylates IκB and targets it for degradation (**Ghosh and Karin** *2002*). NF-κB is thereby released from inhibition and translocated from the cytoplasm to the nucleus where it acts as a transcription factor for a wide range of pro-inflammatory genes. Amongst the diverse range of function, NF-κB mediated signal transduction regulates the expression of Lipooxygenase (LOX), Cyclooxygenase (COX) and MCP-1 which are all involved in the modification of LDL and monocyte chemotaxis (**Aiello** *et al. 1999,* **Burleigh** *et al. 2002*). The expression of several of the adhesion

molecules associated with atherosclerosis, including P-selectin, E-selectin, ICAM1 and VCAM1 are also all regulated by the NF-κB pathway (**Collins** *et al. 2000*).

M-CSF is one such target of NF-κB signalling, released from both monocytes and ECs, responsible for accelerating the monocyte-macrophage transition (**Brach** *et al. 1991*). This is one growth factor among a battery of effects that NF-κB signalling has on both monocytes and ECs thereby resulting in a cycle of self-activation. Myeloperoxidase is also secreted by activated monocytes and plays a role in the formation of atherogenic, dysfunctional lipoproteins by their carbamylation (**Sirpal** *2009*) which is further enhanced by monocyte-derived Reactive Oxygen Species (ROS), which is elevated in some conditions, for example in patients with hyperlipidaemia (**Vasconcelos** *et al. 2009*). Ultimately, most of the inflammatory cytokines found to be up-regulated in atherosclerosis are produced by both monocytes and ECs in an NF-κB-dependent pathway providing further evidence that inflammation and atherogenesis are intimately linked.

2.3.3 Leucocyte Adhesion Cascade

Once mobilised from the bone marrow and into the circulation, monocytes adhere to the vascular endothelium. *Ex-vivo* models have shown that monocytes are able to do so avidly on atherosclerotic arteries but not normal ones (**Ramos** *et al. 1999*). The inability of monocytes to adhere to quiescent endothelium suggests that endothelial activation is a *sine qua non* for monocytes adhesion and diapedesis into a nascent plaque. This process has been well-described and occurs through a tightly regulated multi-step mechanism known as the leucocyte adhesion cascade. Upon activation of endothelium, monocytes are able to attach loosely to roll over the surface, acting to slow down the monocytes during their transit in the circulation. The loose interaction is mediated by the expression of L-selectin, PSGL-1 and CD44 on monocytes interacting with their cognate receptors on endothelial cells (**Alon** *et al. 1996*). The tethering of P-selectin/PSGL1 and L-selectin/CD34 are the most important mediators of 'loose' binding but the ligation of CD44 is responsible for reducing the rolling velocity of monocytes (**Hidalgo** *et al. 2007*) and is particularly important in areas of high arterial shear stress such as at bifurcations, a common place for atherogenesis.
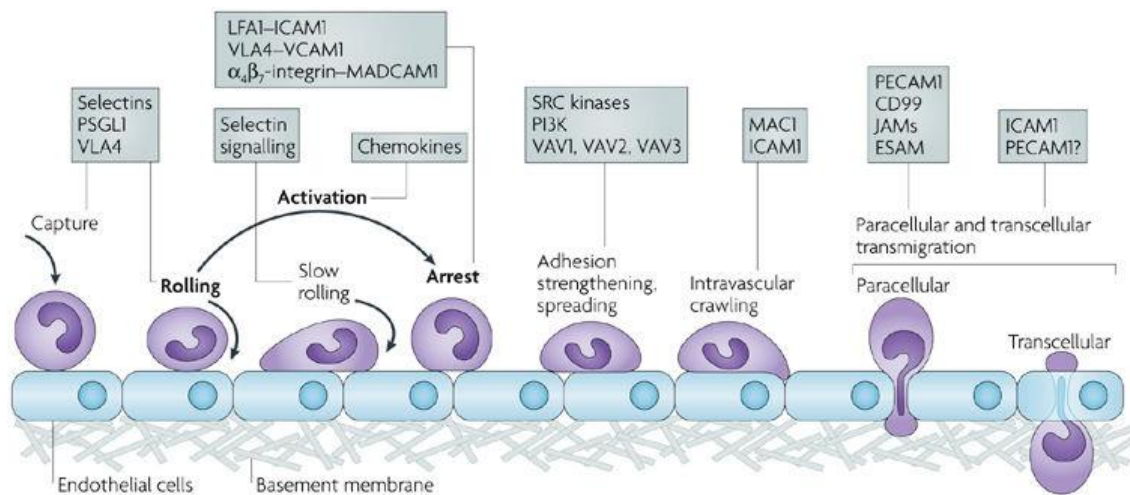
Figure 2.2: Leucocyte Adhesion Cascade. The original three steps are shown in bold: Rolling; mediated by selectins, Activation: by chemokines and Arrest: by integrins. Progress has been made in defining additional steps: capture (or tethering), slow rolling, adhesion strengthening and spreading, intravascular crawling and para/transcellular migration. Key molecules involved in each step are indicated in the boxes. ESAM; endothelial cell-selective adhesion molecule, ICAM1; intercellular adhesion molecule 1, JAM; junctional adhesion molecule, LFA1; lymphocyte function-associated antigen 1 (also known as $\alpha_L\beta_2$ integrin), MAC1; macrophage antigen 1, MADCAM1; mucosal vascular addressing cell adhesion molecule 1, PSGL1; P-selectin glycoprotein ligand 1, PECAM1; platelet/endothelial-cell adhesion molecule 1, P13K; phosphoinositide 3-kinase, VCAM1; vascular cell-adhesion molecule1, VLA4; very late antigen 4 (also known as $\alpha_4\beta_1$ integrin) (**Ley *et al.* 2007**).

The increase in transit time afforded by the loose interactions, render it stochastically favourable for monocytes to be activated by chemokines and/or lipid mediators presented on the endothelial surface (**Jung *et al.* 1998**).The presence of these chemokines, in conjunction with PSGL-1 ligation, induces an increase in the binding affinity and avidity of β_2 integrins (**Gerszten *et al.* 1999**). This is further augmented by the ligation of leucocyte integrins LFA-1, MAC-1 and VLA-4 by the endothelial ICAM1 and VCAM1 (**Ley et al. *2007***). The effect of binding of these surface integrins is that leucocytes then arrest on the endothelial surface which allows for their subsequent transmigration through the endothelial monolayer and into the subendothelial space. The process of transmigration is mediated by a complex response from the endothelial cell involving extensive re-organisation of the endothelial actin cytoskeleton and the activation of intracellular signalling pathways. There is re-organisation of surface expression of integrins (ICAM-1, VCAM-1) to form transmigratory cups (**Barreiro *et al.* 2002**) with the junctional adhesion molecules (JAMs) such as Platelet Endothelial Cell Adhesion Molecule (PECAM-1) and CD99, actively mediating leucocyte transmigration through homophilic interactions (**Muller *et al.* 1993**). In the mouse model, JAM-C is an important adhesion receptor responsible for retaining monocytes within the abluminal compartment. Inhibition of this key protein resulted in decreased overall monocyte egress as there were multiple reverse transmigration events (**Bradfield *et al.* 2007**). This co-ordinated process allows for the egress of luminal monocytes

into a nascent plaque and therefore promotes plaque growth and advancement. The continuing entry, survival and replication of mononuclear cells in atherosclerotic lesions depends partly on M-CSF, GM-CSF and MCP-1. In addition to the mobilisation of monocytes into circulation, chemoattractants (e.g. M-CSF, MCP-1) also support their proliferation and differentiation into macrophages and M-CSF has been shown to promote atherosclerotic plaque progression (**Irvine et al.** *2009*). There is a significant decrease in the burden of atherosclerosis in M-CSF deficient mice and this results largely from the marked decrease in macrophage accumulation within lesions (**Smith *et al.*** *1995*).

2.3.4   Monocyte-Macrophage Differentiation

Driven by M-CSF and other differentiation/survival factors, the majority of monocytes in early atheroma become cells with a macrophage and/or dendritic cell-like feature (**Paulson *et al.*** *2010*). It is often difficult to reconcile the *in-vivo* complexity of macrophages within an atherosclerotic plaque with *in-vitro* models of cultured macrophages. Studies using myeloid cell lines such as THP-1 or U937, transformed these monocytoid cells towards a macrophage-like phenotype with phorbol myristate acetate (PMA) and has shown to induce several markers of dendritic cells but also abnormal morphological changes (**Ibeas *et al.* 2009**). Serving to defend the host from infection, macrophages have developed plasticity with respect to their ability to promote inflammation when needed and to turn it off the inflammatory response when it is no longer needed. Monocytes transform to macrophages in the presence of M-CSF which allows for an 'undifferentiated' M0 macrophage without a specific proclivity towards an immunological response. In the experimental setting, incubation with a combination of IFNγ or LPS induces a classical inflammatory macrophage phenotype known as M1[8]. The M1 macrophage releases a range of pro-inflammatory cytokines such as IL-1β and TNFα as well as chemoattractant proteins such as MCP1 (CCL2) which further promote the recruitment of monocytes to the site of nascent plaque formation. This macrophage subset also upregulates inducible nitric oxide synthase (iNOS) and produces reactive oxygen species (ROS) through NADPH oxidase which further promote inflammation and enhance the ability of this cell to target pathogens for catalytic processing. In contrast, several subtypes of alternatively-activated macrophage populations (termed M2) have been identified *in-vitro* (see **Table 2.1**). This phenotype is induced by incubating macrophages with IL-4 and IL-13 which also inhibit the maturation of M1 macrophages. These cytokines act on the M2 macrophages to induce the production of IL-10 and TGFβ which further act to promote inflammation resolution (**Jenkins *et al.* 2011**).

---

[8] This is loosely analogous to the nomenclature used for T-helper cells (T$_H$1)

Macrophage Subset	Inducers	Markers	Cytokine Production	Function
M1	INFγ, LPS, TNF, GM-CSF	CXCL9, CXCL10, CXCL11, Arg-2	IL-6, TNFα, IL-23, iNOS, ROS	Microbicidal, Pro-inflammatory, Tumour resistance
M2a	IL-4, IL-13	MR, IL1RA, Arg-1, Fizz-1	IL-10, TGFβ, CCL22, CCL17	Tissue remodelling, endocytosis
M2b	LPS, IL-1β, IL1-RA	IL-10, low IL-12	IL-6, TNFα	Immunoregulation
M2c	IL-10, glucocorticoids, TGFβ	MR, Arg-1	IL-10, TGFβ, PTX3	merTK-dependent efferocytosis
M2d	TLR, ATII agonists	Low TNFα, low IL-12	VEGF, IL-10, iNOS	Pro-angiogenic, tumour promotion
Mox	oxLDL	HMOX-1, Srxn1, Txnrd1, Nrf2	IL-10, IL-1β	Pro-atherogenic, weakly phagocytic
M4	CXCL4	MMP7, S100A8, MR, low CD163	MMP12, IL-6, TNFα	Weakly phagocytic, foam cell formation
Mhem	Haem	CD163, ATF1	LXRβ	Anti-atherogenic, Erythrophagocytosis

Table 2.1: Summary Table of Macrophage Subsets. Table shows the main macrophage subsets including a summary of their inducing factors, surface and secreted markers used to characterise them, their predominant cytokine production profile and their putative function in atherosclerotic plaques[9].

The characteristics of macrophage subsets, summarised in the table above, is the result of a number of *in-vitro* studies of isolated macrophages (**Chinetti-Gbaguidi et al.** *2015*). However, macrophages are unlikely to exist as discreet subsets within the atherosclerotic plaque due to the balance of both pro-inflammatory and anti-inflammatory cytokines and a myriad of cellular and non-cellular regulators of plaque biology. However, there is some evidence to suggest that the balance between the M1 pro-inflammatory and M2 anti-inflammatory subsets may help in the determination of plaque stability. Although the numbers of both M1 and M2 subsets increase in human plaque progression, M1 macrophages were the predominant phenotype in rupture-prone should regions whereas M2 markers were found in the adventitia and in stable cell-rich areas of the plaque (**Stoger** *et al.* *2012*). In mouse models of atherosclerosis, the preponderance of either M1 or M2 macrophages determined plaque stability in apoE$^{-/-}$ mice and disease progression correlated with shift from an M2 to an M2 phenotype (**Khallou-Laschet** *et al. 2010*).

---

[9] Table adapted from Chinetti-Gbaguidi, G, S Colin and B Staels. Macrophage Subsets in Atherosclerosis. *Nat Rev Cardiol*.**2015**; **12: 10-17**

2.3.5 Formation of Foam Cells

Once monocytes have entered the vascular intima, in the presence of growth factors such as macrophage-colony stimulating factor (M-CSF), they mature into macrophages. Lipoprotein uptake by monocyte-derived macrophages (MDMs) is thought to be one of the earliest pathogenic events in the nascent plaque and the subsequent formation of foam cells (summarised in **Figure 2.3**) leads to the development of the necrotic, pro-inflammatory core characteristic of an advanced atherosclerotic plaque. The prevailing paradigm is that increased oxidative stress in the artery wall promotes modifications of LDL which acts as a 'danger' signal that are recognised by PRRs on cells of the innate immune system. This is supported by the presence of oxidised LDL (oxLDL) in both humans and mouse atheromas, and of natural IgM antibodies in the circulation that recognise oxidation-specific epitopes of LDL (**Miller *et al.* 2011**). A variety of enzymes, such as 12-15 LOX and myeloperoxidase (MPO) have been identified, as well as free radicals, that could promote LDL oxidation in the artery wall (**Podrez *et al.* 1999**) which, once formed, are avidly endocytosed by macrophages.

Scavenger receptors (SR) are a type of PRR present on monocyte-macrophages that have an important role in atherosclerosis through their ability to recognise and process modified LDL. In contrast to the expression of the classical LDL receptor, the expression of SRs is not downregulated by increased levels of intracellular cholesterol. As a result, SR-mediated uptake of oxLDL leads to continuous internalisation of lipoproteins and the accumulation of excess quantities of lipoprotein-derived lipids by mural macrophages. It has been shown that two scavenger receptors, SR-A1 and CD36 on macrophages, mediate 75-90% of the uptake of LDL that has been modified by acetylation or oxidation (**Kunjathoor *et al.* 2002**). CD36$^{-/-}$ApoE$^{-/-}$ mice show reduced uptake of oxLDL and significantly less atherosclerotic lesion size as compared with their CD36$^{+/+}$ controls (**Podrez *et al.* 2000**). With the progressive internalisation of lipoproteins mediated by SRs, there is excessive accumulation of lipoprotein-derived neutral lipid droplets accumulating in the cytoplasm, giving rise to the typical 'foamy' appearance (**Rios *et al.* 2011**). When internalised, lipoproteins are trafficked into the late endo-lysosomal compartment where the lipoprotein-derived cholesteryl esters are hydrolysed to free cholesterol and fatty acids by lysosomal acid lipase (LAL) to generate free cholesterol, mainly for ATP-binding cassette transporter 1 (ABCA-1) dependent efflux (**Ouimet *et al.* 2011**). The triglycerides from lipoproteins are hydrolysed into glycerol and fatty acids which are then re-esterified into newly formed triglycerides to be stored in lipid droplets. Fatty acids bind to fatty acid binding proteins which are responsible for their intracellular trafficking. In macrophages the absence of aP2, a prominent fatty acid binding protein, protected ApoE$^{-/-}$ mice against atherosclerosis (**Makowski**

et al. 2001). Free cholesterol in the endolysosomal compartment is then trafficked to the endoplasmic reticulum where it undergoes re-esterification by acetyl-coenzyme A: cholesterol acetyltransferase 1 (ACAT1) to cholesteryl fatty acids esters that are stored in cytoplasmic lipid droplets. When stored in the cell as cholesteryl ester, cholesterol is fairly inert but free cholesterol can be toxic to cells through a number of mechanisms (**Tabas** *2002*). Inhibition of ACAT1 activity has been shown to attenuate cholesterol ester accumulation in foam cells *in-vitro* (**Ghosh** *et al. 2003*), however its inhibition in lesional macrophages in LDLR$^{-/-}$ mice actually promoted atherosclerosis (**Fazio** *et al. 2001*). This increased in plaque formation with inhibition of ACAT activity is likely due to the cytotoxic effect of free cholesterol, which crystallises in foam cells. These cholesterol crystals are easily observed in the lipid-rich necrotic core of an atherosclerotic plaque and often in cell-free areas of advanced lesions. The enrichment by free cholesterol of cell membranes enhances inflammatory signalling from lipid rafts triggering TLR4 signalling and activation of NF-κB (**Zhu** *et al. 2010*). Furthermore, trafficking of free cholesterol out of lysosomes may also become defective in these macrophages, which constitute a barrier to cholesterol efflux, resulting in further amplified inflammation. Such dysregulation of lipid metabolism contributes to endoplasmic reticulum stress in macrophages which can promote apoptotic cell death (**Feng** *et al. 2003*). Efficient clearance of apoptotic bodies by surrounding macrophages (efferocytosis) requires intact lipid metabolism (such as cholesterol esterification and efflux) to deal with the ingested lipids from apoptotic bodies. As macrophage lipid metabolism becomes dysregulated, the increase in macrophage apoptosis, combines with defective efferocytosis, and results in secondary necrosis and release of cellular components and lipids that form the necrotic core as dysfunction macrophages are unable to clear apoptotic cells within the plaque.
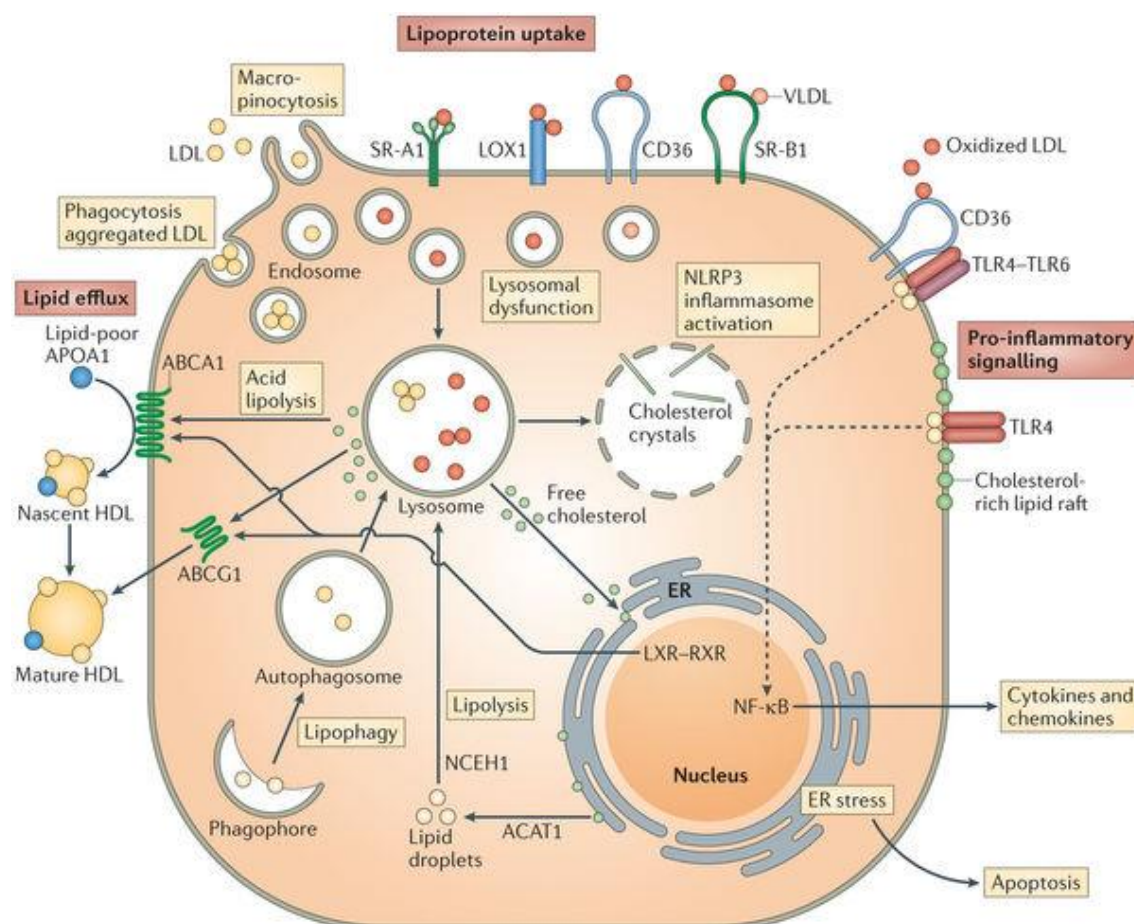
Figure 2.3: Mechanisms of Macrophage Foam Cell Formation. Macrophages internalise native LDL VLDL as well as oxidised lipoproteins in the plaque via micropinocytosis, phagocytosis of aggregated LDL and scavenger receptor-mediated uptake (including by scavenger receptor A1), LOX1, SR-B1 and CD36. The internalised lipoproteins and their associated lipids are digested in the lysosome, which results in the release of free cholesterol that can travel to the plasma membrane and then effluxe from the cell or to the endoplasmic reticulum (ER). In the ER, it can then be esterified by acetyl-coenzyme A:cholesterol acetyltransferase 1 (ACAT1) and is ultimately stored in this form in cytosolic lipid droplets. These stored lipids can be mobilised for efflux either via lipolysis by neutral cholesterol ester hydrolase 1 (NCEH1) or via lipophagy: a form of autophagy resulting in the delivery of lipid droplets to lysosomes. The accumulation of cellular cholesterol activates the liver X receptor (LXR)-retinoid X receptor (RXR) heterodimer transcription factor that upregulates expression of the ATP-binding cassette subfamily A member 1 (ABCA1 and ABCG1). This mediates the transfer of free cholesterol to lipid-poor apolipoprotein A1 (APOA1) to form nascent High-Density Lipoprotein (HDL) or more lipidated HDL particles. The accumulation of free cholesterol can induce cholesterol crystal formation in the lysosome to activate the NLRP3 (NOD-LRR and pyrin-domain-containing 3) inflammasome and may also interfere with the function of the ER which, if prolonged, results in cell death by apoptosis. In addition, lipid rafts are enriched in sphingomyelin which forms a complex with the free cholesterol. As the cholesterol content of lipid rafts increases, pro-inflammatory toll-like receptor 4 (TLR4) signalling is promoted, which can also be induced by oxidised LDL through a heterotrimeric complex composed of CD36-TLR4-TLR6. This signalling results in the activation of NF-kB and in the production of pro-inflammatory cytokines and chemokines[10]

---

[10] Figure taken from Moore, KJ, FJ Sheedy and EA Fisher. Macrophages in Atherosclerosis: A Dynamic Balance. *Nat Rev Immunol.***2013**; **13: 709-721**

The receptor-mediated efflux of cholesterol esters is a major mechanism for the removal of cellular cholesterol and is critical for preventing the formation of foam cells and the development of atherosclerotic lesions. Although passive diffusion plays a minor role (**Yvan-Charvet** *et al. 2010*), the majority of the efflux of cholesterol from macrophages to the serum occurs through an active process mediated by several transporters. ABCA1 and ABCG1 are responsible for the efflux of cholesterol to lipid-poor ApoA1 or to mature HDL respectively (**Adorni** *et al. 2007*). However, while selective deletion of ABCA1 in macrophages (**Brunham** *et al. 2009*) and the overexpression of ABCG1 (**Burgess** *et al. 2008*) did not significantly affect the development of atherosclerotic lesions, the simultaneous deficiency of both transporter proteins significant promoted atherosclerotic lesion (**Yvan-Charvet** *et al. 2007*). The genes encoding ABCA1 and ABCG1 are transcriptionally upregulated in response to elevated cellular cholesterol through LXRs and it has been shown that LXR activation by cholesterol derivatives promoted macrophage cholesterol efflux through the upregulation of ABCG1 and ABCA1 (**Calkin and Tontonoz** *2012*). In addition to ABCA1 and ABCG1, SR-B is a type-B scavenger receptor that promotes cholesterol efflux in macrophages. Suppression of SR-B1 activity in ApoE$^{-/-}$ mice dramatically accelerate the onset of atherosclerosis (**Trigatti** *et al. 1999*) which was further confirmed in ABCA1/SR-B double knockout mice which showed increased formation of foam cells (**Zhao** *et al. 2011*).

The transformation of MDMs to foam cells is therefore a consequence of avid uptake of modified lipoproteins through scavenger receptors with resultant dysregulation of lipid metabolism (see **Figure 2.3**). The progressive accumulation of intracellular lipid droplets leads to the foamy appearance, characteristic of lesional macrophages, accompanied by an intense pro-inflammatory response within atherosclerotic plaques.

2.4   The Role of Monocyte Heterogeneity in Atherosclerosis

The description of monocytes in their role to respond to and active in the presence of inflammatory activation markers is crucial in atherosclerosis. The formation of atherosclerotic plaques relies on the ability of monocytes to egress through areas of activated endothelium and contribute to the fatty necrotic core characteristic of an advanced plaque. It is therefore unsurprising that the levels of absolute monocyte counts have been shown to be associated with cardiovascular disease. In a study of over 300 patients with CAD, high monocyte counts were independent predictors of future ischaemic events and death (**Horne** *et al. 2005*). However, there is growing evidence to show that monocytes are not a homogenous population and that subsets exists that exhibit distinct biological properties and differentially confer cardiac risk.

2.4.1   Markers of Circulating Monocytes

All peripheral blood monocytes possess a surface glycoprotein, namely the myeloid differentiation antigen CD14: a 53kDa protein attached to the cell membrane by a glycophosphatidyl-inositol (GPI) anchor. It is a major surface receptor for lipopolysaccharide (LPS) but also for lipoteichoic acid, peptidoglycans and phospholipids from Gram-positive bacteria. It possesses a wide range of functions and is now widely recognised to serve as a PRR for a variety of ligands ranging from apoptotic cells and fungi to bacterial products (**Pugin** *et al. 1994*). In particular, CD14 has been recognised as the homing receptor for the endotoxin component (LPS) of Gram-negative bacteria (**Ziegler-Heitbrock** *1995*) and the use of anti-CD14 antibodies protects against animal models of endotoxic shock (**Schimke** *et al. 1998*). Membrane-bound CD14 is routinely used as a marker for monocytes as it is expressed, almost exclusively, on this cell type within the circulation.

In addition to the GPI-anchored membrane form (mCD14), CD14 is also present in a soluble form (sCD14) which occurs after shedding of mCD14 or directly secreted from intracellular vesicles (**Kirkland and Viriyakosol** *1998*). Analysis of supernatants of cultured mononuclear cells, activated with PMA, showed prolonged liberation of sCD14 and was associated with the pro-inflammatory cytokine IL-6 in patients with severe burn injuries and sepsis (**Rokita and Menzel** *1997*). This was also associated with a reduction in the surface expression of mCD14 suggesting that the shedding of sCD14 might be important in both inflammation and in the regulation of sCD14 expression (**Bazil and Strominger** *1991*). Soluble CD14 is also believed to facilitate LPS signalling through the LPS Binding Protein (LBP) (**Wright** *et al. 1990*). The use of CD14 as a marker of peripheral blood monocytes is ubiquitous although, with advances in flow cytometry and other detection techniques, CD14 has been found on other cell types such as neutrophils,

basophils, Küpfer cells and dendritic cells albeit in orders of magnitude less abundance (**Morabito *et al.* 1987**). More recently, other monocytic cell types in humans have been shown to express the CD14 antigen, albeit at low levels, of which the CD1c⁺ dendritic cell is an example (**Schwarz *et al.* 2014**).

CD16 is a leucocyte Fcγ type III low-affinity receptor for IgG. It exists as a GPI-anchored protein in macrophages, NK cells and neutrophils. Its function is to bind the Fc portion of IgG in the form of immune complexes or free antibody with a preferential binding affinity for IgG_1 and IgG_3 isotypes. Upon ligation of IgG to CD16, there is initiation of signalling cascades that produce a diverse variety of responses including antibody-dependent cell-mediated cytotoxicity, phagocytosis, degranulation and proliferation. It is believed to be one of the main mechanisms mediating cytotoxicity by Natural Killer cells and has also been shown to perform a similar action in human monocytes (**Yeap *et al.* 2016**). This antigen is of particular importance in monocytes when recognising and differentiating monocyte subsets.

2.4.2   Monocyte Subsets

Monocytes are classically defined as circulating blood cells that constitute approximately 10% of leucocytes in humans and approximately 4% in mice. Since their initial description, monocytes were defined based on morphological parameters and by their ability to adhere to glass (**van Furth and Cohn 1968**) in addition to enzyme staining such as monocyte-specific esterase (**Tucker *et al.* 1977**). It has now been more than 30 years since the first descriptions of human monocyte subsets based on surface antigenicity (**Shen *et al.* 1983**) which is now regarded as a general theme conserved among mammals, with monocyte subsets being reported in cows (**Goff *et al.* 1996**), pigs (**Chamorro *et al.* 2005**), rats (**Ahuja *et al.* 1995**) and mice (**Geissmann *et al.* 2003**).

In humans, monocytes can be classified into two major subsets based on the expression of CD14 and CD16 into the 'classical' (CD14^high CD16^neg) and the 'non-classical' (CD14^dim CD16^pos) subset, the latter of which accounts for less than 10% of all circulating monocytes (**Passlick *et al.* 1989**). These two subsets possess distinct phenotypic variations and have been thoroughly scrutinised using whole genome wide analysis (**Mobley *et al.* 2007**). Although the surface antigenicity between these subsets are readily distinguishable (CD16^pos vs CD16^neg), it has become increasingly clear that there exists further heterogeneity within the minor CD16^pos subset (**Ziegler-Heitbrock *et al.* 2010**). What was traditionally described as the 'non-classical' CD16^pos monocyte subset, was further subdivided into the 'non-classical' monocytes, defined by low expression of CD14 and high expression of CD16 (CD14^dim CD16^high), and also the newly-defined 'intermediate' monocyte subset characterised by high levels of CD14 expression and low-high

levels of CD16 (CD14^{high}CD16^{pos}). Using this schema, the current stratification of monocytes therefore includes three distinct subsets based on the surface expression of CD14 and CD16 that can be identified by flow cytometry (see **Figure 2.4**).
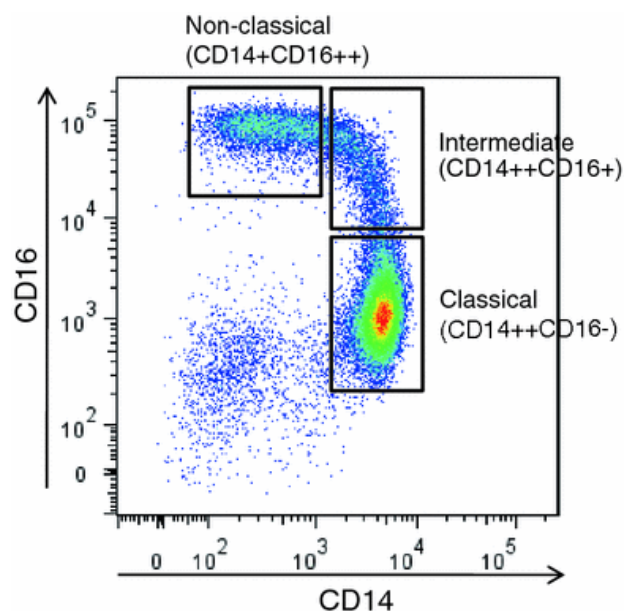
Figure 2.4: Gating Strategy Used to Define 3 Monocyte Subsets. Flow cytometry of monocytes is shown based on surface expression of CD14 and CD16 antigens. A rectangular gating strategy is used to encompass classical (CD14^{high}CD16^{neg}), intermediate (CD14^{high}CD16^{pos}) and non-classical (CD14^{dim}CD16^{neg}) monocyte subsets[11].

Although the three subsets are defined by the expression of two surface antigens, there is evidence from gene expression profiles to support their definition as distinct phenotypes and also how they may be related to each other. Hierarchical clustering of the gene expression profiles (**Cros *et al.* 2010**) showed that non-classical monocytes clustered separately from the classical and intermediate subsets. Their results indicate that classical and intermediate subsets were most closely related while the non-classical was more distant. However, two other independent studies (**Wong *et al.* 2011, Zawada *et al.* 2011**) show that non-classical and the intermediate subset are more closely related which was supported by separate microarray study performed in rhesus monkeys that possess homologous monocyte subpopulations (**Kim *et al.* 2010**). This evidence hints at a direct developmental relationship although this has yet to be formally proven.

---

[11] Taken from Wong, KL, WH Yeap, JJ Tai, SM Ong, TM Dang and SC Wong. The Three Human Monocyte Subsets: Implications for Health and Disease. *Immunol Res.***2012**; **53: 41-57**

Given that the separation of the intermediate and the non-classical subset is based on a relatively arbitrary separation based on the level of expression of CD14, alternative markers have been suggested to differentiate monocyte subsets (**Weber *et al.* 2016**). A monoclonal antibody M-DC8 specifically labelled a subpopulation of leucocytes accounting for 0.5-1% of all leucocytes in blood (**Schakel *et al.* 1998**). These cells were found to be highly phagocytic, expressed CD16 and had the ability to stimulate CD8 T-cells. The epitope was subsequently identified as 6-sulfo LacNAc, a novel O-linked carbohydrate modification of P-selectin glycoprotein ligand also known as Slan (**Schakel *et al.* 2002**). Based on flow cytometry, $Slan^{pos}$ monocytes are nestled within the $CD16^{pos}CD14^{dim}$ population (**de Baey *et al.* 2001**) and constitute about 30-50% of non-classical monocyte in healthy individuals (**Cros et al. 2010**). Analysis of surface marker expression by $Slan^{pos}CD16^{pos}$, $Slan^{neg}CD16^{pos}$ and $CD16^{neg}$ monocyte populations reveal several differences between them. $Slan^{pos}CD16^{pos}$ express the highest levels of the pan-leucocyte CD45-RA antigen that is indicative of 'native' or 'unprimed' leucocytes and C5a complement receptor. They also express the lowest levels of CD11b, CD14, CD32, CD33, CD45RO, CD62L, CD64 and C3a complement receptor which are found in their highest levels on $CD16^{neg}$ monocytes (a list of CD antigens is given in **Table 9.3**). $Slan^{neg}CD16^{pos}$ monocytes most highly expressed HLA-DR and CD86 (**Schakel *et al.* 2006**).

The patterns of expression of these surface molecular markers are similar to that described among the classical, intermediate and non-classical subsets (**Schakel et al. 2006**). $Slan^{pos}CD16^{pos}$ monocytes possess the ability to produce high levels of TNF-α in response to stimulation; a characteristic that is also seen with non-classical subsets. $Slan^{pos}$ monocytes are potent producers of inflammatory cytokines such as TNFα and IL-12 in response to LPS or CD40L (**de Baey et al. 2001**) as compared to $slan^{neg}CD16^{pos}$ cells which are poor producers of IL-12 (**Schakel et al. 2006**). Overall, the evidence suggests that $CD16^{pos}Slan1^{pos}$ monocytes are potent pro-inflammatory T_H1-inducing cells and the current three-subset definition may mask this unique pro-inflammatory subset.

2.4.3   Functional Differences in Monocytes Subsets

The behaviour of monocyte subsets is better understood in mouse models of atherosclerosis where these cells can be distinguished based on their cell surface expression of glycoprotein Ly6C. The murine Ly6 complex are a group of membrane-bound molecules attached to the cell surface via a C-terminal GPI anchor. It is a 14kDa protein found on neutrophils, monocytes, Dendritic Cells and subsets of CD4^{pos} and CD8^{pos} T-cell. Understanding of their function is somewhat elusive but certain Ly6 proteins are in close proximity with essential signalling components of the B-cell and T-cell Receptor Complexes and have been observed with β-integrins (**Harder and Simons** *1999,* **Wang** *et al. 2012*) suggested a pleiotropic role in adaptive immunity and cellular activation. Monocytes expressing the Ly6C antigen in high amounts (Ly6C^{hi}) tend to be short-lived within the circulation and transport antigen to lymph nodes (**Jakubzick** *et al. 2013*). The Ly6C^{hi} subset also express the chemokine receptor CCR2 and migrate from the bone marrow to the site of inflammation (**Serbina and Pamer** *2006*) where they give rise to a number of cell lineages including DCs, Langerhans cells and microglial cells (**Geissmann** *et al. 2003*).

Ly6C[low] monocytes on the other hand are longer-lived, patrol the vasculature, respond early to infection (**Auffray** *et al. 2007*) and survey endothelial integrity (**Carlin** *et al. 2013*). The ratio of these two subsets in the murine circulating is approximately 2:3 Ly6C^{low}: Ly6C^{high} respectively although this balance is perturbed in response to a systemic inflammatory insult (**Yona** *et al. 2013*). In the mouse model of atherosclerosis, as with humans, monocytes are essential to the development and progression of atherosclerotic plaques. The Ly6C^{hi} monocyte readily bind to the endothelium and infiltrate the nascent plaque to form lesional macrophages and their numbers are correlated with the progression of plaque disease (**Swirski** *et al. 2007*). Ly6C^{high} monocytes preferentially accumulate at atherosclerosis prone sites, such as the lesser curvature of the aorta and arterial branch points, to give rise to the inflammatory CD11b/CD11c macrophage (**Varol** *et al. 2009*). The mechanism of action of the Ly6C^{high} monocyte may partly be due to the fact that they tend to exhibit more functional PSGL-1 on their surface which allows them to more avidly adhere to P- and E-selectin as compared with the Ly6C^{low} counterparts, as demonstrated in flow-chamber experiments (**An** *et al. 2008*). This process is augmented by the actions of the chemokine receptors CCR2 and CX3CR1 as inhibition of their target receptors resulted in a 40% attenuation of atherosclerotic burden size (**Tacke** *et al. 2007*).

The origin and fate of Ly6C^{low} remains a topic of debate as does their inter-relationship with Ly6C^{high} monocytes. It is currently understood that the Ly6C^{high} are the steady-state precursors of the Ly6C^{low} subset undergoing maturation within the blood stream (**Yona et al.** *2013*). In

contrast to the Ly6C^{high} subset, the Ly6C^{low} monocytes serves a patrolling roll in mice (**Auffray *et al. 2009***). Their interaction with the vascular endothelium is mediated through LFA-1 as well as the chemokine receptor CX3CR1 which has been shown to be critical in the survival of this subset (**Landsman *et al.* 2009**). There are some data to suggest that this monocyte subset might contribute to plaque stability through the release of CXCL9 and CXCL10 in addition to pro-angiogenic factors (e.g. VEGF) thereby promoting tissue remodelling and phagocytosis (**Martinez *et al.* 2006**). The NR4A1 (Nur77) transcription factor is important in the differentiation of the Ly6C^{low} monocyte subset (**Hanna *et al.* 2011**). In a mouse model of Nur77 deficiency, there were fewer circulating monocytes however, they showed an increase atherosclerotic burden when fed a western diet with resident macrophages polarised towards the M1 phenotype (**Hanna *et al.* 2012**). In a contrasting study however, the transplantation of Nur 77$^{-/-}$ bone marrow into transgenic LDLr$^{-/-}$ mice did not result in increased atherosclerotic burden in the recipient mice when fed a high fat diet (**Chao *et al.* 2013**).

In many respects, the *in-vitro* models of human monocyte subsets recapitulate that seen with the mouse subsets and suggest differential functions amongst the CD16^{pos} and CD16^{neg} subsets. At the transcriptional level, there are over 250 genes that are differentially expressed between the subsets (**Ancuta *et al.* 2009,** **Zawada et al.** *2011*) which is correlated with marked differences in functions such as phagocytosis and antigen presentation. One of the main functions of monocytes is to influence the inflammatory milieu through the production of cytokines however, there is poor agreement in the literature on the preferential production of cytokines by each subset. In one study, isolated peripheral blood monocytes activated with Lipopolysaccharide (LPS) demonstrated significantly greater expression of TNFα by the CD16^{pos} monocyte subset than their CD16^{neg} counterpart (**Belge *et al.* 2002**) but without significant differences between the intermediate and non-classical subset. The preponderance of evidence favours the hypothesis that the intermediate subset (CD14^{pos}CD16^{pos}) is pro-inflammatory and loosely analogous to the monocytes Ly6C^{high} subset. In patients with Rheumatoid Arthritis, the intermediate subset of monocytes were found in higher numbers and shower higher expression of CCR5 and when stimulated with LPS, produced greater amounts pro-inflammatory cytokines such as TNFα, IL-1β and IL-6 (**Rossol *et al.* 2012**). In addition to the induction of inflammation, the intermediate monocyte subset also expresses the fractalkine receptor (CX3CR1) at greater levels and preferentially support its migration across the endothelial cell layer (**Ancuta *et al.* 2003**). This subset also expressed a pro-angiogenic phenotype with increased expression of endoglin (ENG), TEK tyrosine kinase (Tie2, CD202b) and KDR (VEGFR2), all markers of increased angiogenesis (**Zawada et al.** *2011*). This may be particularly relevant in the formation and

stabilisation of an advanced atherosclerotic plaque where intra-plaque haemorrhage can occur through the formation of vaso vasorum.

There is however, contrasting evidence to show that the other monocyte subsets are preferentially involved in inflammation. Classical monocytes express high levels of CCR2 and migrate more efficiently to CCL2 *in-vitro* than do other monocyte subsets (**Ancuta et al.** *2003*) which is of particular relevance in both infective and atherosclerotic aetiologies of inflammation. In further contrasting studies, CD16^{pos} monocytes were weak phagocytes and did not produce ROS or other pro-inflammatory cytokines (such as TNFα) when activated with LPS (**Cros et al.** *2010*) but rather exhibited a patrolling behaviour in the pathogenesis of autoimmune disease, similar to the role played by mouse Ly6C^{low} monocytes. Other studies have shown that the isolated non-classical monocytes (CD14^{dim}CD16^{high}) , in response to LPS stimulation, produced some of the highest levels of TNFα and IL-1β while equivalent amounts of IL-6 and IL-8 were produced by all three subsets (**Wong et al.** *2011*). This was supported by whole blood intracellular staining wherein CD14^{dim} monocyte population produced the greatest amount of TNFα (**Belge et al.** *2002*).

Although loosely analogous, the comparison between human and mouse monocyte subsets should be done tentatively. Central to the comparison is the putative role of the CD16^{pos} and CD16^{neg} monocytes as compared to the differential roles of the Ly6C^{high} versus the Ly6C^{low} subsets. The Ly6C^{high} subset is thought to provide the circulating pool from which tissue macrophages are derived in the presence of inflammation however, both the CD16^{pos} and CD16^{neg} subsets both give rise to DCs and Macrophages with similar voracity. Stimulation of human monocyte subsets with either GM-CSF or M-CSF induced a macrophage morphology in all three subsets with similar secretion of macrophage-associated cytokines and enhanced phagocytosis (**Boyette *et al. 2017***). In fact, the study went on to demonstrate that in contrast to the Ly6C^{low} mouse monocytes, human CD16^{neg} classical monocytes demonstrated increased dendritic cell markers with IL-4 and GM-CSF stimulation and increased allogenic T-cell proliferation suggesting that they augment the inflammatory response. This is in contrast to the Ly6C^{low} monocyte subset where, in a mouse model of arthritis, showed increased recruitment to areas of active synovitis and promoted the shift of resident macrophages from M1 to M2 and therefore attenuate joint inflammation (**Misharin *et al.* 2014**). A similar mechanism has not been demonstrated in human CD16^{neg} monocytes.

2.4.4   Human Monocyte Subsets are Differentially Associated with Atherosclerotic Disease

The understanding of the function of monocyte subsets in human atherosclerotic disease is much less comprehensive than in mouse monocyte subsets and is derived predominantly from associative studies using cohorts of patients with cardiovascular disease. Initial studies have demonstrated that the levels of non-classical monocyte subset were positively correlated with elevated levels of total plasma cholesterol, LDL and Triglycerides and negatively with high-density lipoprotein (HDL) levels (**Rothe *et al.* 1996**). The number of CD16^{pos} monocytes, but not all monocytes, were found to be positively correlated with traditional cardiovascular risk factors such as body mass index (BMI), insulin resistance and intimal-media thickness (**Poitou *et al.* 2011**). This was supported by other studies where the numbers of CD16^{pos} monocytes were associated with obesity and subclinical atherosclerosis (**Rogacev *et al.* 2010**). In the HOM SWEET HOMe[12] study, 951 patients, referred for elective coronary angiography were followed up for the primary endpoint of cardiovascular death, AMI or non-haemorrhagic stroke. It was found that not just higher overall monocyte counts, but numbers of both the classical and intermediate subsets were associated with higher event rates. However, after adjustment for cardiovascular risk factors, only the intermediate subset remained as an independent predictor of adverse outcomes (**Rogacev *et al.* 2012**).

In contrast, a study in the general population (n=659), with no ostensible cardiovascular risk factors, showed that the levels of the classical subset (CD14^{pos}CD16^{neg}) independently predicted cardiovascular events within a mean 15-year follow-up (**Berg *et al.* 2012**). This subset is seen in the infarct border of myocardium in patients who have suffered an MI (**van der Laan *et al.* 2014**) and is associated with an increased production of MCP-1 which stimulates the mobilisation and recruitment of this monocyte subset to myocardium, the levels of which are associated with increased cardiovascular mortality (**de Lemos *et al.* 2007**). Non-classical monocytes have been shown to exhibit a crawling behaviour on the endothelium after being adoptively transferred into mice (**Cros et al. 2010**). This is consistent with other *in-vitro* experiments which has shown the CD16^{pos} subset to be far more mobile than their CD16^{neg} counterparts (**Randolph *et al.* 2002**). The gene expression data supports this as genes associated with cytoskeletal mobility such as the Rho GTPases (RHOC and RHOF) are most highly expressed by the non-classical subset (**Wong et al. 2011**). These findings suggest that the non-classical monocytes are constantly surveying the endothelium for signs of damage and inflammation and are poised to transmigrate rapidly.

---

[12] Heterogeneity of Monocytes in Subjects Who Undergo Elective Coronary Angiography- The HOMburg Evaluation

2.5   The Role of Platelets in Atherosclerosis

Described initially by Giulio Bizzozero in 1882 (**Ribatti and Crivellato** *2007*), platelets are small (2-3µm), anucleate cellular fragments that derive from bone marrow megakaryocytes. Their production is regulated by thrombopoetin (TPO), a glycoprotein hormone, which promotes the growth and development of megakaryocytes from their precursors. TPO induces polyploidy in bone marrow megakaryocytes which go on to form long branching processes consisting of platelet-sized swellings called proplatelets. These bud off into the sinusoidal blood vessels of the bone marrow and are subsequently liberated into the circulation as mature platelets (**Junt** *et al.* *2007*). Once released, they remain in the bloodstream for 7-10 days before they are sequestered and phagocytosed within the reticuloendothelial system in the liver (Küpfer cells) or spleen (**Kaplan and Saba** *1978*).

The primary role of platelets in haemostasis and thrombosis has been recognised since the 19th century where their accumulation at sites of vascular injury, in the form of a primary haemostatic plug, helps to maintain vascular integrity. Further clot formation is amplified by the coagulation cascade to form the secondary haemostatic plug and the generation of a mature thrombus. Their ability to respond to a variety of agonists arises from the multitude of activation receptors they possess on their surface (summarised in **Table 2.2**). The platelet membrane glycoproteins are one such class of receptors that play a key role in haemostasis. Upon vessel damage, they interact with the extracellular matrix to induce conformation change and, through Phospholipase C (PLC-γ), mobilise intracellular Ca^{2+} stores to promote activation. This group of receptors include the GPIb/V/IX complex, GPVI, GPIa-IIa, and GPIIb-IIIa (which also participates in inside-out signalling). Platelets also possess receptors for circulating agonists including the ADP receptors $P2Y_1$ and $P2Y_{12}$, the Thromboxane A_2 (TXA_2) receptors TP-α and TP-β, as well as the Thrombin receptors PAR1 and PAR2[13]. These receptors are all G-protein coupled (GPCR) and also act to increase intracytosolic Ca^{2+} through PLC-β which promotes platelet activation.

---

[13] The other thrombin receptor is the platelet glycoprotein GPIbα

CLASS	SUBCLASS	NAME	LIGAND	FUNCTION
Integrins	β1	α2β1 (GPIa-IIa, VLA-2, CD49b/CD29)	Collagen	Binds collagen and promotes pro-coagulant activity
		α5β1 (GPIc-IIa, VLA-5, CD49e/CD29)	Fibronectin	Pro-coagulant and initiates synthesis of platelet proteins and facilitate adhesion to fibronectin
		α6β1 (GPIc'-IIa, VLA-6, CD49f/CD29)	Laminin	Signals via PI3-K to induce morphological change in platelets
	β2	αLβ2 (CD102, ICAM-2)	LFA-1	Platelet-neutrophil and Platelet-leucocyte interaction
	β3	αIIbβ3 (CD41/CD61, GPIIb-IIIa)	Fibrinogen, Fibrin, vWF, Fibronectin, Vitronectin, Thrombospondin	Upon activation, conformation change is induced from low to high affinity state and promotes platelet aggregation
		αVβ3 (GPv-IIIa, CD51/CD61)	Vitronectin, Fibrinogen, vWF, prothrombin, thrombospondin	Magnesium-dependent activation with ligand binding. Also binds osteopontin in atherosclerotic plaques
IgSF		GPVI	Collagen	Non-covalently associated with ITAM-bearing FcR γ-chain and induces platelet activation
GPCRs	Purinergic Receptors	P2Y$_1$	ADP	Gq-coupled to liberate intracytosolic Ca^{2+} and promote platelet activation
		P2Y$_{12}$	ADP	Gi-coupled to liberate intracytosolic Ca^{2+} and promote platelet activation
	Protease-activated Receptors	PAR1	Thrombin	Activates Gi/Gq/G$_{12/13}$ and liberates intracytosolic Ca^{2+} via PLC-β
		PAR2	Thrombin	Activates Gq/G$_{12/13}$ and liberates intracytosolic Ca^{2+} via PLC-β
	Prostanoid Receptors	TP-α	TXA$_2$	Activates Gq/G$_{12/13}$ and liberates intracytosolic Ca^{2+} via PLC-β and PLA$_2$
		TP-β	TXA$_2$	Activates Gq/G$_{12/13}$ and liberates intracytosolic Ca^{2+} via PLC-β and PLA$_2$

Table 2.2: Nomenclature and Function of Selected Platelet Receptors. Table shows the broad classes of activating platelet receptors including the Integrins, Immunoglobulin Superfamily (IgSF) and the G Protein-Coupled Receptors (GPCRs). Integrins are non- covalently bound heterodimers of α and β subunits and platelets possess three types of integrins (namely β1, β2 and β3) which are constitutively in a closed confirmation. Common agonists inducing platelet activation include Adenosine Diphosphate (ADP), Thrombin and Thromboxane A$_2$ (TXA$_2$) which act synergistically to mobilise intracytosolic Ca^{2+} stores and activate platelets.

Following atherosclerotic plaque rupture, damage to the vessel wall results in the exposure of the subendothelial matrix, an exquisitely thrombogenic substance, allowing for the adherence of platelets and the initiation of thrombus formation. The initial tethering is mediated by platelet GPIbα (of the GPIb-IX-V complex) to the A1 domain of the von Willebrand Factor (vWF) (**Ruggeri** *2002*). More stable interaction is brought about by both GPIa-IIa (integrin $\alpha_2\beta_1$) and GPVI which also induce the activation of platelets. This results in the conformational change of the integrin receptors GPIIb-IIIa fibrinogen receptor (**Arya** *et al.* *2003*) and GPIa-IIa collagen receptor (**Nieswandt** *et al.* *2001*) which firmly bind to their respective extracellular matrix (ECM) components. Both vWF (**Denis** *et al.* *1998*) and GPIbα (**Bergmeier** *et al.* *2006*) knockout mice demonstrate decreased platelet adhesion and defective haemostatic response. The activation of platelets is further supported by the release of soluble agonists at sites of vascular injury. These include thromboxane A_2 (TXA_2), synthesised from arachidonic acid, and ADP released from platelet dense granules. These endogenous agonists can act in an autocrine or paracrine manner to enhance platelet activation by engaging specific G-protein coupled receptors (GPCR). P2Y1 (**Jin** *et al.* *1998*) and P2Y12 (**Hollopeter** *et al.* *2001*) mediate the actions of ADP while the TPα and TPβ (**Huang** *et al.* *2004*) mediate the effect of TXA_2 (see **Figure 2.5**).

The ligation of these surface receptors on platelets results in a dramatic change in the physiology of these cells resulting in a range of effects. Activated platelets undergo significant shape change accompanied by the extrusion of pseudopodia and lamellopodia allowing for their aggregation and interactions with a number of cell types. This is mediated by an extensive submembranous microtubular apparatus that allow for a rapid change in shape and aggregation upon activation (**Patel-Hett** *et al.* *2008*). Platelets also contain, within their cytoplasmic, stores of a range of mediators involved in a diverse array of function. Platelet α-granules are intracellular stores consisting of more than 300 distinct proteins (**Senzel** *et al.* *2009*) which are translocate to the membrane upon activation. Important proteins released from α-granules includes P-selectin, Platelet-Factor 4 and other clotting protein such as thrombospondin. Dense granules are specialised secretory organelles containing low molecular weight compounds such as adenosine diphosphate (ADP), serotonin and ionised calcium which are necessary for the coagulation cascade. Platelets also contain a surface-connected open canalicular system which serves as a final common pathway for the uptake of particulates and the discharge of secretory products, particularly from α-granules, from activated platelets (**Escolar and White** *1991*).

In addition to the release of granule contents, platelets also release several types of membranous extracellular vesicles (EV), specifically microparticles (MP) and exosomes. EVs are released by most cell types (**Quinn** *et al.* *2015*) and following the identification of platelet-

derived EVs (**Heijnen** *et al. 1999*), their role in intercellular communication and as biomarkers in disease states has been increasingly recognised (**Yanez-Mo** *et al. 2015*). Microparticles are large EVs (100-1000nm) with high levels of negatively-charged phospholipids, predominantly phosphatidyl serine (PS), which provide a substrate for their pro-coagulant activity. Importantly, microparticles also retain the surface markers of their cellular origin (e.g. CD61), which allow for their identification, and shown to contain over 500 different proteins, including those involved in coagulation (e.g. fibrinogen) and intracellular signalling (e.g. PKC) (**Garcia** *et al. 2005,* **Jin** *et al. 2005*). Exosomes are smaller than microparticles (40-100nm) and released from cells when multivesicular bodies fuse with the plasma membrane. Unlike MPs, exosomes do not retain their cellular origin markers but instead express tetraspanins at high levels (**Stoorvogel** *et al. 2002,* **Conde-Vancells** *et al. 2008*). Although they contain a limited proteome (**Epple** *et al. 2012*), they are abundant in microRNA along with the necessary cellular machinery to carry out its action and therefore suggests that exosomes are an integral part cellular signalling (**Landry** *et al. 2009,* **Jaiswal** *et al. 2012*).

It has become increasingly recognised that platelets also have other biologically significant roles beyond their haemostatic function (**Jacoby** *et al. 2001*) including localising to the sites of inflammation (**Gawaz** *et al. 2005*) and promoting angiogenesis both in normal vessels and tumours (**Battinelli** *et al. 2011*). This is reflective of their role in both the thrombotic and inflammatory magisteria, crucial to the response to a vascular insult, but dysregulated in the pathogenesis of atherosclerosis.
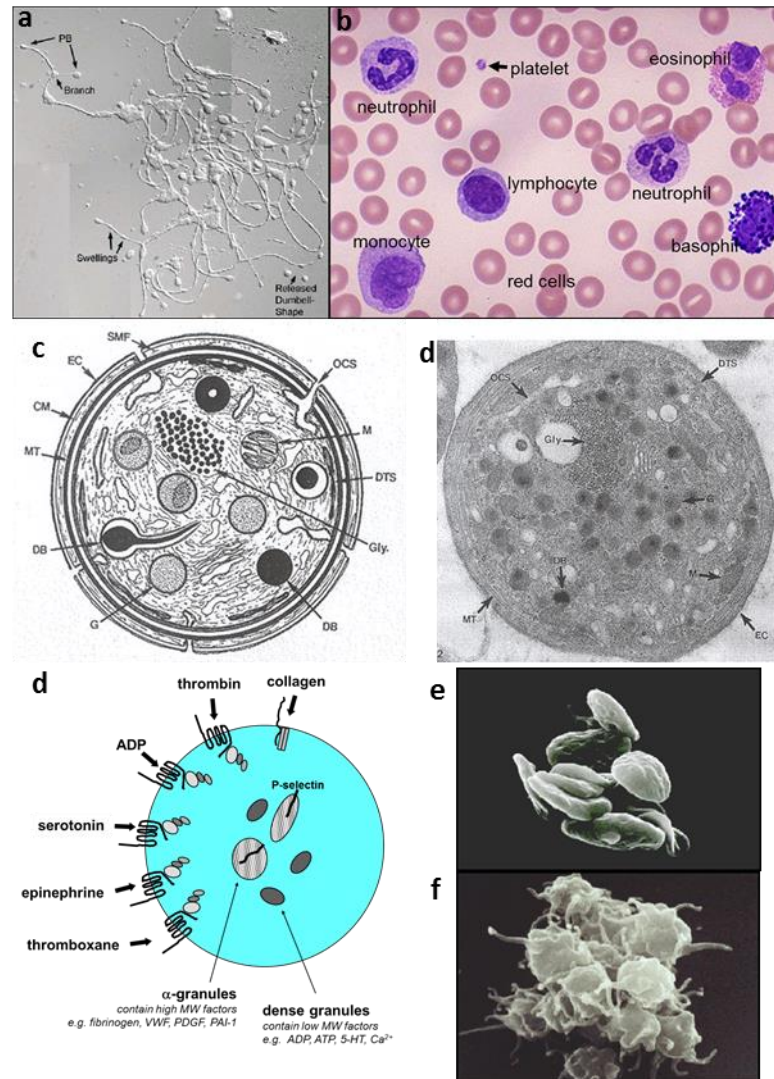
Figure 2.5: Morphological Overview of Platelets. (a) shows light microscopy of a polyploid megakaryocyte. Long branches comprised of platelet-sized swellings in tandem arrays (pro-platelets) are shown which generate platelets as they bud from platelet-bridges (PB). (b) Shows Haematoxylin & Eosin stained blood film under light microscopy to demonstrate the macrostructure of platelets in comparison to other peripheral blood cell constituents. Platelets are significantly smaller than their leucocyte counterparts and reflect their origin as fragments from a parent megakaryocyte. (c) Depicts a schematic diagram of platelet ultrastructure (CM-cell membrane, SMF-specialised microfilaments, MT-microtubules, DB-dense bodies, G-granules (α-granules), DTS-dense tubular system, M-mitrochondria, OCS-open canalicular system, Gly-Glycogen). (d) is an electron microscopy image of a quiescent platelet reflecting many of the features in the schematic diagram including the open canalicular system, dense bodies, α-granules and a microtubular system (d) shows a schematic diagram of the platelet activation receptors from collagen (GPVI), thrombin (PAR), ADP (P2Y) serotonin (5HT2A), epinephrine (α2) and thromboxane (TXA) which act synergistically to induce aggregation and degranulation of platelets. Platelets contain α-granules, comprising of high molecular weight proteins including P-selectin, and dense granules containing low molecular weight compounds such as Ca^{2+} and Adenosine Triphosphate (ATP). Scanning electron micrographs are shown of platelets in the quiescent state (e) and following activation (f). Activated platelets undergo a shape change (mediated by the microtubular system), extrusion of pseudopodia and lamellopodia resulting in aggregation and adherence to the endothelial surface/sub-endothelial matrix.

2.5.1 Platelets Interact with Monocytes

Activated platelets readily bind to all major classes of leucocytes both *in vitro* and *in vivo*. In a range of experimental and clinical models of sepsis, platelets have been shown to bind to neutrophils and contribute to inflammation (**Bozza *et al.* 2009**). The formation of platelet-neutrophil interactions have been shown to contribute to transfusion-related acute lung injury (TRALI) and adverse transfusion reactions in humans (**Keating *et al.* 2008**). Similarly, platelets have also been shown to interact with eosinophils and basophils, believed to be important in the immunopathology of allergic responses (**de Bruijne-Admiraal *et al.* 1992**).

MPAs are heterotopic complexes formed in response to a variety of inflammatory, immune and thrombotic insults and are particularly important in the pathology of atherosclerosis. Patients with stable CAD were found to have more than twice the number of circulating MPAs than healthy age-matched controls (**Furman *et al.* 1998**) with destabilisation of the plaque and subsequent thrombosis associated with a three-fold increase in circulating MPAs (**Brambilla *et al.* 2008**). Even in those patients without an index thrombotic event but who possess risk factors for CAD including hypertension (**Gkaliagkousi *et al.* 2009**) and diabetes (**Harding *et al.* 2004**), the presence of MPAs is directly correlated with adverse clinical outcomes.

MPAs are considered surrogate markers of platelets activation where the primary molecular interaction mediating complex formation is between P-selectin on platelets and its cognate receptor P-selectin Glycoprotein Ligand (PSGL-1) (**Figure 2.6**) on monocytes (**Keating *et al.* 2006**). Inhibition of the P-selectin/PSGL1 couplet abolished MPA formation while their formation was only partially inhibited by blockade of other receptor-ligand couplets such as JAM3-GPIbα (**Santoso *et al.* 2002**). In patients with MI, PSGL-1 blockade both prior to and after platelet stimulation *ex-vivo* markedly reduced the formation of MPAs but *ex-vivo* blockade of $\alpha_{2m}\beta_2$ and $\alpha_{2b}\beta_3$ integrins did not result in a further decrease in MPA formation (**Fernandes *et al.* 2003**).
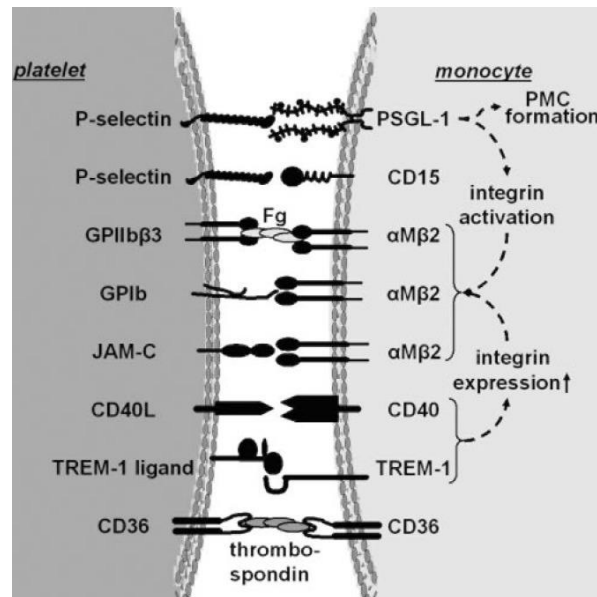
Figure 2.6: Platelet-Monocyte Interactions. Diagram illustrates the myriad of receptor/ligand interactions mediating binding of platelets and monocytes. P-selectin mediates the initial binding contact with monocytes via PSGL-1 and CD15. In addition to triggering the formation of MPAs, the ligation of PSGL1 triggers the activation of $\alpha_M\beta_2$ integrins which form complexes with GPIIbβ_3, JAM-C and GPIb. The CD40L/CD40 and TREM-1 ligand/TREM-1 receptor dyads are important interactions, acting in parallel with P-selectin/PSGL1 to further increase the expression of $\alpha_M\beta_2$ integrins thereby strengthening PMC formation. CD36 on both platelets and monocytes form homodimers mediated by thrombospondin[14]

Besides PSGL1, CD15 on monocytes has also been shown to bind platelet P-selectin (**Larsen *et al. 1990***). The ligation of PSGL-1 leads to increased expression of the β_2 integrin CD11b/CD18 (Mac-1) on monocytes (**Neumann *et al.* 1999**), which itself supports interactions with platelets. Mac-1 on leukocytes binds to GPIb (**Simon *et al.* 2000**) and JAM-C on platelets (**Santoso et al. 2002**). Monocytes also bind to platelets using bridging mechanisms, for example by fibrinogen linking leucocyte Mac-1 to its platelet surface counterpart integrin GPIIb-IIIa (**Gawaz *et al. 1991***). Platelets and monocytes also form bridging interactions through homodimeric interactions, for example of CD36 via thrombospondin (**Silverstein *et al.* 1989**). Additional interactions between platelets and monocytes include CD40-CD40L (**Lindmark *et al.* 2000**) and monocyte triggering receptor expressed on myeloid cell 1 (TREM1) to platelet-expressed TREM-1 ligand (**Haselmayer *et al.* 2007**).

---

[14] Taken from van Gils, JM, JJ Zwaginga and PL Hordijk. Molecular and Functional Interactions among Monocytes, Platelets, and Endothelial Cells and Their Relevance for Cardiovascular Diseases. *J Leukoc Biol*.**2009**; **85: 195-204**

2.5.2 Platelets Activate Monocytes

The cytoplasmic tail of PSGL-1 is linked to the actin cytoskeleton through the ezrin-radixin-moesin (ERM) proteins. This interaction is important in the redistribution of PSGL-1 on the monocyte surface and promotes the rolling of leucocytes on endothelium (**Alonso-Lebrero** *et al. 2000*). In addition to the actin cytoskeleton, ligation of PSGL-1 results in the phosphorylation of ITAM motifs in moesin with subsequent downstream activation of Syk and Src tyrosine kinases (**Hidari** *et al. 1997*). These changes are particularly important in regulating surface integrins, increasing expression and activity of $\alpha_4\beta_1$, $\alpha_m\beta_2$ and $\alpha_L\beta_2$ (**Snapp** *et al. 2002*). In addition to strengthening MPA formation, the induction of these molecules mediates firm adhesion to activated endothelium and therefore promotes monocyte egress. The interaction of P-selectin and PSGL-1 also serves to upregulate key inflammatory genes and expression of pro-inflammatory cytokines in monocytes. There is enhanced translocation of NF-κB and subsequent induction of immediate-early genes such as TNFα and MCP-1 (**Weyrich** *et al. 1995*). Use of a blocking antibody to P-selectin not only abrogated the formation of MPAs with thrombin activation, but also diminished downstream effects on the monocytes consistent with this signalling pathway (**Weyrich** *et al. 1996*). This included key changes such as reduced secretion of MCP-1 and IL-8 which are both dependent on the NF-κB and RANTES signalling. Other ligand couplets are also important in the interaction between platelets and monocytes in addition to the P-selectin/PSGL-1 dyad. Engagement of CD40 with CD40L for example also results in increased monocyte adhesiveness by upregulation of β_1 and β_2 integrins (**Li** *et al. 2008*). The ligation of TREM-1 on monocytes by TREMI-1 ligand on platelets induces upregulation of integrins to promote subsequent secretion of MCP-1, TNFα and IL-8 from monocytes (**Weyrich** *et al. 1996*). These results demonstrate that although the P-selectin/PSGL-1 interaction is a necessary step in the formation of MPAs, other ligand couplets augment this interaction and further promote the activation of monocytes (**Figure 2.6**).

2.5.3 Platelets Promote a Pro-Inflammatory Monocyte Phenotype

Consistent with their role in both thrombosis and inflammation, platelets have also been shown to promote a pro-inflammatory phenotype in circulating monocytes. The evidence for this position comes initially from observational data in patients with significant platelet-activating events. Following ST-elevation Myocardial Infarction (STEMI), there was increased levels of MPA formation which persisted for 30 days, despite the ubiquitous use of anti-platelet therapy (**Tapp et al. 2012**). Upon analysis of monocyte subsets, the platelets tended to form aggregates preferentially with the intermediate followed by the classical monocyte subset (**Tapp et al. 2012**). This is partially supported by *in-vitro* data wherein blood samples from healthy volunteers were activated with an exogenous platelet stimulus and demonstrated that the proportion of MPAs was found to be the highest on the intermediate and non-classical subset (**Boudjeltia et al. 2008**). The study went on to show that this intermediate subset had the highest potential to extravasate into the arterial media which the authors suggest is a mechanism by which MPA formation promotes atherosclerosis.

The association between the intermediate subset and MPA formation is also found in a range of inflammatory conditions. Patients with rheumatoid arthritis have an increased proportion of the CD16^{pos} monocyte subset which was directly correlated with MPA formation (**Rong et al. 2014**). In patients with paroxysmal nocturnal haemoglobinuria and sickle cell anaemia, increased counts of the intermediate phenotype were found with intracellular haemoglobin and increased intracellular markers for platelets (**Rawat et al. 2017**). This finding indicates that circulating monocytes might phagocytose platelets upon MPA formation. The intermediate phenotype might also be induced by an inflammatory stimulus. In one study, MPA formation and monocyte phenotype was quantified in healthy individuals after being subject to influenza immunisation (**Passacquale et al. 2011**). They found that there was a significant increase in MPA and this was correlated with levels of CD16 on those aggregates. These studies provide evidence that MPA formation is correlated with the numbers of intermediate monocyte subsets but provide only circumstantial evidence that this relationship is causal. However, there is limited evidence to suggest that activated platelets might also induce the expression of CD16. In one study examined contaminating monocytes in platelet concentrates as a source of febrile transfusion reactions (**Grey et al. 1998**). Here, the investigators found that increasing levels of IL-6 in platelet concentrates were correlated with monocyte counts and furthermore, these monocytes increased increasing levels of both CD14 and CD16 during storage. This is complimented by an *in*-vitro study wherein human monocytes, when co-cultured with platelets, showed an

upregulation of CD16 (FcγRIII) which was functionally active as assessed by its ability to kill murine anti-CD16 hybridoma cells (**Phillips *et al. 1991***).

2.5.4 Platelets Promote Monocyte Diapedesis

In addition to the direct activation of monocytes, platelets also promote monocyte diapedesis, predominantly through a P-selectin dependent mechanism and thereby accelerate atherosclerosis. P-selectin deficient ApoE$^{-/-}$ mice exhibited a 3-5 fold decreased atherosclerotic lesion burden when compared to P-selectin^{wt} mice (**Dong *et al. 2000***). Furthermore, the P-selectin deficient-mice exhibited more advanced lesions with more smooth muscle infiltration and crucially more monocyte infiltration. P-selectin^{neg} and P-selectin^{wt} mice, bred into an ApoE$^{-/-}$ background were lethally irradiated, to abolish native haemopoesis, before bone marrow from each genotype was transplanted. Although endothelial P-selectin was found to be crucial in the development of atherosclerotic plaques, lesions in wild-type recipients receiving wild-type transplants were 30% larger than those receiving P-selectin deficient platelets (**Burger and Wagner** *2003*). This result suggests that it is predominantly endothelial P-selectin that mediate monocyte transmigration, but platelet P-selectin significantly accelerates this process. This finding was supported by further evidence showing that platelets were present on activated endothelium before the appearance of leucocytes on nascent plaques (**Massberg *et al. 2002***). Repeated infusions of wild-type platelets in ApoE$^{-/-}$ mice accelerated the formation of atherosclerotic lesions whereas infusion with P-selectin-deficient platelets formed much smaller lesions (**Huo *et al. 2003***). In an *in-vitro* study wherein MPAs were perfused over an endothelial cell line (HUVEC) in culture, it was found that monocyte adhesion and cluster formation was increased 2-fold above that found with a pure infusion of monocyte alone. Blocking MPAs by targeting the P-selectin/PSGL1 interaction reversed this adhesion back to baseline with much more modest effects with inhibition of L-selectin (**da Costa Martins *et al. 2004***). This suggests that the presence of MPAs render monocytes more amenable to secondary tethering and increase their transmigratory potential. Furthermore, these platelets are left in the luminal space and are shed from monocytes during their diapedesis (**van Gils *et al. 2008***).

Another mechanism by which platelet promote monocyte diapedesis is through the release of soluble P-selectin (sP-selectin). It is believed to arise from surface P-selectin which is subsequently shed by cleavage (**Michelson *et al. 1996***) and importantly, does not seemed to be influenced by different anticoagulants and/or varying methods of plasma preparation (**Ferroni *et al. 1999***). This fact has enabled sP-selectin to be used as robust marker of platelet and/or endothelial cell activation (**Ridker *et al. 2001***). Mice carrying a mutant p-selectin gene expressing abnormally high levels of sP-selectin, showed larger infarcts in an ischaemic stroke model and

increased susceptibility to atherosclerotic lesions (**Kisucka *et al. 2009***). The mechanism, rather than the direct formation of MPAs, is by activation of PSGL-1 on leucocytes with subsequent upregulation of integrins (MAC-1) and the release of microparticles, which promotes monocyte adhesion and egress into the nascent plaque. However, when measuring levels of this antigen in *in-vivo* models of platelet activation, it is often not clear if what is being measured is true sP-selectin or if it is membrane-bound P-selectin on platelet and endothelial-derived microparticles. This opens up the possibility that platelet-derived microparticles provide an alternate mechanism (from direct platelet-monocyte conjugates and sP-selectin) by which platelets promote monocyte diapedesis and plaque formation.

2.5.5 Platelets Modulate Foam Cell Formation in Monocyte-Derived Macrophages

2.5.5.1 Direct Platelet-MDM Interactions

Platelets readily interact with circulating monocytes however, they may also infiltrate advanced plaques through leakage and/or rupture of newly formed micro vessels (**Kolodgie *et al. 2003***). This is a potential mechanism by which platelets are able to interact with intra-lesional macrophages. By virtue of their close association in the plaque, phagocytosis of platelets by macrophages was one of the earliest mechanisms proposed for foam cell formation. Early studies described lipid-filled leucocytes, known as lipophages, in a rabbit model of atherosclerosis has shown that phagocytosed platelets may be the source of the lipids (**Chandler and Hand *1961***). This was further confirmed by electron microscopy of mural thrombus in baboons (**Poole *1966***) and murine macrophages (**De Meyer *et al. 2002***). These findings are consistent with the observation that platelets themselves are able to bind and uptake LDL. Uptake of LDL by platelets induces changes in the phospholipid composition of platelet plasma membrane as a result of lipid transfer but does not induce their activation (**Engelmann *et al. 1996***). However, in stark contrast, binding of oxLDL and minimally modified LDL induced their activation and promoted thrombus formation (**Maschberger *et al. 2000***). It has also been shown *in-vitro* that various forms of oxLDL bind to human and mouse platelets in a CD36-dependent manner resulting in the activation of platelets with increased surface expression of $\alpha_{2b}\beta_3$ integrins and P-selectin (**Podrez *et al. 2007***). The blockade of CD36 resulted in a reduction in oxLDL binding to platelets (**Volf *et al. 1999***). The Lectin-type Oxidised LDL receptor (LOX-1) is another major binding protein for oxLDL on human platelets working synergistically with CD36. While CD36 is expressed constitutively on human platelets, LOX-1 is induced upon platelet activation, most likely mobilised from intracellular stores, which may further amplify the potential for the uptake of oxLDL by platelets (**Chen *et al. 2001***). In addition to the uptake of oxLDL, platelets can also generate oxLDL by lipid peroxidation as both resting and activated

platelets produce reactive oxygen species (ROS) such as superoxide anions (**Marcus *et al.* 1977**). These mechanisms have been shown to be important in the formation of monocyte-derived foam cells as oxLDL induced the activation of platelets and promoted the rapid formation of MPAs (**Badrnya *et al.* 2014**). The group went on to show that when platelets and monocytes were co-cultured, monocytes took up oxLDL from platelets in a process mediated by CD36-oxLDL interaction and phagocytosis.

There is some evidence to suggest that platelets promote a foam-cell like phenotype in endothelial progenitor cells (EPC). EPCs are circulating bone marrow-derived cell population characterised by the surface expression of CD133, CD34 and VEGFR-2 (**Hristov *et al.* 2003**). Their role appears to be in vascular repair and homeostasis where in response to injury, they contribute to neovascularisation and angiogenesis. Recruitment of EPCs towards vascular lesions has been regarded as a critical initial step in atherosclerosis and a result of the actions of various cardiovascular risk factors (**Xu** *2006*). However, there is controversy in the literature as to the fate of EPCs in atherosclerotic lesions and if indeed they are true precursors of lesional macrophages. In co-cultivation experiments, platelets recruited CD34^{pos} progenitor cells and induce differentiation into mature foam cells (**Daub *et al.* 2006**). The binding of platelets to CD34^{pos} cells induced a change in morphology accompanied by vWF expression and an upregulation of endothelial markers CD146 and CD31. This phenomenon was essentially abrogated in the presence of a P-selectin blocking antibody highlighting, much like platelet-monocyte interactions, the importance of this receptor-ligand interaction in platelet-EPCs binding. Also similar to monocytes, the formation of mature EPC-derived foam cells was driven by the accumulation of oxLDL in platelet dense granules, which are then rapidly internalised by EPCs to become foam cells in a manner dependent on CD36 and SR-A (**Seizer *et al.* 2010**)..

2.5.5.2 Released Factors

In addition to direct interaction of platelets and MDMs, released factors might also promote foam cell formation. Early studies in which thrombin-activated platelets were co-incubated with cultured rat aortic smooth muscle cells, showed increased accumulation of cholesteryl ester lipid droplet formation (**Kruth** *1985*). This effect occurred in the absence of serum lipoproteins and when cholesterol synthesis was blocked suggesting that activated platelets may release cholesterol which was accumulated by SMCs and stored as lipid droplets. In supporting experiments, it was found that both the rate of cholesterol esterification and accumulation of cholesterol esters were increased within 24hrs of co-culture of adherent macrophages with platelets (**Curtiss *et al.* 1987**). Maximal increases in esterification and CE accumulation were observed within 3-4 days of culture and furthermore, products released from platelets after

thrombin stimulation were also active but not to the extent seen with whole platelet incubation (**Curtiss et al.** *1987*). Platelets have within their cytoplasm, numerous α-granules that contain a large range of protein mediators. Proteomic studies have shown over 300 distinct proteins are released from these granules (**Senzel et al.** *2009*). Furthermore, many of these mediators are found at the site of atherosclerotic plaques suggesting that platelet degranulation may be an important modifier of plaque biology. The effects of some of these factors, in particular those found in high abundance, have been studied in detail as illustrated in the following sections.

2.5.5.2.1   Platelet-Factor 4

Chemokine ligand 4 (CXCL4), also known as platelet factor 4 (PF4), was the first chemokine discovered in the platelet releasate and is found in high concentrations within the α-granules (**Brandt** *et al.* *2000*). PF4 is important in atherosclerosis and has effects on various cell types including vascular endothelium, T-cells and cells of the monocyte-macrophage lineage. PF4^{neg} mice, bred into an ApoE^{neg} background showed significantly less atherosclerotic burden when compared to PF4^{pos} mice despite no significant differences in circulating lipids (**Sachais** *et al.* *2007*). PF4 acts as a survival factor for monocytes in culture and furthermore, these monocytes become cytotoxic to endothelial cells predominantly through the effects of reactive oxygen species (**Scheuerer** *et al.* *2000*). In human atherosclerotic plaques, the presence of PF4 correlated with both the histological and clinical severity of disease (**Pitsilos** *et al.* *2003*) and may significantly alter the phenotype of intra-lesional macrophages (see **Table 2.1**) (**Fricke** *et al.* *2004*). The transcriptome of human PF4-induced macrophages was compared to those induced by M-CSF (M0) and shown to have a distinct transcriptome and were thus termed the 'M4' macrophage (**Gleissner** *et al.* *2010*). Although there were similar levels of expression of leucocyte and myeloid markers, there was a significant downregulation of CD163, which correlated inversely with atherosclerotic burden. CD163 is a scavenger receptor for haptoglobin-haemoglobin complexes and is important in the late stages of plaque development in the clearance of haemoglobin. In advanced plaques, the expression of CD163 on macrophages has been described as a distinct subset known as M-hem, which contain intracellular iron and are considered protective in atherosclerosis (**Boyle** *2012*). There is therefore a balance between the PF4-induced M4 macrophage and the M-hem macrophage that modifies plaque biology. In addition, PF4 has been shown to inhibit binding and uptake of LDL through its classical receptor and diverts it to a more inefficient endocytic pathway (**Sachais** *et al.* *2002*). This was correlated with a 10-fold increase in the amount of esterified oxLDL in macrophages and was due to the increased residency time of LDL thus rendering it more susceptible to oxidative modification. This finding is to be contrasted with results comparing gene expression of receptors for both

native and modified LDL in M0 and M4 macrophages. There were similar levels of expression of the ldlr gene (encoding the LDL receptor) but significantly lower levels of expression of CD36 and MSR1 genes, coding for the scavenger receptors CD36 and SR-A respectively, in human MDMs incubated with CXCL4 (**Gleissner** *et al. 2010*). Functional data recapitulated the transcription data and showed that these CXCL4-induced macrophages took up less Dil-labelled acetylated or oxLDL when compared to M0 macrophages differentiated by M-CSF. This finding in human atherosclerotic lesions is contrary to that found in other *in-vitro* models of macrophage biology including CHO cell lines (**Sachais et al.** *2002*) and apoE^{-/-} mice (**Sachais et al.** *2007*) which might be reflective of the different experimental settings. This is supported by the observation that human and mouse monocytes show differing levels of expression of numerous genes involved in lipid uptake, degradation and trafficking, including CD36 (**Ingersoll** *et al. 2010*). By extension, it may be that species difference may play a role in the discrepant effects of CXCL4 on foam cell formation.

2.5.5.2.2 Interleukin 1β

Another cytokine released in abundance from platelets is IL-1β. Interest in IL-1β as a pro-foam cell cytokine stemmed from the observation that an IL-1 receptor antagonist negatively regulated foam cell formation in LDLR[neg] mice (**Devlin** *et al. 2002*). This finding implicated IL-1β as a promoter of foam cell generation in MDMs and levels of this cytokine are increased at sites of atherosclerotic plaques. IL-1β is also known to decrease both ABCA1 and ABCG1 mRNA expression, thereby reducing overall cholesterol efflux (**Chen** *et al. 2007*). This was confirmed in the THP-1 myelomonocytic cell line wherein IL-1β led to increased retention of intracellular cholesterol and triglycerides in a dose-dependent manner (**Persson** *et al. 2008*).

2.5.5.2.3 Peroxisome Proliferator-Activated Receptors

The peroxisome proliferator-activated receptors (PPARs) are a group of nuclear receptor proteins that function as transcription factors. Interestingly, PPARs are expressed in the human platelet despite lacking a nucleus (**Akbiyik** *et al. 2004*). Furthermore, human platelets also contain the PPAR binding partner LXR which is able to form the active heterodimer and is thus capable of biological activity in platelets. This is evidenced by the fact that exposure to PPAR agonists attenuated platelet activation and inflammation (**Ali** *et al. 2006*). PPAR and indeed the functional heterodimer form of PPAR/LXR are released in significant amounts in platelet-derived microparticles and taken-up by THP-1 cells (**Ray** *et al. 2008*). ABCA1 and ABCG1 in macrophages are transcriptionally regulated by ligand-dependent nuclear receptors and PPARγ agonists have been shown to regulate the formation of macrophage foam cells through not only ABCA-dependent and independent mechanisms (**Li** *et al. 2004*). This may partially be explained by the

observation that activators of PPARγ have been shown to upregulate CD36 (**Tontonoz *et al.* 1998**), thereby promoting the uptake of oxLDL into MDMs. However, PPARγ has also been shown to promote reverse cholesterol transport through the induction and upregulation of ABCA1 in macrophages (**Chinetti *et al.* 2001**) and therefore the overall effect on atherosclerosis is likely to reflect a balance of these two mechanisms.

Other members of the PPAR family have less well-defined actions. PPARδ is an isoform that is also found in abundance in platelets and is released upon activation. LDLR^{neg} mice, in which a micro-RNA approach was used to knock down PPARδ, showed decreased lesion development and decreased expression of pro-inflammatory cytokines (**Li *et al.* 2016**). PPARα ligands increase LOX-1 expression in vascular endothelial cells (**Hayashida *et al.* 2001**) and reduce atherosclerotic lesion burden in the mouse model (**Tordjman *et al.* 2001**).

2.5.5.2.4 Transforming Growth-Factor β

Platelets represent one of the major physiological sources of TGFβ, released in abundance upon platelet activation, and an example of an anti-inflammatory cytokine inhibiting foam cell formation. Early studies showed it inhibits scavenger receptor activity in THP-1 cells and may have a similar effect in MDMs (**Bottalico *et al.* 1991**). This was confirmed by two studies that showed that TGFβ inhibited CD36/SR-A expression and oxLDL uptake in human macrophages (**Han *et al.* 2000**) and promoted cholesterol efflux through the upregulation of ABCA-1 mRNA in monocyte-derived macrophages (**Panousis *et al.* 2001**). Furthermore, TGFβ was shown to inhibit lipoprotein lipase (LPL) activity and cholesteryl ester accumulation in murine macrophages with simultaneous enhancement of ABCG1 mRNA expression (**Argmann *et al.* 2001**). These findings suggest that TGFβ may mediate an anti-foam cell effect on monocytes consistent with the role of this cytokine in promoting fibrosis and wound healing. This is to be contrasted with the finding that TGFβ has been shown to upregulate the expression of OLR-1 which would be predicted to increase lipid accumulation and foam cell generation (**Draude and Lorenz 2000**).

2.6 **Conclusions**

When examined together, these studies have demonstrated that in addition to their canonical role in haemostasis and thrombosis, platelets also have an increasingly recognised role in the formation of atherosclerotic plaques. Activated platelets readily bind to circulating monocytes, resulting in pro-atherogenic effects on the monocytes. It has been shown that activated platelets are found to preferentially bind to the CD16^{pos} monocyte subset and the formation of MPAs is correlated with the preponderance of this subset. MPA formation is seen in a wide variety of thrombotic and inflammatory setting, as is the increased prevalence of the CD16^{pos} monocyte subset. However, there are limited data in human studies to show whether this effect is causal. What has been reported in the literature might simply reflect the fact that both of these are independent surrogate markers of inflammation and/or thrombosis and that their association is just that and does not reflect causality. There is limited functional evidence to show that activated platelets, *per se*, induce a CD16^{pos} phenotype in circulating monocytes and furthermore, minimal evidence to show that this phenotype is induced in previously CD16^{neg} cells. The data from mouse models have shown that the Ly6C^{high} is the obligate circulating reserve for the Ly6C^{low} which have been described as loosely analogous to the human monocyte subsets. Given the emerging evidence of the functional heterogeneity of human monocyte subsets, it is an oversimplification to equate human and mouse subsets and studies are needed to explore the functional relevance of platelet activation on human monocyte subsets. This is particularly true with respect to the origin of the CD16^{pos} subset which is, ostensibly, induced in response to an inflammatory or thrombotic stimulus, and strongly correlated with the formation of MPAs. If indeed activated platelets are able to induce a CD16^{pos} phenotype in previously CD16^{neg} cells, this would be another mechanism by which platelets promote atherogenesis.

There is evidence to demonstrate that platelets, and the factors released from platelets, promote the accumulation of intracellular lipid droplets in MDMs and promote their transformation into foam cells. Platelets are known to release a plethora of factors from their α-granules with both pro and anti-foam cell properties. However, the data on the individual factors released from platelets and their effect on foam cells formation does not consider the effect of the platelet *per se*. Furthermore, the experimental conditions used to demonstrate the effect of platelets on foam cells relies on the co-culture of platelets and monocytes. It is argued that this cannot be extrapolated to human disease as it relies on the assumption that platelets and monocytes are co-incident in a nascent atherosclerotic plaque. Although there is evidence that platelet-released proteins are found within a plaque, this is restricted to histological studies at post-mortem of advanced lesions where the formation of vasa vasorum and plaque

haemorrhage results in abundant platelets and may not reflect the conditions of nascent plaques. This thesis addresses these important deficits in the data and provides a better understanding of how activated platelets promote atherosclerosis through their interaction with monocytes.

2.7 <u>Hypothesis</u>

That activated platelets are pro-atherogenic and pro-inflammatory through the binding and modification of the phenotype of circulating monocytes. They promote the formation of foam cells in MDMs through the induction of dysregulated lipid metabolism, increase in surface activation and chemotactic markers on circulating monocytes as well as through the promotion of a CD16^{pos} intermediate monocyte subset. It is also hypothesised that these effects on circulating monocytes and MDMs can be demonstrated not only in an *in-vitro* model of platelet activation, but also using an *in-vivo* model of a physiological platelet-activating event such as myocardial infarction (MI).

In order to address the hypothesis, this thesis will specifically focus on the following objectives;

1 Development of a robust *in-vitro* model of platelet activation allowing for the isolation and culture of primary human monocytes to quantify monocyte activation, phenotype and foam cell formation

2 Description of the effects of platelet activation on monocytes using multiple modalities including quantification of established phenotypic cell surface markers, examination of transcriptomic changes using quantitative real-time PCR and fluorescent microscopy.

3 Quantification of the effect of the early interaction between platelet and monocyte on the subsequent morphology and atherogenicity of MDMs and foam cells. Judicious use of small-molecule inhibitors will be employed to elucidate some of the mechanisms underlying the putative platelet-induced effects on MDMs.

4 To test whether the effects of a 'physiological' platelet-activating event on monocyte phenotype and subsequent foam cell formation in MDMs are seen *in-vivo* in patients with MI.

In order to address the specific aims set out in the hypothesis, this thesis firstly details the development of a methodology whereby monocytes could be isolated from whole blood, without iatrogenic activation (Chapter 4) and cultured so that the formation foam cells can be studied robustly (Chapter 5). In Chapter 6, early interaction of monocytes and platelets are examined, and the phenotype of platelet-activated monocytes is described. Finally, the *in-vitro* methodology was applied to patients with MI in the FOAMI study (Chapter 7:) to ascertain if indeed the findings demonstrated *in-vitro* were recapitulated with an *in-vivo* platelet-activating stimulus.

Chapter 3: Materials & Methods

3.1 <u>Materials</u>

3.1.1 *Phosphate Buffered Saline (PBS)*

A 10x PBS solution was made by combining 80 grams Sodium Chloride (NaCl), 2 g Potassium Chloride (KCl), 11.5 grams disodium phosphate (Na_2HPO_4) and 2 grams Potassium Phosphate Monobasic (KH_2PO_4) in a beaker or conical flask[15]. To this mixture, 800mls of deionised water (H_2O) was added and gently mixed using magnetic stirrer. As the solute dissolved, a further 200mls of deionised water was added up to a final volume of 1000mls. The pH of the solution was tested at room temperature (Mettler Toledo, UK) and adjusted as required to 7.40 with 2M Hydrochloric Acid (HCl) or 0.1M Sodium Hydroxide (NaOH). Subsequent 1x PBS was made by diluting the 10x solution 1:10 in H_2O and filtered using a 0.22µm filter (Merck Millipore).

To prepare the PBS/5mM EDTA solution, 1.861grams of Disodium EDTA was added to 1L of 1xPBS and gently dissolved at room temperature using a magnetic stirrer to give a final concentration of 5mM. This solution was filtered using a 0.22µm filter (Merck Millipore) into a glass bottle and sterilised in an autoclave.

3.1.2 *4% w/v Paraformaldehyde (PFA)*

The preparation of 4% PFA was carried out in a fume hood with eye protection. 4.0 grams of PFA was added to 100mls of filtered PBS in a glass beaker on a hotplate with magnetic stirring. Aluminium foil was placed on top and the suspension was heated to 80°C for 1-2 hours. The mixture was gently stirred at this temperature until all of the PFA has dissolved. Care was taken to not allow the mixture to boil. The solution was left to cool and subsequently stored at 4°C[16].

3.1.3 *HEPES-Buffered Saline (HBS)*

8.766grams of NaCl, 0.373grams Potassium Chloride (KCl), 0.246grams Hydrous Magnesium Sulphate ($MgSO_4 \bullet H_2O$) and 2.383grams HEPES ($C_8H_{18}N_2O_4S$) was added to a volumetric flask and diluted with 1000mls of deionised water. The solution was mixed using a magnetic stirrer until all salts had dissolved. The pH was adjusted to 7.40 or 6.0 using 0.1M NaOH or 2M HCl as required. The HBS was filtered using a 0.22µm filer and was aliquoted into bijou bottle tubes, stored at 2-8°C in single-use aliquots.

---

[15] All chemicals purchased were from Sigma-Aldrich (Poole, UK) unless otherwise stated

[16] 4% PFA was stored for a maximum of 2-3 weeks at 4°C and at -20°C for longer-term storage in single-use aliquots.

3.1.4 Nile Red (9-Diethylamino-5H-benzo-α-phenoxazine-5-one)

500mg of Nile Red powder (Sigma-Aldrich) was dissolved in 500mls of Methanol (CH_3OH) and gently mixed until the powder was completely in solution to give a stock concentration of 1mg/ml. This was stored in the dark at room temperature. For staining of lipid droplets, fresh aliquots were prepared by dilution of stock 1:100 in PBS to give a final working concentration of 10μg/ml.

3.1.5 Human P-selectin (anti-CD62p)

Anti hP-selectin antibody (9E1) (R&D Systems, UK) was used to inhibit the formation of MPAs. The lyophilised powder was reconstituted to a stock concentration of 0.5mg/ml in sterile PBS and aliquoted into smaller vials for storage at -20°C. Each batch was tested using a monocyte-platelet aggregate assay (described in 3.2.5.2) and the minimum concentration required to inhibit MPA formation was selected for further experiments.

3.1.6 Cross-Linked Collagen Related Peptide (CRP-XL)

CRP-XL was purchased from Professor Richard Farndale, University of Cambridge, UK as a lyophilised peptide dissolved in H_2O at a concentration specified by the supplier. Each batch of CRP-XL was tested for efficacy by incubation with whole blood and assessment of platelet activation using a P-selectin flow-cytometric assay (described in flow cytometric methods). The optimum concentration was determined at the minimum dose of CRP-XL required to give maximal (>95%) platelet activation: as determined by P-selectin expression. CRP-XL was kept sterile and stored at 4°C. A fresh working solution was prepared daily by diluting 1μl in 99μl HBS to give a final concentration of 0.1mg/ml. The stock suspension was vortexed prior to sampling to ensure even mixing.

3.1.7 Antibodies Used for Imaging (Flow Cytometry, Fluorescence or Confocal Microscopy

All antibodies were purchased with pre-conjugated fluorochromes suitable for both flow cytometry and fluorescent imaging (**Table 3.1**). All antibodies were individually titrated for use for each assay to determine the optimum dilution for use.

Antibody Name	Clone	Manufacturer	Catalogue Number	Properties
Anti-CD181 (CXCR1)	8F1	Miltenyi Biotec	130-105-393	Binds CXCR1 (IL-8 receptor (IL-8RA)), a member of the GPCR family predominantly promoting neutrophil chemotaxis and activation
Anti-CD182(CXCR2)	REA208	Miltenyi Biotec	130-100-928	Directed against the IL-8β receptor with actions similar to CD181
Anti-CD183(CXCR3)-PE	REA232	Miltenyi Biotec	130-101-380	Binds CXCR3, a receptor for CXCL9, CXCL10 and CXCL11 and increased intracellular Ca^{2+} and activation of PI-3K and MAPK
Anti-CD186(CXCR6)	REA458	Miltenyi Biotec	130-107-730	Binds CXCR6, which has been identified as a co-receptor for HIV and SIV strains[17]
Anti-CD191(CCR1)-PE	REA158	Miltenyi Biotec	130-104-576	Binds CCR1, a member of the beta chemokine receptor family with ligands including CCL3, CCL5, CCL7 and CCL23
Anti-CX3CR1-PE	REA385	Miltenyi Biotec	130-103-899	Targeted against the fractalkine receptor which binds CX3CL1
Anti-human CD54 (ICAM1)-FITC	HA58	BioLegend	353108	Targets the extracellular D1 domain of CD54 (ICAM1) and is a major surface glycoprotein binding to integrins mediating cell-cell interactions
Anti-human CD62p (P-selectin)-FITC	9E1	R&D Systems	BBA34	Targets P-selectin, stored in Weibel-Palade bodies and expressed on the surface upon activation. It is a marker of platelet degranulation
Anti-LOX1-FITC	23C11	Abcam	ab81710	Targets LOX1, a major receptor for oxLDL
Anti-mouse/human CD11b-PerCP-Cy5.5	M1/70	BioLegend	101228	Binds integrin alpha M (ITGAM) which forms the heterodimeric integrin $\alpha_M\beta_2$ also known as Mac-1 or CR3[18]
Anti-Slan (M-DC8)-FITC	DD-1	Miltenyi Biotec	130-093-178	Recognises the 6-sulfoLacNAc carbohydtrate modification of PSGL1
Anti- CD14-VioBlue	TÜK4	Miltenyi Biotec	130-094-364	CD14 is a PRR acting as a co-receptor (with TLR-4) for the detection of LPS. It exists as a GPI[19]-linked and membrane form
Anti- CD16-APC	REA423	Miltenyi Biotec	130-106-705	Also known as FcγRIII and is involved in antibody-dependent cellular cytotoxicity particularly triggering lysis by NK cells
Anti- CD192 (CCR2)-PE	REA264	Miltenyi Biotec	130-103-829	Targets the CCR2 receptor which ligates MCP1, important in monocyte chemotaxis
Anti- CD45-PerCP Vio700	5B1	Miltenyi Biotec	130-097-527	Targets the PTPRC, also known as the common leucocyte antigen, that regulates a variety of cellular processes
IgG1-FITC	Goat anti-human polyclonal	Abcam	ab81051	Most abundant IgG subclass (2/3) in the serum and is used as an isotype negative control
MOPC21 Mouse IgG1κ-FITC	MOPC-21C	BioLegend	400110	Mouse monoclonal antibody used as an isotype for IgG1 kappa light chain antibody

[17] Human and Simian Immunodeficiency Virus

[18] Complement Receptor 3

[19] Glycophosphatidyl Inositol

Mouse anti-human CD42b-PE	HIP1	BD Pharmingen	555473	Platelet glycoprotein Ib alpha (GPIbα) functions as a receptor for vWF and is a marker of platelet activation
Mouse IgG1-FITC	11711	R&D Systems	IC002F	Mouse monoclonal antibody used as an isotype for IgG antibodies
Mouse IgG1κ-PE	MOPC21-C	BD Pharmingen	555749	Alternative mouse monoclonal antibody used as an isotype for IgG1 kappa light chain antibody
Mouse IgG2a-PerCPVio700	S43.10	Miltenyi Biotec	130-097-563	Used as an isotype control for the anti-CD45 antibody
Mouse IgG2a-VioBlue	S43.10	Miltenyi Biotec	130-094-671	Negative Isotype Control Hapten NP (4 hydroxy-3-nitro-phenyl) acetyl
Mouse IgG2b-PE	IgG2bκ	Miltenyi Biotec	130-098-875	Negative isotype control for PE conjugated antibodies
Mouse IgM-FITC	IS5-20C4	Miltenyi Biotec	130-093-178	Negative isotype control for FITC-conjugated antibodies
Rat 1gG2bκ-PerCP/Cy5.5	RTK4530	BioLegend	400632	Negative isotype control for PerCP/Cy5.5-conjugated antibodies
REA Control (S)-APC	REA293	Miltenyi Biotec	130-104-614	Universal isotype control for APC-conjugated REA clone antibodies
REA Control (S)-PE	REA293	Miltenyi Biotec	130-104-612	Universal isotype control for PE-conjugated REA clone antibodies

Table 3.1: List of Antibodies. Names of antibodies are given including the conjugated fluorochrome. Also included are the clone names, supplier, catalogue number and a brief description of the target antigens.

3.2 <u>Methods</u>

3.2.1 Peripheral Venepuncture

Blood was collected using a standardised method, designed to minimise platelet activation, from healthy volunteers within the Department of Cardiovascular Sciences, Glenfield Hospital. Consent was sought from each donor and performed under ethical approval from the University of Leicester (see approval letter in Section 9.4). This allows for the collection of up to 50mls of blood by peripheral venepuncture with a minimum donation frequency of two weeks. Venepuncture and blood collection was performed using the Vacutainer system (Becton-Dickinson, Oxford, UK). A tourniquet was applied to the arm of a donor to identify a suitable vein. Venepuncture was performed using a 21G butterfly needle in the antecubital fossa without alcohol sterilisation (to minimise platelet activation). An initial 2-3mls of blood was collected into an EDTA tube and subsequent samples were collected with the tourniquet removed. Samples were collected into tubes containing Citrate, Theophylline, Adenosine and Dipyridamole (CTAD) or alternatively into 3.2% Sodium Citrate anticoagulant.

3.2.2 Isolation of Cellular Fractions

3.2.2.1 Preparation of Platelet-Rich Plasma

Blood was collected into either Citrate or CTAD tubes and centrifuged (Allegra-X-22R, Beckman-Coulter) at 156g for 20 mins at room temperature with a slow brake. This resulted in the fractionation of whole blood into cellular components, including erythrocytes, pelleted at the bottom of the tube, with the platelet-rich plasma (PRP) supernatant. This PRP layer was careful collected by aspiration using a 3ml Pasteur pipette and care was taken not to disturb the blood-plasma interface.

3.2.2.2 Preparation of Platelet-Poor Plasma

Platelet-poor plasma (PPP) was prepared from either whole blood or from PRP by centrifugation at 1500g for 15mins (Allegra-X-22R, Beckman-Coulter). The supernatant was carefully aspirated and transferred to a new tube which was further centrifuged at 13000g for 2 mins. The supernatant was collected and further depleted of extracellular vesicles by passing the sample through a 0.22µm filter (Acrodisc, Pall) and either used within 30mins or stored in a -80°C freezer.

3.2.2.3 Preparation of Washed Platelets

A working solution of Prostaglandin I_2 (PGI_2, Sigma-Aldrich) was made from a stock solution of 1mg/ml by adding 40µl of HBS (pH 7.4) to 10µl aliquot of stock PGI_2 to give a working solution of 200µg/ml and stored on ice. All freshly prepared working solutions of PGI_2 was used within

10 mins of preparation. PRP collected as outlined previously, into LP4 tubes and 1µl of PGI$_2$ working solution was added per 1000µl of PRP. The PRP was gently mixed by pipetting and centrifuged again for 20mins at 600g. A further working solution of PGI$_2$ was prepared prior to completion of centrifugation. The supernatant was discarded, and the platelet pellet was gently re-suspended in 1ml of HBS (pH 6.0) to which 1µl of PGI$_2$ was added. A further centrifugation step was performed at 600g for 20mins and the platelet pellet was re-suspended in 1ml of HBS (pH 7.4). Platelet count was measured by automated cell counter (Act-T-Diff, Beckman-Coulter, UK). Once prepared, washed platelets were left for a minimum of 30 mins to allow the PGI$_2$ to decay.

3.2.2.4 Isolation of Monocytes from Whole Blood

To Whole Blood collected into 3.2% Trisodium Citrate, 50µl of Whole Blood CD14 MicroBeads (Miltenyi-Biotec) was added per 1ml of blood and incubated for 15mins at 4-8°C. The mixture was then processed through an AutoMACS PRO™ automated cell separator using a POSSELWB/RINSE program to give an isolated CD14^{pos} monocyte fraction.

3.2.2.5 Isolation of Peripheral Blood Mononuclear Cells from Whole Blood

The isolation of PBMCs was performed in a Class II Hood with 0.22µm-filtered and autoclaved solutions to maintain sterility. Whole Blood, collected into either CTAD or Citrate anticoagulant, was centrifuged to generate PRP which was aspirated taking care not to disrupt the buffy coat interface. The PRP-depleted blood was then reconstituted with PBS/5mM EDTA to replace the volume of PRP removed. The mixture was gently mixed and aliquoted into 50ml falcon tubes where the blood was further diluted 1:1 with PBS/5mM EDTA.

Figure 3.1: Appearance of Density-Gradient Centrifugation[20]. Lymphoprep is placed within a 50ml falcon tube (left bottle) and blood is carefully layered on top (middle bottle). Following centrifugation, the contents separate into an erythrocyte layer at the bottom with an overlaying lymphoprep layer. The PBMC layer lies at the interface of lymphoprep and PRP.

---

[20] Image taken from http://www.textbookhaematology4medical-scientist.blogspot.com

Density-gradient centrifugation was employed in the isolation of PBMCs from whole blood. A 50ml falcon tube was prepared with 15mls of sterile Lymphoprep™ (Axis-Shield, Dundee, UK) containing 9.1% w/v Sodium Diatrizoate and 5.7% w/v polysaccharide with a density of 1.077g/ml. To each tube, 30mls of the diluted Blood/PBS/EDTA mixture was carefully overlayed on top of the centrifugation medium taking care to preserve the integrity at the interface. The tube was centrifuged at 800g for 30 mins at room temperature with a slow brake allowing for clear separation of the blood components. The peripheral blood mononuclear cells (PBMCs), found at the interface of the density gradient medium and supernatant (**Figure 3.1**), were then selectively aspirated into clean, sterile 50ml Falcon tube using sterile Pasteur pipettes. To minimise platelet and erythrocyte contamination, the aspirated PBMCs were washed three times by re-suspending in 30mls of PBS/5mM EDTA followed by centrifugation at 300g for 15 mins. The supernatant was discarded, and the cell pellet was re-suspended in 30mls of PBS/5mM EDTA before a second centrifugation step at 200G for 15mins. The supernatant was discarded, and the cells re-suspended in 2mls PBS/5mM EDTA. The cell numbers were quantified using an automated cell counter (Act-T-Diff, Beckman Coulter) and the sample was re-suspended in 15mls of PBS/5mM EDTA for a final centrifugation at 200g for 15 mins. The supernatant was discarded, and cells re-suspended for downstream applications.

3.2.2.6 Double Density Gradient Centrifugation for Isolation of Monocytes

PBMCs were initially isolated from whole blood using Lymphoprep™ as a density gradient medium as outlined above. The PBMC pellet was re-suspended in 30mls of RPMI-1640 (Life Technologies, Paisley, UK) and then carefully overlaid onto 20mls of a 46% isosmotic Percoll solution (GE life Sciences, Amersham, UK), in a 50ml falcon tube, taking care to preserve the integrity of the interface. The tube was centrifuged at 550g for 30 mins, using a slow brake, allowing for the separation of monocytes at the interface. The monocytes were carefully aspirated into a separate 50ml falcon tube and washed by adding 40mls of PBS/EDTA and centrifugation at 400g for 10 mins. The supernatant was discarded, and the pellet was re-suspended for downstream application.

3.2.2.7 Immunomagnetic Depletion of Platelets

Platelets were removed from preparations of PBMCs using an immunomagnetic bead separation method. PBMCs, isolated from whole blood, were re-suspended in 80µl of PBS/5mM EDTA per 10^7 white cells as quantified by the automated cell counter (ActT Diff, Beckman Coulter). To this, 20µl of CD61 microbeads (Miltenyi Biotec, UK) were added per 10^7 cells and incubated for 15 mins at 4-8°C. A further 80µl PBS/EDTA per 10^7 cells was added and mixed gently prior to magnetic separation. This was performed using an automated cell separator (AutoMACS PRO™,

Miltenyi Biotec, UK) housed in a sterile Class II Cabinet. A 'depletes' programme was run which eluted a CD61^{pos} fraction rich in platelets and a CD61^{neg} fraction comprising PBMCs depleted of platelets.

3.2.2.8 Isolation of Monocytes by Positive Immunomagnetic Separation

A cell count was determined on platelet-depleted PBMCs which were pelleted and re-suspended in 80μl of PBS/EDTA per 10^7 cells. To this, 20μl of CD14 Microbeads (Miltenyi-Biotec) was added per 10^7 cells, mixed and incubated for 15mins at 4-8°C. The mixture was then processed through the AutoMACS PRO™ through a POSSEL programme to give preparation of CD14^{pos} monocytes.

3.2.2.9 Isolation of Monocytes by Negative Immunomagnetic Separation

All the biotin-conjugated antibodies and anti-biotin microbeads were provided in the Pan-monocyte Isolation Kit (Miltenyi Biotec). The volumes of reagents described in this section were for up to 10^7 white cells as quantified by automated cell counter. For higher numbers of cells, volumes were scaled up accordingly.

Platelet-depleted PBMCs isolated from whole blood were re-suspended in 30μl of PBS/EDTA. To this, 10μl of a biotin-conjugated antibody cocktail (Miltenyi Biotec) was added along with 10μl of an FcR-blocking reagent[21] (Miltenyi Biotec). The antibody cocktail is directed against CD235a, CD3, CD7, CD15, CD19, CD56, CD123 and CD335 which labels all non-monocytic cells leaving the monocytes unlabelled. The PBMCs-antibody mixture was incubated for 5 mins at 4-8°C and a further 30μl of PBS/EDTA was added. 20μl of anti-biotin magnetic microbeads was added to the solution and incubated for a further 15mins at 4-8°C before processing the mixture through the AutoMACS PRO™. Separation was performed according to the manufacturer's instructions using a 'Depletes' programme. This allowed for the separation of the PBMC/Antibody mixture into a non-monocyte population (positive selection) and the isolated monocyte population (negative selection) into separate Falcon tubes.

3.2.2.10   Isolation of CD16^{pos} Monocytes

Isolation of CD16^{pos} monocytes was performed from PBMCs in a 2-step immunomagnetic procedure. Firstly, PBMCs were isolated from whole blood by density gradient centrifugation and cell number was determined using the automated cell counter. The cells were centrifuged at 400g for 5 mins to form a pellet which was re-suspended in 300μl of PBS per 10^8 cells. To this 100μl of FcR Blocking Reagent and 100μl of Non-Monocyte Depletion Cocktail were added per 10^8 cells. The non-monocyte depletion cocktail contains antibodies to CD15 (granulocytes) and

---

[21] Exact composition of this reagent is proprietary

CD56 (natural killer cells). The mixture was briefly vortexed to ensure mixing and incubated for 15 mins at 4-8°C and then run through the AutoMACS Pro separator on a 'DEPL 05' programme to collect the unlabelled fraction. This was centrifuged at 300G for 10 mins to pellet the cells which were re-suspended in 400μl of PBS. 100μl of CD16 microbeads were added, mixed and incubated for 15 mins at 4-8°C. This mixture was run through the AutoMACS Pro on a 'POSSELD2' programme and the positive fraction was collected.

3.2.2.11 Isolation of CD16^{neg} Monocytes

Isolation of CD16^{neg} monocytes was performed in a 2-step immunomagnetic separation procedure. Firstly, PBMCs were separated by from whole blood by density-gradient centrifugation following which, monocytes were isolated by negative immunomagnetic separation. These isolated monocytes were centrifuged at 300g for 5 mins and the resultant pellet of cells was re-suspended in 400μl of PBS. 100μl of CD16 microbeads were added, mixed and incubated for 15 mins at 4-8°C. This mixture was run through the AutoMACS Pro automated cell separator on a 'DEPLETES' programme and the negative fraction was collected.

3.2.3 Culture of Monocyte-Derived Macrophages

Peripheral blood mononuclear cells were re-suspended in RPMI-1640 (Sigma-Aldrich, UK) at a concentration of 1.0×10^6 cells/ml. For every well in a non-coated 24 well culture plate (Corning Costar 3524, Sigma-Aldrich), 1ml of the cell suspension was added and incubated for 2 hours at 37°C, 5% CO_2. Following this, the medium was gently aspirated, and the cells washed a total of 5 times by gentle addition and aspiration of 500μl per well of RPMI-1640 to remove residual non-adherent lymphocytes. The adherent monocyte/macrophages were subsequently cultured in Macrophage serum-free media (M-SFM) with l-glutamine supplementation (Gibco, UK) without exogenous antibiotics. M-SFM was supplemented with recombinant macrophage-colony stimulating factor (M-CSF) (Miltenyi Biotec, UK) at a concentration of 50ng/ml. 1000μl of M-CSF supplemented media was added to each well and incubated for 24hrs at 37°C, 5% CO_2. On day 1, 4 and 7 of culture, the media was replaced with freshly prepared M-SFM supplemented with 50ng/ml M-CSF.

3.2.4   Cellular Imaging

3.2.4.1 Staining of Monocyte-Derived Macrophages

Fixation and staining of MDMs were performed in-situ in a 24-well plate by adding 400µl of 4% w/v PFA to each well of cells and left to incubate at 4-8°C for 10 mins. The cells were then washed with 400µl of PBS before a second fixing step was performed by adding a further 400µl of PFA for a further 10 mins at 4-8°C. Then, 200µl of a fresh working solution of Nile Red, prepared daily as described earlier, was added to each well and incubated in the dark at room temperature for 20 mins. The cells were washed twice in PBS and finally re-suspended in 500µl of PBS. For identification of the cell nucleus, a stock solution of 4'-6'-diamidino-2-phenylindole (DAPI) (Sigma-Aldrich, UK) was prepared at 1mg/ml in PBS and added to a working solution of Nile Red in a 1:5000 dilution. To each well of a 24-well plate, 200µl of the Nile Red/DAPI solution was added following two fixing steps with PFA, as outlined above, and incubated for 20 mins at room temperature in the dark. The cells were washed in PBS and finally re-suspended in 200µl PBS for fluorescent imaging. Foam cells were defined as those cells with ≥10 discreet intracellular lipid droplets. Both the number of foam cells and the average number of droplets per cell were calculated.
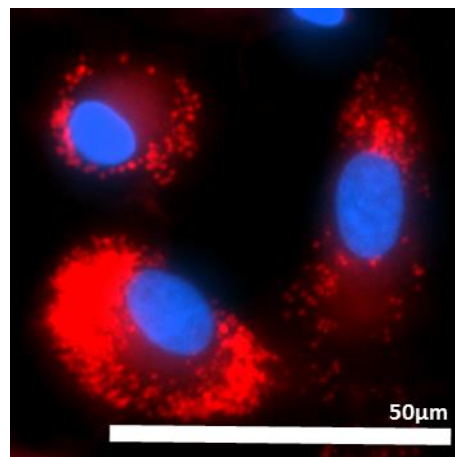
Figure 3.2: Fluorescence Microscopy of Monocyte-Derived Macrophages. Image is representative of macrophages cultured in 7 days in serum-free media supplemented with 50ng/ml M-CSF. Cells were stained with Nile Red and DAPI nuclear counterstain, as per the protocol, and image using EVOS fluorescent microscopy. Multiple intracellular droplets are shown characteristic of foam cells.

3.2.4.2 Staining of Platelets

Isolated platelets (either PRP or Washed Platelets) were centrifuged at 600g for 5 mins to form a pellet which was re-suspended in 250μl of diluent C (Sigma-Aldrich, UK). This was diluted by the addition of 125μl of the cell-suspension to a further 123μl of diluent C and 2μl of PKH67 dye (Sigma-Aldrich, UK). This was incubated on slow rotation for 5 mins at 37°C after which 50μl of 10% Bovine Serum Albumin (Sigma-Aldrich) was added and incubated for a further 5 mins in the dark at room temperature. To remove excess dye, the stained platelets were supplemented with freshly prepared PGI$_2$ to a final concentration of 200ng/ml and placed within a centrifuge at 600g for 5 mins at room temperature. The supernatant was aspirated, and the pellet was re-suspended in 1ml of HBS supplemented with further, freshly prepared, PGI$_2$ (200ng/ml) and placed in a centrifuge again (600g for 5min). This step was repeated a total of 2 times and the PKH67-stained platelet pellet was finally re-suspended in 1ml of HBS for downstream applications.

3.2.4.3 Light Transmission Microscopy

Cultured cells were imaged using an EVOS FL fluorescent microscope (AMG, Fisher Scientific). Plating densities were standardised to $1x10^6$/ml in either 24-well plates or 6-well chamber slides unless otherwise specified. Intensity and contrast were adjusted to give the best image and the individual settings were kept constant for the remainder of the samples. Fluorescent images were captured using separate filters for DAPI (nucleus staining – ex (357/77)/em-(447/60)), GFP (ex-(470/22)/em-(510/42)) and RFP (ex-9531/40)/em-(593/40)).

3.2.4.4 Intracellular Staining

$1x10^6$ cells were pelleted at 600g for 5 mins. The cells with re-suspended in 500μl of PBS/0.2% v/v TWEEN (Sigma) for 10 mins and then pelleted at 600g for 5 mins. The cells were re-suspended in 50μl of PBS/0.5% BSA and incubated with primary antibodies for 30mins at room temperature. The cells were then fixed with 450μl of 0.2% Formyl Saline for downstream applications.

3.2.4.5 Confocal Microscopy

Imaging of cultured MDMs was performed using an Olympus FV1000 confocal microscope. Monocyte-derived macrophages, cultured in 8-well chamber slides (Lab-Tek) for up to 7 days were stained with Nile Red and DAPI as previously described, washing twice with PBS after staining. The supernatant was aspirated and the partitions between wells were removed according to the manufacturer's protocol, to leave the slide bare. A small drop of prolong gold antifade mountant (ThermoFisher Scientific) was added onto the slide and covered with a

coverslip taking care to ensure that bubbles were extruded from the preparation. The slide was sealed with nail varnish and ready for confocal imaging.

3.2.5 Flow Cytometric Methods

Flow cytometry was used to identify and quantify cells as well as measuring the level of expression of cellular antigens. All experiments were performed using a Gallios®, 10-colour flow cytometer (Beckman-Coulter, UK) which was calibrated on a daily basis using Flow-Check and Flow-Set beads (Beckman Coulter). The optimum cell concentrations for all sample suspensions were determined by running samples at different concentrations until the optimum event rate was reached. Additionally, all antibodies were titrated to determine the optimum concentration. Directly-conjugated antibodies were used for all assays and fluorochromes were chosen with minimal overlap spectra. Colour compensation was carried out using single labelled samples, Negative controls were used for all experiments and set at 2% positive and consisted of nonspecific isotype control antibodies.

3.2.5.1 P-selectin

This assay was used to quantify expression of P-selectin on the surface of platelets as a marker of platelet degranulation. In LP3 flow cytometry tubes, 2µl of anti-human P-selectin-FITC (BD Pharmingen, UK) or 2µl of IgG-FITC isotype control was added to 50µl of HBS. To this 5µl of sample (Whole Blood, PRP or PBMC as appropriate) was added, mixed gently, and incubated at room temperature for 20 mins. The samples were then diluted with 450µl of 0.2% (w/v) Formyl Saline and left to incubate for 10mins at room temperature before diluting 1:10 with a further 450µl of 0.2% (w/v) Formyl Saline ready for flow cytometry.
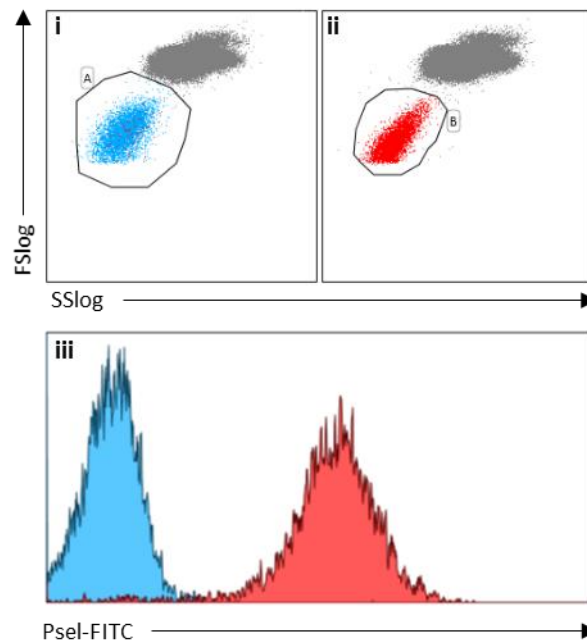
Figure 3.3: Representative Histogram of P-selectin Assay. Plots (i) and (ii) show forward (FS) and side scatter (SS) signals of whole blood from resting and CRP-activated samples respectively, prepared as detailed above (Paragraph 3.2.5.1), plotted on a logarithmic scale. There is an appreciable shape change, as reflected by SS and SS plots, when comparing CRP-activated (red) to resting platelets (blue). Activation is recorded in the overlay histogram (iii) showing the fluorescence of P-selectin from platelets gated from both blue gate A (quiescent) and red gate B (activated). There is a clear and demonstrable shift in the fluorescence intensity of surface P-selectin upon activation.

3.2.5.2 Monocyte-Platelet Aggregate Assay

This assay was used to quantify the proportion of monocytes with adherent platelets. LP3 tubes were prepared with 50µl of HBS and fluorochrome-conjugated antibodies to leucocyte and platelet antigens. To each tube, 5µl of anti-CD45-PerCPVio700, 3µl of anti-CD14-VioBlue and 1µl of anti-CD42b-PE was added. Negative isotype controls were also set up with LP3 tubes containing IgG2a-PerCPVio700 for CD45, IgG2-VioBlue for CD14 and IgGκ-PE for CD42b. To the HBS/antibody mixture, 50µl of sample was added, mixed and incubated for 30 mins at room temperature. Following this, erythrolysis was performed with the addition of 1ml of Versalyse lysis solution (Beckman Coulter, UK). This was briefly vortexed to mix the sample and incubated for a further 20 mins at room temperature. The samples were then run through the flow cytometer within 1hour of preparation. Monocytes were identified based on typical Forward and Side Scatter properties in addition to CD45 and CD14 expression. Monocyte-Platelet aggregates were identified as those monocytes that co-expressed the CD42b antigen and expressed as a proportion of all monocytes.
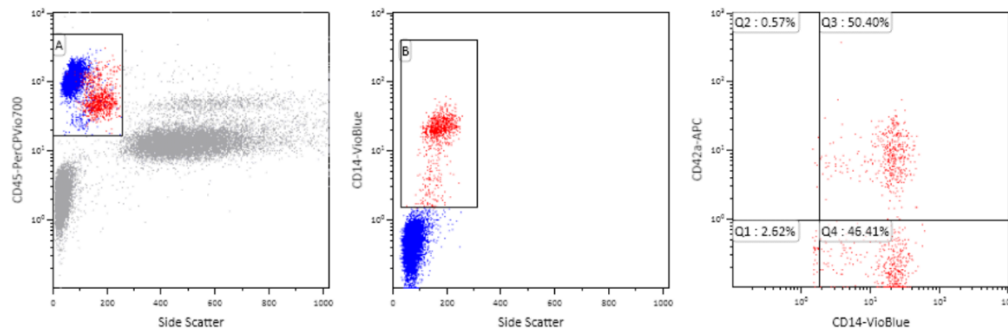
Figure 3.4: Representative Flow Cytometry of Monocyte-Platelet Assay. Panel of the left shows a plot of CD45-PerCPVio700 (y-axis) against Side Scatter (x-axis). Cells highlighted in box A include the mononuclear cells comprising lymphocytes and monocytes. Excluded from the box are the platelets (below) and the granulocytes which exhibit a large SS signal. The middle panel is gated from A and shows the separation of mononuclear cells based on the expression of surface CD14-VioBlue (y-axis). The CD14^{pos} cells were gated (gate B), the lower border of which was determined by an isotype control. The panel on the right includes all events within gate B and is a plot of CD42-APC (y-axis) versus CD14-VioBlue (x-axis). Cells are split into 4 quadrants and the proportion of cells within Q3 are the proportion of monocytes with adherent platelets i.e. monocyte-platelet aggregates.

3.2.5.3 Detection of Cellular DNA Content by Flow Cytometry.

Cells were prepared in PBS to a concentration of 2.5×10^6/ml. To 500μl of cell suspension, 2mls of ice cold 70% (v/v) ethanol was added and incubated on ice for 60 mins. The cells were then incubated overnight at 4°C in the fridge. Cell were centrifuged at 1200rpm for 5 mins and the supernatant was discarded. Cells were washed with PBS with a further spin at 1200rpm for 5 mins and the pellet was re-suspended in 800μl PBS. To this, 100μl of RNAase (20mg/ml) (Sigma Aldrich, UK) and 100μl Propidium Iodide (50μg/ml) (Sigma Aldrich, UK) was added and incubated for 30mins. The cells were spun for a final time at 1200rpm for 5 mins and re-suspended in 500μl of buffer for flow cytometry. Cells were identified based on Forward Scatter (FS) and Side Scatter (SS) properties. Fluorescence of propidium iodide was recorded in the FL3 channel as both peak impulse height (PH) and peak impulse area (PA) to exclude doublets from analysis. The percentage of cells in each phase of the cell cycle was quantified using a histogram of FL3-PA.
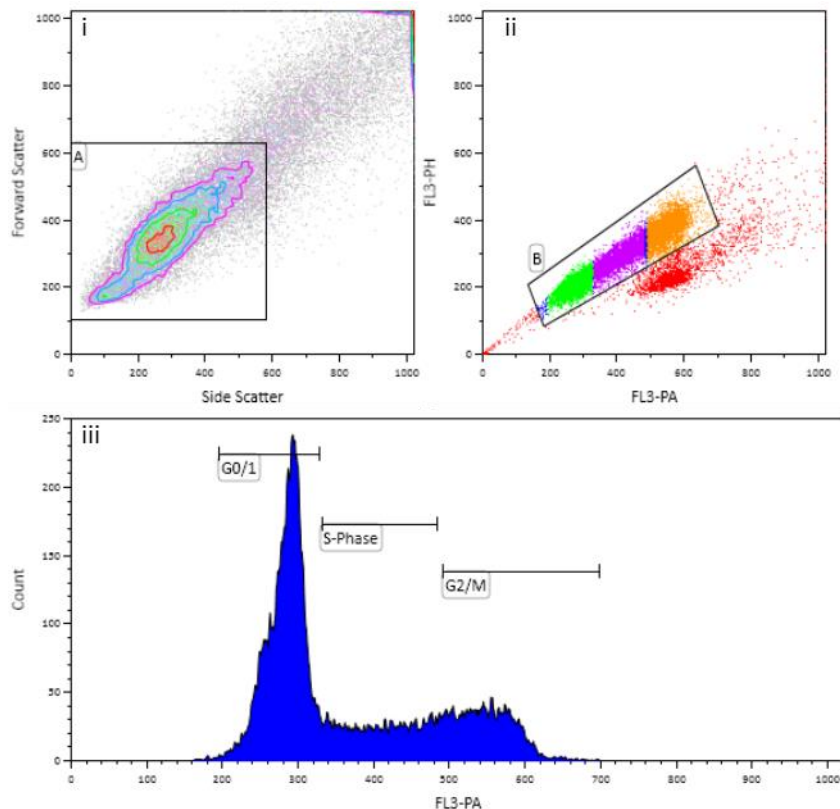
Figure 3.5: Flow Cytometric Quantification of Cell Cycle. Graphs show representative flow cytometry of THP-1 cells stained with propidium iodide as outlined above (3.2.5.3). (i) shows a Forward Scatter (y-axis) vs Side Scatter (x-axis) contour plot of prepared THP1. Gate 'A' has been drawn around to encompass these cells and to exclude cellular debris. (ii) shows a plot of propidium iodide staining (in the FL3 channel) measures by other pulse height (FL3-PH) and pulse area (FL3-PA). Doublets were excluded (red events) and singular THP-1 cells were gated. (iii) is a histogram of all gated cells 'B' and demonstrates the proportion of cells within the G0/1, S or G2/M phases of cell cycle.

3.2.5.4 Quantification of Lipid Droplet Formation in Whole Blood

Whole blood (50µl) was mixed with 50µl of HBS in LP4 flow cytometry tubes and erythrolysis and fixing was performed by adding 500µl of Optilyse C® lysis solution (Beckman-Coulter, UK) which contains 1.5% formaldehyde. The solution was briefly mixed by vortex and incubated for 20 mins at room temperature until the solution became clear. 5µl of the Nile Red working solution was added to each sample tube and incubated for a further 20mins at room temperature in the dark. A washing step was performed by adding 1-2mls of PBS to each sample followed by centrifugation at 400g for 5mins. The supernatant was discarded, and the pellet was re-suspended in 500µl of PBS in LP4 tubes suitable for flow cytometry.
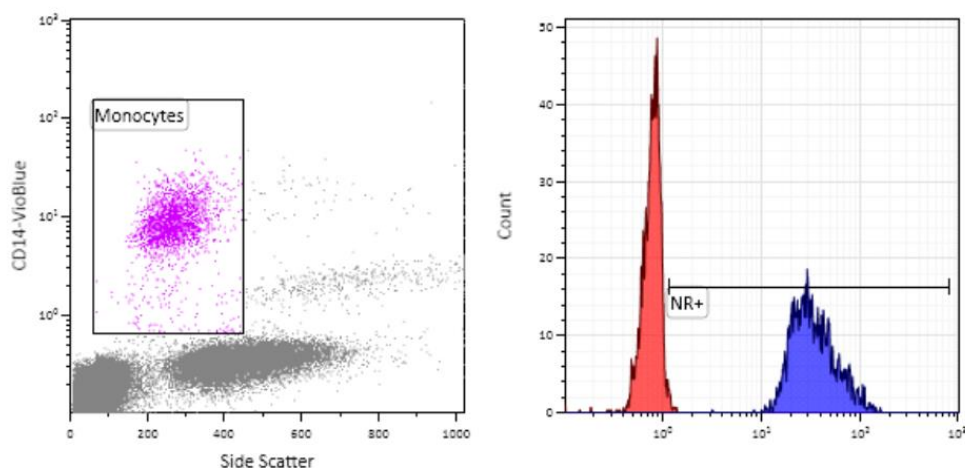
Figure 3.6: Representative Flow Cytometry of Whole Blood Nile Red Assay. Monocytes were gated (left hand panel) based on Side Scatter and CD14 fluorescence. A representative overlay histogram is shown (right hand panel) showing Nile Red fluorescence (in the FL3 channel) of stained, resting monocytes (red histogram) and CRP-activated monocytes following 24 hours of incubation (blue histogram). Both the median fluorescence intensity and the percentage of monocytes staining for Nile Red can be calculated.

3.2.5.5 Quantification of lipid droplet staining in cultured monocyte-derived macrophages

Monocyte-Derived Macrophages in culture were stained with Nile Red. These cells were scrapped using a rubber-tipped syringe and the cell suspension was aspirated into LP4 tubes for flow cytometry. Cells were identified by FS and SS properties and the fluorescence of Nile Red was quantified in the FL3 channel. Baseline fluorescence (autofluorescence) was set using unstained MDMs and voltages were adjusted so that this remained within the 1st log decade. Both the percentage of cells positive for Nile Red staining and median fluorescence intensity of those cells were recorded.

Stained MDM were scrapped from wells using a 2ml rubber-tipped syringe and the cell suspension was aspirated into LP4 tubes for flow cytometry. Cells were identified by Forward and Side Scatter and the fluorescence of Nile Red was quantified in the FL3 channel. Baseline fluorescence was set using unstained cells and voltages were adjusted so that this lied within the first log decade.
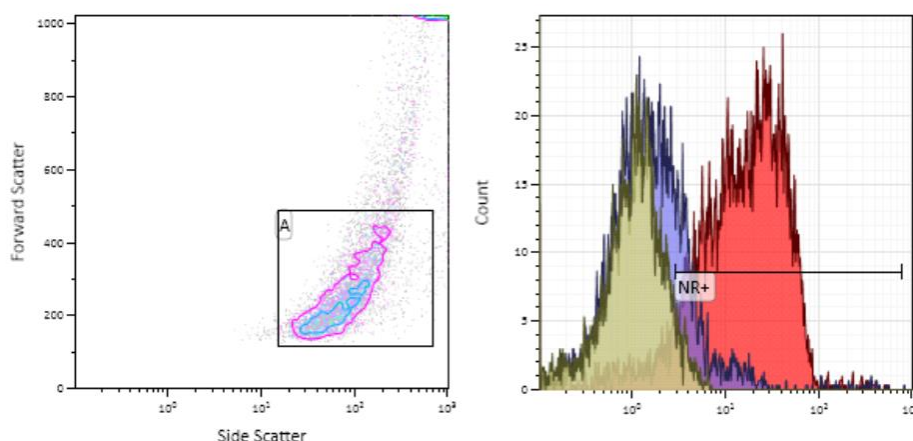
Figure 3.7: Representative Flow Cytometry of Macrophage Foam Cell Quantification. Prepared, cultured macrophages were gated (left panel) by forward and side scatter (plotted on a logarithmic scale). Nile Red Fluorescence was recorded in the FL3 channel as shown in the overlay histogram (right panel). Histograms are shown for un-activated (yellow) and CRP-activated MDMs (blue) following 24hrs of incubation. Fluorescence histogram is also shown for CRP-activated MDMs cultured for 5 days (red histogram). Both the percentage of cells staining for Nile Red and Median Fluorescence Intensity was quantified.

3.2.5.6 Quantification of Viability

Cell viability was assessed by flow cytometry based on the property of dead cells to readily take up Propidium Iodide staining. Cells were re-suspended in 1ml PBS at a concentration of 1×10^6 cells/ml. 50µl of propidium iodide (50µg/ml) was added and incubated for 5 mins at room temperature. Samples were centrifuged briefly (1200rpm for 5 mins) in a microfuge and re-suspended 500µl PBS for flow cytometry[22]. Cells were identified by FS and SS and fluorescence was recorded in the FL3 channel. Baseline fluorescence was set using unstained samples and all positively staining cells were classified as non-viable and expressed as a percentage of all viable cells.

3.2.5.7 Phenotyping of Monocytes by Flow Cytometry

This method was developed to classify monocytes based on CD14 and CD16 expression in both whole blood and isolated cellular preparations. LP4 flow cytometry tubes were prepared with 50µl of HBS along with 5µl of anti-CD45-PerCPVio700, 3µl of anti-CD14-VioBlue and 3µl of anti-CD16-APC. To the prepared tubes, 50µl of sample (either whole blood or isolated cells) were added, mixed and incubated for 30mins at room temperature. Fixation was performed with 500ml of Optilyse C lysis solution when using whole blood or with 500µl of 0.2% Formyl saline when using cell preparations. The solutions were mixed briefly and left to incubate at room

---

[22] Samples were analysed as soon as possible after preparation (within 10mins) as PI staining increases with increasing incubation times

temperature for a further 20mins after which it was ready for flow cytometry. Leucocytes were gated based on CD45 expression and monocyte subsets were identified by both CD14 and CD16 fluorescence.

3.2.6 Colorimetric Quantification of Cholesterol

Cholesterol was quantified in cultured monocyte-derived macrophages by a coupled enzyme assay using a Cholesterol Quantitation Kit (MAK043, Sigma Aldrich) as per the manufacturer's instructions. Cells were cultured in 24-well plates at a density of 1.0×10^6 cells per well. A cholesterol extraction solution was prepared using Chloroform, Isopropranolol and IGEPAL CA-630 (all reagents purchased from Sigma-Aldrich) at a ratio of 70:110:1. This solution was prepared in a glass tube, stored at room temperature and protected from light and 200µl was added to each well of a 24-well plate. The cells were macerated and scrapped using a pipette tip, and the solution was carefully aspirated into a 1.5ml Eppendorf tube and vortexed to thoroughly mix the sample. Samples were then centrifuged at 13,000g for 10 mins to pellet any insoluble material, and the organic supernatant was aspirated into a new Eppendorf tube. Samples were left to dry in an incubator set at 50-70°C for 1hr to remove excess chloroform followed by incubation for a further 30 mins in a vacuum concentrator (SpeedVac SPD1010, ThermoFisher Scientific) to remove any residual organic solvent. Dried lipids were dissolved with 100µl of cholesterol assay buffer (Sigma-Aldrich).

For the colorimetric assay, a Mastermix Reaction Buffer was prepared by mixing 44µl of Cholesterol Assay Buffer, 2µl of Cholesterol Probe, 2µl of Cholesterol Enzyme Mix and 2µl of Cholesterol Esterase for every sample due to be run. A 96-well flat-bottomed plate was used to which 20µl a prepared lipid sample was added to each well along with 30µl of the Mastermix Reaction Buffer. Samples were run in duplicate and a standard curve was performed for every plate using manufacturer-supplied, serially diluted cholesterol samples. Absorbance was measured at 560nm using an automated absorbance plate reader (Biotek ELS800) and cholesterol content in each of the sample wells were calculated based on the values obtained for the standard curve.

3.2.7 Molecular Biology Methods

3.2.7.1 RNA Extraction

Isolated cells were re-suspended in 1ml of TRIzol Reagent in an Eppendorf tube. To this, 200µl of Chloroform was added, shaken vigorously for 10-15 seconds in a vortex, and left to incubate at room temperature for 2-3mins. The samples were then centrifuged at 12000g at 4°C to separate the aqueous phase, which was then carefully transferred to a clean Eppendorf taking

care not to disrupt the interface. An equal volume of 70% Ethanol was added and mixed well by vortex. Up to 700µl of the mixture was added onto a RNeasy Mini spin column (Qiagen, UK) placed within a 2ml collection tube. The sample was centrifuged for 15secs at 8000g and the flow-through was discarded. The remainder of the sample was added to the spin column and centrifuged again at 8000g for 15secs. 700µl of RW1 buffer (Qiagen, UK) was added to the spin column and centrifuged at 8000rpm for 15secs. The flow-through was discarded and 500µl of RPE buffer was added to the spin column. The column was centrifuged at 800g for 15secs and the flow-through was discarded. A final further 500µl of RPE buffer was added to the spin column and centrifuged for 2mins at 8000g. The flow-through was discarded and the membrane was left uncovered to dry. The spin column was replaced in a new 1.5ml Eppendorf and 30-50µl of RNAse-free water was added directly onto the membrane. The sample was centrifuged for 1min at 8000g to elute the RNA.

RNA was quantified using a NanoDrop (Thermo Scientific). 1-2µl of sample was placed on the NanoDrop and the A230/260 ratio was recorded in addition to the concentration in ng/ml.

3.2.7.2 Reverse Transcription

Reverse transcription was performed using a recombinant murine leukaemia virus reverse transcriptase (MultiScribe™ RT) optimised for the TaqMan-based assay (Thermo Fischer Scientific) using a 0.2ml PCR reaction well. A mastermix was prepared comprising 2.0µl of 10x RT buffer, 1.5µl MgCl2, 4µl of 10mM dNTP mix, 1.0µl RNase inhibitor (20U/µl), 1.0µl MultiScribe RT (50U/µl), 4.6µl of DEPC-treated water and either 1.0µl of 50µM Oligo(dT)16 or 1.0µl of 50µM random hexamers per 20µl reaction. This was thorough mixed and 15µl of this was added to each 0.2ml PCR reaction well in addition to 5µl of RNA ensuring that all of the mixture was at the bottom of the well. A G-Storm Multi-Block thermal cycler was used under manufacturer-specified cycling conditions depending on if oligo(dT)16 or random hexamers were used in the PCR mixture. For oligo(dT)16 the cycle conditions were set at 65°C for 5mins, 4°C for 2mins, 37°C for 30mins and 95°C for 5mins. When using random hexamers, cycle conditions were set at 25°C for 10mins, 37°C for 30mins, 95°C for 5mins. The subsequent cDNA samples generated by the PCR were stored at -80°C until they were used for downstream applications.

3.2.7.3 Quantitative Real-Time PCR

All work was carried out in a clean cabinet designated for PCR and all work surfaces were cleaned with industrial methylated spirit (IMS) and RNAzap spray (Thermo Fisher) prior to use. All reactions were done using a MicroAMP Endura Optical 96-well Fast Clear Reaction Plates (ThermoFisher) with 20µl reaction volumes.

Prior to reach reaction, a mastermix was prepared in a sterile, irradiated 1.5ml Eppendorf according to the total number of wells used in the reaction. For every 20µl reaction, a mastermix was made by mixing 1µl of primer solution, 4µl of DEPC-treated water and 10µl of Taqman Fast Advanced MasterMix (ThermoFisher). To each well, 16µl of mastermix was added along with either 4µl of cDNA or 4µl of DEPC-treated water for the non-template controls. Each well was mixed gently by pipetting and tapped to ensure all of the mixture was at the bottom of the well. The plate was sealed with a MicroAMP Optical adhesive film (ThermoFischer) ensuring that there were no gaps. To ensure that all the mixture was at the bottom of the well, the plate was centrifuged at 1000rpm for 1min.

Quantification was performed using a ViiA7 Real-Time PCR machine using a 96 well block and 'FAST' conditions. The ViiA7RUO software was used to label the different wells of the PCR plate, set the dyes to read and also to enable the comparative CT method of quantification. The software was also used to set the thermal cycling conditions as follows; Fast ramp rate, Hold 50°C for 5mins, Hold 95°C for 20secs followed by 40 cycles of 95°C for 1sec and 60°C for 20sec.

Samples were repeated in triplicate and a mean Ct value calculated for each. All Ct values were normalised to an internal B2M control to give a ΔCt value. To quantify the effect of treatment on gene expression, ΔCt values were compared between treatment and control samples to give a ΔΔCt value. A $2^{-\Delta\Delta Ct}$ calculation was performed to give a fold-change expression and was used to quantify gene expression.

3.2.8 Platelet Function Testing

3.2.8.1 Impedance Aggregometry

Whole blood was collected into Hirudin anticoagulant (Roche) and left on slow rotation for a minimum of 30mins and no more than 2 hours after venepuncture. Platelet aggregation was measured using a Multiplate™ Impedance Aggregometer (Roche). Prior to use, the machine was allowed to come to temperature (37°C) and electronic controls were run. 0.9% NaCl solution was gently warmed in the incubation block prior to use as were the test reagents (ADP, ASPI & TRAP).
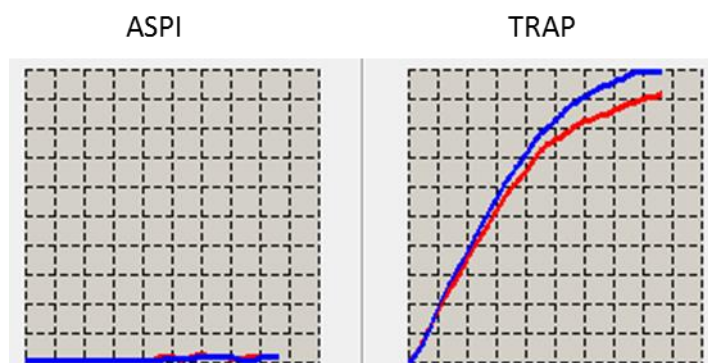
Figure 3.8: Representative Multiplate Aggregometer Trace from a Patient Taking Aspirin. Graphs show impedance traces (y-axis) over a 6-minute incubation period (x-axis) from 2 electrodes within each cuvette (red and blue). The coefficient of variance between the 2 electrodes should be <10% for the results to be valid. Increasing impedance is a surrogate marker for platelet aggregation and the aggregometry traces show blood activated with either arachiodonic acid (ASPI) or TRAP. There is no aggregation with ASPI as compared with a robust activation with TRAP.

To each test cuvette, 300µl of whole blood was added and mixed with an equal volume of 0.9% NaCl solution. This was incubated for 2mins in the incubation block before 20µl of either ADP (Adenosine diphosphate), ASPI (Arachiodonic Acid) or TRAP (Thrombin receptor activated peptide) test reagents were added to separate cuvettes. The impedance between the measuring electrodes was recorded over a 6-minute incubation period. Aggregation was quantified as the total area under the curve (AUC) for all three activating agents.

3.2.9 Statistical Methods

All data obtained from experimental work were collated in Microsoft Office Excel. Results are reported as mean±standard deviation unless otherwise stated. Statistical analysis was performed using PRISM software 5 (GraphPad Inc, California, USA). ANOVA was performed with Tukey's or Bonferroni's multiple comparison tests and all data was assumed to be parametric unless otherwise specified. Correlation was assessed by Spearman's rank correlation coefficient. Differences were considered significant (*) at $p < 0.05$, and very significant (**) at $p < 0.01$ or $p < 0.001$ (***).

Chapter 4: Development of Core Methods

4.1 <u>Introduction</u>

In order to address the stated hypothesis (Section 2.7), a robust method of monocyte isolation and culture of MDMs was developed. To study the effect of platelets on foam cell formation, a pure population of monocytes is required, free to platelet contamination, to be isolated from whole blood and cultured to generate MDMs. Blood from healthy volunteers is a readily accessible source of leucocytes but monocytes only comprise between 2-10% of all circulating leucocytes with most clinical laboratories setting the 'normal' range between $0.2\text{-}0.8\text{x}10^9$/L. Therefore, any method employed to isolate these cells, must also consider the yield obtained from any given sample.
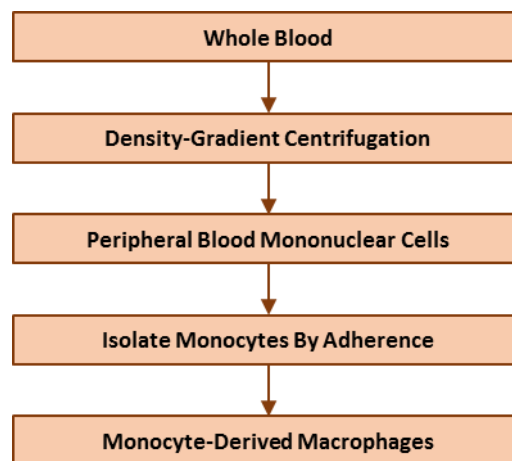
Figure 4.1: Overview of the 'Standard' Method of Isolating Monocytes and Culture into MDMs. From whole blood, PBMCs are separated by density-gradient centrifugation. Monocytes are then isolated from PBMCs, by their adherence to plastic plates, and cultured to become MDMs.

One of the most commonly used methods to obtain monocytes from whole blood relies on the principle of density-gradient separation of PBMCs and isolation of monocytes by adherence (**Davies and Gordon** *2005*). Density-gradient centrifugation is based on the principle that PBMCs have a lower buoyant density (<1.077g/ml) than other cellular components of blood (granulocytes and erythrocytes) (**Bennett and Cohn** *1966*). Therefore, centrifugation onto an isosmotic medium, with density greater than PBMCs but lower than other cellular components, permits erythrocytes and granulocytes to sediment through the medium, as PBMCs are retained to form a distinct layer at the plasma/medium interface (see **Figure 3.1**). Although viable and functional PBMCs are purified from this process, they are often contaminated with free platelets that have co-sedimented with the PBMCs, or through iatrogenic activation of platelets resulting in their adherence to monocytes and co-sedimentation in the PBMC layer. Nevertheless, the

main advantage of this technique is that functional PBMCs are purified, relatively rapidly, in a non-adherent state, which allows for the subsequent positive selection of monocytes based on adherence to plastic (**Bennett and Cohn** *1966*). The final purity and yield of monocytes are dependent on the type of surface to which cells adhere and the medium used (**Koller** *et al.* *1973*). Various surfaces have been used to isolate and purify human monocytes from PBMCs by adherence. These have included glass, tissue culture-treated plastic cytodex microcarriers and extracellular matrix components such as fibronectin and gelatin. Tissue culture-treated plasticware is perhaps the most commonly used adherence surface but often favours the adherence of other mononuclear cells. It has been shown that as much as 25% of the remaining cells within 24hrs of culture of PBMCs are lymphocytes despite four vigorous washes (**Bennett** *et al. 1992*). These contaminating lymphoid cells can be reduced to approximately 19%, with preservation of monocyte viability and function, when untreated plastic products were used (**Bennett et al.** *1992*). However, after 48 hours in serum-free culture, contaminating cells are substantially reduced (1-2%) on both tissue culture-treated and untreated plastic surfaces. Although adherence is a simple, straightforward method for purifying monocytes, it has some other disadvantages. Adherence is a known activation signal for monocytes, albeit transient, with prompt restitution to the resting state (**Shaw** *et al. 1990*). There are also difficulties in detaching the monocytes for further studies. For instance, mechanical detachment with a rubber policeman can result in cell damage, and chemical methods, using for example EDTA and trypsin, are known to modify cell function (**Nielsen** *1987*). This is because many of the cell surface receptors are calcium-dependent and therefore disrupted by EDTA or cleaved by trypsin.

This 'standard' method will be explored and optimised in this chapter to isolate a pure population of monocytes, with minimal iatrogenic activation and platelet contamination, so that both monocyte phenotype and foam cell formation can be studied to address the stated hypotheses.

4.2   The Isolation of Monocytes from Whole Blood

4.2.1   Evaluation of Different Density-Gradient Methods on the Isolation of Peripheral Blood Mononuclear Cells from Whole Blood

A number of different density-gradient media have been used in the isolation of cellular components of blood. A comparison was made of Ficoll, Nycoprep and Percoll. Ficoll-Hypaque contains sodium metrizoate 9.1% (w/v) and polysaccharide 5.7% (w/v) adjusted to a density of 1.077g/ml allowing for a single-step centrifugation of whole blood to obtain PBMCs (**Boyum** *1968*). Nycoprep contains a non-ionic, iodinated Nycodenz (in place of the sodium metrizoate in Ficoll) and allows for a single step centrifugation from whole blood to give PBMCs (**Boyum** *1983*). Importantly, Nycoprep does not contain any polysaccharide and, in particular, mitogenic lectins (e.g. phytohaemagglutinin and concanavalin A) that have been shown to induce activation of PBMCs in *in-vitro* models (**Ashraf and Khan** *2003*), therefore offering an advantage over Lymphoprep. Percoll consists of colloidal silica particles (23% w/v) coated with polyvinylpyrrolidone and has been used in the preparation of cells, subcellular particles and large viruses (**Pertoft** *et al. 1978*). This density gradient medium is diluted with an inert buffer to generate a continuous density gradient medium suitable for the 2-step separation of monocytes from PBMCs, following their initial isolation by Ficoll centrifugation (**de Almeida** *et al. 2000*). The putative advantage of this technique is that, as Percoll can be adjusted in both density and osmolality, it allows for the more specific separation of monocytes *per se* as opposed to PBMCs.

Single-step density-gradient centrifugation of whole blood using either Lymphoprep or Nycoprep; or double-step centrifugation employing Percoll were compared for their ability to isolate monocytes and PBMCs with respect to purity and yield. Blood samples (45mls) were taken from healthy volunteers (n=3) into 3.2% trisodium citrate and separated into three equal aliquots from which PBMCs were isolated by all three methods in parallel. For the determination of yield and purity, a Full Blood Count (FBC) was performed by automated cell counter which determined the concentration of leucocytes (WCC $\times 10^6$/ml) in both whole blood and mononuclear cell isolates. Additionally, the proportion of CD45^{pos} leucocytes, that co-expressed the CD14 antigen, was quantified by flow cytometry in both whole blood and leucocyte isolates and expressed as the percentage purity of monocytes. Using these two values, the concentration of monocytes (in either whole blood or leucocyte preparations) was calculated as follows:

$$\text{Monocyte Count } (\times 10^6/\text{ml}) = \text{Monocyte Purity (\%)} \times \text{White Cell Count } (\times 10^6/\text{ml})$$

For the determination of yield, the total number of monocytes within the leucocyte preparation of interest was calculated by multiplication of the monocyte count (as determined above) by the total volume of sample in question. The number of monocytes in the original starting volume of whole blood, used for subsequent isolation, was also determined similarly and the ratio of these two values was expressed as a percentage yield:

$$\text{Yield (\%)} = \frac{\text{Monocyte Count in Sample } (\times 10^6/\text{ml}) \times \text{Volume of Sample (ml)}}{\text{Monocyte Count in Whole Blood } (\times 10^6/\text{ml}) \ \times \text{Volume of Blood (ml)}} \times 100$$
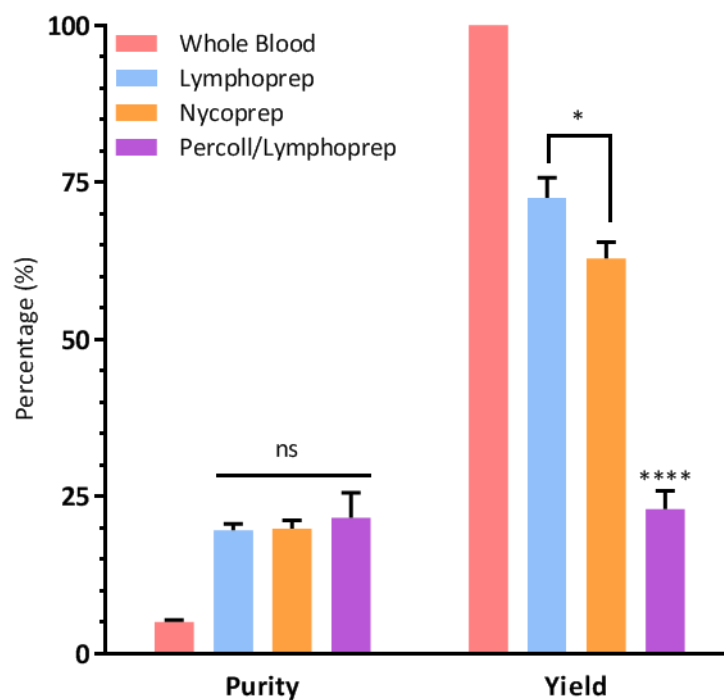
Figure 4.2: Purity and Yield of Monocytes with Different Density-Gradient Isolation Methods. Graph shows yield of monocytes in PBMC preps isolated by Lymphoprep (blue), Nycoprep (yellow) and double density-gradient (purple) centrifugation. Lymphoprep separation gave the highest yield of monocytes which was significantly more than both Nycoprep and Percoll (p<0.05). Separation using Percoll/Lymphoprep offered the lowest yield of monocytes (~23%, p<0.0001). There was no significant difference in the purity of isolated monocytes using different density-gradient media (p>0.05). Bars show mean±SD; *=p<0.01, ****=p<0.0001, ns=non-significant.

Monocytes in whole blood accounted for 5.0±0.3% of all leucocytes. In PBMCs isolated using Lymphoprep density-gradient centrifugation, 19.6±1.0% of leucocytes were identified as monocytes with comparable figures in Nycoprep and double density gradient-derived PBMCs. Monocyte purity ranged from 19.6±1.0% to 21.6±4.00% in the PBMCs isolated using the different density-gradient methods but there were no significant differences overall (p=0.60, ANOVA). There were significant differences in the yield of monocytes within the leucocyte

preparations obtained using the different isolation methods (p<0.0001). The best yield of monocytes was given by density-gradient centrifugation with Lymphoprep (72.5±3.2%) which was significantly more (p=0.0069) than isolating monocytes using Nycoprep (62.9±2.6%). Double-density gradient gave a much lower yield of 23.0±2.9% (p<0.0001).

4.2.2 Immunomagnetic Bead Isolation of Monocytes

Monocytes can also be specifically isolated from both whole blood and PBMCs using immunomagnetic beads. This method is based on the principle that small, magnetic particles can attach to cells via antibodies or lectins. When the mixed population of cells is placed in a magnetic field, those cells with adherent beads will be attracted to the magnet and may be separated from unlabelled cells. Several manufactured beads are available, some of which are designed specifically for cell sorting and other that are designed for purifying molecules (particularly nucleic acids) that may be adapted for cell sorting if necessary. They all work on the same principle, but the strength of the magnetic field required to separate the cells differs depending on the size of the beads. The larger beads (>2μm), although commonly used, are not suitable for every type of cell because they have been shown to strip antigens from the cell surface (**Manyonda *et al.* 1992**). Furthermore, due to their size, steric interference may, disrupt studies of cell-cell interactions, their attachment to culture surfaces and render them more difficult to use during analysis by flow cytometry. Smaller beads, such as those produced by the MACS system (Miltenyi Biotec), consist of iron oxide and polysaccharide and are approximately 50nm in diameter. In contrast to the larger beads, they are not internalised by cells, do not interfere with adhesion and are more suitable for analysis by flow cytometry (**Plouffe *et al.* 2015**). As isolated monocytes will be required for downstream applications including cell culture, the smaller magnetic microbeads were evaluated.

In addition to positive selection, cells may also be separated using the 'negative selection' method. In this case, all unwanted cell types are immunomagnetically labelled, a process that often requires a cocktail of antibodies depending on the mixture of cells from which to isolate the cell of interest. The labelling procedure is the same as for positive sorting except it is the unlabelled fraction that is retained, and the labelled cells are discarded. The advantage with this technique is that the cell of interest, in this case monocytes, are 'untouched' by beads and therefore experimental manipulation is kept to a minimum. A further consideration, and particularly pertinent to monocytes, is the preservation of heterogeneity found *in-vivo* within the circulation. In order to develop a representative *in-vitro* model, isolated monocytes should retain this heterogeneity as much as possible. Monocyte subsets may be classified based on the

level of expression of CD14 and positive selection may therefore exclude the lower expressing monocytes.

4.2.2.1 Method

Monocytes were isolated using two complimentary methods, both based on immunomagnetic bead separation, that positively select CD14^{pos} monocytes either directly from whole blood or from PBMCs. Blood (18mls) was collected from healthy volunteers (n=3) into citrate and split into two equal aliquots of 9 ml. One aliquot was mixed with 450µl of Whole Blood CD14 Microbeads and incubated for 15 mins at 4-8°C. The second aliquot was diluted with an equal volume (1:1) of PBS and carefully overlayed onto Lymphoprep for density-gradient isolation. The isolated PBMCs were incubated with CD14 microbeads and CD14^{pos} monocytes were isolated by positive selection using an automated cell separator as per the manufacturer's instructions (methods 3.2.2.8). Monocytes were also isolated by negative immunomagnetic separation. Blood from healthy volunteers (n=3) was used to separate PBMCs following which they were incubated with a Fc-blocking antibody and a biotinylated antibody cocktail against non-monocyte antigens (Pan-Monocyte Isolation Kit). Cells were separated as per the manufacturer's protocol (see methods 3.2.2.9) following which all the isolated cells were analysed to calculate purity and yield as well as the quantification of surface expression of CD16 on CD14^{pos} monocytes.

4.2.2.2 Results

Monocytes accounted for approximately 5% of the circulating leucocytes in the original blood samples but consistently constituted >90% in the isolated cellular fractions. The monocyte purity in the preparations isolated by negative selection were 95.6±3.3%, which was comparable (p=0.46) to the purity of monocytes isolated by positive selection from PBMCs (97.4%±1.7%). Isolating monocytes by positive selection directly from whole blood gave a slightly lower purity of monocytes (91.7±5.0%) but this was not statistically significant (p>0.05).

Similarly, there were no significant differences in the yield of monocytes obtained with either positive or negative selection methods (p>0.05). In addition to yield and purity, the proportion of monocytes that express the CD16 antigen were quantified on all isolated preparations (Figure 4.3). Expression levels were low (<5%) on positively- selected cells from both PBMCs (2.6±0.3%) and cells isolated directly from whole blood (2.7±0.5%), which was not significantly different (p>0.05, t-test). However, monocytes isolated by negative selection expressed a significantly higher (p=0.0002, t-test) proportion of cells expressing CD16 (11.3%±2.1%) than either of the positive selection methods.
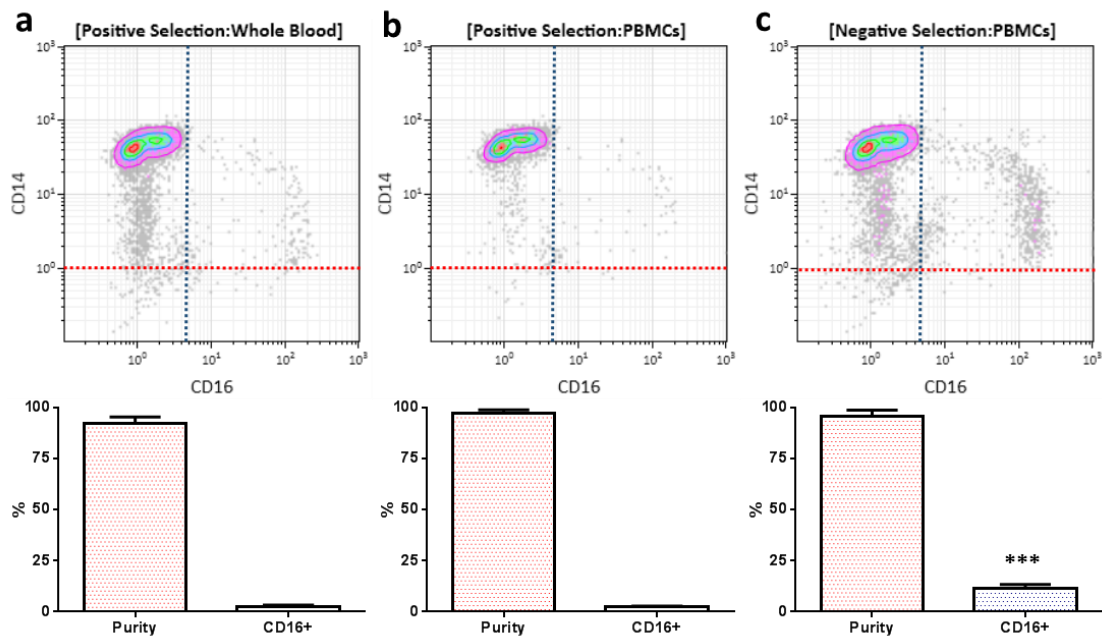
Figure 4.3: Monocyte Purity and Heterogeneity with Positive and Negative Immunomagnetic Separation. Figure depicts representative density and contour plots (CD14 vs CD16) of monocytes isolated by both positive and negative selection methods. Graph depicts both the purity of monocytes (as a percentage of all CD45^{pos} events) and percentage of monocytes that were CD16^{pos}. Representative histograms and collated data (n=3) is shown for cells isolated by positive selection direct from Whole Blood (a), positive selection from PBMCs (b) and negative selection from PBMCs(c).

4.3 Minimising Platelet Contamination

The combination of density-gradient centrifugation and immunomagnetic separation of monocytes rely on both their size and surface immunogenicity. However, current methods do little to minimise the contamination of leucocyte preparations with platelets. Platelets are the most abundant (150-450 x10^9/L) non-erythroid circulating cell and readily form aggregates with circulating monocytes. Therefore, in a preparation of isolated monocytes, platelets often co-segregate either as free, unbound platelets or as MPAs. A method was therefore sought to minimise platelet contamination and iatrogenic platelet activation.

4.3.1 Effect of PRP Removal Prior to Density-Gradient Centrifugation on Residual Platelet Counts and Activation in PBMCs

Blood was collected from healthy volunteers (n=3) into 3.2% sodium citrate and centrifuged at 160g for 20 mins. The resultant supernatant (PRP) was aspirated and the platelet-depleted blood was re-constituted with an equal volume of PBS/5mM EDTA. This was further diluted 1:1 with PBS/5mM EDTA and layered onto Ficoll density gradient medium and centrifuged to separate

PBMCs. This method was compared to isolated PBMCs from whole blood without an initial PRP-removal step. Platelets counts were quantified by automated cell counter and the activation of platelets was quantified by flow cytometry using a P-selectin assay (methods 3.2.5.1).
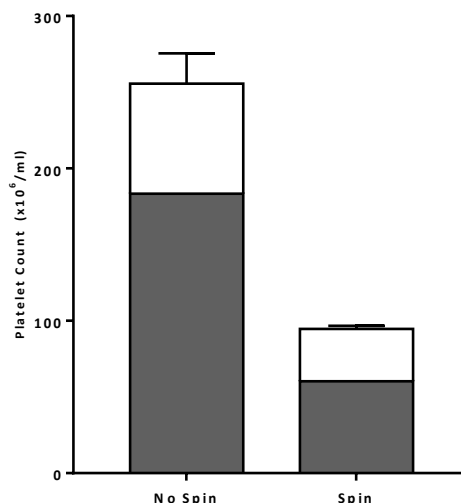
Figure 4.4: Platelet Contamination in PBMC Preparations. Graphs depicts mean±SD of platelet count (x10^6/ml) in PBMCs isolated by density-gradient centrifugation both with (Spin) and without (No Spin) an initial centrifugation to decant PRP. The addition of an initial spin significantly decreased the number of contaminating platelets in a preparation of PBMCs (p<0.05, n=3). Also shown is the activation state of platelets. The grey shaded area denotes the proportion of platelets in the 'Spin' and 'No Spin' groups that express surface P-selectin. Bars denote mean ±SD

In both sets of PBMCs preparation, the presence of contaminating platelets could be detected both by automated cell counting and by flow cytometry. The addition of a PRP removal step prior to density gradient centrifugation led to a significant (p=0.0419, t-test) decrease in the presence of contaminating platelets (94.7±5.7 x 10^6/ml vs 255.7±54.2 x 10^6/ml). When platelet P-selectin expression was measured by flow cytometry, there was no significant difference in the proportion of contaminating platelets that expressed surface P-selectin (65.6%vs 64.1% p>0.05).

4.3.2 Effect of CD61-immunomagnetic bead separation on residual platelets in a leucocyte preparation

Immunomagnetic bead separation methods can also be employed to deplete platelets from a preparation of PBMCs using an antibody directed at platelet-specific surface antigen such as CD61 (see **Table 9.3**). Whole blood from healthy volunteers (n=5) was collected into 3.2% trisodium citrate and centrifuged at 160g for 20 mins. The PRP supernatant was aspirated and the remaining platelet-poor blood was reconstituted with PBS/5mM EDTA equivalent to the volume of PRP removed, diluted a further 1:1 and layered onto Lymphoprep for density-gradient

separation. The PBMCs were incubated with either anti-CD61 microbeads (20µl per 10^7 leucocytes) or a vehicle control (20µl of PBS/0.1%BSA/0.01% Sodium Azide) for 15 mins at 4-8°C. PBMCs were then run through an automated cell separator to collect the negative fraction (see methods 3.2.2.7).

Numbers of residual platelets were quantified in the PBMCs preparation by automated cell counting in addition to flow cytometric quantification of platelet activation markers including P-selectin expression and MPA formation. Additionally, PBMCs were re-suspended in RPMI and allowed to adhere onto plastic 24-well plates for 2 hrs. Monocytes were isolated by adherence and viewed under light microscopy to visually confirm the presence of MPAs.

CD61 immunomagnetic depletion led to a significant reduction (p=0.0231, t-test) in the numbers of residual platelets in the PBMCs from 183.2±144.6 $x10^6$/ml to 2.0±0.4 $x10^6$/ml. This was confirmed by flow cytometry as the number of CD42b^{pos} events fell by >99% (p<0.0001, t-test). In non-depleted samples, P-selectin was expressed on 75.13±12.11% of residual platelets. This was not significantly different to the levels of P-selectin expression on residual platelets in the CD61-depleted samples (56.4±36.4%, p>0.05, Welches t-test[23]) There were however no significant differences in the proportion of platelets that expressed the P-selectin antigen (p>0.05, t-test). CD61 depletion also led to a significant reduction in the proportion of monocytes with adherent platelets. Without an initial CD61 depletion step, 18.47±2.18% of monocytes had adherent platelets which fell significantly (p<0.001, t-test) to 1.64±0.51% following bead depletion (p<0.001, t-test).

---

[23] Numbers of platelets were significantly lower in the CD61-depleted samples and therefore there were unequal variances in P-selectin expression when comparing the depleted and non-depleted samples
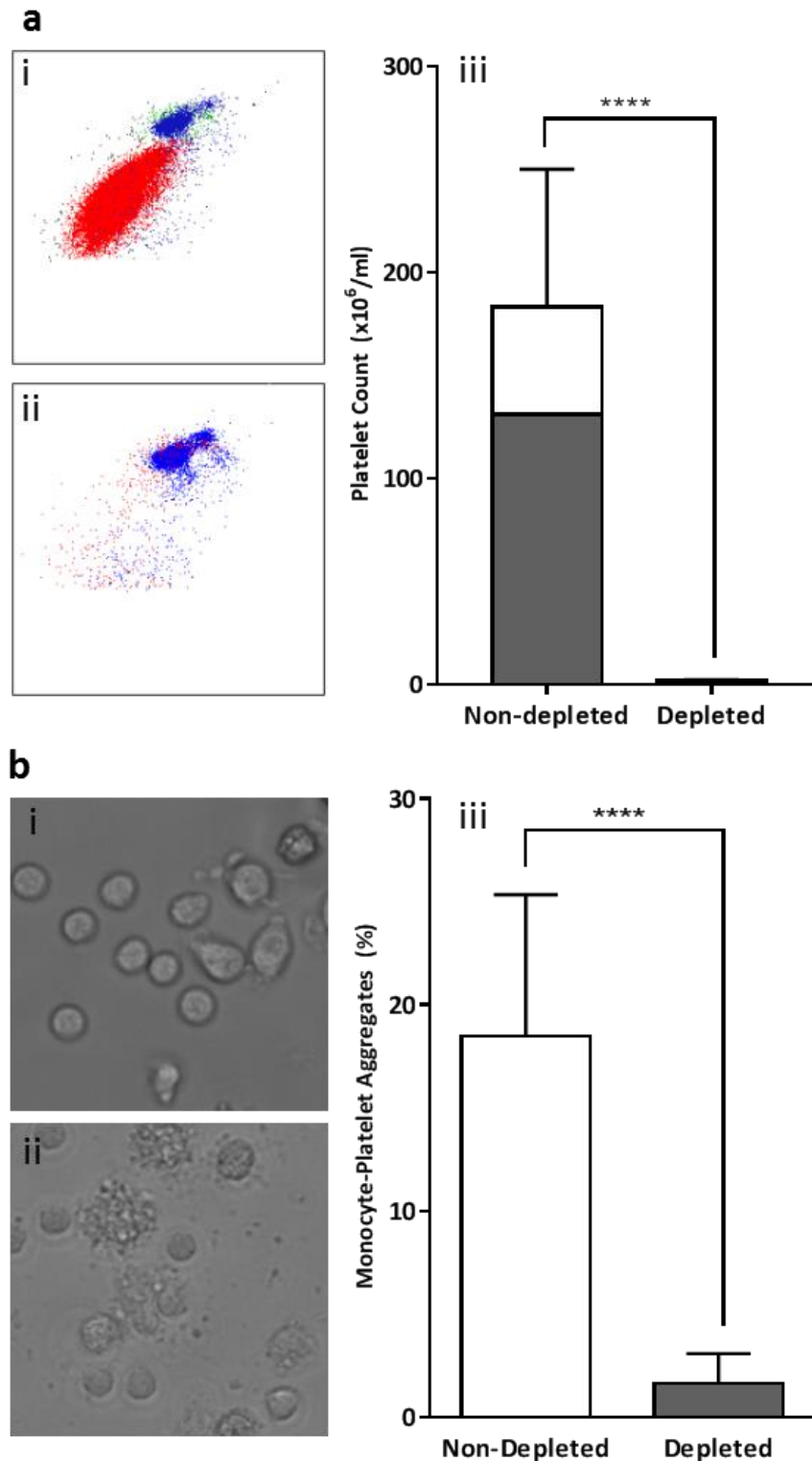
Figure 4.5: CD61 Immunomagnetic Depletion of Platelets from PBMCs. (a) depicts residual platelet counts in a PBMCs before and after platelet depletion. Forward (y-axis) and Side Scatter (x-axis) plots of PBMCs with CD45^{pos} leucocytes (blue) and CD42b^{pos} platelets (red) both before (i) and after (ii) CD61 immunomagnetic bead depletion. Also shown are both the platelets counts (iii). Bars represent mean±SD and the grey shaded area represents the proportion of those residual platelets that expressed surface P-selectin. (b) depicts MPAs in PBMCs before and after platelet depletion. Representative light microscopy of cultured, adherent monocytes is shown (b) both with (b,i) and without (b,ii) initial CD61 depletion. Aggregated data is shown depicting the percentage of isolated monocytes with adherent platelets (iii). n=5, ****=p<0.0001

4.4 Minimising Iatrogenic Activation within Leucocyte Preparations

Isolating monocytes from whole blood is a time-consuming process and requires the experimental manipulation of leucocytes and platelets which may lead to their iatrogenic activation. The effect of density-gradient media on leucocyte activation has been described (**Ashraf and Khan** *2003*) but care must also be taken to minimise the activation of platelets. The experiments conducted so far have not shown significant differences in the levels of platelet activation between the methods and therefore the methodological considerations to minimise this are described in this section.

4.4.1 Effect of anticoagulant medium on residual platelet counts and activation in PBMCs

For the study of platelet function, blood samples are commonly anticoagulated with sodium citrate solution which act a chelator of free Ca^{2+} and therefore reduce the activity of the coagulation cascade (**Mody *et al.*** *1999*). Furthermore, Ca^{2+} is required for platelet aggregation and blood stored in citrate for 24hrs has been shown to exhibit continued inhibition of activity when compared to other anticoagulants such as heparin (**Truss *et al.*** *2009*). CTAD is an alternative anticoagulant that consists of a mixture of Sodium Citrate, Citric Acid, Theophylline, Adenosine and Dipyridamole. It was first developed for use in coagulation assays and designed to minimise the activation of platelets (**van den Besselaar *et al.*** *1987*). When compared to blood taken into EDTA anticoagulant, platelet activation was significantly less in CTAD but returned to normal function when removed from this medium (**Ahnadi *et al.*** *2003*).

During the production of therapeutic concentrates from human donor blood, platelet-rich plasma (PRP) shows significant increases in surface markers such as P-selectin and Annexin V when compared to whole blood indicating that artificial activation can occur through the isolation and storage of cellular concentrates (**Metcalfe *et al.*** *1997*). The levels of platelets activation were therefore quantified during the isolation of PBMCs to ascertain the difference, if any, between CTAD and Sodium Citrate anticoagulant media.

Equal volumes of whole blood from healthy volunteers (n=3) was collected into both Citrate and CTAD anticoagulant and diluted with an equal volume (1:1) of PBS/5mM EDTA solution. PBMCs were separated from the blood mixture by density-gradient centrifugation using Lymphoprep and the resulting cells were washed three times by repeated centrifugation (400G, 15mins) and discarding of the supernatant. The number of residual platelets in the final preparation of PBMCs was measured by automated cell counting (Act-T-Diff, Beckman-Coulter) and activation was quantified by P-selectin expression (**Figure 4.6**).
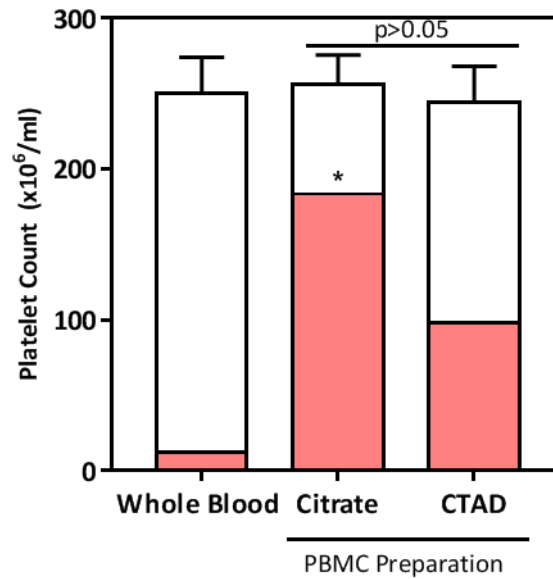
Figure 4.6: Effect of Anticoagulants on Residual Platelet Numbers. Graph shows concentration of platelets (mean±SD) in whole blood and PBMCs isolated from blood collected into either Citrate anticoagulant or CTAD. There was no significant difference in the concentration of platelets in either whole blood or PBMCs (p>0.05). Bars also show the proportion of platelets that are activated. The red shaded area represents the proportion of platelets that expressed P-selectin. Residual platelets in PBMC isolated from citrated blood showed significantly more (p<0.05) P-selectin expression than from CTAD anticoagulant. '*'=p<0.05

Density-gradient separated leucocytes yielded equivalent numbers of cells from either 3.2% trisodium citrate or CTAD (15.24 ±4.28 x10^6/ml vs 14.69±2.71x10^6/ml, p=0.82, t-test) with no significant difference in the proportion of CD14^{pos} monocytes (p>0.05, t-test). Residual platelet count was lower in PBMCs isolated from CTAD blood (244±53.1x10^6/ml) than Citrate (255±93.9x10^6/ml) although these differences were not statistically significant (p=0.62, t-test). Levels of P-selectin expression on platelets in whole blood were low (4.8±0.9%) but significantly higher (p=0.0039, t-test) in residual platelets in PBMC preparations isolated from both Citrated (71.1±2.5%) and CTAD (39.69±6.9%) blood (**Figure 4.6**).

The proportion of monocytes with adherent platelets in (MPAs) was quantified, by flow cytometry, in whole blood and in PBMC preparations isolated from CTAD and Citrated blood (**Figure 4.7**). In whole blood, 6.83±3.8% of monocytes had adherent platelets as compared with 19.3±1.3% in PBMCs isolated from Citrated blood. When isolated from CTAD blood, only 12.8±2.8% of monocytes in the PBMC isolate had adherent platelets which was significantly less than with Citrated blood (p=0.02, t-test).
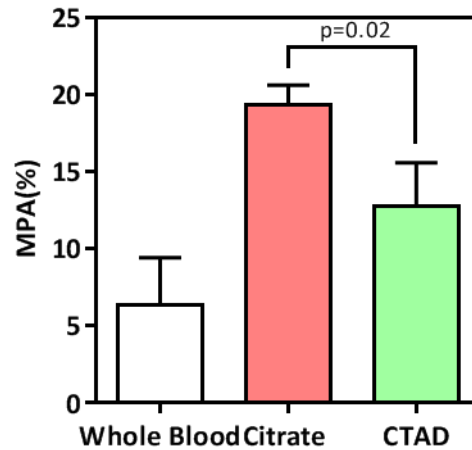
Figure 4.7: Effect of Anticoagulant Medium on MPA Formation. Graph shows the percentage of monocytes with adherent platelets (%MPA) in whole blood, and in PBMCs collected from either Citrated (red bar) or CTAD blood (green bar). There was significantly greater (p=.0.02) MPA formation in Citrated PBMCs than with CTAD. Bars denote mean±SD.

4.4.2   Effect of Anticoagulant Medium and Platelet Depletion on Monocyte Activation

Whole blood from healthy volunteers (n=5) was collected into both Citrate and CTAD anticoagulant and PBMCs were isolated by density gradient centrifugation followed by CD61 immunomagnetic depletion. Monocyte activation was quantified by expression of ICAM1 both in the preparation of PBMCs and in whole blood for comparison (**Figure 4.8**).

ICAM1 expression, used as an early marker of monocyte activation, on monocytes in whole blood was low (<5%) and there was no significant difference between Citrate and CTAD samples (p=0.231, t-test). When ICAM1 expression was quantified on monocytes in a PBMC preparation, levels were marginally higher (21.1±11.5% vs 16.0±4.1%) when isolated with Citrated as oppose to CTAD blood in the samples without CD61 depletion, although this was not statistically significant (p>0.05, ANOVA). However, when a CD61 depletion step was employed, ICAM1 expression was significantly lower (19.4±5.9% vs 6.0±4.8%, p=0.009, ANOVA) on monocytes isolated from CTAD vs Citrated blood. Furthermore, levels of ICAM1 expression in the isolated mononuclear preparations, using all permutations of methodology, were significantly higher (p<0.05, ANOVA) than found on monocytes directly in whole blood (3.1±0.3%).
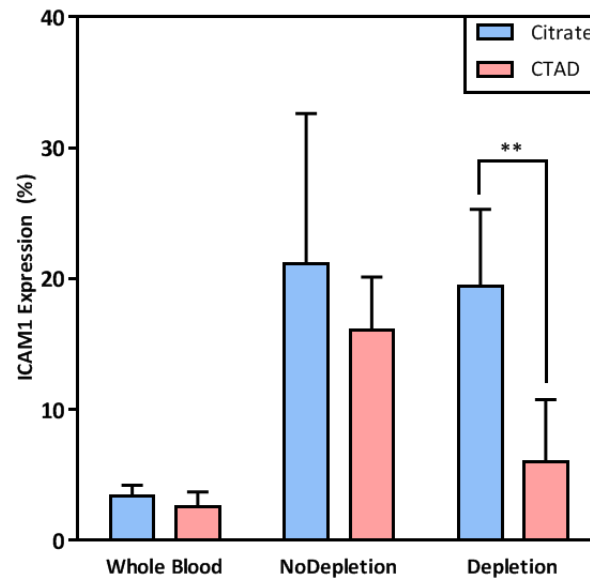
Figure 4.8: Effect of Anticoagulant Medium and Platelet Depletion on Monocyte Activation. Graph shows the proportion of monocytes expressing surface ICAM1 in whole blood and in PBMCs preparations isolated both with (depletion) and without (nodepletion) CD61 immunomagnetic depletion. Bars show mean±SD (n=5) of ICAM1 expression in whole blood and PBMCs isolated from Citrated (blue) and CTAD (red) anticoagulant. Both platelet depletion and the use of CTAD resulted in a significant (p<0.05) decrease in the expression of monocyte ICAM1.'**' = p<0.01

4.4.3 Activation of Monocytes in a PBMC Preparation is Dependent on Residual Platelets

Blood was collected from healthy volunteers (n=3) into 3.2% Trisodium Citrate and PBMCs were isolated by centrifugation on Lymphoprep density-gradient. The resultant PBMCs underwent either CD61 platelet depletion or sham depletion using an automated magnetic cell separator (AutoMACS Pro, Miltenyi Biotec). To both CD61^{pos} and CD61^{neg} PBMCs, CRP-XL (1.0μg/ml) was added and incubated at 37°C for 4 hours on slow rotation. The leucocyte sample was then analysed by flow cytometry for MPA formation and expression of ICAM1 on monocytes (**Figure 4.9**).

In a preparation of PBMCs, CRP-XL incubation for 4 hrs resulted in a mean increase in monocyte-platelet aggregate of 73.99±8.55% (p<0.0001, 2-way ANOVA with Sidak's multiple comparisons). There was no significant increase (p>0.05, 2-way ANOVA) in MPA formation when platelet-depleted PBMCs were incubated with CRP-XL and similarly for ICAM1 expression (p>0.05, 2-way ANOVA). However, without platelet depletion, CRP-XL led to a 20.84±2.32% increase in ICAM1 expression on monocytes which was statistically significant (p<0.001, 2-way ANOVA with Sidaks multiple comparisons).
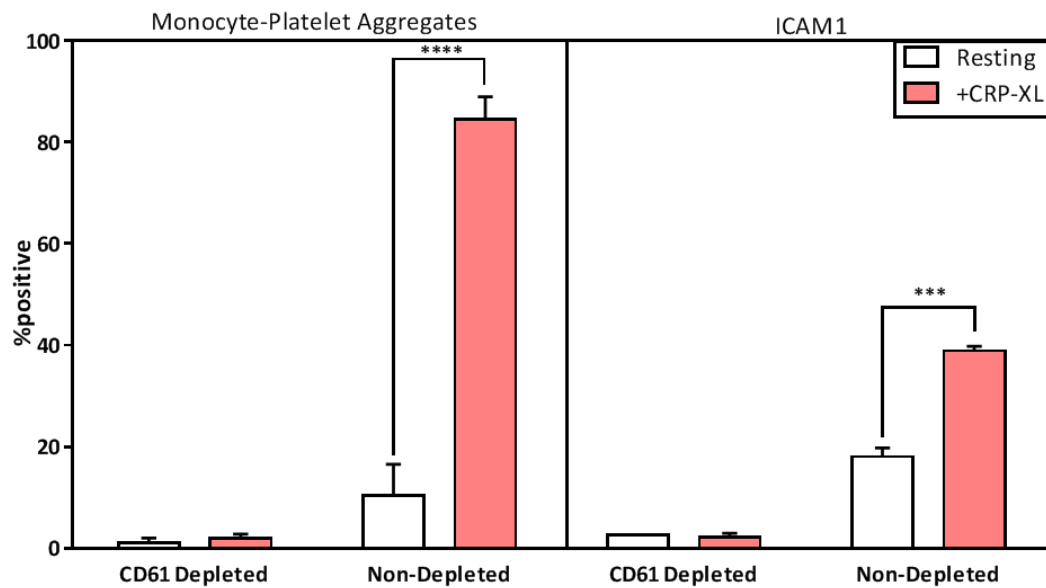
Figure 4.9: MPA Formation and Monocyte Activation is Dependent on Contaminating Platelets. Graph shows both percentage MPA formation (left panel) and percentage ICAM1 expression on monocytes (right panel). Data is shown for PBMCs isolated from blood both with and without CD61 immunomagnetic depletion. Bars represent mean±SD with clear bars depicting non-activated samples whereas red bars represent samples activated with CRP-XL. There was a significant increase ($p < 0.05$, n=3) in both MPA formation and ICAM1 expression on monocytes with CRP-XL activation. However, this difference was not seen with CD61 depleted samples.

4.5   The Culture of Monocyte-Derived Macrophages

One of the aims of the thesis is to examine the effects of monocyte stimulation by platelets with respect to the formation of foam cells. A method was therefore optimised for the culture of MDMs in order to study foam cell formation.

4.5.1   Studies of Monocyte Viability

4.5.1.1 Effect of Activation with CRP-XL in Whole Blood

Blood from healthy donors (n=2) was collected into 3.2% Trisodium Citrate and incubated for 4 hours at 37°C with and without 1.0μg/ml CRP-XL. Monocytes were isolated by density gradient centrifugation followed by negative immunomagnetic separation and re-suspended in PBS. Cells were stained with Propidium Iodide and viability was quantified by flow cytometry (**Figure 4.10**). After the incubation period, >90% of isolated monocytes were viable with no significant difference demonstrated ($p > 0.087$, t-test) between CRP-activated and non-activated monocytes.
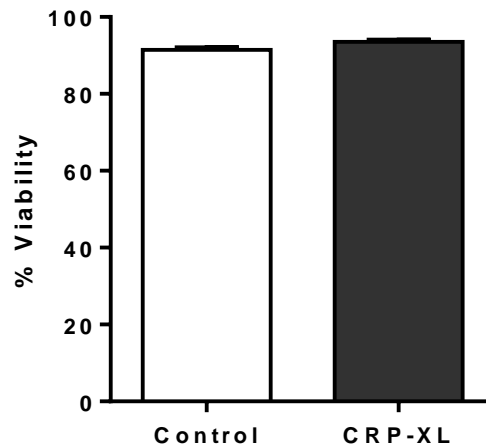
Figure 4.10: Viability of CRP-Activated Monocytes. Graph shows viability of cultured monocytes from whole blood either with or without CRP-XL stimulation. There was no significant difference in viability between the two groups (p>0.05, t-test, n=2)

4.5.1.2 Effect of Activation with CRP-XL on MDMs

In parallel experiments, monocytes were isolated from whole blood (n=3) as above and re-suspended in either RPMI-1640, Macrophage Serum-Free Media (MSFM) or Dulbecco Modified Eagle Media (DMEM)[24] at a concentration of 1.0×10^6/ml. The monocytes were incubated with autologous platelets at a concentration of 250×10^6/ml with either 1.0µg/ml of CRP-XL or an equivalent volume of HBS pH7.4 for a period of 16hrs overnight in a 37°C incubator. Following this, cells were stained with Propidium Iodide and assessed for viability by flow cytometry (**Figure 4.11**).

---

[24] All culture media was purchased from Gibco
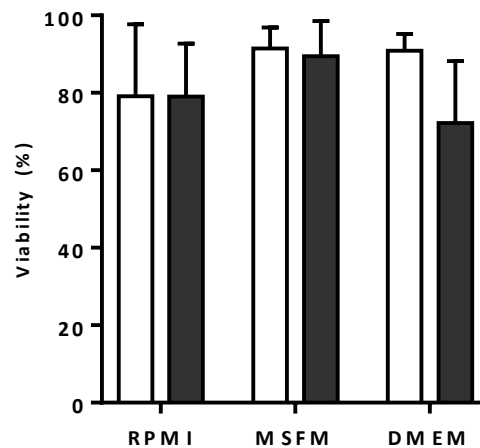
Figure 4.11: Effects of Prolonged CRP-Activation and Culture Medium on Monocyte Viability. Viability of monocytes after 16hrs incubation with (grey bars) or without (white bars) CRP-XL and autologous washed platelets. Monocytes and platelets were incubated in either RPMI-1640 (RPMI), Macrophage Serum-Free Media (MSFM) or Dulbecco Modified Eagle Media (DMEM). Overall, there was no significant difference in viability (p>0.05, ANOVA) across the different incubation conditions. Bars denote mean ± SD (n=3).

In isolated and cultured monocytes, without the addition of autologous platelets, viability in all conditions was >75% with no overall difference with the use of different media (p=0.29, ANOVA). Viability was marginally lower in cells incubated in RPMI-1640 (79.16%±18.59%) when compared to MSFM (91.42%±5.48%) or DMEM (90.89%±4.33%). As with incubation in whole blood, viability in isolated monocytes incubated with autologous platelets was not significantly different with co-incubated with CRP-XL (p=0.26, 2way ANOVA).

4.5.2   Isolation of Monocytes by Adherence

The purest population of monocytes was obtained by immunomagnetic bead selection, but this was at the expense of yield. Given the relatively small number of cells obtained from a single donor (~3.0-4.0x10^6 cells), use of a standard plating density of 1.0x10^6 cells/ml often resulted in insufficient cells to perform a time course over 7 days especially when different incubation were required. Isolation of monocytes by adherence is another commonly used method was evaluated.

PBMCs were isolated from healthy donors (n=2) and re-suspended in RPMI-1640 at a concentration of 1.0x10^6/ml. Aliquots of this cell suspension (1ml, 1.0x10^6 cells) were placed into individual wells of 24-well plates and incubated for 2 hrs at 37°C, 5% CO_2. Following this incubation period, cells were washed with RPMI up to 5 times and following each wash, cells were scraped into LP4 tubes for flow cytometric quantification of monocyte purity. PBMCs suspended in RPMI showed a monocyte purity of 16.95%±6.64% which increased to

55.34%±5.64% (p<0.05, t-test) after 1 wash with RPMI. With successive washes, the purity of monocytes increased progressively (p<0.05, ANOVA) up to 5 washes which resulted in a monocyte purity of 72.84%±4.5 in adherent cells.

4.5.3 Validation of Flow Cytometric Quantification of Foam Cells

PBMCs were isolated from whole blood by density-gradient centrifugation and adherence, and cultured in RPMI culture medium supplemented with 10% autologous serum for up to 7 days. On each day of culture, cells were dual-stained with both Nile Red and DAPI after which intracellular lipid droplets were quantified manually. The total number of discreet intracellular droplets within the cytoplasm of MDMs were counted as well as the total number of cells within a fixed field of zoom (60x) to calculate a mean number of droplets per cell. For those cells with more than 10 quantifiable droplets or if the intracellular lipid droplets staining was not discreet, a value of 10 was assigned as it was visually difficult to assign a value beyond this point. Following fluorescent microscopy, the dual-stained cells were scrapped into a suspension of PBS and analysed by flow cytometry for Nile Red fluorescence. A negative control was set, to exclude background staining, using parallel samples in which PBMCs were isolated from whole blood (from the same donor), stained with Nile red and analysed by flow cytometry to set a baseline at 2%. Both median fluorescence intensity and the percentage of cells that stained for Nile Red was recorded and plotted alongside the manual quantification of intracellular lipid droplets (**Figure 4.12**).
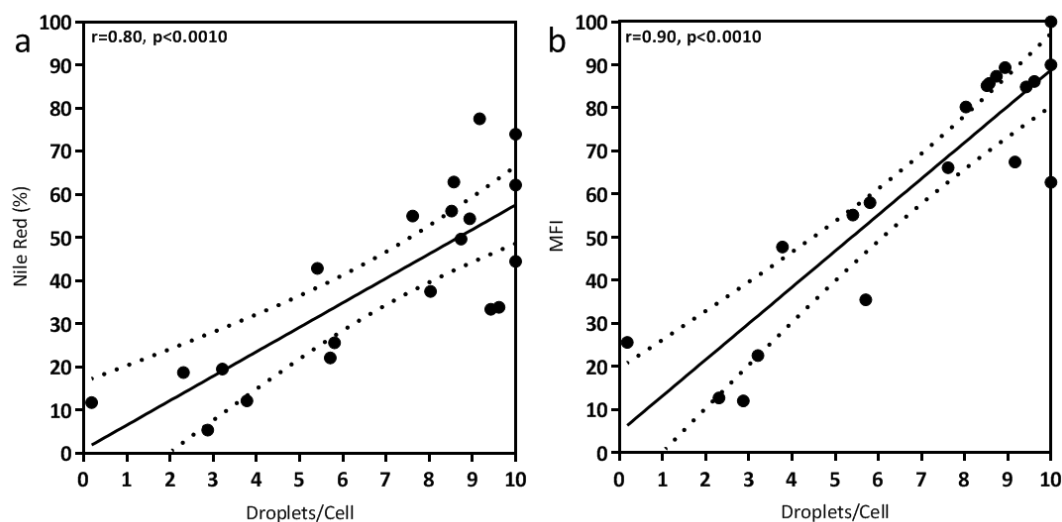
Figure 4.12: Correlation of Flow Cytometric and Manual Quantification of Lipid Droplets. (a) shows scatter plot of mean droplets/cell as quantified by fluorescent microscopy versus the percentage the cells that show Nile Red staining (Nile Red %). (b) Also shows the light microscopic quantification of lipid droplets on the x-axis but shows the median fluorescence intensity of Nile Red on the y-axis. The line of best fit is shown (solid line) with 95% confidence interval (dotted line).

Both the median fluorescence intensity of Nile Red staining (r=0.903, p<0.0001) and the percentage of Nile Red positive MDMs (r=0.802, p<0.0001) were found to be correlated with the mean number of droplets per cell. The correlation of MFI was marginally stronger than for percentage Nile Red staining.

4.5.4   Selection of Serum for the Culture of MDMs

Serum is commonly used as a nutritive supplement in cell culture and provides hormones, mitogenic peptides and growth factors that are necessary for growth and survival. However, there are a number of caveats with its use, particularly with respect to the culture of primary MDMs. Serum may contain undefined factors that influence the growth of cells in an idiosyncratic or batch-dependent manner and also might promote the growth of contaminating lymphocytes. Furthermore, serum may contain endotoxins which activate monocytes and alters monocyte-macrophage function. Finally, and particularly important with regards to lipid homeostasis, serum contains a range of free fatty acids, cholesterol, lipoproteins and chylomicrons which may significantly alter cholesterol homeostasis in monocyte-derived macrophages and promote foam cell formation. Culture media, without the addition of serum supplementation, has been used in the growth of monocytes and was found to be less adherent (**Vogel *et al.* 1988**) and differentiate into macrophages more slowly (**Andreesen *et al.* 1990**) than those cultured in serum-supplemented media. Using the culture system, the effect of serum supplementation and serum-free media on the formation of intracellular lipid droplets and foam cell formation in MDMs was ascertained.

PBMCs were isolated from whole blood by density-gradient centrifugation and depleted of platelets by immunomagnetic bead separation. Cells were re-suspended in RPMI-1640 at a concentration of 1.0×10^6/ml and plated into 24-well plates and left to adhere for 2hrs at 37°C, 5% CO_2. Residual lymphocytes were washed away with 5 washes of RPMI and the adherent monocytes were cultured in RPMI-1640 supplemented with 10% autologous serum. Cells were stained with Nile Red and analysed by light microscopy and flow cytometry for morphology and intracellular lipid droplet formation (Figure 4.13).

Cells cultured in 10% autologous serum demonstrated a morphological change towards a macrophage phenotype with increased intracellular lipid droplets as quantified by Nile Red staining. The lipid droplets occurred spontaneously (i.e. without the addition of an exogenous stimulus) and were found within 24 hours of culture. The frequency and density of these intracellular droplets increased progressively over 7 days in culture and by day 7, more than 90% of cells had the appearance of lipid-laden foam cells.
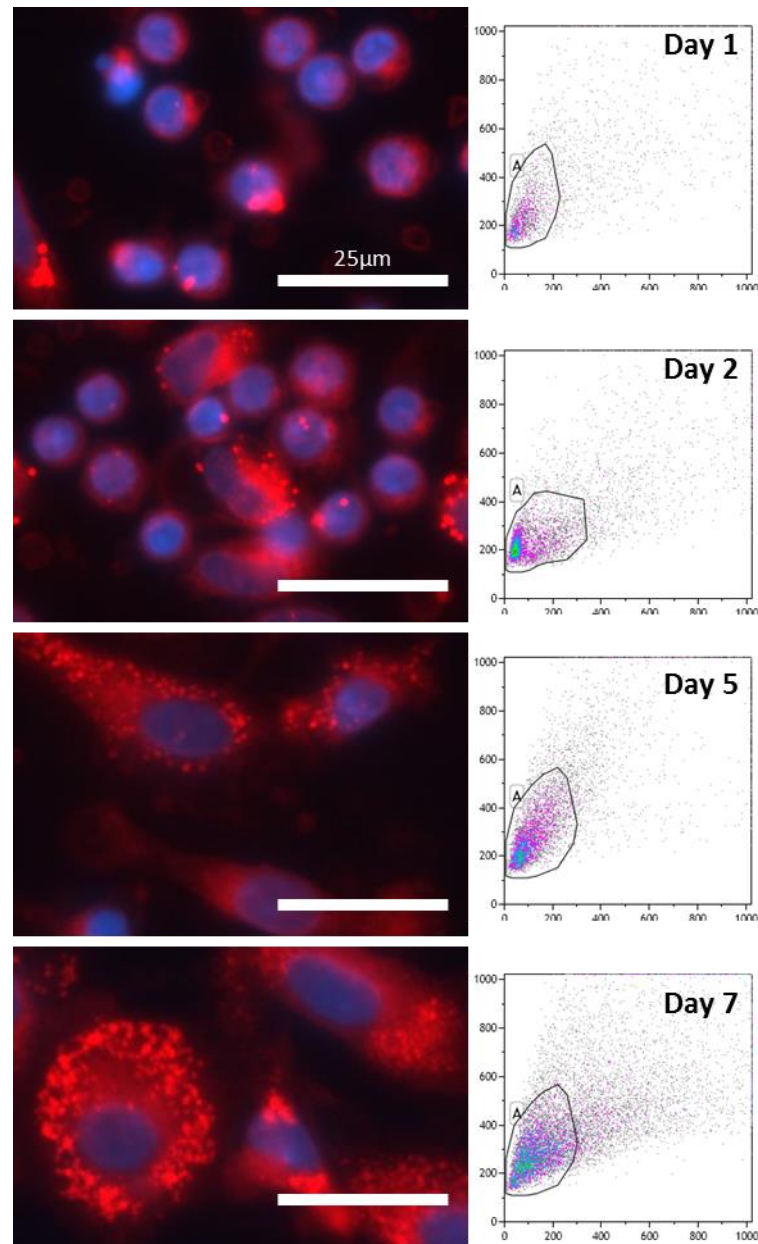
Figure 4.13: Formation of Foam Cells in MDMs. Images show monocytes cultured in RPMI1640 + 10% autologous serum and stained with Nile Red and DAPI (blue). Scale bars are shown (25μm). Shown also are accompanying FS/SS density plots taken form cultured MDMs on Days 1, 2, 5 and 7. MDMs show a change in their morphology from simple cells with large nuclear:cytoplasmic ratio to larger, more granular cells with increased intracellular lipid droplets. This progressive increase in size and granularity is confirmed by the FS/SS signals.

To assess the effect of serum supplementation on foam cell formation, monocytes were isolated by adherence and cultured in either serum-supplemented RPMI-1640 or Macrophage Serum-Free Medium supplemented with 50ng/ml M-CSF for 7 days. The formation of intracellular lipid droplets was quantified by flow cytometry (Figure 4.14). MDMs cultured in both serum-free and

serum-supplemented media showed a progressive increase in NR fluorescence (both MFI and percentage positive) over 7 days in culture ($p < 0.05$, ANOVA). There were no significant appreciable differences in gross morphology between the culture conditions nor were there significant differences in SS or FS ($p > 0.05$, ANOVA). Cells cultured in serum-free media however exhibited less Nile Red staining than in serum-conditioned medium however, there was no overall statistically significant difference on multiple t-testing ($p > 0.05$).
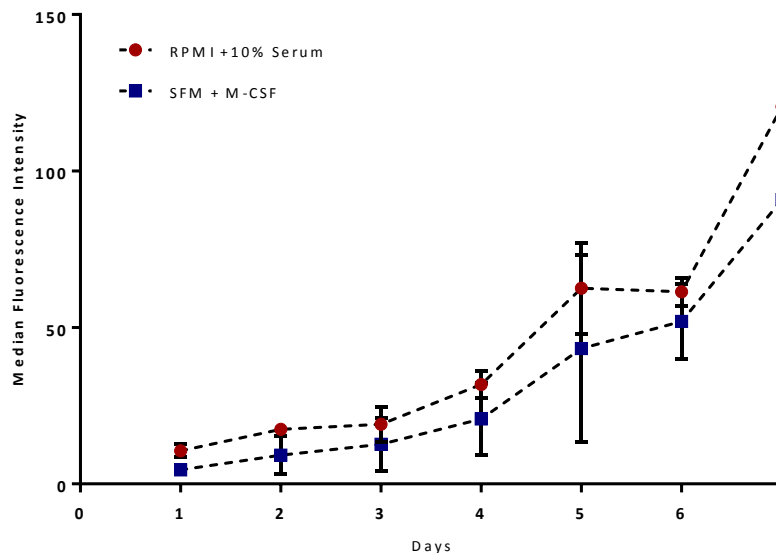
Figure 4.14: Effects of Serum-Supplementation on Foam Cell Formation in MDMs. Graph shows median fluorescence intensity (MFI) of Nile Red fluorescence in monocytes cultured in with RPMI + autologous serum (red dots) and macrophage serum-free medium supplemented with M-CSF (blue squares) over 7 days in culture. Points depicts mean ±SD.

4.5.5 Culture of Monocytes and Transformation into MDMs

PBMCs were isolated from whole blood from healthy volunteers (n=8) by density gradient centrifugation and platelets were depleted by immunomagnetic bead separation. The platelet-free PBMCs were then plated into 24 well plates, allowed to adhere and washed with RPMI. The resultant adherent monocytes were then cultured in macrophage serum-free medium (Gibco) supplemented with 50ng/ml M-CSF (Miltenyi Biotec) for 7 days. On each day in culture, cells were imaged by light microscopy and also gently scrapped into PBS to be analysed by flow cytometry for forward and side scatter as well as to quantify the expression of the macrophage differentiation marker CD68 (Figure 4.15).

Within 24hrs of culture, adherent cells exhibited typical characteristics of circulating monocytes including an agranular cytoplasm and a large nuclear:cytoplasmic ratio. With increasing days in culture, the morphology of these adherent cells changes to resemble either typical

macrophages, or long spindle-shaped cells consistent with the appearance of dendritic cells. Both of these cell morphologies were accompanied by increased cell size and cytoplasmic granularity when assessed by light microscopy. This was confirmed by flow cytometry which showed progressive increases in forward scatter and side scatter over the 7-day culture period. The expression of CD68 increased on cultured monocytes from 28.6±9.6% on Day 1 of culture to 62.5±11.4% on Day 7. This was not linear as the expression levels showed small increases over Days 1 to 5 followed by a marked rise at day 6.
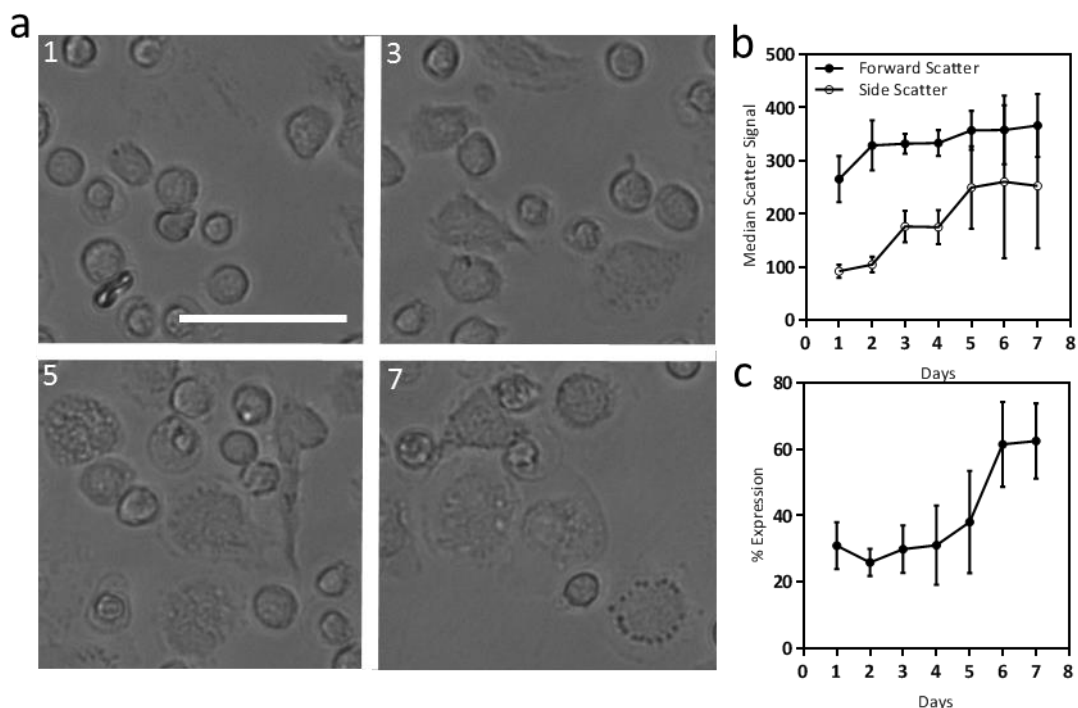
Figure 4.15: Morphological Features of Cultured Monocyte-Derived Macrophages. (a) shows representative images of monocytes cultured in Serum-Free medium supplemented with 50ng/ml M-CSF on Day 1, Day 3, Day 5 and Day 7 of culture. White bar scale bar denotes 25µm. (b) shows median scatter signals for both forward and side scatter of MDMs and (c) shows the % of CD68 expression on MDMs. Graphs show mean±SD, n=8.

4.5.6   The Effect of Different Density-Gradient media on Foam Cell Formation

In addition to the effect on monocyte purity and activation, the choice of density-gradient medium might also affect the phenotype of cultured MDMs. Ficoll is a hydrophilic polysaccharide and its use as a density-gradient medium may stimulate monocytes during their isolation and induce phenotypic changes in culture: particularly phagocytic activity which is relevant with respect to foam cell formation (**Zhou *et al.* 2012**). Nycoprep is an alternative density-gradient medium, containing Nycodenz which replaces the Ficoll while maintaining the

correct osmotic environment. This is medium does not contain polysaccharide, it is believed to be less likely to cause iatrogenic stimulation of monocytes.

PBMCs were isolated from whole blood using either Lymphoprep or Nycoprep density-gradient medium in a single-step process. The PBMCs were depleted of platelets, monocytes isolated by adherence and subsequently cultured in macrophage serum-free medium supplemented with 50ng/ml M-CSF for 6 days. Intracellular lipid droplet formation was quantified by flow cytometry by staining the cells with Nile Red.
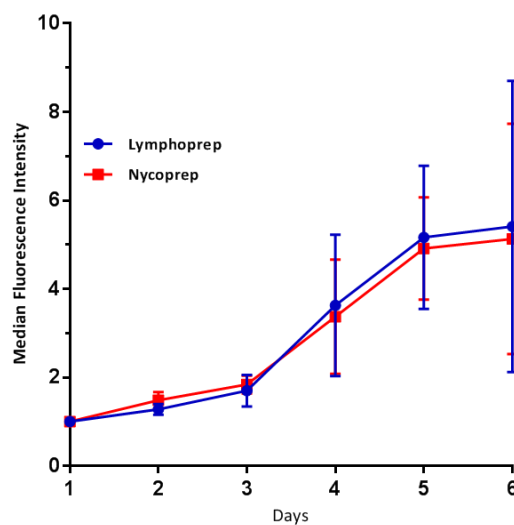
Figure 4.16: Effect of Density-Gradient Medium on Nile Red Fluorescence Intensity in Cultured MDMs. Fluorescence intensity of cultured MDMs in serum-free medium supplemented with 50ng/ml M-CSF. Cells were isolated by density gradient separation using either Lymphoprep or Nycoprep. There was no overall significant difference ($p>0.05$, ANOVA) when using the two density gradient media. Results show mean±SD.

As with previous experiments, there was a progressive increase in Nile Red fluorescence in MDMs over 6 days in culture ($p<0.05$, ANOVA) using either Lymphoprep or Nycoprep as density-gradient media. Cells obtained with Nycoprep demonstrated less Nile Red staining, but this was not significantly different to those obtained with Lymphoprep ($p>0.05$, ANOVA).

4.6 <u>Summary</u>

In this chapter, the iterations and testing of the methodology to isolate a pure population of monocytes was demonstrated as well as the selection of an optimal culture system in order to quantify foam cell formation.

Of the density-gradient media investigated in this chapter, the use of Lymphoprep provided the best overall balance of yield and purity (**Figure 4.2**). The addition of a second density-gradient step using Percoll was designed to improve the purity of isolated monocytes but demonstrated a prohibitively low yield, unsuitable for downstream applications. The use of the lymphoprep single-step density gradient method resulted in significant numbers of both co-segregated platelets and monocyte platelet aggregates (Figure 4.5). Flow cytometry both confirmed the presence of these platelets, and demonstrated them to be moderately activated as shown by the surface expression of P-selectin (**Figure 4.6**). In order to reduce the numbers of contaminating platelets, an initial centrifugation step to remove platelet-rich plasma was instituted. This resulted in decreased platelet counts in the final preparation of PBMCs but did not remove them entirely (**Figure 4.4**). Therefore an immunomagnetic depletion mechanism was employed, resulting in an almost complete removed of residual platelets from the PBMC preparation (Figure 4.5). Furthermore, the use of CD61 microbeads essentially abrogated the effects of CRP-XL that indirectly activated the monocyte through the activation of the residual platelets seen in the non-depleted preparation (**Figure 4.9**).

In order to further enrich the isolated cellular fractions with monocytes, both positive and negative immunomagnetic separation methods were analysed (**Figure 4.3**). Although positive selection provided a pure population of monocytes from both PBMCs and directly from whole blood, the use of negative selection preserved the heterogeneity of monocyte subsets and therefore allows for the subsequent analysis and selection of both CD16^{pos} and CD16^{neg} fractions.

Cultured monocytes, isolated either by immunomagnetic separation or by virtue of their adherence to the plastic plates, show a robust transformation into macrophages when cultured in media supplemented with M-CSF (Figure 4.13). Furthermore, even in the absence of exogenous activation or addition of exogenous lipids, these cultured cells show a spontaneous accumulation of intracellular lipid droplets and formation of foam cells. The assay of foam cells using the fluorescence of Nile Red as a surrogate marker was robust and correlated strongly with the visual quantification of intracellular lipid droplets (**Figure 4.12**). Using this method, it was also shown that the use of Ficoll as a density-gradient medium did not have a demonstrably different effect on the formation of foam cells when compared to Nycoprep.

From experimental manipulation of the 'standard' method of monocyte isolation, an optimised methodology was developed that allowed for the isolation of a pure population of monocytes with limited platelet contamination (**Figure 4.17**). Whole blood was collected into 3.2% trisodium citrate with an initial centrifugation step to remove PRP. This reduced the number of platelets in the PBMC preparation in subsequent density-gradient centrifugation and washing steps. Once PBMCs had been isolated, monocytes were isolated by negative immunomagnetic separation for downstream applications such as flow cytometry or with selective incubation with platelets. For the culture of monocyte-derived macrophages, monocytes were isolated by adherence to plastic wells as this provides the optimum combination of yield and purity.
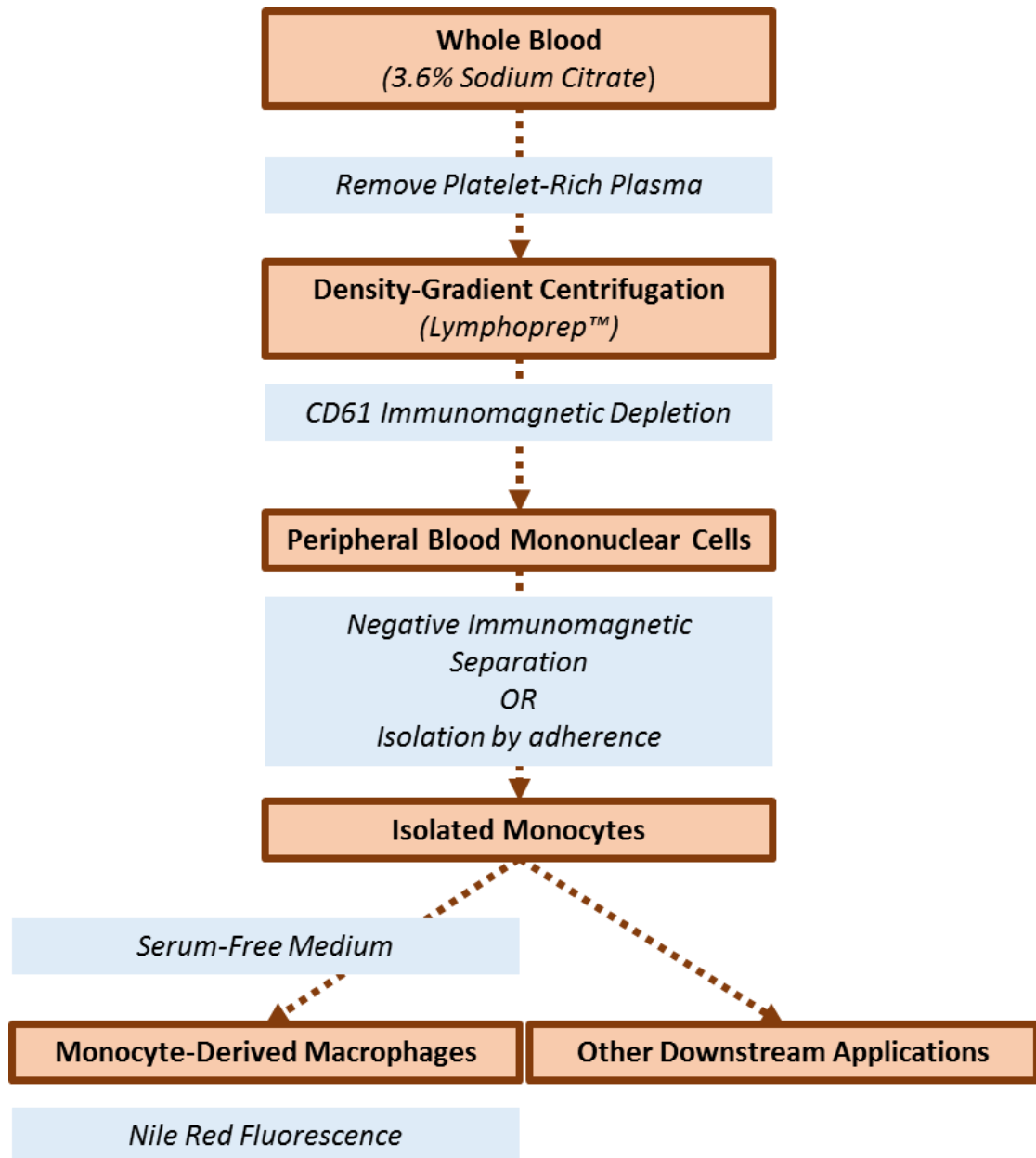
Figure 4.17: Schematic Overview of Optimised Methodology. Text in blues shows the additional steps added to the 'standard' method to improve the purity of isolated monocytes.

Chapter 5: Platelets Promote a Pro-Atherogenic Phenotype in Monocytes and Monocyte-Derived Macrophages

5.1 <u>Introduction</u>

In addition to their canonical role in haemostasis and thrombosis, activated platelets are able to readily form complexes with circulating monocytes and influence their phenotype as discussed in the introduction to this thesis. Platelets may also influence the formation of foam cells in MDMs however, the preponderance of experimental data has focussed on either individual factors released from platelets and/or derived from co-culture experiments with both platelets and monocytes-MDMs. In this chapter, the role of the early interaction between platelets and monocytes in whole blood, prior to the formation of MDMs, on subsequent effects on foam cell formation. Employing the techniques of monocyte isolation and culture, developed from the previous chapter, a model where whole blood is activated with CRP-XL prior to culture of MDMs and study of foam cell formation will be used.

CRP-XL is a cross-linked collagen peptide mimetic and is a selective agonist for the platelet collagen receptor GPVI (**Smethurst *et al.* 2007**). CRP readily adopts a triple helical structure containing GPO[25] triplets, which are recognised by GPVI, but is a potent platelet agonist only after cross-linking (CRP-XL) so that it may induce quaternary structuring (**Asselin *et al.* 1997**). Importantly, and unlike the receptors for other commonly used platelet agonists, it is specifically found on platelets and is not present on other leucocytes including monocytes (**Jandrot-Perrus *et al.* 2000**). Therefore, a model wherein whole blood is incubated with CRP-XL results in the specific activation of platelets and any effect on monocytes is therefore a result of this.

This model was therefore employed in this chapter to examine the effects of platelet activation on foam cell formation.

---

[25] Single letter amino acid code; G=Glycine, P=Proline, O=Hydroxyproline

5.2 Platelets Induce Foam Cell Formation in Monocyte-Derived Macrophages

5.2.1 Foam Cell Formation in Platelet-Activated MDMs from Whole Blood

Whole blood (WB) from healthy volunteers (n=7) was collected into 3.2% trisodium citrate anticoagulant (BD Vacutainer) and activated with 1.0µg/ml of CRP-XL for 4hrs at 37°C. Following the incubation period, WB was layered on a density-gradient medium and centrifuged to generate PBMCs which were re-suspended in RPMI-1640. The cells were plated at a density of $1.0x10^6$ cells/ml into 24-well plates and allowed to adhere for 2hrs at 37°C, 5% CO_2. Cells were washed with RPMI to remove non-adherent lymphocytes and cultured in serum-free media supplemented with 50ng/ml M-CSF for up to 7 days. The cell culture medium was changed on Day 1 and Day 4.

On each day of culture, 4% PFA was added to fix cells which were stained with Nile Red and DAPI nuclear counterstain. Fluorescent images were acquired by fluorescent microscopy to quantify foam cells and also the cells were scrapped and passed through a flow cytometer (Gallios, Beckman-Coulter) to analyse foam cells by fluorescence intensity (**Figure 5.1**).
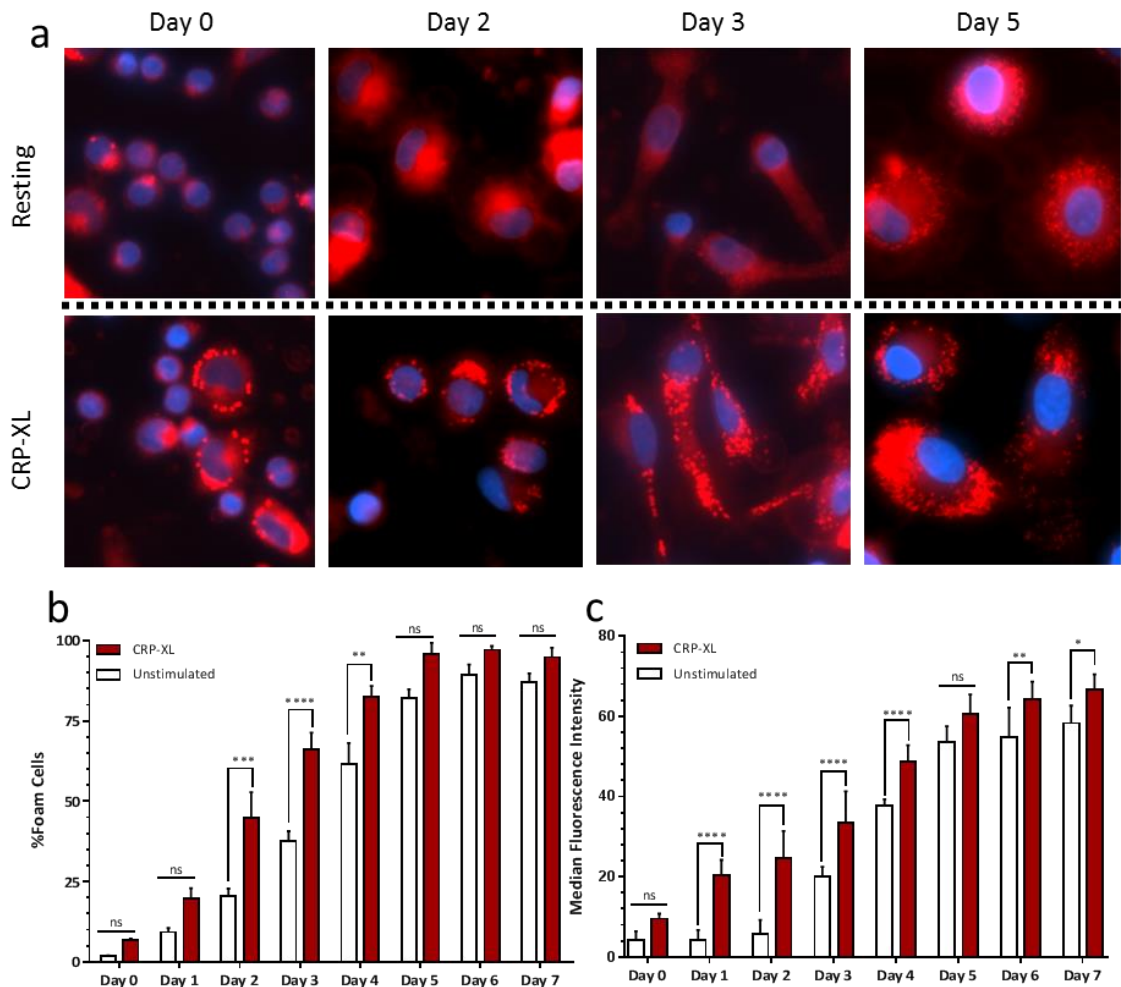
Figure 5.1: Foam Cell Formation of MDMs. Representative Images are shown (a) of cultured monocyte-derived macrophages stained with Nile Red and DAPI. Images are shown from Days 0, 2, 3 and 5 in culture of both unstimulated monocytes (resting) and CRP-XL activated samples (bottom panel). The formation of foam cells was quantified by fluorescent microscopy by manual counting of foam cells. The percentage of cells with greater than 10 lipid droplets is shown (b) over the 7-day culture period. Additionally, the median fluorescence intensity of cells was quantified by flow cytometry (c). Graphs show data from both unstimulated (white) and CRP-XL stimulated MDMs (red). 'ns' = non-significant, *=$p<0.05$, **=$p<0.01$, ***=$p<0.005$, ****=$p<0.0001$ ANOVA with Sidak's multiple comparisons, (n=7).

Consistent with the studies in isolated PBMCs and washed platelets earlier in the chapter, the formation of intracellular lipid droplets could be visualised within 24hrs of culture. Morphologically, the cells took the appearance of circulating monocytes with a circular appearance and increased nuclear:cytoplasmic ratio. Nile Red staining identified the presence of intracellular droplets both in the unstimulated and the CRP-activated samples. However, there was greater median fluorescence intensity of the latter accompanied by increased manual quantification of foam cells, but this failed to reach statistical significance ($p>0.05$, ANOVA with Sidaks multiple comparisons. There was however an overall increase in both the percentage of foam cells and median Nile red fluorescence intensity of cells cultured over 5 days ($p<0.001$,

ANOVA) with a significantly more staining in CRP-XL activated samples (p<0.001, ANOVA). This difference was most marked at Day 3 (p<0.0001, ANOVA) with more modest, but still significant, differences thereafter.

5.2.1.1 Blocking MPA Formation Inhibits Foam-Cell Formation

Whole blood from healthy donors (n=5) was stimulated as before with 1.0μg/ml of CRP-XL for 4hrs at 37°C with and without the presence of a blocking antibody to hpselectin (9E1, R&D Systems). PBMCs were prepared as per the standard protocol and monocytes were isolated by adherence to plastic 24-well plates. Cells were cultured for 3 days in serum-free medium supplemented with 50ng/ml M-CSF following which they were fixed with 4% PFA and stained with both Nile Red and DAPI nuclear counterstain. Foam Cell formation was assessed by flow cytometry (**Figure 5.2**).
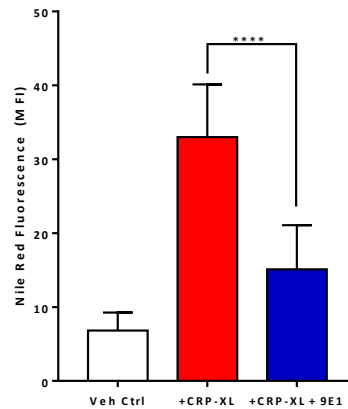
Figure 5.2: Fluorescence of MDMs with CRP-XL Activation in Whole Blood With(out) the Presence of a Blocking 9E1 Antibody. Data are shown as mean±SD of median fluorescence intensity of CRP-activated (red) samples and CRP-activated samples in the presence of 9E1 blocking antibody (blue). Values for the vehicle control (HBS) are shown as the clear bar (n=5).

MDMs isolated and cultured from whole blood activated with CRP-XL demonstrated a significantly greater (p<0.05, t-test) fluorescence of Nile red following 3 days of culture than unactivated samples. When MPA formation was inhibited with 9E1, the fluorescence intensity of Nile Red was abrogated by 50% (p<0.05, t-test) but not back to the levels seen at baseline. This suggests that the platelet-induced formation of foam cells in this assay is predominantly due to MPA formation but also involves factors released from the platelets.

5.2.1.2 Platelet Releasate Does Not Induce Foam Cell Formation in MDMs

To assess the effect of released factors from platelets (releasate) on monocyte foam cell formation, blood was obtained from healthy volunteers (n=5) and collected into 3.2% trisodium citrate. PBMCs were isolated by density-gradient centrifugation and platelets were depleted by immunomagnetic CD61 bead separation. Washed platelets were prepared from the platelet-rich fraction, re-suspended in HBS pH 7.4 and adjusted to a platelet count of $1000x10^6$/ml. Platelets were then activated with TRAP for 10 mins to induce maximal platelet degranulation. The activated washed platelets were then centrifuged (1600g, 20mins) to pellet the cellular components and the supernatant was removed. This was filtered (0.2μm Acrodisc) to remove any residual platelets or platelet-derived microparticles and the filtrate was diluted in serum-free media in 4 times the volume of the original washed platelet solution to give a platelet-conditioned medium from an effective platelet concentration of $250x10^6$/ml. The isolated PBMCs were allowed to adhere in 24-well plates for 2 hours (37°C, 5% CO_2) at a concentration of $1.0x10^6$ cells/ml and the contaminating lymphocytes were removed by repeated washing steps. 1ml of platelet-conditioned medium was added to each well and supplemented with 50ng/ml M-CSF to culture the cells for up to 7 days. For analysis of foam cell formation, cells were fixed with 4% PFA and stained with Nile Red for analysis by flow cytometry (**Figure 5.3**).
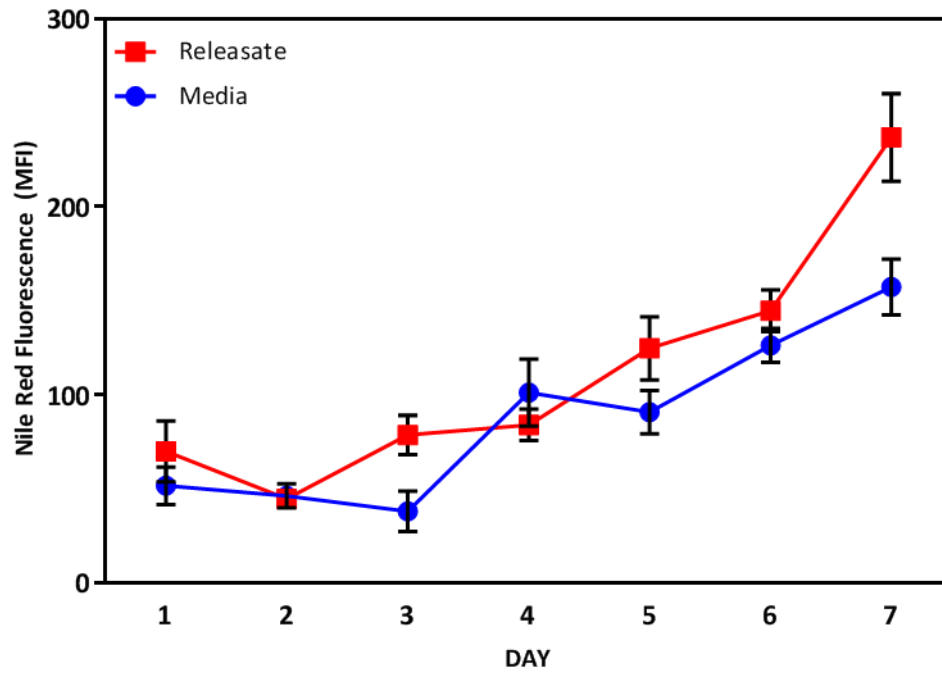
Figure 5.3: Effect of Platelet-Releasate on Foam Cell Formation in Cultured MDMS. Graph depicts mean±SD of Nile Red median fluorescence intensity of cultured MDMs incubated with either standard (blue) or platelet-conditioned (red) media. There is no overall significant difference in MFI over the culture period (p>0.05, ANOVA, n=5).

Cells cultured in either serum-free or platelet-conditioned media showed no difference in morphology over the 7-day culture period. When foam cell formation was quantified by median fluorescence intensity, there was overall no significant difference between media and platelet-conditioned media (p>0.05, ANOVA). These results demonstrate that the increase in foam cells with platelet activation requires direct cell-cell contact.

5.2.2 Demonstration that Lipid Droplet Formation in Platelet-Activated MDMs is a Result of Cholesterol Accumulation

The Cholesterol Quantitation Kit (Sigma-Aldrich) relies on the initial hydrolysis of cholesterol ester by cholesterol esterase into free cholesterol (**Figure 5.4**). The free cholesterol is then incubated with cholesterol oxidase to generate choleste-4-ene-3-one and hydrogen peroxide in a 1:1 stoichiometry. The presence of H_2O_2 is detected with a horse-radish peroxidase coupled to a fluorimetric probe detected at 570nm.
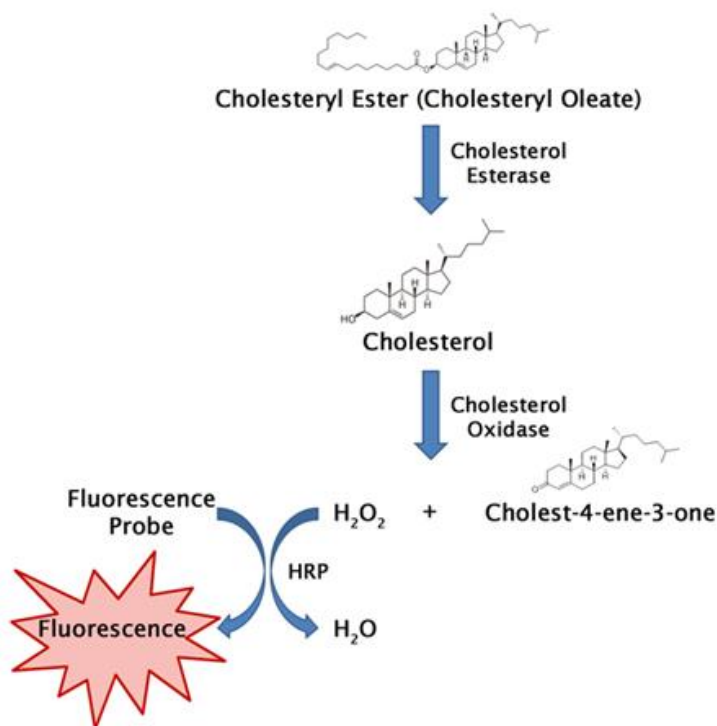
Figure 5.4: Colorimetric Cholesterol Assay. Schematic diagram of colorimetric cholesterol assay wherein cholesterol esters are hydrolysed to free cholesterol by cholesterol esterase. Further oxidation occurs to generate cholest-4-ene-3-one and hydrogen peroxide in a 1:1 stoichiometry. A fluorescence probe with a horseradish peroxidase is used to quantify H_2O_2 measured by fluorescence.

5.2.2.1 Validation of cholesterol assay

To validate the cholesterol assay, PBMCs were isolated from whole blood, by density-gradient centrifugation and plated into 24-well platelets at a concentration of 1.0×10^6/ml into 5 separate wells. PBMCs were also plated at 1.0×10^6/ml increments from 1.0×10^6/ml to 10.0×10^6/ml into a 24-well plate. All cells were cultured for 3 days in serum-free media supplemented with 50ng/ml M-CSF after which cells were scrapped into 500µl of IGEPAL (Sigma-Aldrich) and briefly vortexed to ensure homogenisation of lysate. This was then incubated with the enzyme cocktail and the HRP/colorimetric conjugate to quantify absorbance at 570nm (**Figure 5.5**).
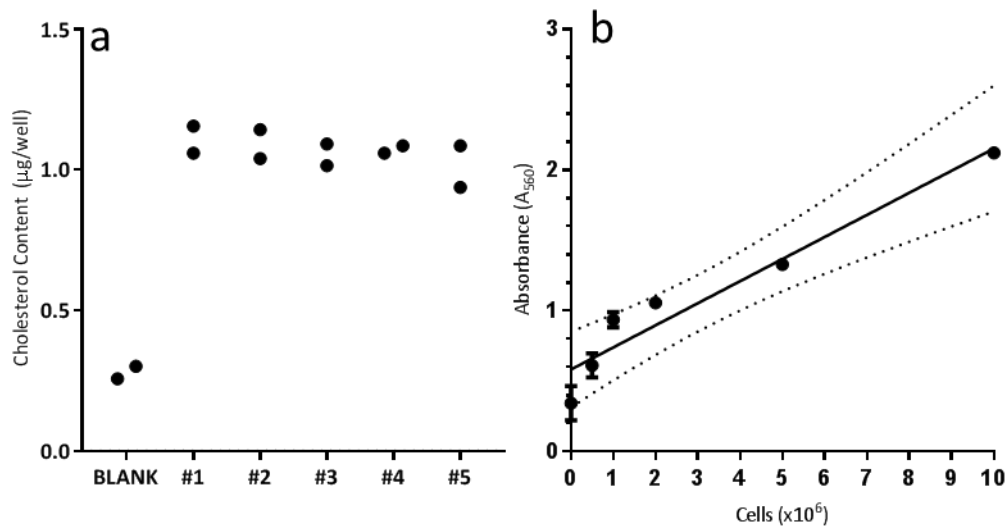
Figure 5.5: Validation of Cholesterol Quantification Assay. (a) Absorbance is shown at 570nm for 5 replicate wells containing 1.0×10^6 cells/ml. Shown also is the mean±SD absorbance at 570nm for wells of increasing plating densities (b). Solid line shows line of best fit with 95% confidence intervals. There is a strong correlation (r=0.966, p=0.0017) between absorbance and the number of cells within the lysate.

Using known concentrations of manufacturer-supplied cholesterol, absorbance at 570nm was recorded and a standard curve was produced. This was used to quantify cholesterol content in the test samples. Upon repeated quantification of cholesterol content in wells with 1.0×10^6 cells/well, there was no significant difference (p=0.69, ANOVA) in the measured Absorbance at 570nm. Furthermore, there was strong association (r=0.966) between the absorbance$_{530nm}$ at the number of cells plated within the well (p=0.0017) which demonstrates that the colorimetric assay is a reproducible and sensitive method to quantify cholesterol in MDMs.

5.2.2.2 GPVI-Activated Platelets Induce Increased Cholesterol Content in MDMs

To measure cholesterol content in platelet-activated MDMs, whole blood from healthy volunteers (n=5) was incubated with $1.0 \mu g$/ml of CRP-XL. To quantify the role of MPA formation, samples were also incubated with 20mg/ml of 9E1 (R&D Systems) blocking antibody to P-selectin. Following a 4-hour incubation period, PBMCs were isolated by density-gradient centrifugation and re-suspended in RPMI at 1.0×10^6 cells/ml to be plated onto 24-well plastic culture plates and allowed to adhere for 2hrs at 37°C, 5% CO_2. The non-adherent cells were removed with repeated washes with RPMI and cultured from up to 7 days in serum-free media. On each day of culture, the supernatant was aspirated, and replaced with a $500 \mu l$ of IGEPAL (Sigma-Aldrich). Cells were scrapped using a rubber tip and the suspension homogenised using a vortex mixer. Cholesterol was quantified by colorimetry in both the cell suspension and the culture supernatant. On samples collected from days 3 and 7, in addition to the total cholesterol,

free cholesterol was quantified by omitting the cholesterol esterase in the colorimetric assay allowing for the quantification of both free cholesterol and cholesterol esters specifically (**Figure 5.6**).

There was a progressive increase in the absorbance measured at 530nm in MDMs with increasing days in culture ($p < 0.05$, ANOVA). CRP-stimulated MDMs showed a significant increase in the quantity of cholesterol ($p < 0.05$) from day 3 onwards. This was significantly inhibited ($p < 0.05$) by blocking MPA formation with 9E1 although the content of cholesterol was still higher than baseline. On day 3 of culture, CRP-stimulated MDMs showed significantly more ($p < 0.05$) cholesterol content than either baseline or when incubated with 9E1, and the majority (>80%) of this was attributable to cholesterol esters. On day 7 of culture, although CRP-stimulated samples continued to show a greater amount of cholesterol, there was an increased proportion of free cholesterol when compared to either baseline or 9E1 samples. The results from quantification of cholesterol content in MDMs is complemented by measuring cholesterol in the culture medium supernatant (**Figure 5.6**). Over the 7-day period, there was significantly more cholesterol in the supernatant of un-activated MDMs that in CRP-activated MDMs ($p < 0.05$). When CRP-activated samples were co-incubated with 9E1, the FC content in the supernatant rose to the levels seen with the un-activated samples. This suggests that the increase in intracellular cholesterol in MDMs activated with CRP is accompanied by reduced FC in the culture supernatant and the presumption that this is therefore retained within the MDMs.
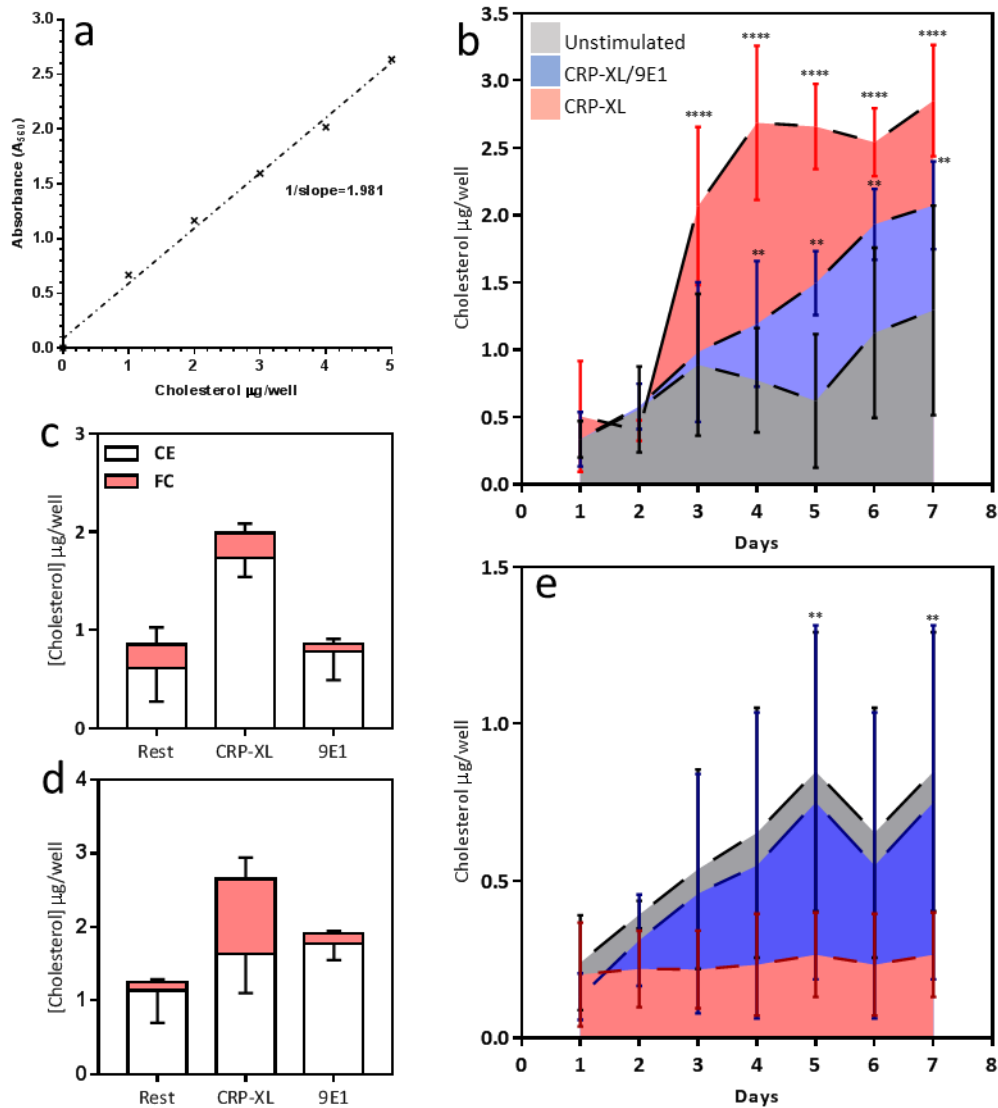
Figure 5.6: Cholesterol Content in Platelet-Activated MDMs. A standard curve is shown (a) using manufacturer-supplied known concentrations of cholesterol for which corresponding absorbance at 570nm was recorded. Total cholesterol content in MDMs is shown (b) for samples activated with CRP-XL (red), CRP-XL and 9E1 (blue) and a HBS vehicle control (grey). Graph shows mean±SD of cholesterol content at on different days in culture. CRP-XL induced significantly more cholesterol content in MDM than both unstimulated and 9E1 incubated samples. Colorimetric assay was performed for cells on day 3 (c) and day 7 (d) of culture showing total cholesterol content expressed as constituent cholesterol ester (CE-white) and free cholesterol (FC-red). Bars depicts mean±SD. Finally, cholesterol content was quantified in the culture medium of MDMs (e) stimulated with CRP-XL (red), CRP-XL and 9E1 (blue) or with a vehicle control (grey). * = p<0.05, ** = p<0.01, *** = p<0.005, ****=p<0.001.

5.2.3 Inhibitors of cholesterol metabolism in cultured MDMs

We have demonstrated that uptake of platelets by monocytes is an important mechanism by which foam cells are formed using the current cell culture model. The formation of foam cells in MDMs is a result of the delicate balance between cellular processes that mediate uptake, synthesis and efflux of cholesterol and its intermediaries (**Figure 5.7**). We sought to examine the effects of platelets on individual mechanisms of lipid droplet synthesis in MDMs. Lipid, and specifically LDL, is taken up by cells through clathrin-mediated endocytosis. Agents are available to inhibit this process but were not used as within the serum-free methodology employed in this thesis, there were no exogenous LDLs added to the culture system. However, lipids are ingested into MDMs by both pinocytosis and phagocytosis with are inhibited by amiloride and cytochalasin D, the latter being an inhibitor of tubulin arrangement required for both processes. Cholesterol is also synthesised within the cell and can be inhibited through blockage of HMG Co-A reductase using simvastatin. Finally, efflux of cholesterol can be inhibited using Glibenclamide which is a potent inhibitor of the ABCA1 and ABCG1 transporter cassette proteins.
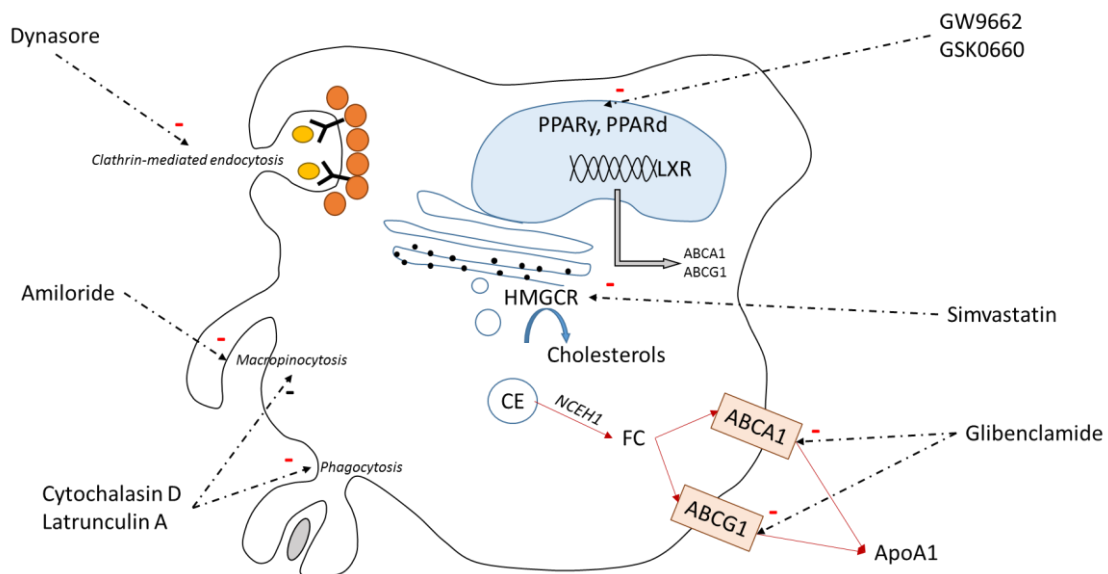
Figure 5.7: Overview of the Main Mechanisms of Lipid Droplet Formation in MDMs. Clathrin-mediated endocytosis is responsible for the uptake of LDL receptors complexed to LDL. Both pinocytosis and phagocytosis rely on the re-arrangement of the actin cytoskeleton. Pinocytosis is a mode of endocytosis in which small particles suspended in extra-cellular medium. Phagocytosis is responsible for the endocytosis of solid particles and internalisation as a phagosome. Cytochalasin D and Latrunculin A is a potent inhibitor of actin polymerisation and therefore inhibits both pinocytosis and phagocytosis. Amiloride inhibits epithelial sodium channels and therefore inhibits pinocytosis. Both PPARγ and PPARδ is responsible for the transcription of ABCA1 and ABCG1 through LXR and is inhibited by the compounds GW9662 and GSK0660. Cholesterol esters, stored as intracellular lipid droplets, is degraded into free cholesterol (FC) by NCEH1. The intracellular free cholesterol is toxic and is exported by ABCA1 and ABCG1 to ApoA1. Glibenclamide acts to inhibit the effects of ABCA1 and ABCG1 to inhibit cholesterol export. Another major mechanism of cholesterol synthesis is mediated by the HMGCR enzymes tethered to the endoplasmic reticulum. This is readily inhibited by Simvastatin.

The selection of concentration of different inhibitors was based on the existing literature. Cytochalasin D was used to inhibit phagocytosis of microglial cells at 10µM (**Ting-Beall *et al.* 1995**) and in more recent studies a concentration of 10µM was shown to inhibit >90% of phagocytosis of Streptococcus *pneumoniae* by murine microglia (**Ribes *et al.* 2010**). Macropinocytosis is differentiated from other types of endocytosis by its unique susceptibility to inhibitors of Na$^+$/H$^+$ exchange. Amiloride (1mM) or Latrunculin B (10µM) both are effective inhibitors of micropinocytosis acting predominantly through lowering submembranous pH (**Koivusalo *et al.* 2010**). This was confirmed in other studies of vaccinia virus entry into dendritic cells (**Sandgren *et al.* 2010**) at a similar concentration of Amiloride (1mM). By virtue of their structural similarity, the ATP Cassette transporters ABCA1 and ABCG1 are inhibited by the sulphonylurea antagonists (**Hasko *et al.* 2002**) and other members within this family of inhibitors (**Dean *et al.* 2001**). Glibenclamide at a dose of 10µM was found to inhibit the ATP-dependent cassette transporters (**Hasko et al. *2002***). Finally, statins have a well-established role in reducing cholesterol and its main mechanism of action is through inhibition of the HMG CoA Reductase enzyme required for cholesterol synthesis (**Stancu and Sima *2001***). They have been used at concentrations of 1µM in THP-1 cells to inhibit cholesterol synthesis (**Yoshida *et al.* 2001**). Importantly, all of these concentrations are within the range wherein viability is maintained in the cultured MDMs and yet has been shown to be effective in inhibiting the relevant mechanism of action.

5.2.3.1 *Effects of Inhibitors of Cholesterol Metabolism on Platelet-Induced Foam Cell Formation*

Blood from healthy donors (n=3) was collected into 3.2% trisodium citrate anticoagulant (BD Vacutainer) and prepared to give both washed platelets and isolated monocytes as per the standardised method. Both isolated monocytes and platelets were re-suspended in HBS (pH 7.4) at a concentration of 1x10^6/ml and 1000x10^6/ml respectively. For each donor, aliquots of monocytes were incubated either un-activated platelets or platelets with 1.0µg/ml CRP-XL in a fixed 1:250 stoichiometry of monocytes to platelets and compared with a control HBS sample. In addition to the comparison between quiescent and activated platelets, samples were also incubated within various inhibitors of cholesterol metabolism. Samples were incubated with Amiloride (1mM), Cytochalasin D (10µM), Glibenclamide (10µM) and Simvastatin (1µM) and incubated for 4 hours at 37°C on slow rotation. Following the incubation period, samples were then centrifuged at 1500G for 5mins to pellet the cells, re-suspended in serum-free medium at a concentration of 1x10^6/ml monocytes and cultured in 24-well plates. To these cells, the corresponding inhibitor was added at the same effective concentration and cultured for 3 days. Following this incubation period, the cholesterol content in these MDMs were quantified by

colorimetric assay Following the 3-day incubation period, cholesterol content in monocyte-derived macrophages was quantified by colorimetric assay and expressed as the Absorbance at 560nm (**Figure 5.8**).
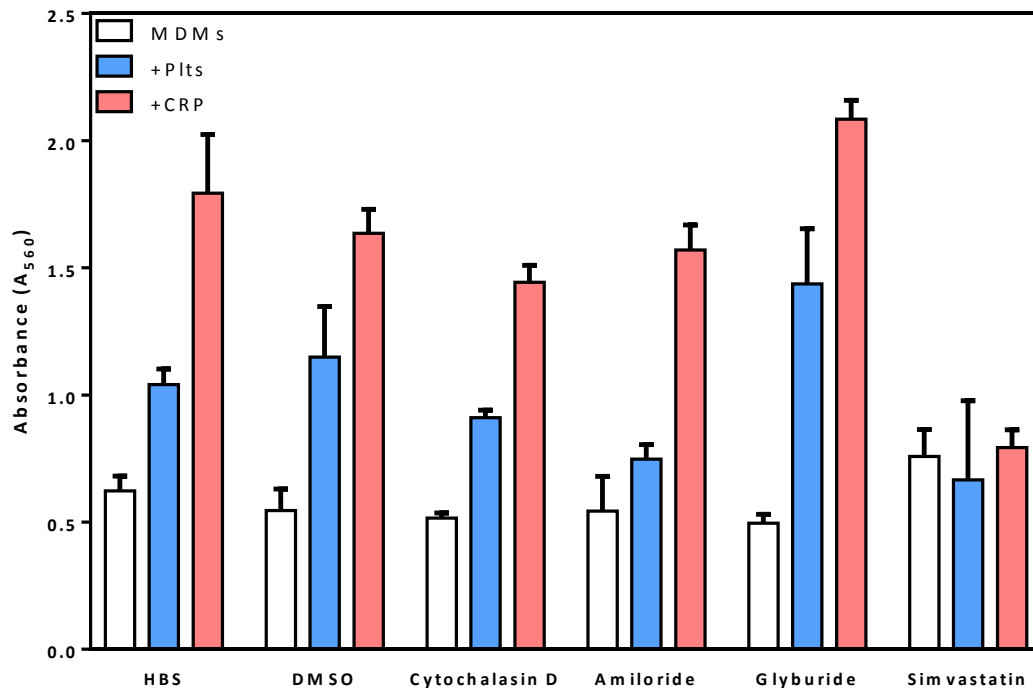
Figure 5.8: Cholesterol Content of Platelet-Activated MDMs with Inhibitors of Lipid Metabolism. Bars represent mean±SD of absorbance at 560nm from a total of n=3 donors which correlates with cholesterol content. Data is shown from unstimulated MDMs (white), MDMs incubated with platelets (blue) and MDMs incubated with CRP-activated platelets (red). Additionally, culture was performed in the presence of HBS, DMSO, Cytochalasin D, Amiloride, Glyburide (Glibenclamide) and Simvastatin at previously pre-specified doses.

In the MDMs incubated either with a control HBS or DMSO (1%), CRP-XL induced a significant (p<0.05) increase in the cholesterol content when compared to un-activated MDMs. Neither Cytochalasin D nor Amiloride had a significant effect on the increase in MDM cholesterol content in the platelet-activated MDMs (p>0.05). Furthermore, there was no effect of either drug on platelet-naïve samples indicating that neither uptake of exogenous lipids is not the major mechanisms by which foam cells are formed using this culture system. Incubation with Glyburide led to significantly increased formation of intracellular cholesterol in MDMs when incubated with both quiescent (p=0.024) and CRP-activated platelets (p=0.035). Conversely, simvastatin led to a significant attenuation (52.9%, p<0.0001) of CRP-induced increase in intracellular cholesterol content. These data suggest that both cholesterol efflux and synthesis are involved.

5.3 Platelets Induce Lipid Droplet Formation in Circulating Monocytes

The results from this chapter have demonstrated that activated platelets promote a foam-cell phenotype in MDMs. However, one of the central tenants of the hypotheses posed at the start of this thesis is that it is the early interaction of platelets with monocytes that drive this pro-atherogenic change. Following on from the analysis of MDMs, the effect of activated platelets on circulating monocytes was therefore examined with respect to the formation of intracellular lipid droplets and promotion of a pro-atherogenic phenotype.

5.3.1 Transcriptomic Analysis of Platelet-Activated Monocytes

Transcriptomic data from work previously conducted within the laboratory by Dr Unni Krishnan[26] was re-analysed, focussing on genes involved in lipid metabolism. This previous study had explored gene expression, using genome-wide microarray analysis, of monocytes extracted from citrated blood from 19 healthy subjects, that has been incubated for 4 hours with CRP-XL at a final concentration of 1µg/ml; a concentration selected to induce maximal MPA formation and P-selectin expression (>90%). Monocytes were isolated from both stimulated and unstimulated blood samples (collected into EDTA anticoagulant), using CD14-coated Dynabeads (Invitrogen #11149D) according to manufacturer's instruction (25µl beads/ml blood). Monocytes attached to beads were washed with PBS and lysed for 5 mins with TRIzol reagent (Ambion #15596-026). RNA was then isolated using a combination of chloroform/phenol extraction and purification using a membrane column (RNeasy Columns, Qiagen #74106). Samples were hybridised to an Ilumina Human-6 v2 expression BeadChip array (Illumina Inc, San Diego, CA). The single colour fluorescent signal intensities of each probe set on the array were quantified by the BeadArray Reader and then analysed using BeadStudio (Ilumina).

5.3.1.1 Results

Based on their involvement in cholesterol metabolism and lipoprotein signalling, 93 genes were identified in the literature and corroborated with those probes found on the SAB Biosciences Human Lipoprotein Signalling & Cholesterol Metabolism PCR array (**Zhou *et al.* 2009**). Of those, 45 were present as probes on the original microarray and the expression of these genes was compared between unstimulated monocytes and monocytes after 4 hours of incubation with CRP-XL. Signal intensity of the probes were compared between resting and stimulated samples and expressed a $\log_2$ fold-change (**Figure 5.9**).

---

[26] Identification of Novel Genes Involved In Coronary Atherothrombosis by Blood Cell Transcriptome Profiling. Unni Krishnan (PhD thesis 2012)
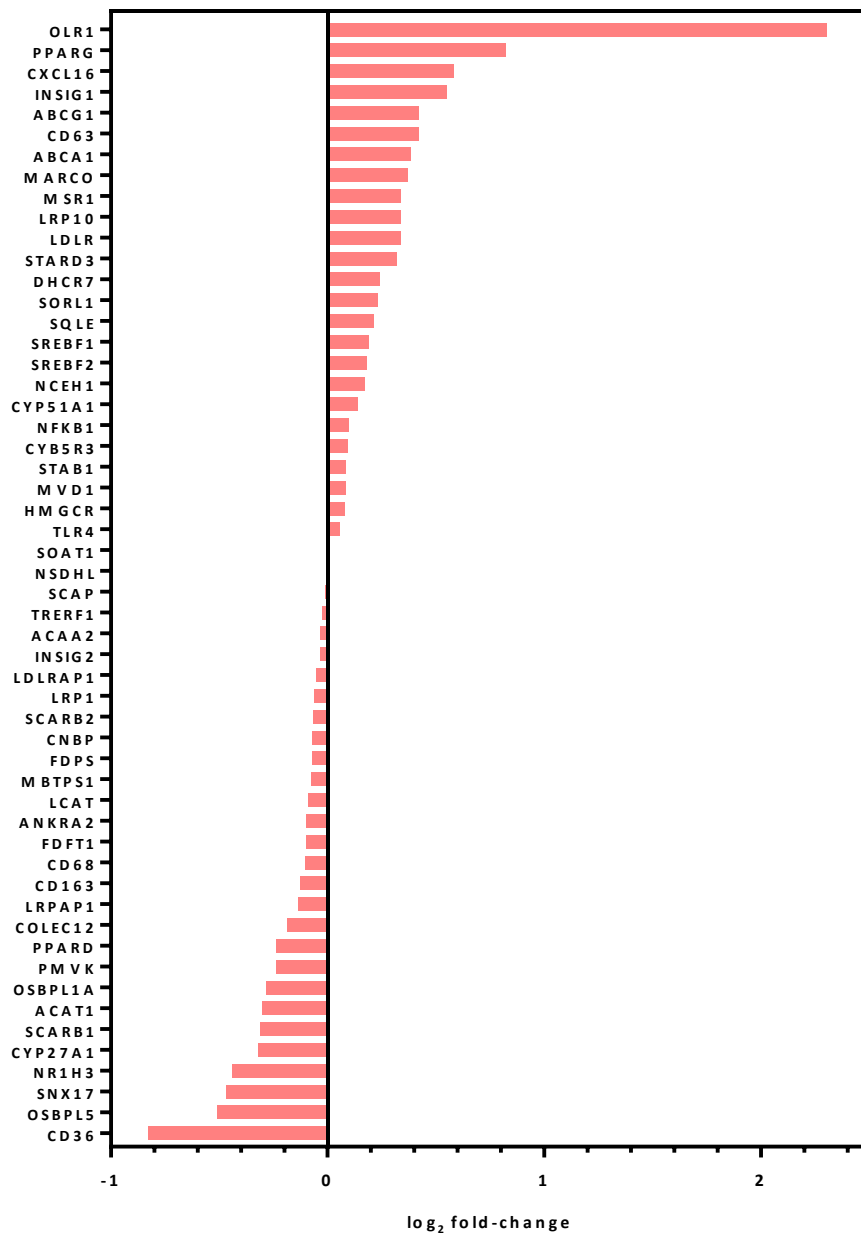
Figure 5.9: Expression of Genes involved in Cholesterol Metabolism in Platelet-Activated Monocytes. Data is expressed as $\log_2$ fold-change of signal-intensity on the Illumina probe. Gene IDs are given for individual genes and arranged from the highest to lowest expressing.

There was significant differential regulation of a key number of genes relating to the uptake, efflux and degradation in platelet-activated monocytes. One of the most highly upregulated genes was OLR1 (>200-fold) which encodes the oxidised LDL receptor (LOX-1); a member of the C-type lectin superfamily, its function is to bind, internalise and degrade oxLDL and plays a role as a scavenger receptor. This is one of a number of scavenger receptors (SR) involved in the

uptake of oxidised lipid and its role has been identified as of paramount importance in the formation of foam cells and pathogenesis of atherosclerosis (**Xu *et al.* 2013**). Other scavenger receptors were also upregulated in platelet-stimulated monocytes. These included MARCO (2.34-fold) and MSR1 (2.19-fold), which are both members of the macrophage class A scavenger receptor and avidly take up oxLDL. PPARγ and PPARδ are both members of a superfamily of ligand-dependent transcription factors that have key roles in macrophage foam cell formation. Mouse models have shown that genetic deletion of PPARγ resulted in an increased development of atherosclerotic plaques (**Chawla *et al.* 2001**) whereas PPARδ resulted in an increased development of atherosclerotic plaques (**Lee *et al.* 2003**). Both of these genes were upregulated in platelet-stimulated monocytes, which further supports the idea that the action of platelets per se can be both pro and anti-atherogenic. There was increased expression of cholesterol transporters ABCA1 and ABCG1 accompanied by increased expression of STARD3 encoding the StAR-related lipid transfer domain protein 2, responsible for the trafficking of free cholesterol from the late endosome to mitochondria. These transcriptional changes suggest that the interaction of platelets 'prime' the monocytes to deal with an increased lipid load. Interestingly, there was also upregulation of the LDLR gene encoding the low-density lipoprotein receptors responsible for the uptake of native LDL into monocyte-macrophages.

Other genes that were upregulated included those involved in cholesterol biosynthesis including HMCGR encoding the HMG CoA reductase and MVD encoding mevalonate decarboxylase. Conversely, PRKAG2 was upregulated which encodes for the AMP-activated protein kinase (AMPK), which inactivates key enzymes involved in de-novo synthesis of fatty acids and cholesterol.

A number of genes were also significantly downregulated. OSBPL5 encodes for oxysterol binding protein and belongs to a large and evolutionarily conserved family of lipid-binding proteins that target organelle membranes to mediate sterol signalling and/or transport. Knockdown of OSBPL5 causes cholesterol accumulation in late endosomes and lysosomes and co-operates with NPC1 to mediate exit of cholesterol from these organelles (**Du *et al.* 2011**). Monocytes downregulated OSBPL5 and OBBPL1 in response to platelet activation. There was also significant downregulation of SNX17 encoding the sorting nexin-17 protein. This is an adaptor protein known to play a key role in the recycling of low-density lipoprotein receptor-related protein (LRP1) (**Farfan *et al.* 2013**) and thus its downregulation promotes the expression of LDL receptors on monocytes. Another significantly downregulated gene was CYP27A1 encoding sterol 27-hydroxylase. Overexpression has been shown to enhance LXR-dependent apoA1 and ABCA1-dependent cholesterol efflux (**Taylor *et al.* 2010**)

The genes on the array were additionally grouped according to their predominant function[27] on intracellular cholesterol stores (**Figure 5.10**). This includes uptake, synthesis, degradation, efflux and genes involved in intracellular trafficking.
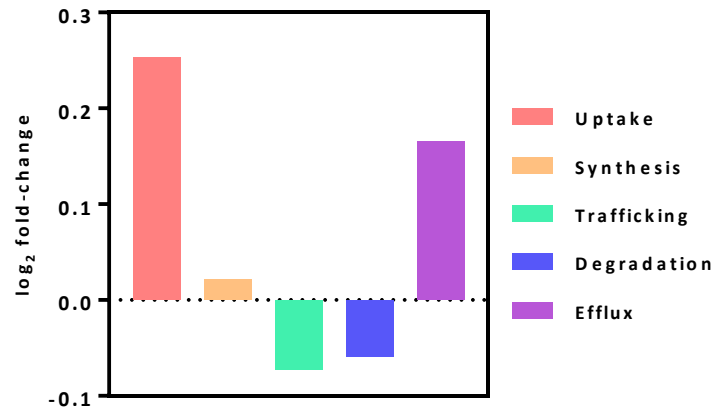
Figure 5.10: Aggregated Expression of Cholesterol-Related Genes. Data is expressed as mean $\log_2$ fold-change signal intensity of genes in platelet-activated monocytes. Bars represent the mean of all genes that are grouped into different functional classes.

This method serves as an overview of the functional relevance of differential gene expression in platelet-activated monocytes. There was an overall increase in the expression of genes involved in cellular cholesterol uptake driven predominantly by the upregulation of scavenger receptors. This was accompanied by more modest decreases in genes responsible for intracellular degradation and trafficking of lipids. In contrast to these findings, there was an increased expression of genes involved in the efflux of intracellular cholesterol esters driven predominantly by the ABCG1 and ABCA1 genes. It is interesting to note that activated platelets induce the upregulation of both cholesterol efflux genes and those involved in the uptake of lipids and is likely a physiological response to an increased overall lipid load.

---

[27] This was guided by the KEGG Pathway Database

5.3.1.2 OLR1 Protein (LOX-1) is Increased on Platelet-Activated Monocytes

To assess if changes in gene transcription were reflected in the protein expression, confirmatory experiments were performed to quantify the expression of LOX-1, the protein encoded by OLR1, the most highly upregulated gene in platelet-activated monocytes. Blood from healthy volunteers (n=3) was collected into either CTAD (to minimise platelet activation) or citrate tubes and incubated for up to 8 hours at 37°C. To the Citrated tubes, CRP-XL was added (1.0µg/ml) and the surface expression of LOX-1 was quantified by flow cytometry (**Figure 5.11**).
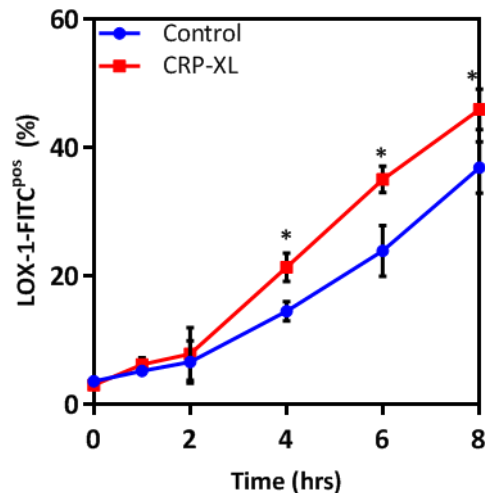
Figure 5.11: Expression of LOX-1 on Platelet-Activated Monocytes. Graph shows the percentage of monocytes that stained for LOX-1-FITC antibody (percentage positive) over an 8-hour incubation period. Surface expression of LOX-1 is increased in both samples but is more so in platelet-activated monocytes. '*'=p<0.05.

Un-activated monocytes show a progressive increase in the surface expression of LOX-1 over the 8-hour incubation period to a peak of 36.9±4.0%. However, monocytes from samples activated with CRP-XL showed a maximum expression of 45.9±3.2% at 8 hours which was significantly more than with un-activated monocytes (p=0.037). This difference in surface expression of LOX-1 was observed from 4 hours onwards (p=0.011).

5.3.2 Platelets Induce the Formation of Intracellular Lipid Droplets in Primary Human Monocytes

To follow on from the transcriptomic analysis, a whole blood model was used to quantify lipid droplets in monocytes using flow cytometry. Blood from healthy volunteers was collected into 3.2% trisodium citrate (BD Vacutainer) and incubated, with appropriate agonists and inhibitors, for up to 24hrs at 37°C on slow rotation. During the incubation period, 50μl aliquots of blood was taken at regular time intervals, stained and analysed by flow cytometry for fluorescence intensity of Nile Red as a marker for intracellular lipid droplet formation (see Methods 3.2.5.4).

5.3.2.1 Activated platelets induce intracellular lipid droplet accumulation in monocytes

Aliquots of 1ml of whole blood from healthy volunteers (n=5) was incubated for up to 24hrs with CRP-XL (1.0μg/ml) to specifically activate platelets through GPVI. CRP-activated samples were compared with samples incubated with both Lipopolysaccharide (LPS) or a vehicle control (HBS). In this instance, LPS was used as a positive control as it has been shown to induce foam cell formation (**An** *et al. 2017*). Flow cytometric analysis of Nile Red Fluorescence intensity was performed after 10mins, 1hr, 2 hrs, 4hrs, 6hrs and 24hrs of incubation. Both LPS and CRP-XL significantly increased the Nile red fluorescence intensity of circulating monocytes over a 24hr period, above that seen with a vehicle control alone (p=0.0003, 2-way RM-ANOVA). Over this same time period, there was no overall significant difference between the two agonists with respect to Nile Red fluorescence intensity (p=0.27, 2-way RM-ANOVA). Upon comparison of individual time points, CRP-stimulated samples showed significantly greater formation of monocyte lipid droplets than either vehicle control or LPS-activated samples at 10mins (p=0.022) and 1hr (0.021) but no significant difference thereafter (p>0.05, multiple t-tests). This difference was most marked within 10mins of activation with either CRP or LPS.

Although LPS is known to be a direct activator of monocytes, confirmatory experiments were performed to ascertain whether it also caused platelet activation. Whole blood (n=1) was activated with either LPS (0.5μg/m) or CRP-XL (1.0μg/ml) for 30mins at room temperature on slow rotation. Samples were taken for analysis by flow cytometry for both the expression of P-selectin on the surface of platelets (P-selectin assay) and the formation of monocyte-platelet aggregates (MPA assay) using standard protocols (described in sections 3.2.5.1 and 3.2.5.2 Consistent with the experimental work so far, CRP-XL induced maximal (>98%) expression of surface P-selectin on platelets and >90% formation of monocyte-platelet aggregates. LPS on the other hand did not induce expression of P-selectin any more than that seen in the isotype control, although it did induce a 10.4% increase in the MPA formation.

Next, the important of direct platelet contact with monocytes (as detected by MPA formation) and induction of gene transcription in the accumulation of lipid droplets by monocytes was ascertained. Whole blood from healthy volunteers (n=5), activated with CRP-XL, was co-incubated with 20mg/ml of the anti-hpselectin antibody (Abcam) to inhibit MPA formation and 20mg/ml Actinomycin D (Sigma-Aldrich) to inhibit gene transcription. Samples were incubated for 24hrs at 37°C and analysed, by flow cytometry, at regular time intervals for Nile Red fluorescence intensity as a marker for lipid droplet formation (**Figure 5.12**).

Recapitulating previous experimental data, CRP-XL induced a significant ($p<0.001$) and sustained increase in both the proportion of monocytes that stained with NR (**Figure 5.12**, d) and their median fluorescence intensity (**Figure 5.12**, c) ($p<0.0001$ for both). This difference began at 10 minutes, fell slightly by 1 hour but then increased steadily up to 24hrs when compared to a vehicle control. When activated in the presence of 9E1, overall Nile Red fluorescence (over the 24-hour incubation period) was attenuated by 54.5±4.2% (Area under curve, $p<0.05$) but not back down to the levels seen with a vehicle control alone. This observed difference was particularly apparent in samples incubated for up to 4 hours of incubation after which levels of NR staining plateau or, at most, rise modestly. The addition of Actinomycin D to CRP-activated whole blood led to an overall modest reduction in NR fluorescence (AUC 24.26±1.557%, $p<0.05$) but this was only seen after 4 hours. When both 9E1 and Actinomycin D were incubated with CRP-activated samples, the combination further reduced NR fluorescence by 60.93% ($p<0.05$) and this effect was seen from 10mins onwards and sustained for the 24-hour incubation period. From 4 hours onwards, the addition of Actinomycin D led to a greater inhibition of NR fluorescence than 9E1 alone but did not reduce overall staining back down to levels seen with the vehicle control. These results suggest that the induced increase in monocyte NR staining is dependent on direct contact of monocyte and platelets up to the 4-hour time point, and then on gene transcription thereafter.
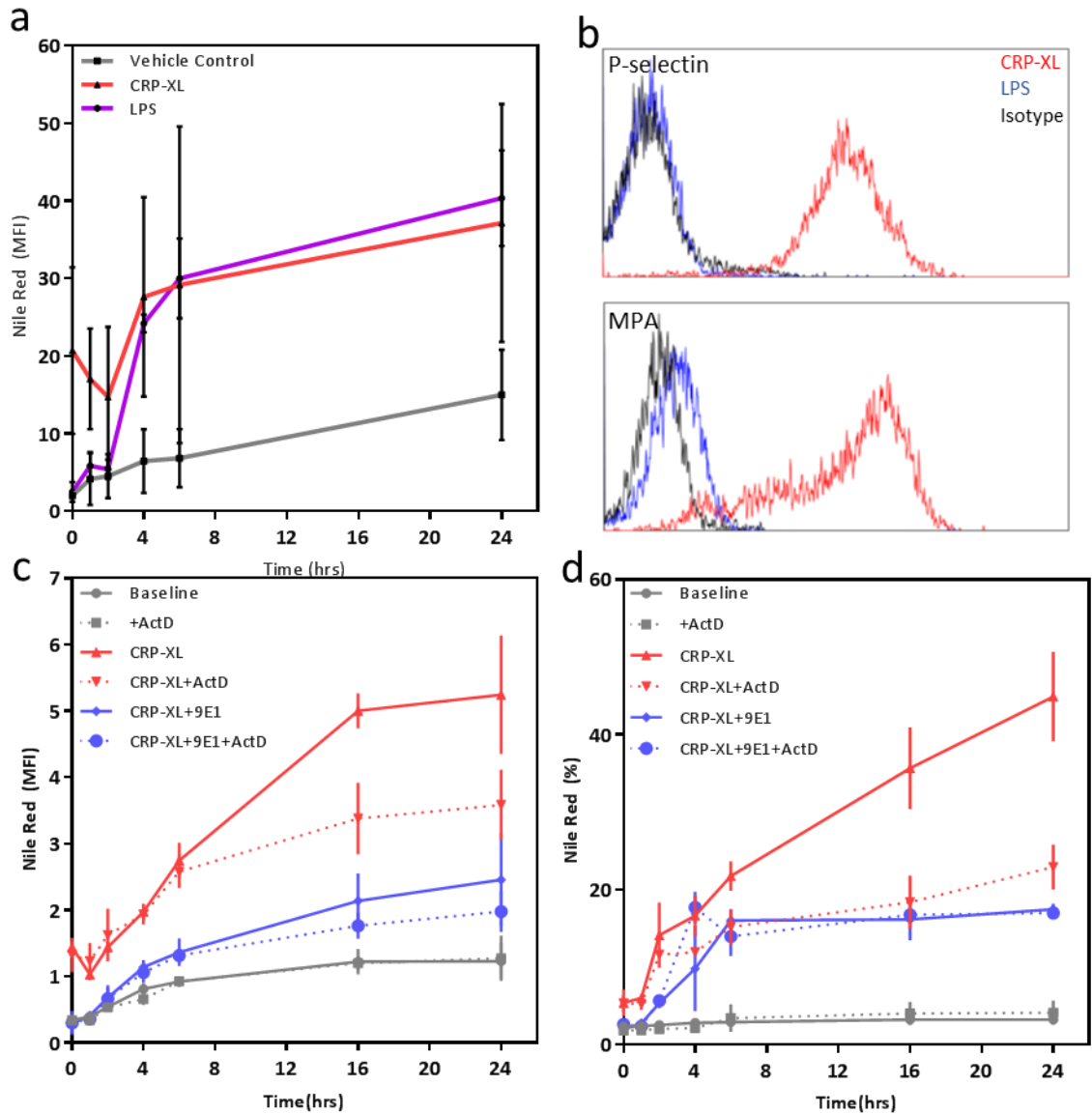
Figure 5.12: Flow Cytometric Quantification of Intracellular Lipid Droplets in Platelet-Activated Monocytes. (a) median fluorescence intensity (MFI) of Nile red in whole blood monocytes is shown, stimulated with either CRP-XL (red), Lipopolysaccharide (LPS-purple) or a vehicle control (grey). Data is shown over a 24hr period and points represent mean±SD. (b) shows representative histogram of both p-selectin and MPA formation on whole blood monocytes stimulated with either LPS or CRP-XL, along with an isotype control. CRP-XL induces almost maximal expression of P-selectin and MPA formation but not LPS. Whole blood was activated with CRP-XL (red) with(out) 9E1 (blue) to inhibit the formation of MPAs. Additionally, samples were incubated with actinomycin D (dotted line) to inhibit gene transcription. Data is shown for both median fluorescence intensity (c) and % positive (d) of Nile red fluorescence in monocytes. Data are shown as mean±SD.

5.3.2.2 Confocal Microscopic Confirmation of Intracellular Location of NR^pos Lipid Droplets

WB was incubated with 1.0μg/ml of CRP-XL for 4 hrs at 37°C on slow rotation. PBMCs were isolated by density-gradient centrifugation and depleted of platelets and MPAs by CD61 immunomagnetic separation. The platelet-free PBMCs were re-suspended in RPMI-1640 (Sigma-Aldrich) and plated in 6-well slides (LabTek, Thermo-Fisher) at a concentration of 1.0×10^6/ml. Excess contaminating lymphocytes, and any residual platelets, were washed off and the adherent monocytes were immediately fixed with 4% PFA. Cells were stained with Nile Red for lipid droplets and DAPI (Sigma-Aldrich) as a nuclear counterstain. Cells were washed, and the slides were viewed under confocal microscopy (Olympus FV1000) (**Figure 5.13**).

Nile Red was found to homogenously stain the cell membrane in line with its mechanism of action as a marker of neutral cholesterol esters. In addition to this, discreet droplets of cholesterol esters were visible within the cell cytoplasm that were readily distinguished from the cell membrane. The intracellular location of discreet lipid droplets was confirmed by multiple images taken within the XZ plan and Z-stacked to create a 3D reconstruction using Fiji Software. Lipid droplets seen initially in the XY plane were mapped to the corresponding lipid droplet both in the XY and YZ plane which correlated with an intracellular location.
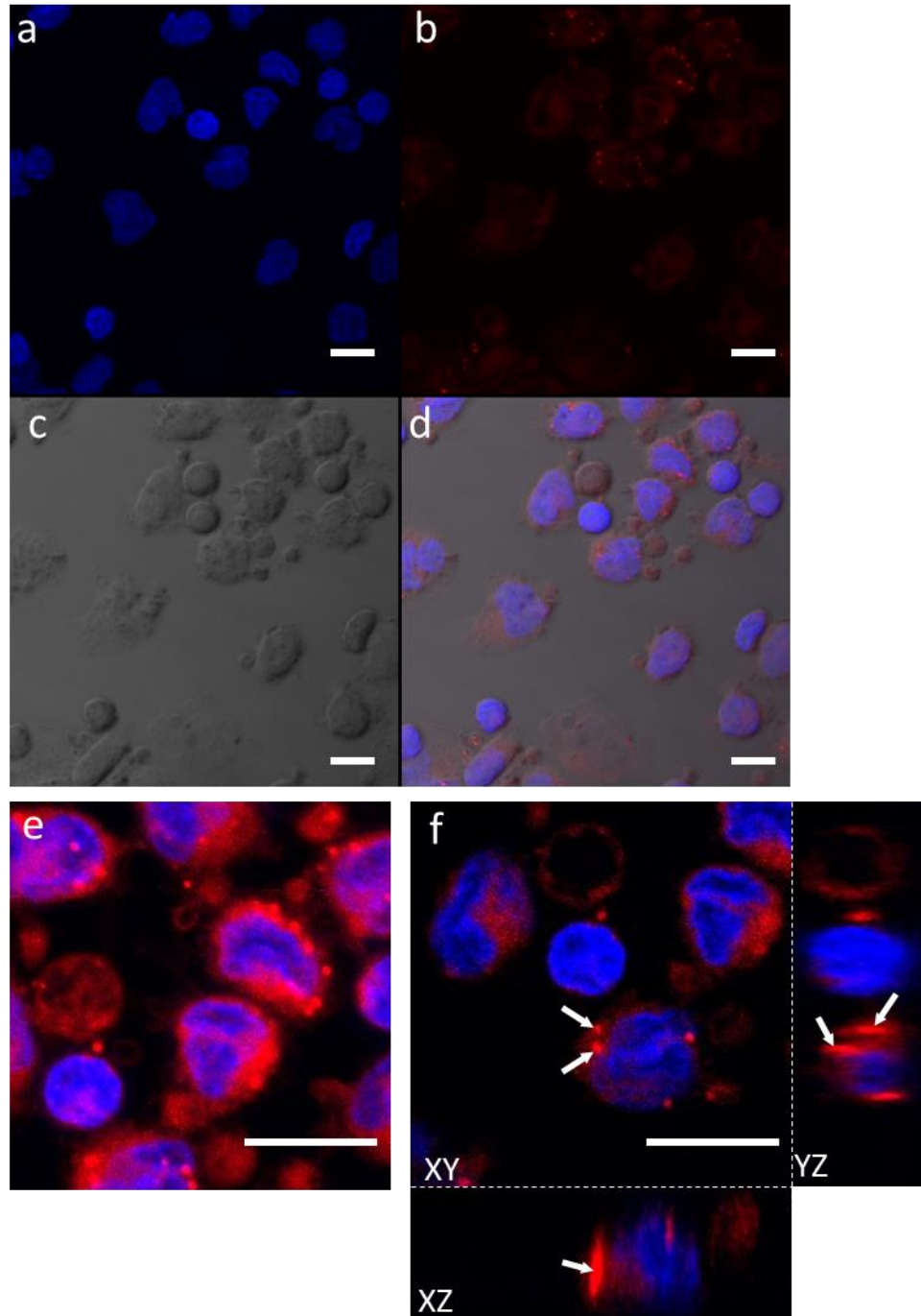
Figure 5.13: Confocal Microscopy of Platelet-Activated Monocytes. Panels (a) and (b) show representative images of platelet-activated monocyte visualised through a DAPI filter (a) and a Nile Red filter (b). Cells were also visualised by transmission light microscopy (c) and combined to give image (d). A maximum intensity projection is shown in (e) with the exclusion of light transmission. This does not clearly delineate the location of lipid droplets. However, confocal imaging (panel f) shows the location of these droplets, initially seen in the XY plane, in the XZ and YZ planes (white arrows). White bars represent 10μm.

5.3.2.3 Activated Platelets are Endocytosed by Monocytes

5.3.2.3.1   Uptake of Platelets by Monocytes

Blood was from healthy volunteers (n=3) was collected in 3.2% trisodium citrate and centrifuged to separate PRP and platelet-deplete blood. From PRP, washed platelets were prepared (Section 3.2.2.3) and stained with PKH67 membrane-linker dye (Section 3.2.4.2) and the excess stain was removed from the supernatant by centrifugation and re-suspension in HBS. Autologous PBMCs were prepared in parallel and platelets were depleted using CD61 immunomagnetic bead separation. The PKH67-stained platelets were then incubated with (unstained) PBMCs in a 1:250 fixed stoichiometry, for 30mins. Samples were also incubated with either 1.0µg/ml CRP or 1.0µg/ml CRP + 20µg/ml anti-hpselectin (9E1) to inhibit MPA formation. The samples were then passed through a magnetic cell separator using CD61 microbeads (Miltenyi Biotec) to remove residual free platelets and monocytes with attached platelets. PBMCs were analysed by flow cytometry both before and after CD61 depletion to quantify PKH67 staining in monocytes (**Figure 5.14**).

In PBMCs incubated with PKH67^{pos} platelets, there was a significant increase in both the proportion (p=0.0001) and median fluorescence intensity (p=0.0028) of PKH67 staining on monocytes. This difference was more marked in when platelets were activated with CRP-XL as, in these samples, 24.53% of monocytes were PKH67^{pos} as compared with 7.27% when incubated with platelets alone. Samples activated in the presence of 9E1 to inhibit MPA formation showed that 9.67% of monocytes were positive for PKH67 however there was no significant difference in the median fluorescence intensity above control (p>0.05).

Following CD61 immunomagnetic depletion, monocytes from PBMCs incubated with un-activated platelets showed a significant decrease (p<0.0001) in the proportion of PKH67^{pos} monocytes accompanied by a significant decrease in the median fluorescence intensity (p=0.004). The magnitude of difference between CD61-depleted and non-depleted samples was found to be greater for CRP-activated samples (p<0.001). However, CD61-depletion did not reduce levels of PKH67 staining back to baseline. These results show that activated platelets form complexes with monocytes through the p-selectin/PSGL1 interaction. However, even in the presence of 9E1, ~10% of monocytes stain positive for PKH67 which is not significantly reduced (p>0.05) following depletion with CD61 microbeads suggesting that this increase in staining is not due to adherent platelets. Furthermore, following activation with CRP, depletion of platelets led to a >50% attenuation in PKH67 staining (p<0.001) however, it did not reduce to baseline. This suggests, along with the data on 9E1, that part of the PKH67 staining seen in monocytes is attributable to intracellular accumulation of platelet-derived PKH67 dye.
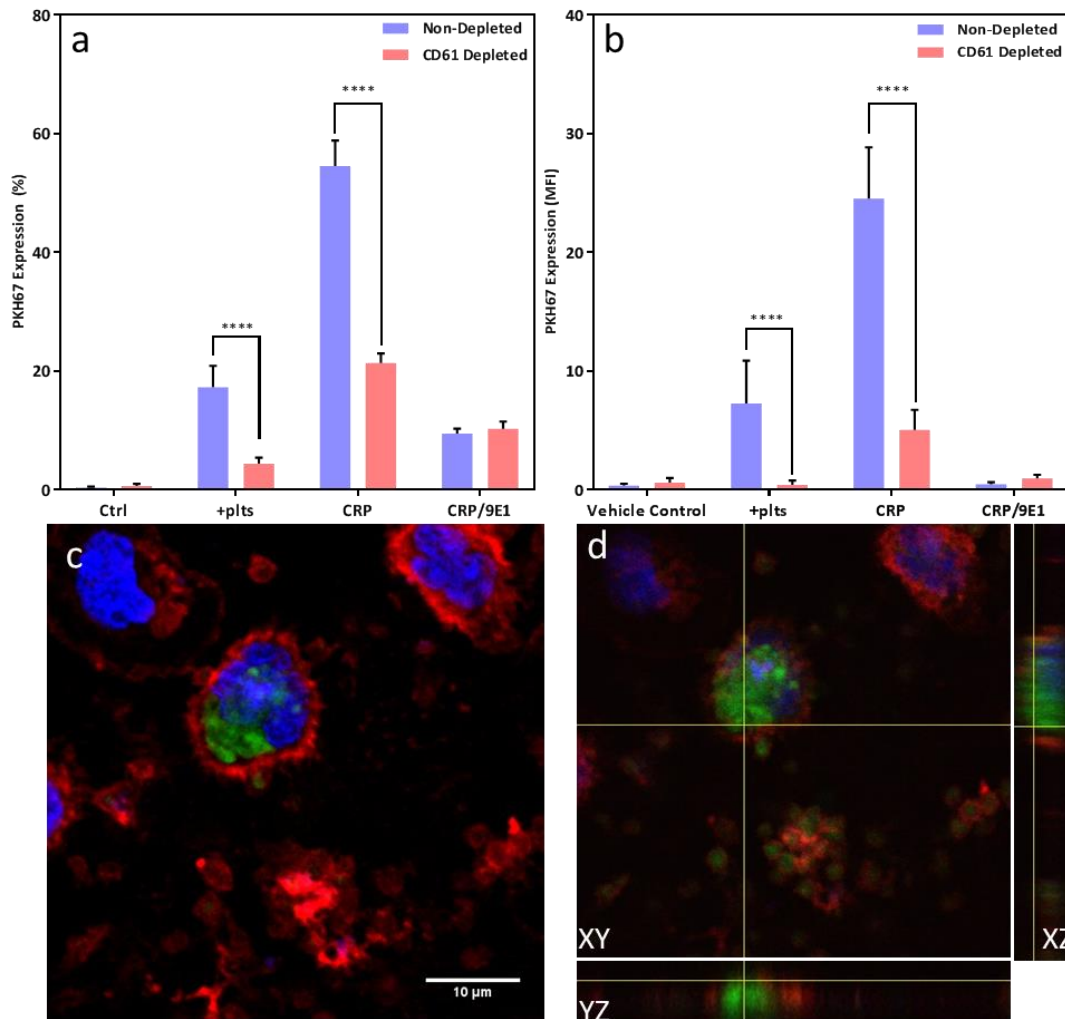
Figure 5.14: Uptake of PKH67^pos Platelets by Monocytes. Graphs depicts both % positive (a) and median fluorescence intensity (b) of monocytes in different incubation conditions. PKH67^pos platelets were incubated with PBMCs (+plts) and activated (+CRP) with an additional anti-hpselectin antibody to inhibit MPA formation (CRP/9E1). Bars depict mean±SD (n=3) with blue bars shows samples without and red bars with depletion with CD61 microbeads. (c) and (d) both show confocal microscopy images of monocytes incubated with PKH67^pos platelets. (c) and (d) show representative confocal microscopy of monocytes stained with wheat germ agglutinin (red) and a DAPI (blue) nuclear counterstain. Platelets are stained with PKH67 (green). (c) shows maximum intensity projection of platelet fragments mount within the cell membrane of monocytes. (d) confirms the intracellular location and demonstrates a single z-stack segment with the location of platelet fragments intracellularly in all three planes.

5.3.2.3.2   Confocal Microscopy confirms that platelets are taken up by monocytes

Both PBMCs and washed platelet were prepared from whole blood collected into 3.2% trisodium citrate. Washed platelets were stained with the PKH67 membrane dye and incubated with PBMCs for 10mins at 37°C on slow rotation along with 1.0μg/ml CRP-XL. Following incubation, PBMCs were re-suspended in RPMI-1640 and plated onto 6-well microscope slides and allowed to adhere for 2hrs at 37°C, 5% CO_2. Following incubation, the adherent cells were washed 5 times with RPMI 1640 to remove all non-adherent lymphocytes and free platelets. Samples were fixed with 4% PFA and stained with DAPI nuclear counterstain and WGA (Texas Red) as a

membrane stain. Following staining, samples were imaged using an Olympus FV1000 confocal microscope (**Figure 5.14**). Confocal microscopy demonstrated both monocytes and platelets within the culture model. Platelets were present as free cells, adherent to monocytes in the form of monocyte-platelet aggregates, and also as clumps of platelets in the form of platelet-platelet aggregates. Importantly, the confocal images of the monocytes demonstrated the presence of intracellular staining with PKH67 suggesting that platelets were indeed ingested by monocytes and therefore confirming the findings from flow cytometry.

5.3.2.3.3 Formation of intracellular droplets is independent of platelet uptake by monocytes.

Fluorescent microscopy was used to assess if the endocytosed platelets co-localised with Lipid droplets. Both PBMCs and washed platelets were prepared from whole blood from healthy volunteers. Washed platelets were then stained with PKH67 membrane linker dye and incubated with PBMCs for 4 hours at 37°C on slow rotation along with 1.0μg/ml CRP-XL. Following incubation, the platelet-activated PBMCs were plated at 1.0×10^6/ml in RPMI in 24-well plates and allowed to adhere for 2hrs at 37°C, 5%CO_2. The non-adherent cells and free platelets were washed away with further RPMI and the cells were fixed (4% PFA) and stained with LipidTox Deep Red (Invitrogen) and DAPI nuclear counterstain. Cells were imaged in an EVOS fluorescent microscope (EVOS FL).
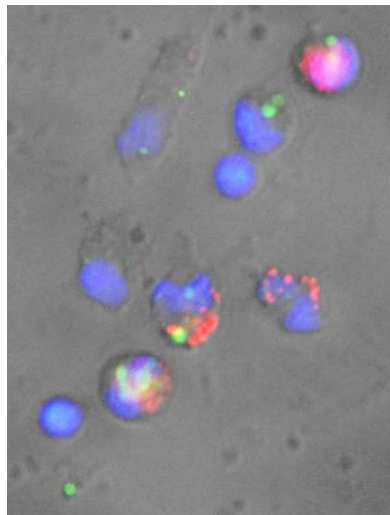
Figure 5.15: Fluorescent Microscopy of Platelet-Incubated Monocytes. Representative image of adherent monocytes (60x zoom) visualised through fluorescent microscopy. Image shows overlay of monocytes viewed by light microscopy with LipidTOX (Cy5 filter), PKH67 (FITC filter) and DAPI nuclear counterstain filter (blue). Images show both intracellular lipid droplets (LipidTOX) and intracellular platelets (FITC) without co-localisation of the staining.

Monocytes activated with platelets demonstrated accumulation of intracellular lipid droplets as quantified by LipidTOX staining. The staining of platelets however did not co-localise with intracellular lipid droplets. These results demonstrate that although phagocytosis of platelets may represent an important mechanism by which monocytes and MDMs also accumulate intracellular lipids, the droplets observed in these experiments accumulated through an independent mechanism.

5.4 Summary

Activation of whole blood with the platelet-specific agonist CRP-XL led to a significant increase in the formation of foam cells in cultured MDMs (Section 5.2.1). Over the 7-day culture period, there were progressive increases in the number and intensity of intracellular lipid droplets in MDMs which suggests that the majority, if not all, are a result of *de-novo* formation. This is supported by the fact that there is no addition of exogenous lipids or lipid intermediaries within the culture system nor is the ingestion of platelets sufficient to account for the lipid droplets seen in MDMs, particularly with increasing days in culture. The formation of *de-novo* lipid droplets is further supported by evidence from the colorimetric cholesterol assays (Section 5.2.2). Firstly, they confirmed the nature of these lipid droplets as cholesteryl esters and the activation of monocytes by CRP-stimulated platelets led to increased concentrations of CE in both the cultured MDMs and in the culture medium from these cells. Examination of the culture supernatant also revealed that significantly less cholesterol is released from platelet-activated, as oppose to un-activated, MDMs which suggests that CE are retained to a greater extent in these macrophages. This is partially in line with the transcriptomic data which has shown decreased expression of genes involved in intracellular trafficking and increased expression of cholesterol synthesis genes in platelet-activated monocytes (Section 5.3.1.1). Assuming that these transcriptomic signals are transmitted to phenotypic signals in MDMs, one would expect increased synthesis and intracellular retention of CE. Conversely, platelet-activated monocytes also expressed a greater amount of cholesterol efflux and transport proteins and would therefore expect an increased amount of CE in the supernatant of platelet-activated MDMs. It is important to note that as the transcriptomic data is derived from 4-hour platelet-activated monocytes, extrapolating the data must be done with caution.

Use of inhibitors of cholesterol metabolism allowed an insight into the likely mechanism(s) by which platelets promote foam cell formation (Section 5.2.3.1). The use of Simvastatin essentially abrogated the increased in foam cell formation attributable to activated platelets. This is

consistent with the transcriptomic data which showed that platelet-activated monocytes exhibited an increase in HMGCR mRNA and therefore, one mechanism of foam cell formation may be through increased production of CE in platelet-activated MDMs with increased intracellular retention through maladaptive cholesterol trafficking mechanisms. Interestingly, the use of Simvastatin, in the absence of activated platelets, did not reduce foam cell formation below that seen with either DMSO or HBS controls. This suggests that the baseline formation of foam cells in this assay is at least partly due to the ingestion of lipids, by MDMs, through other routes and platelets add to this through direct provision of lipid material or through the promotion of *de-novo* lipid synthesis. Conversely, the use of glibenclamide, which inhibits cholesterol efflux through the ABCA/ABCG transporters, led to increased accumulation of intracellular CE in platelet-activated MDMs. The transcriptome of platelet-activated monocytes showed an increase in the expression of the ATP-cassette transporters and may be a mechanism by which platelet 'prime' monocytes for an increased lipid load in MDMs, generated by both platelet-dependent and independent mechanisms. In this assay, inhibition of ABCA/ABCG meant that a mechanism used to efflux the platelet-induced increase in intracellular lipids has been compromised and therefore led to increased accumulation of CE and increased foam cell formation.

In addition to the formation of MDMs, activated platelets also promote the formation of lipid droplets in circulating monocytes. This claim is initially supported by the transcriptomic data (Section 5.3.1.1) which shows differential regulation of a number of genes involved in lipid metabolism. The majority of the analysed genes have perfunctory roles in cellular homeostasis and therefore an extrapolation to their effects on foam cell formation is *non sequitur*. However, there are hints within the platelet-induced transcriptomic signature that suggest that platelet do indeed 'prime' monocytes to become foam cells. Firstly, platelets induce upregulation of a number of scavenger receptors, including OLR1 which is increased over 200-fold in platelet-stimulated samples. Although gene transcription is not always temporally associated with protein expression, in this whole blood assay, OLR1 gene expression is accompanied by surface expression of LOX1 at a 4-hour incubation period.

The transcriptomic signature was mirrored by increased accumulation of intracellular lipids as shown by increased NR staining in circulating monocytes (Section 5.3.2). Within 10mins of activation of CRP-XL, there was a sharp increase in NR staining, not seen with LPS, which was essentially abrogated in the presence of 9E1 to block MPA formation. Nile Red however is a neutral lipid stain and therefore stains the cell membranes of both platelets and monocytes. Platelets also contain lipids other than membrane lipids and therefore the initial NR staining on

monocytes is likely due to bound platelets. However, both CRP-XL and LPS produced a comparable magnitude of NR fluorescence in monocytes after 4 hours of activation which was sustained over the 24hour incubation period suggesting that both stimuli induce intracellular lipid droplets to a similar magnitude. Co-incubation with Actinomycin D, a potent inhibitor of gene transcription, had no significant effect on NR fluorescence within the first 4 hours of incubation. However, from that point onwards, Actinomycin D significantly inhibited monocyte NR staining which once again supports the assertion that the early transcriptomic changes, as a result of platelet activation, are responsible for lipid accumulation in monocytes. This was confirmed with both fluorescent and confocal microscopy demonstrating the intracellular location of these droplets. The earliest studies of the effects of platelets on monocytes showed that platelets are active lipid donors and that the co-incubation of platelets with MDMs resulted in increased phagocytosis and thereby increased foam cell formation (Section 5.3.2.3). This was confirmed by the demonstration that platelets accumulated intracellularly upon activation. Furthermore, the increased intracellular lipid droplet formation within 24hours of activation in monocytes were not necessarily co-incident with platelets. The results of this suggests that the increase in monocyte foam cell formation may be due to both increased gene transcription and increased phagocytosis of platelets by monocytes and MDMs. The use of 9E1 in the WB model inhibited the formation of intracellular lipid droplets and therefore the direct interaction of platelets and monocytes are shown to be important in this process and is consistent with the same finding in MDMs.

Chapter 6: Monocyte Subset Switching in Response to Platelet Activation

6.1 <u>Introduction</u>

Monocyte heterogeneity is a consistent feature across a number of mammalian species and in various models of atherosclerosis, different subsets of monocytes have been shown to have varying effects on plaque formation (**Woollard and Geissmann** *2010*). In addition to the activation of monocytes, platelets, and the subsequent formation of MPAs, have been shown to be associated with increased expression of CD16 on monocytes. However, it is yet to be established if this relationship between MPA formation and CD16 expression is purely associative or indeed if platelets themselves promote the expression of CD16 in previously CD16^{neg} monocytes. This chapter will aim to examine this relationship between platelet activation and CD16 expression on circulating monocytes as well as analysing the phenotypic implications of this.

6.1.1 Differential Formation of Foam Cells in Monocyte Subsets

Blood from healthy volunteers (n=6) was collected into 3.2% trisodium citrate tubes (BD Vacutainer) and PBMCs were isolated by density-gradient centrifugation. Platelets were depleted with a combination of centrifugation to remove PRP and CD61 immunomagnetic bead separation (see methods 3.2.2.7). From the platelet-deplete PBMCs fraction, the CD16^{pos} monocytes were isolated by first depleting the pool of granulocytes (CD15^{pos}) and natural killer cells (CD56^{pos}). This was followed by positive immunomagnetic separation using CD16 microbeads to select the CD16^{pos} monocyte subpopulation (see methods 3.2.2.11). The negative fraction contained the CD16^{neg} monocytes and both fractions were cultured in serum-free media for 3 days and foam cell formation was quantified by flow cytometry as before. An additional arm of the study included the pre-incubation of CD16^{neg} monocytes with CRP-activated, washed platelets for 4hrs prior to their culture in serum-free media.
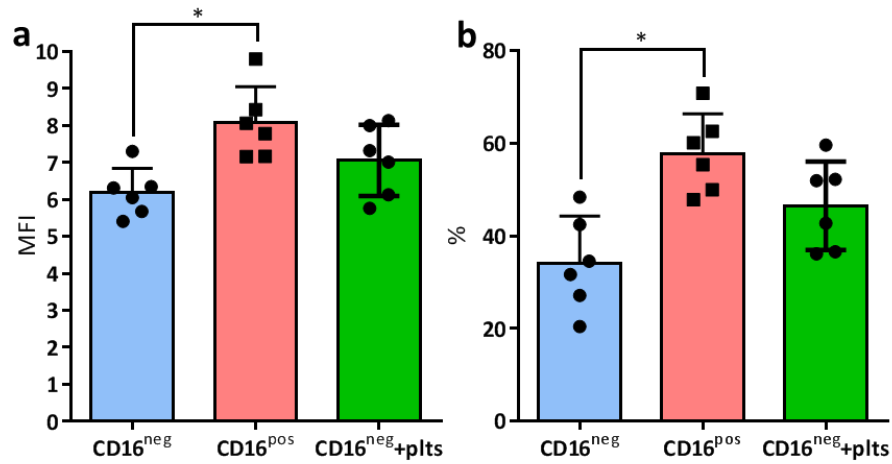
Figure 6.1: Quantification of Foam Cells in CD16^pos and CD16^neg MDMs. Graphs show both median fluorescence intensity (a) and percentage of cells that were positive for Nile Red (b) in cultured MDMs. Cells were cultured from isolated CD16^neg and CD16^pos monocytes in addition to CD16^neg monocytes incubated with activated platelets. Bars show mean±SD (n=6), *=p<0.05.

When compared with CD16^neg monocytes, the CD16^pos subset showed significantly greater formation of foam cells as quantified by both fluorescence intensity (p=0.057, t-test) and percentage of cells staining for Nile Red (p=0.016, t-test). Activated platelets enhances the formation of foam cells in the CD16^neg monocyte population compared to platelet-naïve CD16^neg monocytes, but this did not reach the levels of foam cell formation seen in the CD16^pos monocytes however this was not significantly different (p>0.05).

6.2   MPA formation is induced by platelet activation

To determine whether activated platelets induce the formation of MPAs, whole blood from healthy volunteers (n=3) was collected into 3.2% trisodium citrate and centrifuged to separate PRP and the platelet-poor, erythrocyte fraction. The PRP was decanted into separate tubes, from which washed platelets were prepared. The platelet-poor fraction was diluted in PBS/5mM EDTA and separated on a density-gradient medium to isolate monocytes (as outlined in methods section 3.2.2.5). The isolated monocytes and washed platelets were combined in a fixed 250:1 stoichiometry and incubated for up to 24 hours on slow rotation with 1.0μg/ml CRP-XL to activate platelets with and without the addition of hp-selectin blocking antibody (9E1) to inhibit the formation of MPAs. During the incubation, small aliquots were removed at regular time intervals and analysed by flow cytometry for markers of MPA formation (**Figure 6.2**).

Within this *in-vitro* assay, activation with CRP-XL shown a significant (p<0.0001) increase in the proportion of MPAs within 10mins of stimulation. Levels of MPAs were consistently above 90% however, there was a slow dissociation over time to a mean of 72.9±15.3% by 24hrs. Incubation of monocytes with platelets without addition of CRP-XL led to significant (p<0.001) increases in the proportion of MPAs, albeit to a lower level, reaching a maximum of 24.6% at 4 hours, which was significantly less (p<0.001) than that seen in the CRP-activated samples at any time point. The use of 9E1 abrogated MPA formation over the 24 hour period by >90%, reaching a peak of only 7.0%. These findings illustrate that CRP-XL is a potent platelet activating agent resulting in a rapid and robust formation of MPAs which is inhibited by 9E1. Monocytes incubated with platelets, without the addition of CRP-XL, demonstrated the spontaneous formation of MPAs although not to the levels seen with CRP-XL (**Figure 6.2**).
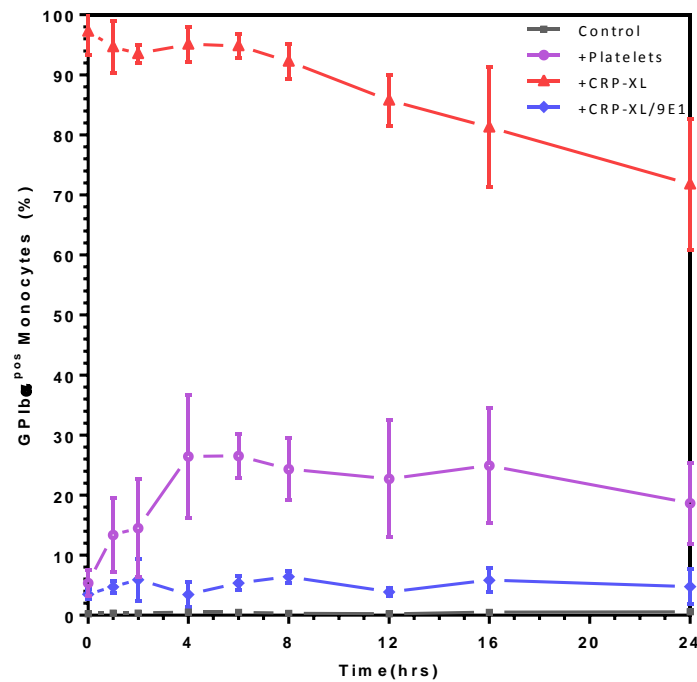
Figure 6.2: MPA Formation During Co-Incubation of Isolated Monocytes and Platelets. Graph depicts the proportion (%) of monocytes with adherent platelets (GPIbα^{pos}) incubated over a 24hr time course. CRP-XL activated samples (red) show a greater than 90% increase in MPA formation which falls slowly over the 24hour period but remains significantly more (p<0.0001) than un-activated samples. Samples incubated with washed platelets without CRP-XL activation (purple) also show increased MPA formation but less so than with CRP-XL. The co-incubation with 9E1 (blue) effectively abrogated the formation of MPAs almost back to levels seen with control (grey). Graphs show mean±SD, (n=3).

6.3 Association of CD16 Expression on Circulating Monocytes and the Formation of Monocyte-Platelet Aggregates

For the investigation of CD16 expression, blood was collected from healthy volunteers and incubated for up to 24 hours at 37°C with slow rotation. Activation of platelets was performed with the addition of CRP-XL and MPA formation was inhibited with 9E1 in the same way as with the isolated cell preparations. A whole blood flow cytometric assay was employed to ascertain both the proportion of MPAs and also the phenotype of monocytes.

6.3.1 Correlation of CD16 expression with MPA formation

Blood from healthy volunteers (n=15) was collected into 3.2% trisodium citrate and incubated at 37°C with slow rotation for 24 hours. Flow cytometry was performed after the incubation period to quantify both MPA formation and expression of surface CD16 on monocytes.
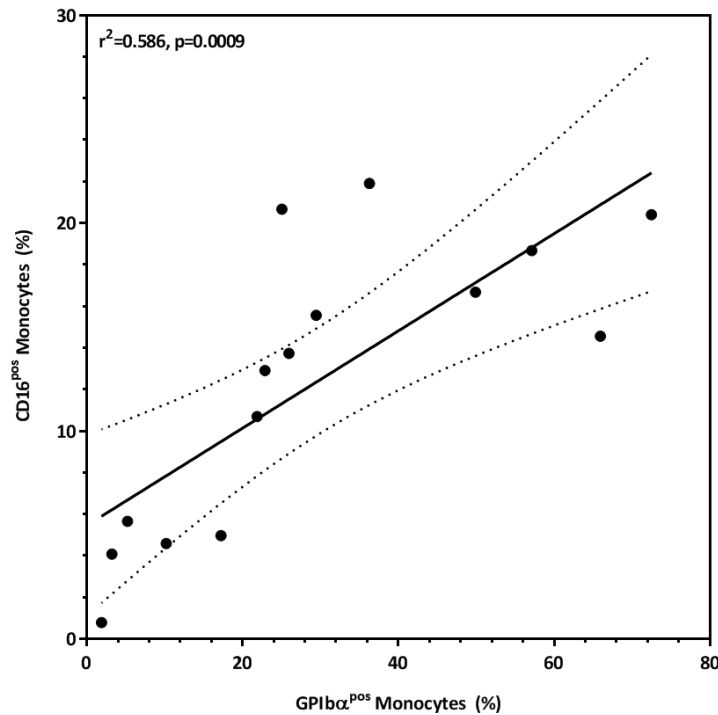
Figure 6.3: Expression of CD16 and Platelet GPIbα on Whole Blood Monocytes. Graph is a scatter plot of percentage expression of both the CD16 (FcγRIII) and GPIbα (CD42b) antigens on whole blood monocytes incubated for 24hrs. Circles represent values from individual healthy volunteers (n=15), solid line is the line of best fit with 95% confidence bands (dotted line). (r^2=0.586, p=0.0009, Pearson Correlation Coefficient)

Using this model, it was found that monocytes, at 24hrs, there was a large variation in the proportion of monocytes with bound platelets (from 1.91 to 72.48%) with a mean of 29.7±22.5% of MPAs. Similarly, the expression of CD16 on blood monocytes ranged from 0.8% to 21.9% with an overall mean of 12.4±6.9%. It was found that the expression of CD16 on monocytes correlated with the percentage of monocytes with adherent platelets (Pearson r^2=0.58, p=0.0009, n=15). This positive correlation (1/slope = 4.27) therefore confirms previous reports in the literature that MPA formation is associated with increasing levels of CD16 expression on monocytes.

6.3.2 Expression of CD16 on monocytes with and without adherent platelets

The demonstration that MPA formation and levels of CD16 expression on monocytes were correlated, was investigated further in experiments in which blood from healthy volunteers (n=4) was incubated for up to 24hr at 37°C. Aliquots of blood (50μl) were removed at regular time intervals over the incubation period and analysed by flow cytometry to identify monocytes and subdivide them into those with adherent platelets and those without (GPIbα^{pos} vs GPIbα^{neg}). The expression of CD16 was quantified on each monocyte subgroup over the 24hour incubation period (**Figure 6.4**).
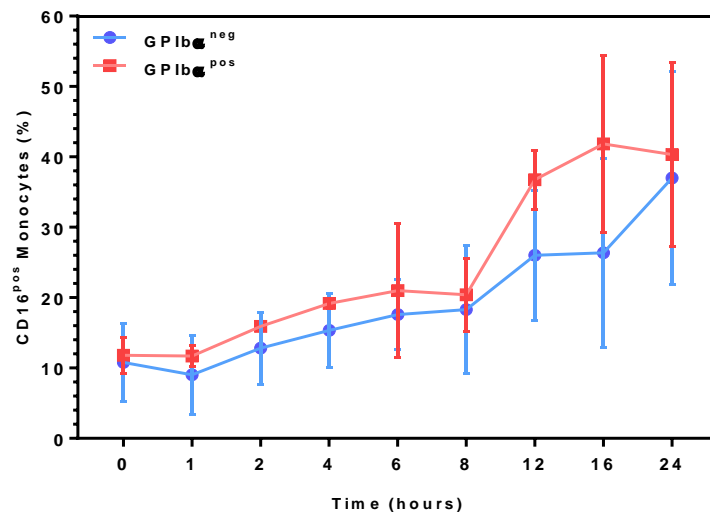
Figure 6.4: Expression of CD16 on Platelet-Bound and Platelet-Free Monocytes. Graph shows expression of the CD16 antigen on both platelet-bound (GPIbα^{pos}, red line) and free monocytes (GPIbα^{neg}, blue line) The expression of CD16 increased with incubation time on both platelet-bound (r=0.93) and free monocytes (r=0.97). There is a trend towards increased expression of CD16 on platelet-bound as compared with free monocytes and a trend towards an increased difference with longer incubation periods however this was not statistically significant (p>0.05, 2way RM-ANOVA). Points represent mean±SD for n=4.

On both GPIbα^{pos} and GPIbα^{neg} monocytes, the proportion of CD16^{pos} cells correlated with increasing period of incubation (r=0.93, p=0.0003 and r=0.97, p<0.0001 respectively). When comparing GPIbα^{pos} with GPIbα^{neg} monocytes, there was a trend towards increased expression of CD16 on platelet-bound monocytes however this was not statistically significant (p=0.0572, n=4, 2way ANOVA). Furthermore, there was no significant difference upon multiple comparisons testing of CD16 expression at different time points (p>0.05, Holm-Sidak).

6.4 Predilection of Activated Platelets to Bind Preferentially to the Classical Subset

Having confirmed an association between the formation of MPAs and the expression of CD16 on monocytes, we sought to ascertain if this was due to platelets preferentially binding the CD16^{pos} monocyte subset. To do this, blood was collected from healthy volunteers (n=5) and incubated with CRP-XL to activate platelets with(out) 9E1 to inhibit MPA formation.

Blood was collected from healthy volunteers (n=5) into 3.2% trisodium citrate and incubated at 37°C with slow rotation. To induce the formation of MPAs, platelets were selectively activated in whole blood with 1.0μg/ml of CRP-XL. In parallel tubes, 20mg/ml of an anti-hPselectin (9E1, R&D Systems) antibody was used to inhibit MPA formation. Blood was sampled across all reaction conditions after 1 and 16 hours of incubation and analysed by flow cytometry. Based on the expression levels of both the CD14 and CD16[28] antigens, monocytes (CD45^{pos}CD14^{pos}) were stratified into Classical, Intermediate and Non-Classical monocyte and the proportion of platelet-bound (GPIbα^{pos}) monocytes were quantified on each subset (**Figure 6.5**).

Following 1 hour of incubation, there was a minimal level of MPA formation in the control group (8.6%±3.0%) which increased to 30.8%±12.9% following an overnight 16hr incubation. Activation with CRP-XL led to a greater than 80% increase in the levels of GPIbα^{pos} monocytes across all monocyte subsets when compared to a vehicle control (p<0.0001, 2way ANOVA). The formation of MPAs upon activation of platelets with CRP was significant reduced (p<0.0001) when co-incubated with 9E1 both at 1 hour (3.3%±1.7%) and at 16 hrs (5.9%±3.7%). This effect was seen equally across all three subsets (p>0.05, 1way ANOVA).

When comparing the Classical and Intermediate subsets, there were equivalent levels of MPA formation induced by CRP-XL both at 1 (89.2%±1.1% vs 90.3%±3.1%, p>0.05, t-test) and 16 hours

---

[28] Selection of these two time points was based on preliminary time-course experiments not presented here.

(93.7%±1.8% vs 91.9%±3.6%, p>0.05, t-test) of incubation. However, when levels of MPAs on both classical and intermediate subsets were compared to levels on the non-classical subset; there were significant differences. Following 1-hour incubation with CRP-XL, there was a smaller proportion of non-classical monocytes with adherent platelets (62.9%±20.9%) than either the Classical (p<0.001) or the Intermediate (p<0.001) monocyte subsets. After 16 hours of incubation with CRP-XL, a similar proportion of non-classical monocytes had adherent platelets (60.9%±15.7%) which was once again significantly less (p<0.001) than either the intermediate or classical monocyte subsets (**Figure 6.5**).

These results demonstrate that activated platelets are preferentially bound to both CD14^{high} monocytes; the Classical and Intermediate subsets. The formation of these MPAs are robust and persist over the 16hr incubation period of the experiment. Furthermore, the formation of the MPAs was equally inhibited by a hp-selectin blocking antibody (9E1) in all subsets indicating that the P-selectin/PSGL1 dyad is equally important in the formation MPAs across all three monocyte subtypes. Given that the classical and intermediate monocyte subsets tend to express lower levels of CD16 than the non-classical subsets, we can surmise that activated platelets tend to preferentially bind the CD16^{neg} rather than the CD16^{pos} subset as originally hypothesised.
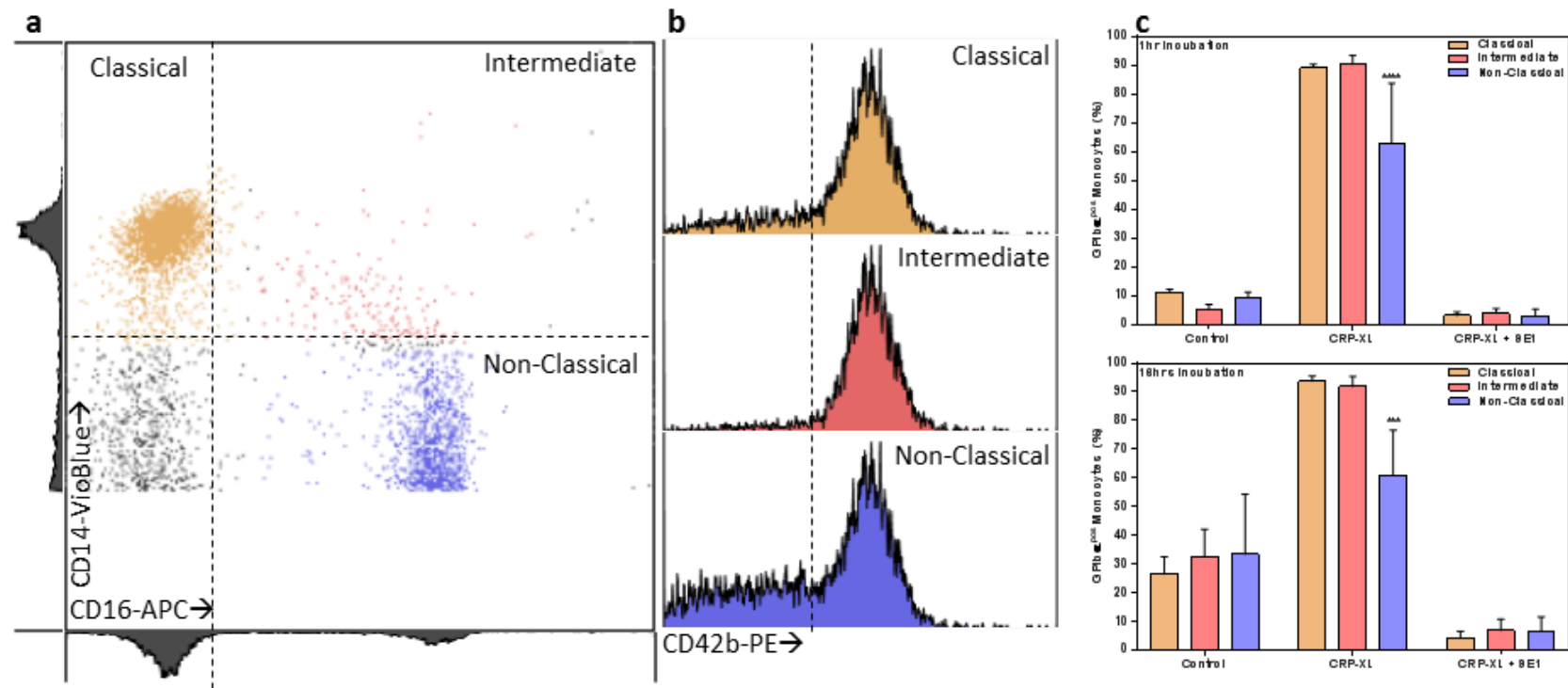
Figure 6.5: Formation of MPAs on Monocyte Subsets. (a) shows representative flow cytometric plot (including histograms) of CD14 (y-axis) vs CD16 (x-axis) was used to gate Classical (yellow) Intermediate (red) and Non-Classical (blue). Whole blood was activated for 1 hour with 1.0μg/ml CRP-XL and (b) shows representative histograms of CD42b-PE fluorescence gated from Classical, Intermediate and Non-Classical monocytes. Images show greater than 80% of Classical and Intermediate monocytes are GPIbα^{pos} as compared with 60% of Non-Classical monocytes. Results from all healthy donors (n=5) are shown (c) following incubation for 1 and 16 hours. The proportion of monocytes with adherent platelets (GPIbα^{pos} monocytes) are shown for each monocyte subset in the control, CRP-XL activated, and blood activated with CRP-XL in the presence of 9E1. There was no significant difference in GPIbα expression between monocyte subsets when incubated with either vehicle control or when MPA formation was inhibited. There was significantly less (p<0.001, 2way ANOVA, Tukey's Multiple Comparisons) GP1bα expression on Non-Classical subsets than either Classical or Intermediate when blood was activated with CRP-XL after 1hour of incubation and persisting until 24hrs. All bars depict mean±SD, n=4,'***' = p<0.001

6.4.1 Platelets Preferentially Activate the Classical Monocyte Subset

In order to ascertain if platelets that bind to monocytes of whatever subset influence their phenotype, an *in-vitro* model was conducted using isolated cells, to look at the changes to the monocyte subsets in response to platelet activation. Blood from healthy volunteers (n=3) was collected into 3.2% trisodium citrate and separated into PRP, from which washed platelets were prepared (methods section 3.2.2.3) and PBMCs (methods section 3.2.2.5). From the PBMCs, monocytes were isolated (described in method section 3.2.2.9) and incubated with autologous washed platelets adjusted to a final concentration of 250×10^6 per ml. Samples were incubated for 4 hours at 37°C with slow rotation and with 1.0μg/ml of CRP-XL, with and without anti-hpselectin (20mg/ml). An equivalent volume of HBS was used as a vehicle control. Samples were analysed by flow cytometry wherein monocytes were classified into Classical, Intermediate and Non-Classical subsets based on expression of CD14 and CD16 surface antigens. Cells were additionally stained with anti-ICAM1/FITC (Abcam) and the fluorescence of FITC was quantified on each of the subsets to assess monocyte activation (**Figure 6.6**). Freshly isolated monocytes demonstrated a low level of ICAM1 expression (<5%) on all three subsets. Following incubation with a vehicle control for 4hours, there was no significant increase in ICAM1 expression ($p>0.05$) in any of the three subsets ($p>0.05$, 2way ANOVA with Tukey's Multiple Comparisons). Incubation with autologous, washed platelets led to a significant ($p<0.0001$, 2way ANOVA with Tukey's Multiple Comparisons) increase in ICAM1 expression on the Classical subset but not the Intermediate or Non-Classical. A similar pattern was seen when monocytes were incubated with autologous, CRP-activated washed platelets; there was a further significant increase in ICAM1 expression above monocytes incubated with non-activated platelets ($p<0.0001$, 2way ANOVA with Tukey's Multiple Comparisons) across all three subsets. However, the greatest increase was seen on the Classical subset ($p<0.0001$) with no significant difference between the intermediate and the non-classical subsets ($p>0.05$). When MPA formation was inhibited with 9E1, it did not inhibit the CRP-XL induced expression of ICAM1 on monocytes ($p>0.05$, 2way ANOVA). Classical monocytes were the most highly activated in this group ($p<0.001$, 2way ANOVA, Tukey's Multiple Comparisons) and the Non-classical subset was significantly more activated than the intermediate subset ($p<0.01$). This suggest that the activation of the classical subset is not dependent on MPA formation.
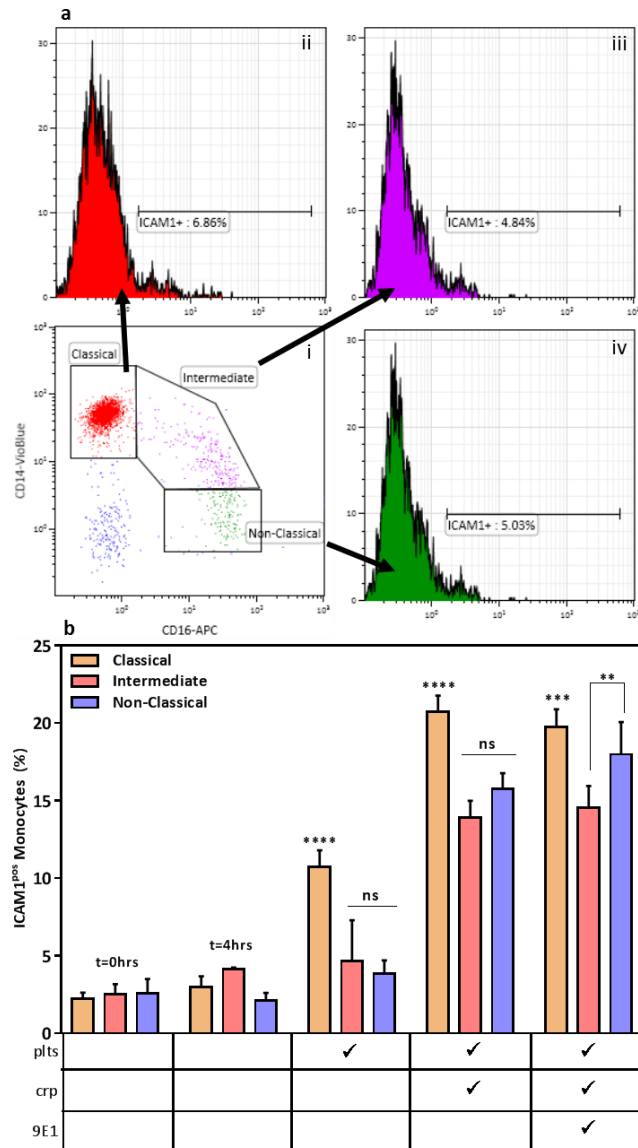
Figure 6.6: Effect of Activated Platelets on ICAM1 Expression on Monocyte Subsets. Flow cytometric gating strategy is shown (a) where monocytes are gated from CD45^{pos} cells and on a CD14/CD16 plot (i). Classical, Intermediate and Non-Classical Monocytes were gated and the expression of ICAM1 was quantified on each subset (ii-iv). Data is shown (b) where coloured bars represent the percentage of monocytes, within each subset, that expressed ICAM-1 (percentage positive). Data is shown for freshly isolated monocytes "t=0hrs" and for monocytes incubated with platelets "plts", CRP-XL "crp" and anti-hpselectin antibody "9E1". ICAM1 expression was increased on all 3 monocyte subsets with platelet activation but significantly more so (p<0.001) on the Classical subset. Inhibiting MPA formation did not inhibit the platelet-induced expression of ICAM1 on monocytes. All bars represent mean ±SD, n=3, 'ns' = p>0.05, *** = p<0.001, *** = p<0.0001, ** = p<0.01.

6.5 Activated Platelets Induce Surface Expression of CD16 on Previously CD16^{neg} Monocytes

To ascertain the effect of activated platelets on CD16^{neg} monocytes, this subset was isolated and incubated with activated, autologous platelets using an *in-vitro* model of platelet activation. Whole blood from healthy volunteers (n=5) was collected into 3.2% trisodium citrate and separated to generate washed platelets and CD61-depleted PBMCs as previously. Classical monocytes were isolated by first depleting CD16^{pos} non-monocytes using an antibody cocktail directed against CD15 and CD56 (described in methods section 3.2.2.10). This resulted in a pre-enriched leucocyte fraction from which all CD16^{pos} monocytes were removed by incubation with anti-CD16 microbeads and separation on a magnetic column. The CD16^{pos} fraction was separated and discarded to leave a classical (CD16^{neg}) monocyte population.

From each donor, freshly isolated classical monocytes were incubated with either autologous platelets alone, with CRP-XL to activate platelets, or CRP-XL and an anti-hpselectin antibody (9E1) to stop MPA formation. Within a 1ml reaction well, 1.0×10^6/ml of isolated CD16^{neg} monocytes were incubated with 250×10^6 autologous washed platelets. These cell preparations were incubated for up to 24hrs at 37°C on slow rotation and 50µl aliquots were taken at regular intervals for analysis by flow cytometry where both MPA formation and surface CD16 expression were quantified. CD16^{neg} monocytes were identified by flow cytometry based on expression of CD45 and CD14 and lack of expression of CD16.
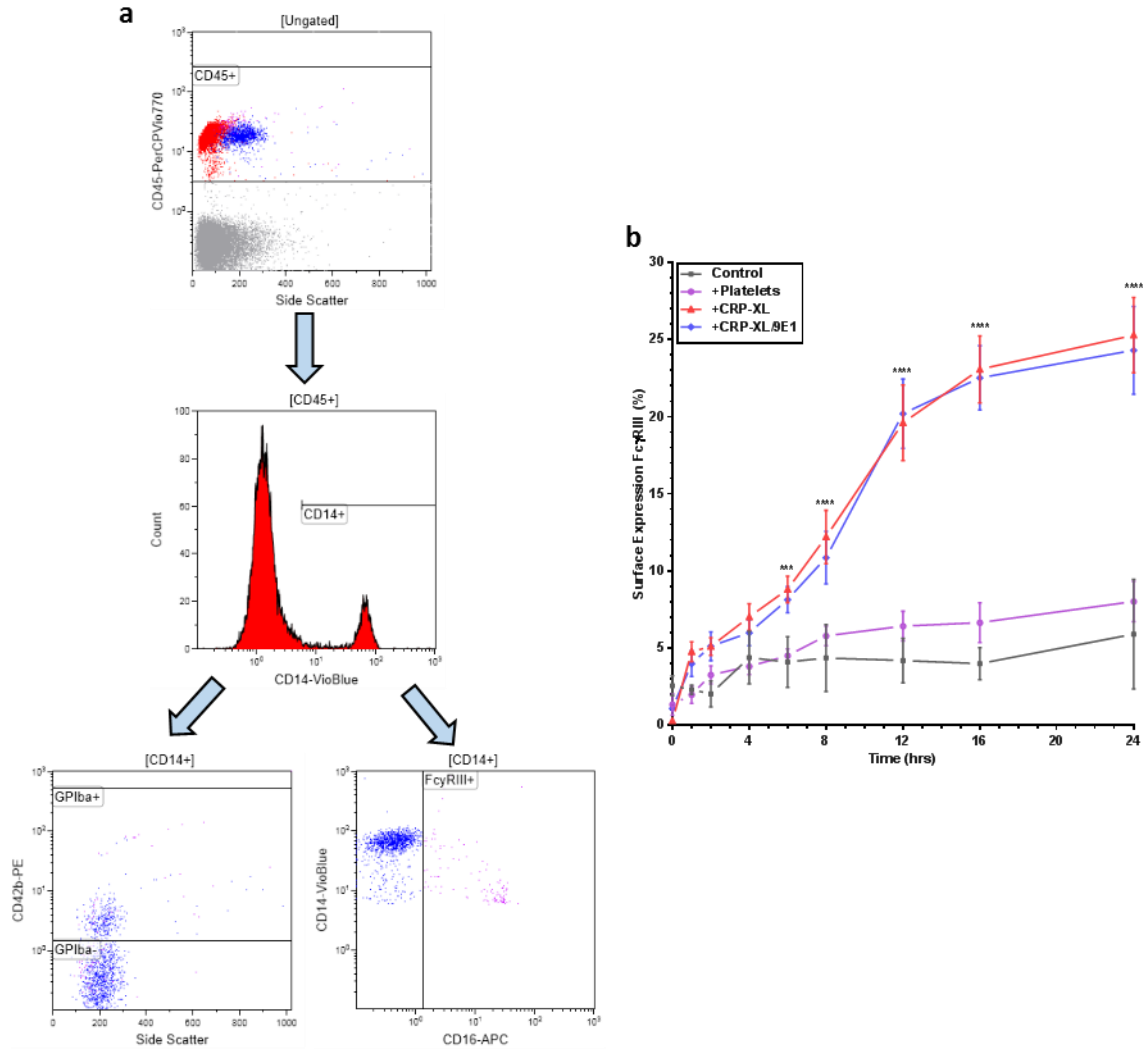
Figure 6.7: Induction of CD16 Expression on Classical Monocytes by Activated Platelets. (a) Flow cytometric gating strategy (from top to bottom) used to identify CD16^{neg} monocytes. CD14^{pos} monocytes were gated from CD45^{pos} leucocytes. An IgG2κ isotype control was used to set the CD14^{neg} population and all CD14^{pos} events were gated to record both CD42b (GPIbα) and CD16 (FcγRIII) fluorescence. (b) Time course of the percentage of monocytes expressing CD16 (FcγRIII) with either a HBS vehicle control, 250x10^6/ml of autologous platelets (+Platelets) or incubation with autologous platelets and 1.0μg/ml CRP-XL (+CRP-XL). Additionally, platelets were activated in the presence of 9E1 to inhibit the formation of MPAs (+CRP-XL/9E1). Points represent mean ± SD, ***=p<0.001, ****=p<0.0001, 2way ANOVA and Tukey's Multiple Comparison testing

When incubated with autologous, un-activated, platelets, CD16^{neg} monocytes readily formed low levels of MPAs, reaching a maximum of 26.5±10.2% at 4 hours but with no significant change over the subsequent incubation period (r^2=0.16, p=0.28, Pearsons r). Incubation with CRP-activated autologous platelets however, led to a rapid and significant increase in MPA formation to >90% which was significantly greater than that seen with un-activated platelets (p<0.0001, ANOVA, Tukey's Multiple comparisons). CD16^{neg} monocytes incubated over 24hrs all showed an increase in CD16 expression with time (r>0.8, p<0.01, Pearson r). However, when incubated with CRP-activated platelets, there was a significant increase in CD16 expression compared to

monocytes incubated with un-activated platelets (p<0.0001, 2way ANOVA). This difference was seen after 4hours of incubation (p<0.01, 2way ANOVA with Tukey's Multiple Comparisons) and increased steadily up to 24hrs (p<0.0001). It was therefore demonstrated that activated platelets induce surface expression of CD16 on previously CD16^{neg} monocytes.

6.5.1 Activated Platelets Promote a CD14^{dim} Expression Phenotype at the Expense of CD14^{high}

To further investigate the effect of activated platelets and direct cell-cell contact on the phenotype of monocytes, the phenotype of monocytes using a 4-colour flow cytometric assay, was examined.

In parallel experiments, blood from healthy volunteers was collected into 3.2% trisodium citrate and both CD16-depleted PBMCs and autologous washed platelets were prepared as before. Samples were incubated for up to 24hrs and 50μl aliquots were removed at different time points for analysis by flow cytometry. The expression of CD14 was first set on isolated classical monocytes using an IgG2b isotype control (IgG2b-VioBlue™, Miltenyi Biotec) to exclude 98% of all events and was thus deemed as a negative background control. A monoclonal antibody (TÜK4 clone) was used to identify all CD14^{pos} events and thereby classed as monocytes. Within the CD14^{pos} gate, separate populations of high and lower expressers of CD14 were identified and quantified over a 24hr time course with and without activated platelets (**Figure 6.8**).

It was found that CD16^{neg} monocytes gradually lost CD14 expression with time (p<0.0001, Pearson r) regardless of concomitant platelet activation. When examining the expression of CD14^{high} on the monocyte population, there is a gradual loss of staining with time (p<0.0001, Pearson r) however this loss is accelerated with platelet activation after 6hrs of incubation (p<0.001, 2way ANOVA with Tukeys Multiple Comparisons). There was no significant difference in the expression of CD14^{high} when monocytes were incubated with activated platelets with or without anti-hpselectin antibody (p>0.05, 2way ANOVA). Conversely, there is an overall increase in the population of CD14^{dim} (p<0.05, Pearson r) with increasing incubation times. Activation with platelets (both with and without the presence of 9E1 blocking antibody) led to an increase in the proportion of cells expressing CD14^{dim} (p<0.0001, 2way ANOVA) following a minimum of 6 hours incubation. Overall, activated platelets promote the loss of high expressing CD14^{pos} monocytes and promote the CD14^{dim} population.
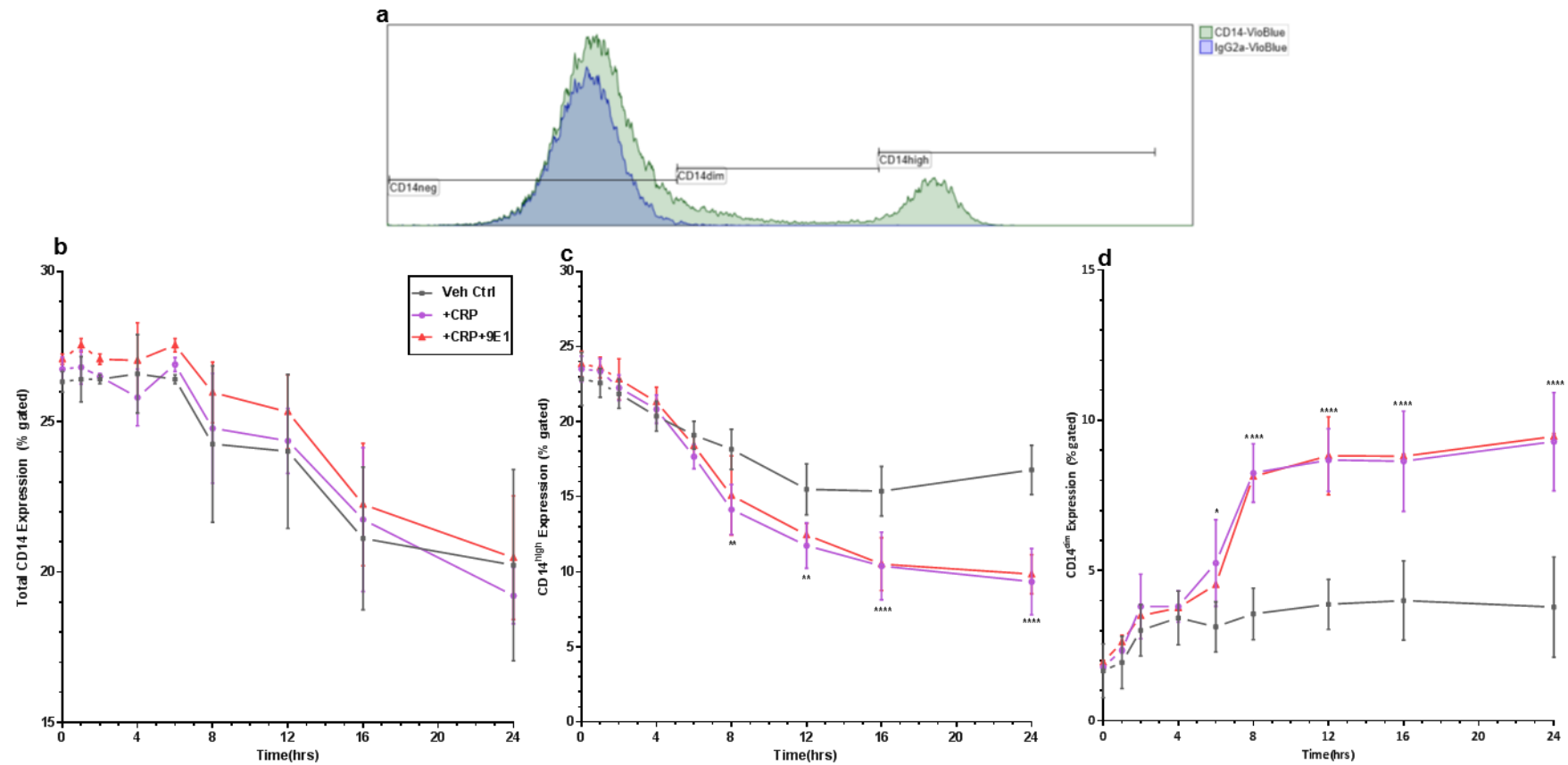
Figure 6.8: Expression of CD14 on CD16^{neg} Monocytes Incubated with Activated Platelets. (a) Representative overlay histogram of CD14-VioBlue (FL9) fluorescence of CD16^{neg}CD56^{neg}CD15^{neg} PBMCs. A mouse IgG2a isotype control was used to set baseline fluorescence and both the CD14^{dim} and CD14^{high} populations were defined. Total CD14 fluorescence was the sum of both the dim and high populations. (b), (c) and (d) show collated results (n=5) of total, CD14^{high} and CD14^{dim} populations respectively. There is an overall trend towards loss of CD14 expression ($p<0.0001$, ANOVA) with time. However, there is increased loss of the CD14^{high} and an increase in the proportion of cells that are CD14^{dim}. ****=$p<0.0001$, *=$p<0.05$

6.5.2 Activated Platelets Promote an Intermediate Monocyte Phenotype at the Expense of the Classical Phenotype

In parallel analysis, the effect of activated platelets on the isolated population of $CD16^{neg}$ monocytes was analysed by flow cytometry. Monocytes were identified based on fluorescence of CD45 and CD14. Of all $CD14^{pos}$ events, monocytes were further stratified according to $CD14^{high}$ and $CD14^{dim}$ expressers and expression of CD16, allowing the separation of monocytes into $CD14^{high}CD16^{neg}$ (Classical), $CD14^{high}CD16^{pos}$ (Intermediate) and $CD14^{dim}CD16^{pos}$ (Non-Classical) subsets (**Figure 6.9**).

More than 95% of all monocytes were classified as 'Classical' at the start of the incubation period. Following incubation with HBS alone, there was a progressive reduction in the proportion of cells classified as 'Classical' ($p<0.001$, $r^2=0.83$, Pearsons) and a concomitant increase in both the 'Intermediate' ($p=0.004$, $r^2=0.72$) and 'Non-Classical' ($p=0.001$, $r^2=0.89$) monocyte subsets. When $CD16^{neg}$ monocytes were incubated with GPVI-activated platelets, the proportion of 'Classical' monocytes fell significantly ($p<0.0001$, ANOVA) when compared to controls with the greatest differences appreciable after 24 hours incubation. Furthermore, there was also a parallel increase in the proportion of 'Intermediate' monocytes following platelet activation ($p<0.0001$, ANOVA) seen most distinctly after 6hrs of incubation. Blocking MPA formation in CRP-XL stimulated samples with anti-hpselectin antibody (9E1), significantly reduced this decrease in the 'Classical' monocyte subset ($p<0.01$, ANOVA) and increase in the 'Intermediate' subset ($p<0.001$, ANOVA). Once again, the differences were apparent and became statistically significant ($p<0.05$) following a minimum of 6hrs incubation.
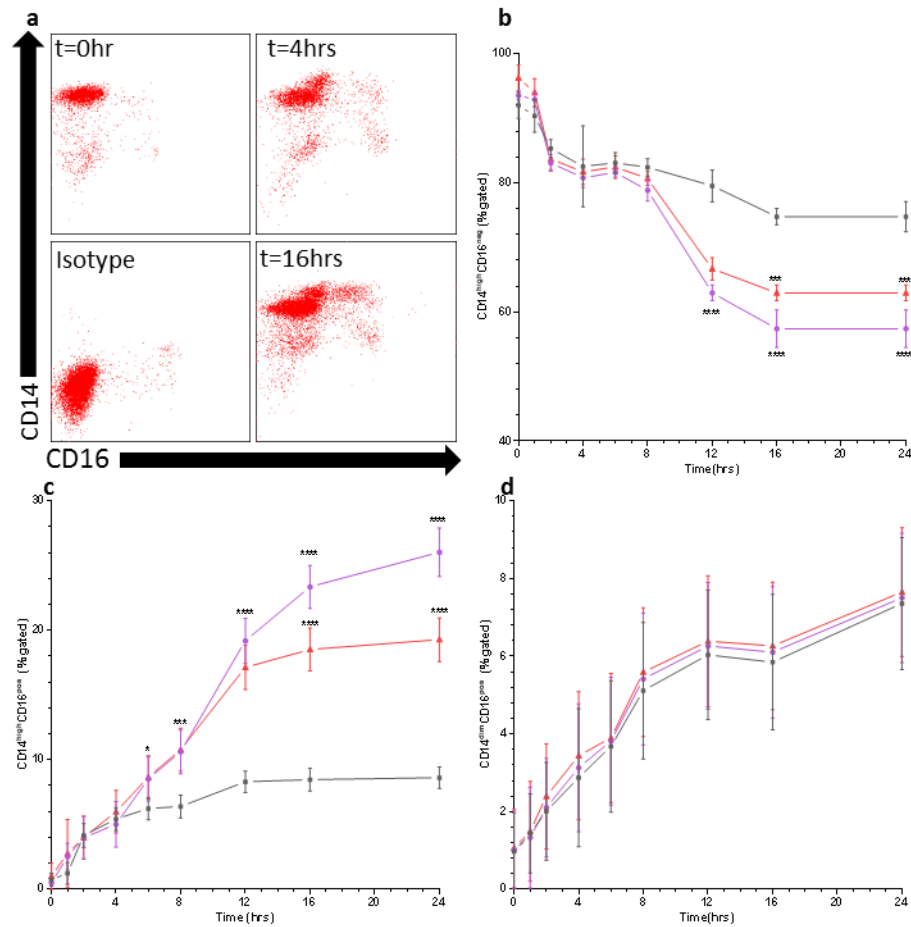
Figure 6.9: Phenotyping of CD16^{neg} Monocytes Incubated with Activated Platelets. (a) Representative flow cytometry of isolated CD16^{neg} monocytes. Cells are gated from CD45^{pos} events and depicts a CD14-VioBlue (FL9) vs CD16-APC (FL6) fluorescence plot. Bottom left panel shows isotype control with top left, top right and bottom right plots showing monocytes incubated with activated platelets at t=0hr, t=4hrs and t=16hrs respectively. Graphs in (b), (c) and (d) show the percentage of cells within the CD14^{high}CD16^{neg}, CD14^{high}CD16^{pos} and CD14^{high}CD16^{pos} gates respectively. Grey line shows isolated CD16^{neg} monocytes incubated with HBS alone while the purple and red lines represent incubation with CRP-activated platelets or CRP-activated platelets + 9E1. Graphs show a decrease in the number of the 'Classical' subset and an increase in the 'intermediate' phenotype (p<0.0001). Inhibition of MPA formation partially inhibited this change (p<0.05). There was no significant difference in the Non-Classical Subset. Graphs show mean ± SD for n=4. *=p<0.05, ***=p<0.001, ****=p<0.0001.

6.6 Increase in the CD16^{pos} monocyte subset is not due to proliferation of the classical subset

The data so far has demonstrated that activated platelets promote the CD16^{pos} monocyte subset and in particular the intermediate subset. One potential mechanism by which this may occur is through the proliferation of monocytes and in particular the CD16^{pos} subset. To investigate this, the effect of activated platelets on the proliferation status of monocytes was studied using a cell cycle assay. An assay using THP-1 human myelomonocytic cell line was set up which shows many features of peripheral blood monocytes, but unlike them, proliferates with an average doubling time of between 19-50 hours and lacks replicative senescence (**Tsuchiya *et al.* 1980**).

A suspension of 5.0×10^6 THP-1 cells in RPMI-1640 + 10% FCS was taken and centrifuged at 400g for 15mins to form a pellet[29]. This was stained with propidium iodide (PI) as described in Section 3.2.5.3 and re-suspended in 500µl of PBS for flow cytometry. Cells were identified based on forward and side scatter properties and fluorescence of PI was quantified in the FL3 channel. Exclusion of doublets was performed by gating all cells on the y=x line on a plot of FL3-PA vs FL3-PH as illustrated in **Figure 6.10**, and the proportion of cells within each phase of the cell cycle was quantified using a histogram of FL3-PA.

---

[29] The culture and maintenance of the THP-1 cell line was undertaken by Dr Ashley Ambrose. Ambrose A 2016. *Platelet extracellular vesicles and the transfer of microRNA in atherosclerosis*. Thesis, (PhD). University of Leicester
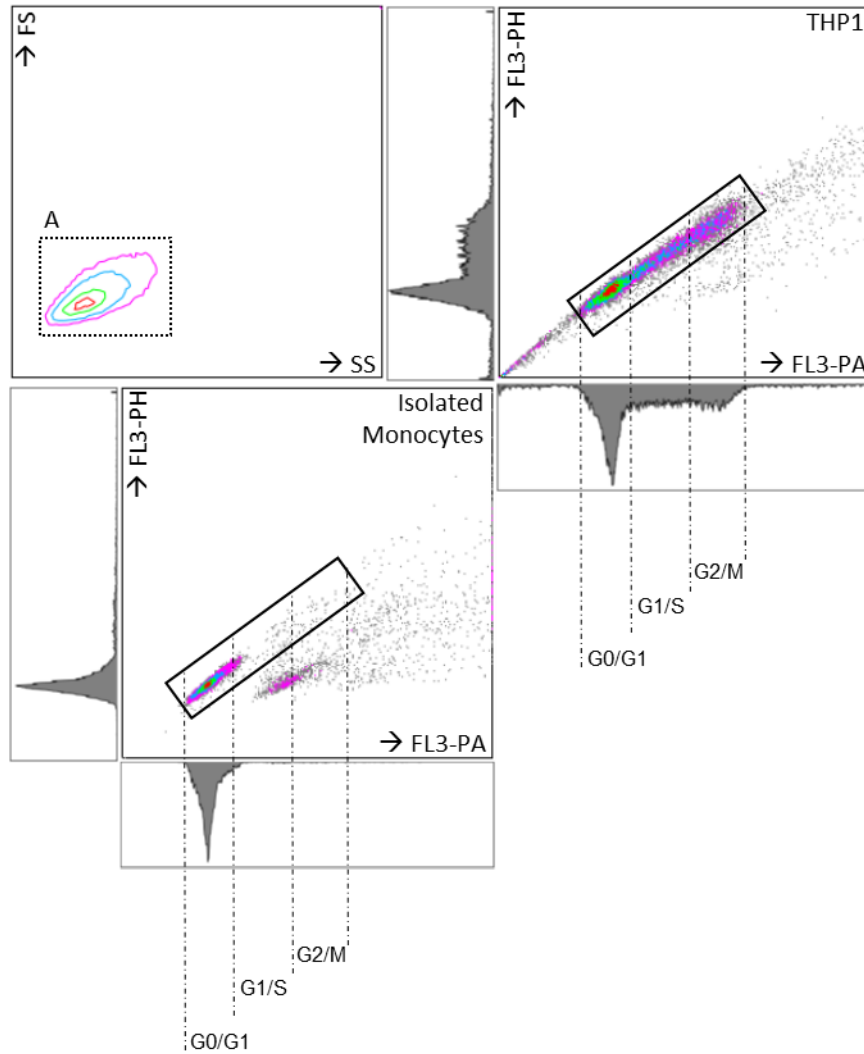
Figure 6.10: Gating Strategy for Cell Cycle Analysis. Top left plot shows a forward scatter (FS) and side scatter (SS) plot of THP-1 cells from which cells were identified (gate A) based on size and granularity. From these gated cells, Propidium Iodide fluorescence in the FL3 channel was quantified both as signal area (FL3-PA) and peak signal intensity (FL3-PH). A plot of FL3-PA vs FL3-PH was drawn to exclude doublets but gating out the single cells. After doublet discrimination, cell cycle was determined on a linear plot of FL3-PA into G0/G1, G1/S and G2/M. Figure shows FL3-PA vs FL3-PH plots for both THP1 cells (from which cell cycle boundaries were standardised) and from isolated monocytes (from which doublets were effectively excluded from final analyses).

For analysis of cell cycle on peripheral blood mononuclear cells, both PBMCs and washed platelets were produced from whole blood (n=3) using the standard methodology (3.2.2.5). An aliquot of PBMCs was kept aside and monocytes were isolated from the remaining PBMCs by negative immunomagnetic bead separation. The isolated monocytes were incubated for 24hrs with either an HBS control or autologous washed platelets (250x10^6/ml) with 1.0µg/ml CRP-XL. Both PBMCs and THP-1 cells were also incubated at 37°C for 24hrs in parallel with either an HBS control or washed platelets. Following the 24hr incubation period, cells were stained with PI as described previously (Section 3.2.5.3) and analysed by flow cytometry.

Overall, there was a significant difference in the proportion of cells in each of the cell-cycle phases (p<0.0001, 2way ANOVA) with the vast majority of cells in the G0/1 phase. THP-1 cells and PBMCs (monocytes and lymphocytes) both demonstrated greater than 50% of their population within G0/G1 and ~20% within the G1/S phase. Isolated monocytes showed that >80% of their cell population was within the G0/G1 phase. Monocytes incubated with activated platelets showed a marginally reduced proportion of cells within the G0/G1 phase (8.9% mean difference) which was statistically significant (p<0.05, ANOVA). There was however no significant difference in the proportion of monocytes in either the G1/S or G2/M phases either with or without platelet incubation (p>0.05, ANOVA) which confirms that platelets do not induce proliferation of isolated monocytes. This is in contrast with the THP-1 cell line wherein ~18% of cells were in G2/M indicating an actively replicating monocytic cell line.
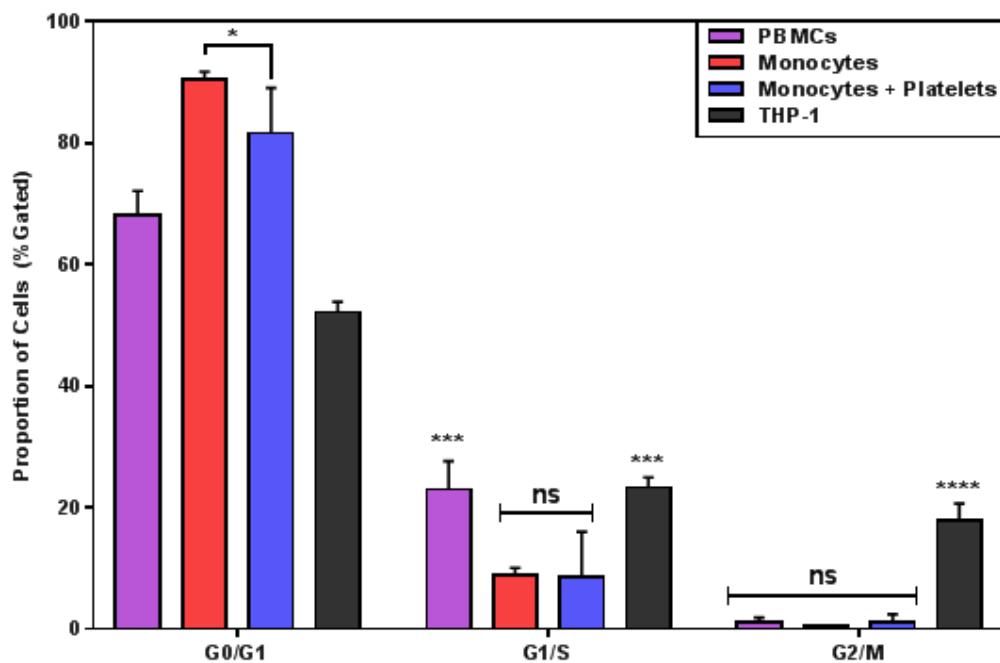
Figure 6.11: Cell-Cycle Analysis of Mononuclear Leucocytes. Graph shows the proportion of cells (gated after doublet discrimination) within each phase of the cell cycle (G0/1, G1/S, and G2/M). Results are shown for PBMCs, isolated monocytes, isolated monocytes incubated with activated platelets for 24hrs and a THP-1 cell line. Bars represent mean ± SD, n=3, '*' = p<0.05, '***'=p<0.001, '****' = p<0.0001, 2-way ANOVA with Tukeys Multiple Comparisons.

6.7   Expression of FCGR3 mRNA in platelet-activated monocytes

The previous data has demonstrated that activated platelets induce the expression of the CD16 antigen on the surface of monocytes which did not previously express this protein with a consequent increase in the proportion of CD16^{pos} monocytes, and it has been shown that this is not due to proliferation. To test whether platelets induce the expression of CD16 at the transcriptomic level, real-time PCR was used to look for de-novo expression of *FCGR3*; the FCγRIII (CD16) gene.

6.7.1   Setup of Method

For this, a real-time PCR method was selected from the TaqMan® probe system (Thermo-Fischer). This is based on a 5' nuclease chemistry which uses a fluorogenic probe to enable the detection of a specific PCR product as it accumulates during thermal cycling conditions. Each assay contains unlabelled primers for the transcript of interest, and a TaqMan probe with either a FAM™ or VIC™ dye label on the 5' end. Additionally, the probe also contains a minor groove binder (MGB) and a non-fluorescent quencher (NFQ) on the 3' end (**Figure 6.12**). The temperature is raised at the start of real-time PCR to denature the double-stranded cDNA during which the fluorescent dye at the 5' end is quenched by the NFQ at the 3' end. When the reaction temperature is reduced, the primers and probes anneal to their specific target sequences. The DNA Taq polymerase then synthesises new strands using the unlabelled primers and the template cDNA. When it reaches the probe, the endogenous 5' nuclease activity of the DNA polymerase cleaves the probe and separates the dye from the quencher. With each cycle of PCR, the increase in fluorescence intensity is proportional to the amount of amplicon synthesised.
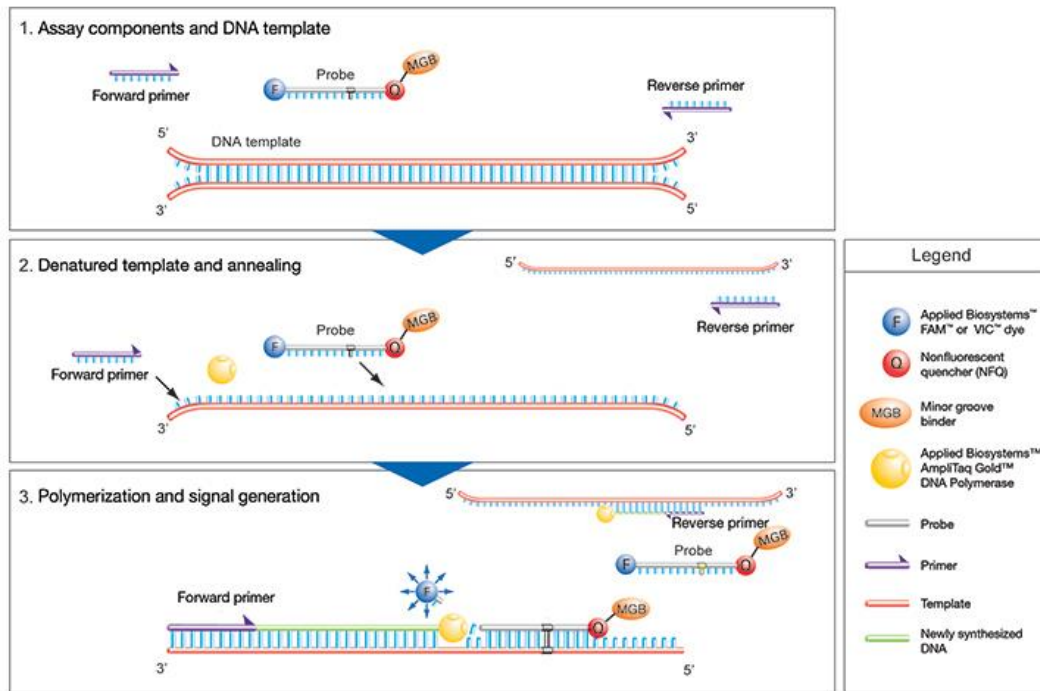
Figure 6.12: Graphical Representation of the Taqman® Gene Expression Assay. Pictures show a schematic representation of the (1) assay components and DNA template, (2) the process during denaturing and annealing of the template DNA and finally (3) the process during polymerisation and signal generation. Image taken from Thermo-Fisher (https://www.thermofisher.com/uk/en/home/life-science/pcr/real-time-pcr/qpcr-education/how-taqman-assays-work.html)

This assay was validated using PBMCs isolated from whole blood by density-gradient centrifugation. Cells were then pelleted by centrifugation and re-suspended in TRIzol at a concentration of 1.0×10^6 cells/ml. RNA was isolated by a combination of Chloroform/TRIzol and column separation and both yield, and purity was quantified using the Nanodrop spectral analyser (see methods 3.2.7.1). Reverse transcription was performed both with and without the addition of AMV reverse transcriptase (RT) to give an RT[neg] control sample; this was used in the real-time PCR reaction to test for the presence of genomic DNA.

Serial 10-fold dilutions of cDNA was added to the assay plate along with a mastermix including both *FCGR3* and *B2M*[30] primers conjugated to FAM and VIC dyes respectively. cDNA samples were also titrated in an assay plate with both *B2M* and *FCGR3* primers in separate reaction wells to ensure that there was no spill-over of emission spectra. All samples were run in triplicate and with a non-template control.

---

[30] B2M is a primer for the β_2 microglobulin gene, a serum protein found in association with the MHC Class I heavy chain on the surface of nearly all nucleated cells. It is employed regularly, as is the case in this assay, as a housekeeping gene

There was a strong correlation between log (cDNA) and Cycle Threshold (Ct) for both FCGR3 (r^2=0.990) and B2M (r^2=0.998) (**Figure 6.13**). Amplification efficiency was given by the formula;

$$E = 10^{\frac{-1}{\text{slope}}}$$

Which was expressed as a percentage as follows;

Percentage Efficiency = (E-1) x 100

Efficiency for *B2M* was 93.1% across 6 log decades and 106.9% across 3 log decades for *FCGR3*. These preliminary experiments confirmed that the assay system was valid, with good yields of high-quality RNA and good efficiency of the PCR reaction approaching 100% (see figure **Figure 6.13**).
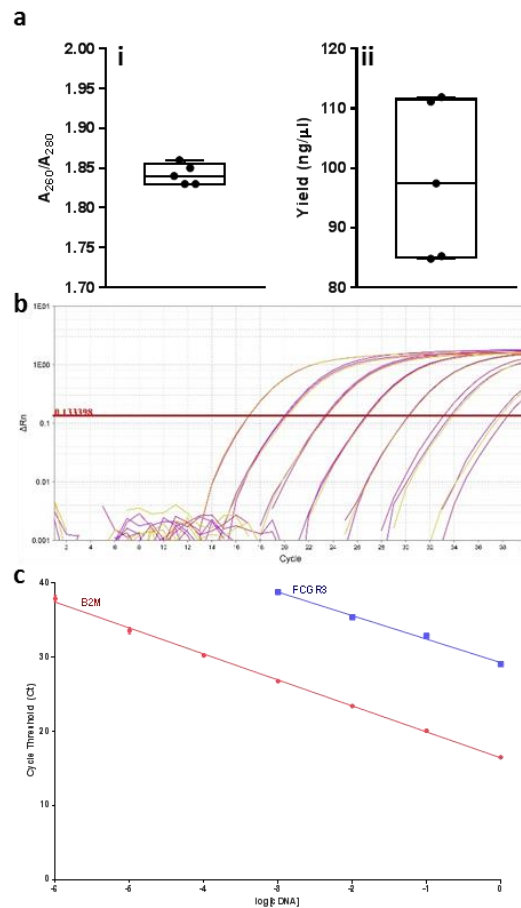
Figure 6.13: Validation of Real-Time Quantitative PCR. (a) shows both purity (i) and yield (ii) of RNA isolated from PBMCs. Purity is shown as the ratio of absorbance at A260 and A280. Graphs depicts min-max values and median. (b) Typical amplification plot of serial dilutions of cDNA, (c) shows a plot of Ct values against log(cDNA) concentrations from which PCR efficiency was calculated. Line of best fit is shown for both B2M (red) and FCGR3 (blue).

6.7.2 Expression of FCGR3 mRNA is Induced in CD16^{neg} Monocytes by Activated Platelets

6.7.2 Expression of FCGR3 mRNA is Induced in CD16ⁿᵉᵍ Monocytes by Activated Platelets

PBMCs were isolated from whole blood (n=4) by density-gradient separation and CD61 immunomagnetic bead depletion (Methods 3.2.2.5). Washed platelets were also prepared from the PRP fraction in parallel (Methods 3.2.2.3) and of the isolated PBMCs, $1x10^6$ cells were separated into an aliquot and re-suspended in 1ml of TRIzol for RNA extraction. From the remaining PBMCs, the CD16^{pos} monocytes were removed by 2-step immunomagnetic depletion (Methods 3.2.2.11) and the resultant CD16^{neg} monocytes were split into equal aliquots of $0.5x10^6$ cells incubated either with or without autologous platelets ($250x10^6$/ml). Samples were also stimulated with 1.0µg/ml of CRP-XL alone and in the presence of 9E1 to block MPA formation. Finally, Actinomycin D (20mg/L) was added to inhibit gene transcription and was used as a negative control. All these samples were incubated for 8 hours at 37°C with slow rotation after which cells were pelleted and RNA isolated and purified (Methods 3.2.7.1). The purified RNA was then reverse transcribed into cDNA using a recombinant murine leukaemia virus reverse transcriptase (MultiScribe™ RT) optimised for the TaqMan-based assay (Thermo-Fischer) (Methods 3.2.7.2). To test for the presence of contaminating genomic DNA (gDNA), the thermal cycling reaction was performed was performed for the purified RNA without the reverse transcriptase (RT negative control).

For real-time PCR, all samples were carried out in triplicate in a 96-well plate including a non-template control and a RT negative control to confirm there is no gDNA[31]. The mastermix included primers for *B2M* (Hs00187842_m1) and *FCGR3* (Hs00275547_m1) conjugated to VIC and FAM reporter dyes respectively. This allowed for duplexing of the real-time reaction. Cycle threshold (Ct) values were recorded for both FCGR3 and B2M and the difference between the two ($Ct_{FCGR3} - Ct_{B2M}$) was designated as ΔCt. The ΔCt value for PBMCs (t=0hrs) was used as the baseline value and all ΔCt were normalised to this. Relative expression of the FCGR3 gene was calculated as;

$$\Delta Ct_{sample\ of\ interest} - \Delta Ct_{baseline} = \Delta\Delta Ct$$

Fold-change expression of FCGR3 was imputed ($2^{-\Delta\Delta Ct}$) and transformed logarithmically (**Figure 6.14**).

---

[31] gDNA denotes genomic DNA

Platelets		+	+	+	+
CRP-XL			+	+	+
9E1				+	
ActD					+
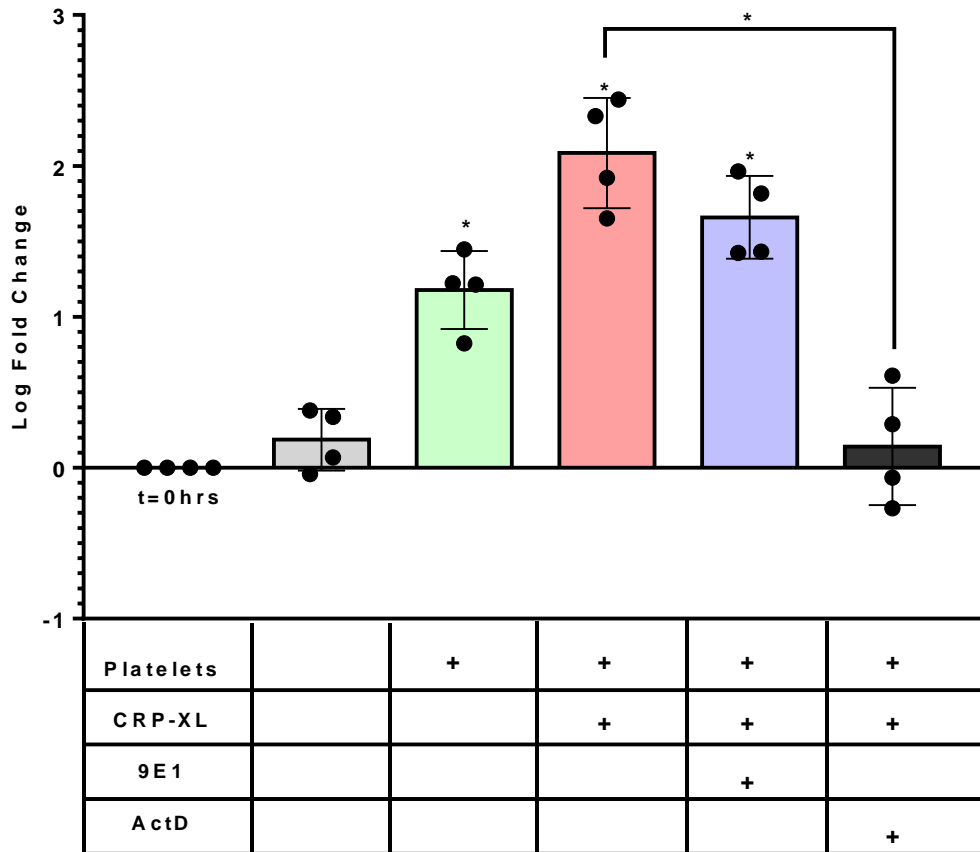
Figure 6.14: Expression of FCGR3 in CD16^{neg} Monocytes. Graph shows fold-change expression of FCGR3 in isolated CD16 negative monocytes normalised to expression on PBMCs at t=0hrs. Table below shows reaction conditions including the addition of platelets, CRP-XL, 9E1 or Actinomycin D (ActD). Y-axis represents log$_{10}$ of fold change as calculated by 2$^{-\Delta\Delta Ct}$ method, bars represent mean ± SD and includes individual values (black dots). Incubation with platelets alone and activated platelets led to a significant (p<0.05) increase in the expression of FCGR3. There was no significant inhibition of FCGR3 by inhibiting MPA formation (9E1). Actinomycin D was effective at inhibiting the gene transcription induced by activated platelets. '*' = p<0.05, (n=4) analysis performed using students t-test.

Following an 8-hour incubation period, there was a minimal increase in the expression of *FCGR3* in CD16^{neg} monocytes although this was not significantly more than t=0hr control (p=0.12, t-test). Incubation with platelets alone led to a significant increase in *FCGR3* expression above CD16^{neg} monocytes alone (p=0.0129, t-test). However, activation with CRP-XL led to further increases in *FCGR3* expression in CD16^{neg} monocytes (p=0.0303, t-test). Inhibition of MPA formation with 9E1 did not abrogate the significant increases in *FCGR3* expression when compared to the control (p=0.0174, t-test) and although there was a trend towards lower expression of *FCGR3* when compared to activation with CRP-XL alone, this difference was not statistically significant (p=0.122, t-test). The use of Actinomycin D, however, completely inhibited *FCGR3* gene expression.

6.8 Further Characterisation of Monocyte Subsets and the Effect of Platelet Activation

Thus far, the strategy employed to stratify monocytes into their constituent subsets has relied on the fluorescence intensity of both CD14 and CD16. Classical monocytes can be differentiated readily based on the fluorescence of CD16 in which the 2% negative population is set with an appropriate isotype control (see **Table 3.1**). By definition, Classical monocytes are CD16^{neg} and therefore this subset can be readily identified. Difficulty arises when examining the CD16^{pos} monocyte subset and the distinction between the intermediate and non-classical subset. As both subsets are CD16^{pos}, the distinction between the two relies on a split between CD14 high and low expressing cells. Different gating strategies have been proposed to differentiate between the intermediate and non-classical subsets (**Zawada *et al.* 2015**) but still rely on a subjective stratification based on CD14 fluorescence.

Additional markers have therefore been proposed to stratify monocytes, in particular CCR2 and Slan1 (**Weber et al.** *2016*). A 5-colour flow cytometric assay was therefore set up to differentiate monocyte subsets based on the expression of these antigens in addition to CD45, CD14 and CD16, using CCR2-PE and Slan1-FITC as additional markers to distinguish these monocyte subsets.

6.8.1 Development of a 5-colour Assay for Flow-Cytometric Quantification of Monocyte Subsets

Leucocytes were first identified by the CD45 pan-leucocyte marker and all CD14^{pos} events were identified as monocytes. Of the CD45^{pos}CD14^{pos} population, the expression of CD16 was quantified and the cells were discriminated into CD16^{neg} and CD16^{pos} population. The discrimination of the 2 subsets was based on a pre-set 2% positive control using an appropriate isotype control conjugated to APC (**Figure 6.15**).

All monocytes that were CD16^{neg} were also negative for the Slan1 marker and showed a high expression of the CCR2 antigen. This subset was therefore designated as CD16^{neg}CCR2^{high}Slan1^{neg} and analogous to the classical monocyte subset traditionally defined by CD14 and CD16 fluorescence alone. The CD16^{pos} monocytes were all found to express CCR2 but with variable, bimodal intensity. Overall, there was a lower expression of CCR2 (CCR2^{dim}) within the CD16^{pos} population and was therefore not a good marker to discriminate between the intermediate and non-classical subsets but rather correlated with the CD16^{pos} and CD16^{neg} subsets. The

differentiation of the CD16^{pos} monocytes by Slan1 showed a much closer relationship to the expression of CD16 and was therefore used for further experiments to discriminate the different monocyte subsets.
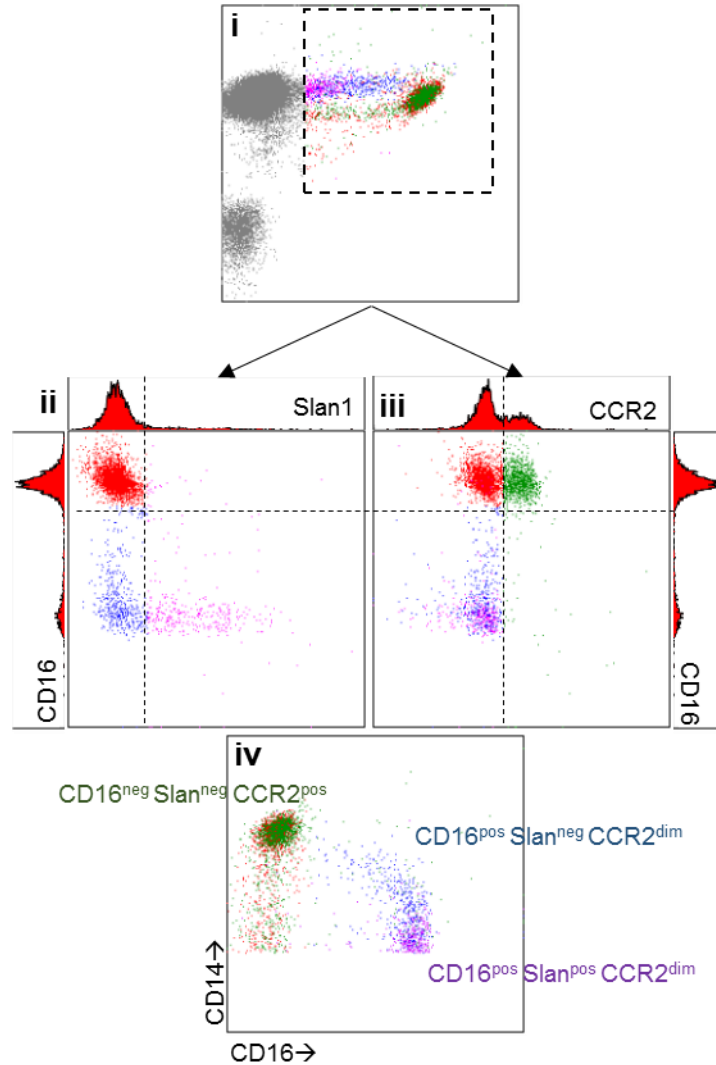
Figure 6.15: Deep Phenotyping of Monocyte Subsets. (i) Gating of monocytes based on CD45 expression (y-axis) and CD14 (x-axis). The CD45^{pos}CD14^{pos} cells were further analysed for expression of slan1 (ii) and CCR2 (iii). CD16^{neg} monocytes are all slan1^{neg} whereas CD16^{pos} monocytes were further stratified in those that do and do not express slan1. All CD45^{pos}CD14^{pos} cells expressed the CCR2 antigen (iii) however the expression intensity was bimodal. The CD16^{neg} monocytes expressed CCR2 in a bimodal distribution whereas CD16^{pos} monocytes were all CCR2^{dim} expressers. The composite CD14 vs CD16 plot (iv) can therefore be further stratified and accurately defined.

CD16^{pos} monocytes were gated and the expression of Slan1-FITC was quantified. The negative population was set using an appropriate 2% isotype control and the proportion of Slan1 positive and Slan1 negative cells were quantified. In this way, two further populations of monocytes were identified, namely the CD16^{pos}CCR2^{dim}Slan1^{neg} and the CD16^{pos}CCR2^{dim}Slan1^{pos} cells.

6.8.2   Validation of Five-Colour Assay

To validate this assay, we examine the classification of monocyte subsets using the 5-colour method to the traditional gating strategies used to stratify monocytes based on CD14 and CD16 fluorescence. Blood from healthy volunteers (n=3) was centrifuged on a density-gradient medium to isolate PBMCs. Cells were stained with fluorochrome-conjugated antibodies directed against CD45, CD14, CD16-, CCR2 and Slan1 and analysed by flow cytometry using 3 complimentary methods. Methods 1 and 2 gated monocytes based on CD14 and CD16 fluorescence however method 1 relies on rectangular gates to demarcate the different subtypes. Method 2 on the other hand still uses a rectangular gate to demarcate the classical subset but used a trapezoid gate to distinguish between the classical and intermediate subsets. Both of these methods were compared to a 3rd method (method 3) which employs the CCR2 and Slan1 antigens as additional markers of monocyte subsets (**Figure 6.16**).

When using a box gating strategy, 69.1±12.6% of cells were classified as 'Classical' with 7.4±1.2% and intermediate and 15.0±8.2% and non-classical (see

Table 6.1). When comparing to a trapezoid gating strategy (Method 2), there was an overall significant difference in the proportion of cells within each gate (p=0.0016, 2way RM-ANOVA). Upon multiple comparisons testing, there were significantly fewer intermediate monocytes and more non-classical monocytes when using the trapezoid gating strategy (p<0.001, Sidaks).

	Classical	Intermediate	Non-Classical
Box Gating	69.1±12.6	7.4±1.2	15.0±8.2
Trapezoid Gating	68.8±12.7	3.5±0.5	19.1±8.3

Table 6.1: Monocyte Subset Counts Using Differing Gating Strategies. Table shows comparison of flow-cytometric methods to classify monocyte subsets using both a box and trapezoid gating strategy. Values show mean±SD from 3 donors.

The 5-colour assay showed that of all (>95%) of the monocytes (CD45^{pos}CD14^{pos}), expressed the CCR2 antigen (>95%) in a bimodal distribution. The majority (84.4±5.7%) of CD16^{neg} monocytes expressed CCR2 at high levels and did not express the Slan1 antigen. They were therefore classified as CD16^{neg}CCR2^{high}Slan1^{neg} cells. Overall, 76.3±9.3% of all monocytes were classified as CD16^{neg}CCR2^{high}Slan1^{neg} which was significantly more than with either Method 1 or Method 2 (p<0.001, ANOVA). CD16^{pos} monocytes expressed CCR2 at lower levels (CCR2^{dim}) and were stratified based on the expression of the Slan1 antigen into either CD16^{pos}CCR2^{dim}Slan1^{neg} (11.6±2.6%) or CD16^{pos}CCR2^{dim}Slan1^{pos} (12.1±4.7%).

The correlation of CCR2/Slan1-defined subsets and the CD14/CD16-defined subsets was also investigated. Cells that fell within each of the gates (Classical, Intermediate, Non-Classical) were analysed to record what proportion of each of these cells were CD16^{neg}CCR2^{high}Slan1^{neg}, CD16^{pos}CCR2^{dim}Slan1^{neg} or CD16^{pos}CCR2^{dim}Slan1^{pos}. Over 99% of Classical monocytes, gated by both methods, were CD16^{neg}CCR2^{high}Slan1^{neg} which suggests that these two classification methodologies are synonymous with respect to this particular subset. When comparing the intermediate gate from the box and trapezoid gating strategies, 81.9±7.7% and 83.2±7.7% were CD16^{pos}CCR2^{dim}Slan1^{neg} respectively and the remainder were CD16^{pos}CCR2^{dim}Slan1^{pos}. When the non-classical gate was analysed, 62.6±5.8% and 52.2±7.3% cells were CD16^{pos}CCR2^{dim}Slan1^{pos} using Methods 1 and 2 respectively and the remainder of cells were CD16^{pos}CCR2^{dim}Slan1^{neg} (**Figure 6.16**). These results, taken in concert, suggest that CCR2/Slan1-defined subsets correlate well with the Classical monocyte subset but there is overlap of either Slan1^{pos} or Slan1^{neg} expression within the CD16^{pos} population which means that drawing the intermediate and non-classical gates does not necessarily correlate with the CCR2/Slan1-defined subsets. There is however a tendency for the Slan1^{neg} subset to fall within the intermediate gate and the Slan1^{pos} subset to lie within the non-classical gate.
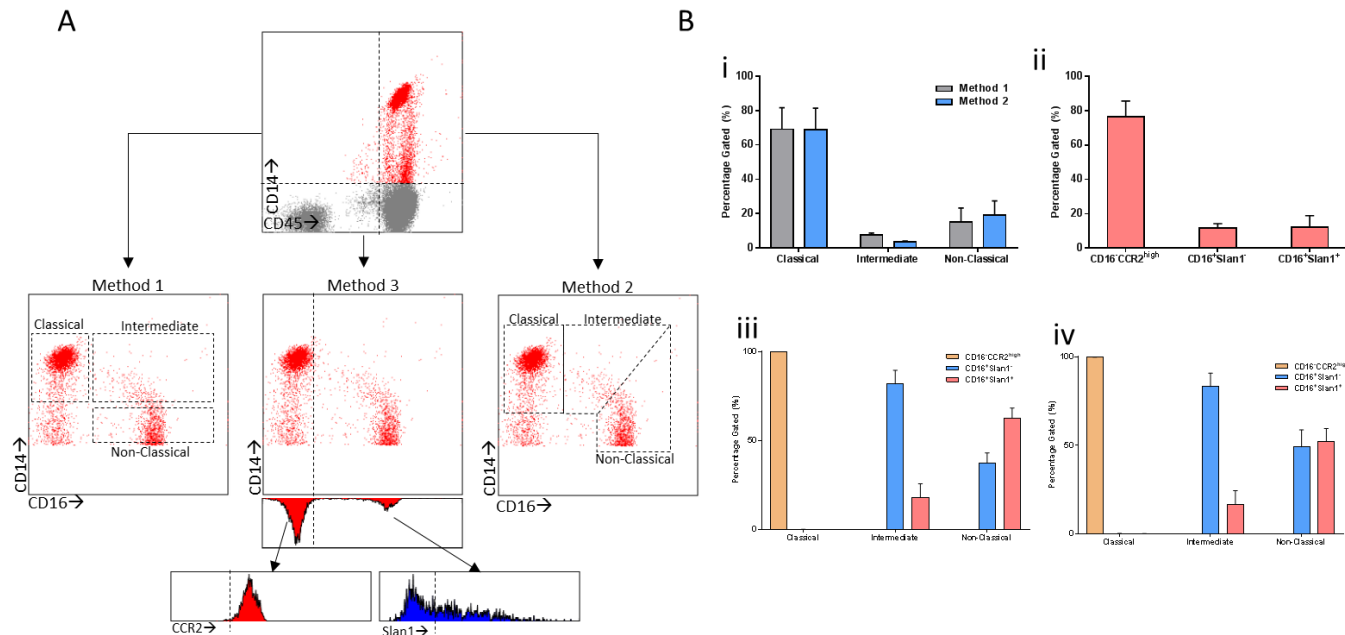
Figure 6.16: 'Standard' Gating Strategies Used to Sub-Classify Monocytes and their Relation to CCR2/Slan1 Expression. Figure shows results from isolated PBMCs from healthy volunteers (n=3). (A) shows gating strategies used to classify monocyte subsets. Monocytes were first identified by CD45 and CD14 staining and then sub stratified according to 3 different methods. Methods 1 and 2 rely on a CD14 vs CD16 plot and boxes are drawn around the Classical, Intermediate and Non-Classical subsets. Method 1 employs rectangular gates while Method 2 employs polygonal gates. Method 3 classifies cells according to CD16 expression and identified a CCR2high population from the CD16^{neg} monocytes. The CD16^{pos} monocytes were further subdivided into Slan1^{pos} and Slan1^{neg} cells. (B) shows collated results from healthy volunteers (n=3). (i) shows the proportion of monocytes within each of the Classical, Intermediate or Non-Classical gates using the gating techniques of Methods 1 and 2. There was a trend towards a greater proportion of 'Intermediate' monocytes and less 'Non-Classical' monocytes using polygonal gates (Method 2) however this was not statistically significant ($p>0.05$, RM-ANOVA with multiple comparisons). (ii) shows the proportion of monocytes stratified using CCR2 and Slan1 as markers in addition to CD14 and CD16 (Method 3).$76.3\pm9.3\%$ of cells were classified as CD16^{neg}CCR2^{high} and the remaining CD16^{pos} cells were equally split between Slan1^{pos} and negative cells. (iii) depicts the proportion of CCR2/Slan classified cells within each of the Classical, Intermediate and Non-Classical gates as per Method 1. 100% of Classical Monocytes were CD16^{neg}CCR2^{high} whereas the Intermediate and Non-Classical gates contained a mixture of Slan1^{pos} and Slan1^{neg} monocytes. There were significantly more CD16^{pos}Slan1^{neg} monocytes within the intermediate gate than in the Non-Classical gate ($p<0.001$, RM-ANOVA). (iv) shows the same data but for cells gated using Method 2. Using this method, a greater proportion of cells within the Non-Classical gate were designated as CD16^{pos}Slan1^{neg} than with Method 1. (RM-ANOVA with Tukey's multiple comparison.

6.8.3 Immuno-Magnetically Isolated CD16^pos and CD16^neg Monocytes Show Differential Expression of CCR2 and Slan1

Blood was collected from healthy volunteers (n=3) and PBMCs were separated by density gradient centrifugation. A 2-step immunomagnetic bead separation was performed to first deplete both granulocytes and NK cells using CD56 and CD15 microbeads. The pre-enriched cellular fraction was then further separated by CD16 immunomagnetic beads into a CD16 positive and CD16 negative cellular population (methods 3.2.2.10). Both populations of cells were analysed by flow cytometry for extended phenotypic markers of monocyte subpopulations (**Figure 6.17**).
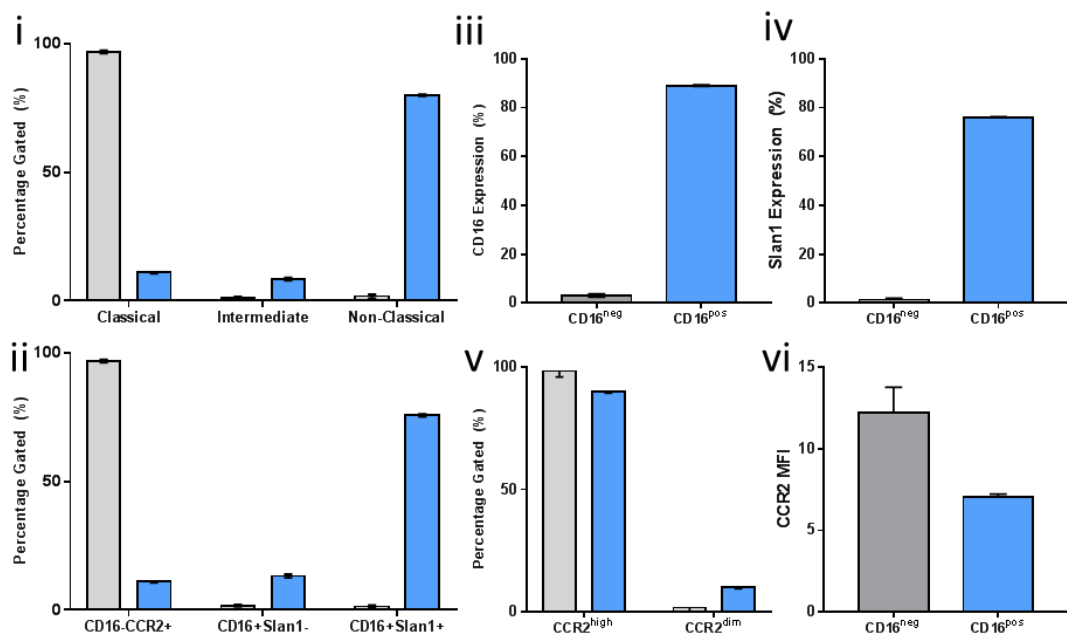

Figure 6.17: CCR2/Slan1 Quantification on CD16^pos and CD16^neg Monocytes. Graphs show the surface phenotypic markers of both CD16^neg (grey) and CD16^pos (blue) monocytes. (i) shows the proportion of monocytes classified as either Classical, Intermediate and Non-Classical based on CD14 and CD16 fluorescence using a box gating strategy. CD16^neg negative monocytes are predominantly classified as 'Classical' whereas CD16^pos monocytes are predominantly non-classical (ii) demonstrates the stratification of CD16^pos and CD16^neg monocytes according to expression of CCR2 and Slan1. CD16^neg monocytes are overwhelmingly CCR2^pos whereas CD16^neg monocytes are predominantly Slan1^pos although a significant minority (13.3%) are Slan1^neg. (iii) shows the proportion of isolated cells that express the CD16 antigen. Isolated CD16^neg monocytes do not show any expression of CD16 and therefore indicates a successful isolation procedure. (iv) shows the expression of Slan1 on both CD16^neg and CD16^pos monocytes. CD16^neg monocyte do not exhibit Slan1 staining whereas ~80% of CD16^pos monocytes do. (v) shows the percentage of cells that express CCR2 in high amounts (CCR2^high) and low amounts (CCR2^dim). The majority of both CD16^neg and CD16^pos cells are high expressers of CCR2 however a significant minority of CD16^pos cells express CCR2 at diminished levels. Finally, this was confirmed by measuring the fluorescence intensity of CCR2 staining (vi) which shows that CD16^neg monocytes express significantly more CCR2 than their CD16^pos counterparts (p=0.0006, n=3, t-test).

To verify separation, the expression of CD16 was quantified on both isolated cell types. On the CD16 depleted cellular fraction, mean expression of CD16 was 3.1±0.6% as compared with the CD16^{pos} fraction which showed a mean expression of 89.0±0.3% confirming that the separation procedure was effective.

It was found that the 98.1±0.6% of CD16^{neg} monocytes were classified as CD16^{neg}CCR2^{high} in contrast to only 11.0±0.3% of CD16^{pos} cells (p<0.001, t-test). Furthermore, within the CD16^{pos} fraction, 13.35±0.7% of cells were classified as CD16^{pos}CCR2^{dim}Slan1^{neg} with the vast majority (75.8±0.6%) classified as CD16^{pos}CCR2^{dim}Slan1^{pos}. Slan1 is also an excellent marker to distinguish between the CD16^{pos} and CD16^{neg} isolated cell types as 1.4±0.6% of CD16^{neg} cells expressed Slan1 as compared with 75.8±0.6% of CD16^{pos} cells. That is to say that all CD16^{neg} cells are additionally Slan1^{neg} but not all CD16^{pos} cells are Slan1^{pos}. There were also differences in the intensity of CCR2 expression between the CD16^{pos} and CD16^{neg} subsets. The median fluorescence intensity of CCR2 in CD16^{neg} monocytes was 12.3±0.8 and compared with 7.3±0.1 in the CD16^{pos} fraction. This difference was statistically significant (p=0.0006, t-test) suggesting that the CD16^{pos} fraction expressed the CCR2 antigen as a lower level than their CD16^{neg} counterpart. Within the CD16^{pos} population there was no statistically significant difference in CCR2 fluorescence intensity when comparing Slan1^{pos} against Slan1^{neg} cells (p>0.05, t-test).

6.9 Activated Platelets Induce a CD16^{pos}CCR2^{dim}Slan1^{neg} Monocyte Phenotype in CD16^{neg} Monocytes

These experiments have demonstrated that classification of monocytes using CCR2 and Slan1 as additional markers is clearly able to distinguish CD16^{neg} from CD16^{pos} monocytes and furthermore, is able to distinguish subsets within the CD16^{pos} population. Given that platelets have been shown to induce CD16 in previously CD16^{neg} monocytes, this finding was to be confirmed using this more comprehensive measure of phenotype with CCR2 and Slan1 as additional markers.

Blood from healthy volunteers (n=3) was collected and PBMCs were isolated by density-gradient centrifugation. From this cell suspension, platelets were depleted (CD61 microbeads) and both a CD16^{neg} and CD16^{pos} populations were isolated. From autologous whole blood, PRP was prepared and washed platelets were made. CD16^{neg} cells were incubated with autologous washed platelets with and without 1.0µg/ml CRP-XL to activate platelets for 4hrs at 37°C on slow

rotation. Cells were analysed at t=0hrs and after 4 hours of incubation to quantify monocyte phenotype (**Figure 6.18**).
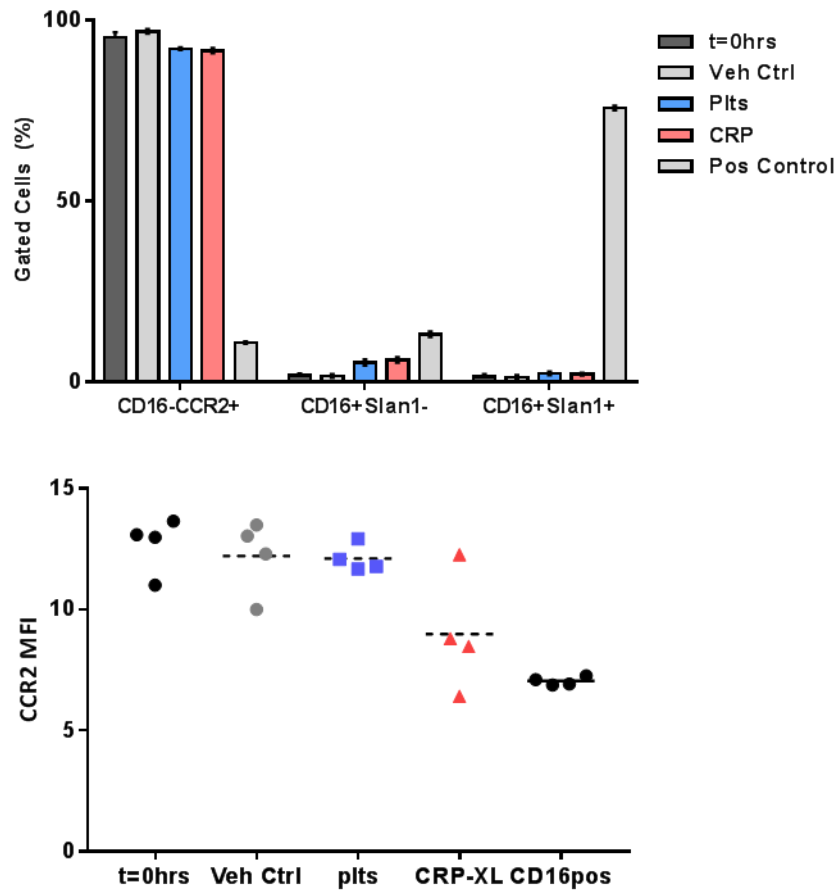

Figure 6.18: Extended Monocyte Phenotype of CD16^{neg} Monocytes with Platelet Activation. Graphs shows the extended phenotype of monocytes using both CCR2 and Slan1 as markers in addition to CD14 and CD16. CD16^{neg} monocytes are shown immediately following isolation (t=0hrs) followed by 4hours incubation with a vehicle control (Veh Ctrl). CD16^{neg} monocytes were also incubated with autologous platelets alone (Plts) and autologous platelets + 1.0µg/ml CRP-XL (CRP). The positive control was CD16^{pos} isolated monocytes. Graph shows the percentage of cells gated to either the CD16^{neg}CCR2^{pos}, CD16^{pos}Slan1^{neg} or CD16^{pos}Slan1^{pos} phenotypes. Incubation with platelets and activated platelets led to a significant decrease in the CD16^{neg}CCR2^{pos} population (p<0.01, ANOVA). Furthermore, there was a significant increase in the proportion of cells that were CD16^{pos}Slan1^{neg} (p<0.01, ANOVA) when comparing to a vehicle control. However, there was no statistically significant difference when comparing CRP-activated vs non-activated platelets. There was no overall statistically significant difference in the CD16^{pos}Slan1^{pos} population with platelet incubation (p>0.05, ANOVA). When comparing data for the median fluorescence intensity of CCR2 staining (CCR2 MFI), there was overall a significant effect of platelet incubation in reducing CCR2 MFI (p=0.0386, 1way ANOVA). There was no statistically significant difference on multiple comparisons testing

Freshly isolated CD16^{neg} negative monocytes were 95.2±1.4% CD16^{neg}CCR2^{high}Slan1^{neg} with less than 2% of cells were designated as CD16^{pos}. There was no overall significant change in the proportion of cells within each subset upon incubation with a vehicle control (p=0.087, RM-ANOVA) however there were marginally fewer CD16^{neg}CCR2^{high}Slan1^{neg} monocytes (p=0.047, ANOVA with Sidaks). When the addition of vehicle control was compared to CD16 negative cells incubated with autologous platelets, there was a statistically significant (p<0.001, ANOVA)

increase in the CD16^{pos}CCR2^{dim}Slan1^{neg} and a decrease in CD16^{neg}CCR2^{high}Slan1^{neg} subsets. This difference was even more marked when the addition of a vehicle control was compared to the addition of autologous, CRP-XL activated platelet (p<0.0001, ANOVA). There was no significant difference in the proportion of CD16^{neg}CCR2^{dim}Slan1^{pos} monocytes across all reaction conditions (p>0.05, ANOVA). CD16^{pos} monocytes were analysed as a positive control and the pattern of expression with platelet-activated CD16^{neg} monocytes tended towards a CD16^{pos} population with the exception of the CD16^{pos}CCR2^{dom}Slan1^{pos} subset which remained low despite platelet activation. This was further confirmed when examining the fluorescence intensity of CCR2 expression (**Figure 6.19**). There was no significant difference when comparing CCR2 MFI on t=0hr CD16^{neg} monocytes to either 4 hours with a vehicle control (p=0.12, paired t-test) or with autologous washed platelets (p=0.55, paired t-test). There was lower expression of CCR2 when CD16^{neg} monocytes were incubated with activated platelets (12.2±0.8 vs 9.0±1.2) however this was not statistically significant (p=0.066, t-test). Overall, platelet activation, in addition to inducing CD16 expression, leads to a decreased expression of CCR2 and a slightly increased expression of Slan1 in previously CD16^{neg} monocytes.
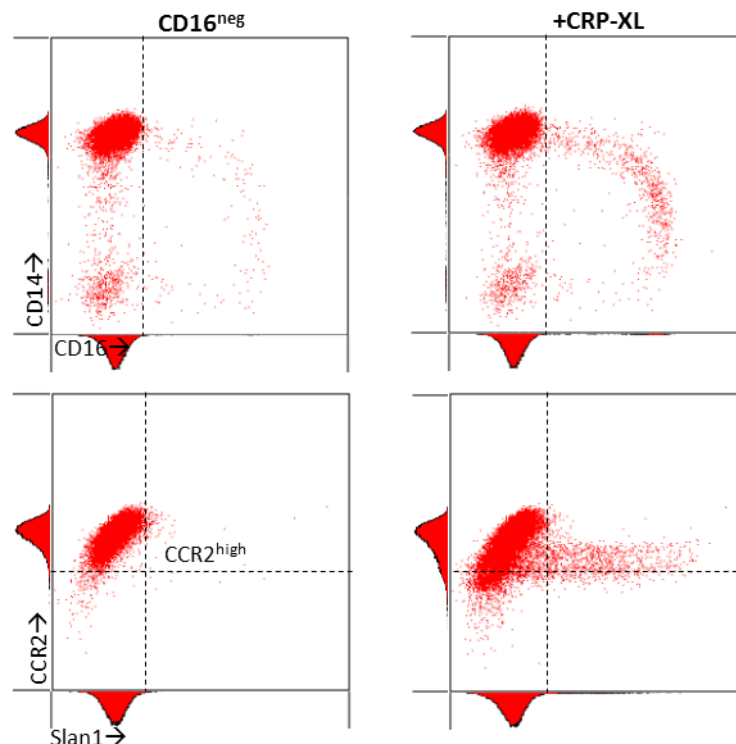
Figure 6.19: Representative Flow Cytometry of CD16^{neg} Monocytes Incubated with Activated Platelets. Images are for CD16^{neg} monocytes (left hand column) and those monocytes incubated with CRP-activated platelets (right hand column). Top row shows plot of CD14 (y-axis) vs CD16 (x-axis) with the vertical dashed line representing the demarcation between the CD16 positive and negative cells. Stimulation with CRP-XL leads to a rise in the proportion of CD16 positive monocytes. Bottom row shows plots of CCR2 (y-axis) vs Slan1 (x-axis) with the vertical line representing the demarcation between Slan1^{neg} and Slan1^{pos}. The horizontal dashed line represents the demarcation between CCR2 high expressing cells and CCR2 dim. With platelet activation, there is an increase in the overall proportion of cell expressing Slan1 and a tendency towards decreased expression of CCR2 towards the dim population

6.10 <u>Expression of Chemokines on Platelet-Activated Monocytes</u>

Chemokine receptors are constitutively expressed by monocytes and exist in both surface and intracellular forms. The levels of expression of these receptors and the release of the cognate chemokines, not only from monocytes but from leucocytes of all classes, is a mechanism by which the phenotype of these cells is regulated (see **Table 9.1** for a list of chemokines). The ligation of chemokines to their cognate receptor allows for the migration of monocytes through the endothelial barrier and also modulates their phenotype to make them, in some instances, pro-inflammatory. This is contrasted with the 'anti-inflammatory' chemokines which regulate monocyte behaviour to render them more protective of the endothelium. The corollary with respect to foam cell formation is that the levels of expression of chemokines, which subsequently affect the migration and atherogenicity of monocytes, likely contribute to the formation of an advanced atherosclerotic plaque.

Platelets contain a range of chemokines and might influence the phenotype of monocytes through modulation of chemokines and chemokine receptors. Using the same dataset from which the expression of lipid-regulatory genes was analysed (Section 5.3.1), the transcriptome of platelet-activated monocytes was analysed with respect to expression of chemokine genes. This demonstrates that the genes belonging to the chemokines and their receptors were some of the most highly upregulated in platelet-activated monocytes. In particular, IL-8, CCL20, CCL2 and CCL7 were among the top 25 most highly upregulated genes on the array. CCL3, CCR2, CXCL10 and CX3CR1 were downregulated in platelet-activated monocytes. At the transcriptomic level at least, activated platelets lead to significant changes in the expression of chemokines and their receptors which may have significant effects on the phenotype of platelet-activated monocytes. Furthermore, the analysis performed to date is an aggregate of all monocytes and does not distinguish between monocyte subsets. It has been demonstrated that platelets can differentially activate monocyte subsets (see section 6.4.1) and it may be the case that platelets preferentially induce a chemokine receptor profile that is different in CD16^{pos} vs CD16^{neg} monocytes that might account partly for their different atherogenicity. The effect of activated platelets on the expression of a selected group of chemokine receptors on monocytes was therefore examined along with the effects of platelets on the release of chemokines from monocytes.

6.10.1 Expression of Chemokine Receptors on Whole Blood Monocytes

6.10.1.1 Method

The effect of activated platelets on the expression of surface chemokine receptors was initially quantified using a whole blood model. Blood from healthy volunteers (n=2) was collected into 3.2% trisodium citrate and incubated for up to 8hrs on slow rotation at 37°C either with or without the addition of CRP-XL at a final concentration of 1.0µg/ml. At regular time intervals over the incubation period, 50µl aliquots were taken at 0, 2, 4, 6, and 8 hours for analysis by flow cytometry and prepared according to a standard protocol (as outlined in 3.2.5.2). To identify monocytes, leucocytes were labelled with CD45-PerCPVio700 pan-leucocyte marker followed by identification of monocytes by CD14-VioBlue. Up to 7 samples was collected at any one time point wherein PE-conjugated antibodies directed against surface chemokine receptors, namely CCR1, CCR2, CX3CR1, CXCR1, CXCR2, CXCR3 and CXCR6 was used. A REA isotype control was used (and a PE-conjugated IgG2b for the CXCR1-PE antibody) to set the baseline fluorescence at 2% (see **Table 3.1** for list of antibodies). Both the percentage of monocytes expressing the respective chemokine receptors and their median fluorescence intensity was recorded (**Figure 6.20**). Samples from 2 donors was investigated but the final measurement (at t=8hrs) for one of the donors was rejected due to sample degradation.

6.10.1.2 Results

Overall, there were no significant differences between CRP-activated samples and vehicle control in any of the chemokines analysed over the 8 hour incubation period with respect to either the percentage of cells expressing each chemokine receptor, or the median fluorescence intensity. The results confirmed the constitutive expression of the receptors on the surface of monocytes however this model failed to demonstrate any appreciable change with platelet activation (**Figure 6.20**). While there was some increased expression at the longer time points of CXC3CR1, CXCR2, CXCR3 and CXCR6, none of this reached statistical significant ($p > 0.05$).
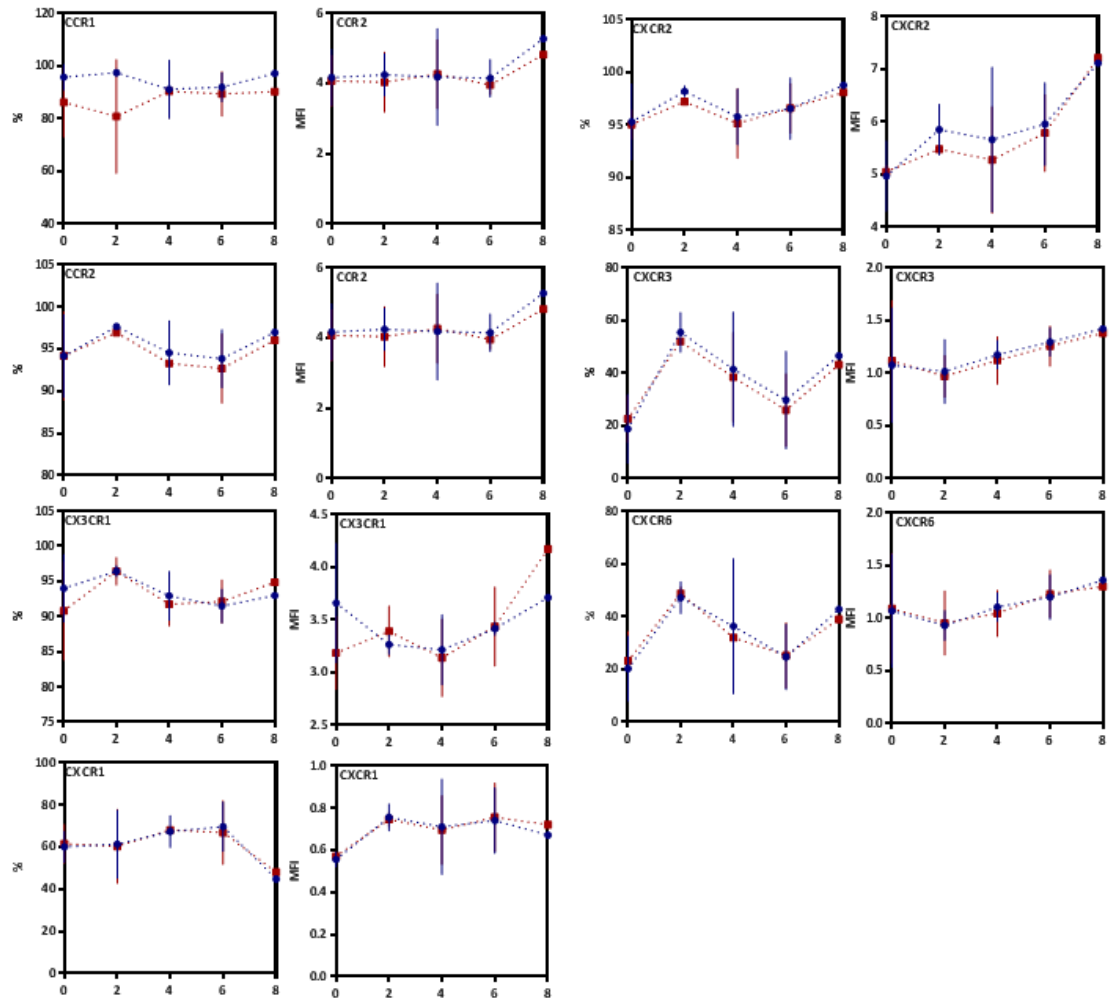
Figure 6.20: Expression of Chemokine Receptors on Whole Blood Monocytes. Graphs show both percentage of monocytes that express the respective chemokines (%) and their median fluorescence intensity (MFI). Graphs show mean±SD where blue dots/lines represent un-activated whole blood and red denotes CRP-activated samples. Over the 8 hour incubation period, there is no significant difference between control and test samples in either MFI or percentage positive for any of the above chemokines (p>0.05, multiple t-tests).

6.10.2 Expression of Chemokine Receptors on Isolated Monocytes

Given that there was no demonstrable evidence that activated platelet induce a change in the expression of chemokine receptors in a whole blood model, a model using isolated monocytes was employed instead.

6.10.2.1   Method

Whole blood (n=5), collected into 3.2% trisodium citrate, was centrifuged to separate PRP (see methods 3.2.2.1) from which washed platelets were prepared (section 3.2.2.3). The remaining platelet-poor blood fraction was diluted with PBS/5mM EDTA and carefully overlayed onto lymphoprep for the isolation of PBMCs by density-gradient centrifugation (see methods section 3.2.2.5). From this, CD61 immunomagnetic bead depletion was performed (section 3.2.2.7) followed by negative isolation of monocytes (section 3.2.2.9). Following isolation of the cellular fractions, washed platelets were added to an aliquot of isolated monocytes in a 250:1 stoichiometry[32].   Monocytes were incubated alone in HBS, with un-activated platelets or with platelets and CRP-XL at a final concentration of 1.0μg/ml. The expression of chemokine receptors was quantified on monocytes at t=0hrs and after a 4hr incubation period at 37°C on slow rotation under different conditions as outlined above (**Figure 6.21**).

6.10.2.2   Results

Monocytes incubated alone in HBS showed no overall significant difference (ANOVA, $p>0.05$) in chemokine expression when compared to the t=0hr sample. However, when compared to the HBS control, there was a significant increase ($p<0.01$, RM-ANOVA) in the expression of CXCR6 when monocytes were incubated with platelets and an even greater difference (21.9% vs 12.7% increase) when incubated with CRP-activated platelets ($p<0.0001$). A similar magnitude of increase was observed with CXCR3 expression on monocytes when incubated with platelets (5.8% increase $p=0.038$) which increased with activated platelets (15.7%, $p<0.0001$). A similar result was found when recording median fluorescence intensity for CXCR6 ($p<0.01$) however there was no overall significant difference in MFI with CXCR3 ($p>0.05$, RM-ANOVA). Activation with platelets resulted in a significant increase (27.1%, $p<0.0001$) in the expression of CX3CR1 which was not matched by a concomitant increase in the median fluorescence intensity ($p>0.05$). Conversely, activation with platelets led to a significant decrease in the surface expression of CCR2 by 7.7% ($p=0.0047$) which was matched by a significant fall in the median fluorescence intensity ($p<0.001$). There was a greater fall (78.4%, $p<0.001$) in the surface

---

[32] In most instances, this equated to $1.0x10^6$ monocytes in a 1ml Eppendorf with $250x10^6$ platelets all constituted to a final 1000μl volume.

expression of CCR1 with concomitant decreases in the median fluorescence intensity (p=0.014). There were no overall significant differences (p>0.05) in the surface expression of CXCR2 and CXCR1.
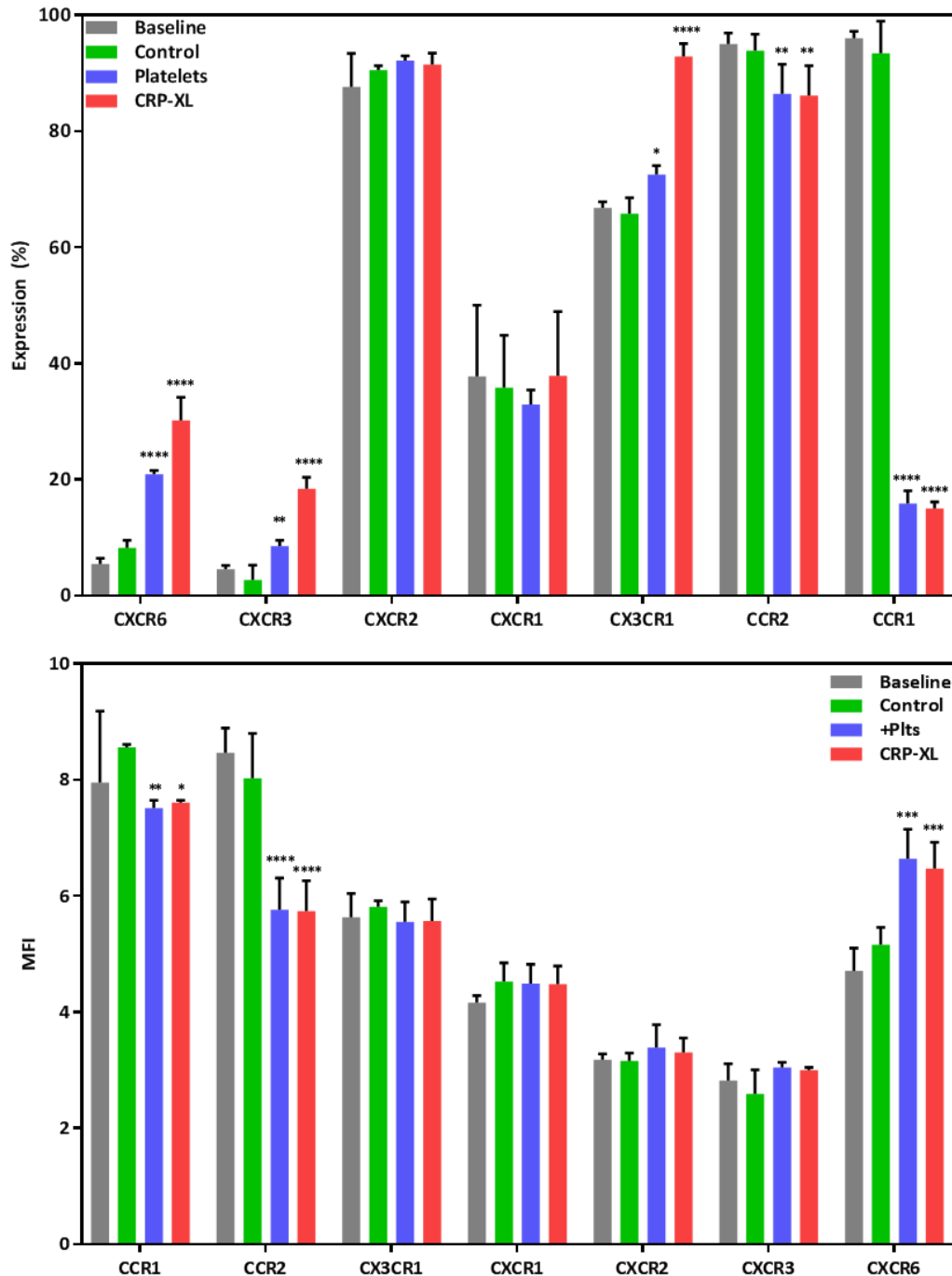

Figure 6.21: Chemokine Receptor Expression on Platelet-Activated Monocytes. Graphs show both the percentage expression (top panel) and median fluorescence intensity (bottom panel) of chemokine receptor expression on isolated monocytes. Bars show mean±SD of chemokine receptor expression from monocytes at t=0 (baseline), following 4 hours of incubation (control) and following incubation with washed platelets (+Plts) or with activated washed platelets (CRP-XL). Samples were compared to control. ('****'=p<0.0001, '***'=p<0.001, '**'=p<0.01, '*'=p<0.05, 2-way RM ANOVA with Dunnetts multiple comparisons). Overall, CCR1 and CCR2 showed a significant decrease in expression with platelet activation whereas CXCR6, CXCR3 and CX3CR1 showed a significant increase in expression with platelet activation.

6.10.3 Quantification of Intracellular Chemokine Receptor Expression

The flow cytometric assay allowed only for the quantification of the surface expression of chemokine receptor. To see if the expression of protein recapitulates the transcriptomic signature, flow cytometry was employed to examine the expression of chemokine receptors both on the surface and intracellularly.

6.10.3.1   Method

Blood from healthy volunteers (n=3) was collected into 3.2% trisodium citrate and both monocytes and washed platelets were prepared as before (section 6.10.2.1). Monocytes were incubated with washed platelets in a 250:1 stoichiometry as before and incubated for 4 hours with CRP-XL at 37°C. Following this incubation period, the monocytes (with and without co-incubated platelets) were pelleted and re-suspended in PBS/0.2% TWEEN to permeabilise the cells (methods section 3.2.4.4). After further washing, cells were incubated with primary antibodies including CD45-PerCPVio700, CD14-VioBlue and PE-conjugated antibodies to chemokine receptors. After fixation with 0.2% Formyl Saline, cells were analysed as before for the expression of chemokine receptors by median fluorescence intensity (**Figure 6.22**).

6.10.3.2   Results

From the t=0hr time point to a 4 hour incubation period, there was a trend towards increasing expression of chemokine receptors with a decreasing expression of CX3CR1. None of these reached statistical significant except for CCR2 and CXCR1 which both showed increased expression (adjusted p=0.030 and 0.046 respectively, multiple t-test with Holm-Sidak correction).

When samples were activated using CRP-XL, there was a trend towards decreased expression of the chemokine receptors CCR1, CCR2, CXCR1 and CXCR2. Conversely, there was a trend towards increased expression of CX3CR1 however, using the same statistical methods as before, an unadjusted p<0.05 was found only for CCR2 which was not significant after correction for multiple testing.
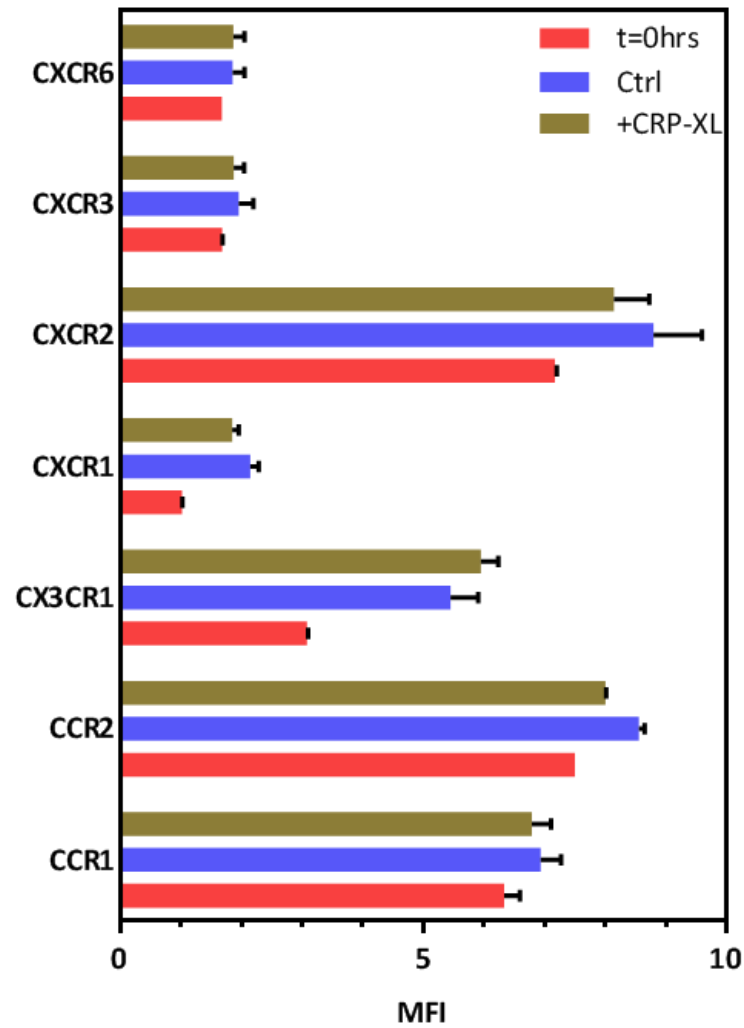
Figure 6.22: Expression of Intracellular Chemokine Receptors. Graphs show median fluorescence intensity of chemokine receptors in monocytes permeabilised prior to staining thus reflecting intracellular antigens. There is a trend towards decreased expression of CCR1, CCR2, CXCR1 and CXCR2 with CRP-XL activation while the expression of CX2CR1 increased. There was no appreciable difference in expression of CXCR6 and CXCR3. None of these results reached statistical significance. Bars show mean±SD (n=3).

6.10.4 Expression of Chemokine Receptors on Monocyte Subsets

The mixed results from flow cytometry might partly be accounted for in the light of previous experiments which has demonstrated that platelets induce a change in the phenotype of monocytes (section 6.5). Furthermore, monocyte subsets are known to express differing levels of chemokine receptors such as CCR2 and CX3CR1 and therefore, the observed difference in chemokine receptor expression may be accounted for by differing levels of CD16^{pos} and CD16^{neg} monocytes. Monocytes were isolated from whole blood (n=3) by density-gradient centrifugation followed by immunomagnetic depletion of CD61^{pos} platelets and CD14^{pos} leucocytes (see section 3.2.2.9 for method). These isolated monocytes were prepared for flow cytometry where subsets were identified based on the surface expression of CD14 and CD16 (see methods section 3.2.5.7). Furthermore, the surface expression of chemokine receptors was quantified on each subset (see **Figure 6.23**).

Following incubation with platelets, CCR1 showed a >95% expression on the Mon1 subset[33] with a 20.9% reduction on Mon2 with a further 11.3% decrease on Mon3 monocytes (p<0.001). A similar pattern was seen for CCR2 where the Mon3 subset showed significantly less than on Mon1 (p<0.001). Conversely, CX3CR1, CXCR3 and CXCR6 all showed significantly more expression on the CD16^{pos} subsets than on the 'classical' Mon1 subset (p<0.001 and p<0.0001 respectively). CXCR1 showed a greater expression on the Mon2 subset than either the Mon1 or Mon3 subsets (p<0.0001). There was no overall significant difference between any of the subsets with respect to the expression of the chemokine receptor CXCR2 (p>0.05).

---

[33] Mon1 is an alternative nomenclature for Classical monocytes with Mon2 and Mon3 used to describe Intermediate and Non-Classical subsets respectively
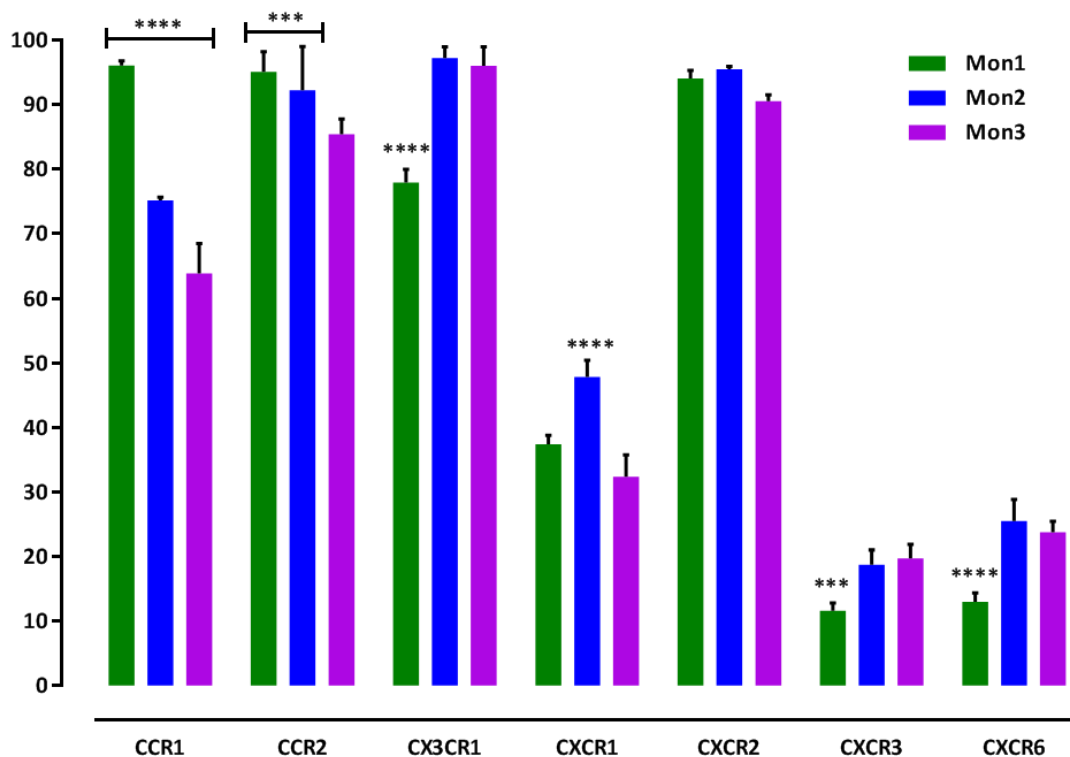
Figure 6.23: Expression of Chemokine Receptors on Monocyte Subsets. Isolated monocytes were classified by the expression of CD14 and CD16 into Mon1, Mon2 and Mon3 subtypes. Using flow-cytometric gating of these subtypes, surface expression of chemokine receptors was quantified. Bars depict mean±SD of percentage expression of chemokine receptors on different monocyte subsets. CXCR6 and CXCR3 are expressed more on the Mon2 and Mon 3 subsets. There is a progressive decrease in the expression of CCR1 and CCR2 with Mon3 as compared with Mon1 subsets. CX3CR1 is expressed more on the Mon3 and Mon2 subsets than the Mon1. '****'=p<0.0001, '***'=p<0.001, 2-way ANOVA.

6.10.4.1 *Expression of Chemokine Receptors on CD16^pos and CD16^neg Monocyte Subsets*

For the analysis of monocyte subsets, both CD16^pos and CD16^neg monocytes were isolated from PBMCs. Whole blood, collected into 3.2% trisodium citrate (n=3) was carefully layered onto Lymphoprep™ to generate PBMCs while washed platelets were prepared simultaneously from the PRP (**Figure 6.24**).
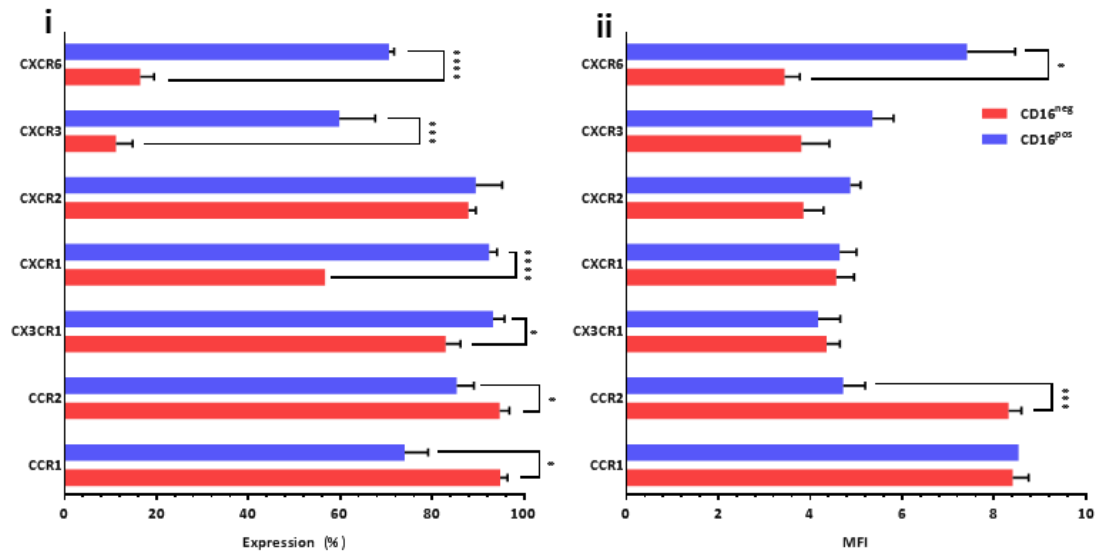

Figure 6.24: Expression of Chemokine Receptor on CD16^pos and CD16^neg Monocytes. Graphs show chemokine receptor expression of both percentage positive (i) and median fluorescence intensity (ii) on isolated CD16^pos (blue) and CD16^neg (red) monocytes. All of the analysed chemokine receptors, except for CXCR2, show significant differences between the CD16^pos and CD16^neg monocytes. The differences in median fluorescence intensity mirror that of the percentage positive expression but only reached statistical significance with CXCR6 expression and CCR2. Bars represent mean±SD, '*'=p<0.05, '**'=p<0.01, '***'=p<0.001, '****'=p<0.0001.

Upon analysis of both the percentage positive and median fluorescence intensity of chemokine receptor expression, there were significant differences when comparing isolated CD16^neg and CD16^pos monocyte fractions. The CD16^pos monocyte subset showed a greater expression of a range of chemokine receptors including CXCR6 (p<0.0001), CXCR3 (p<0.01), CXCR1 (p<0.0001) and CX3CR1 (p<0.05). There were more modest differences in the median fluorescence intensity of receptors with CXCR6 being expressed with greater intensity on CD16^pos monocytes. There was also significantly less (p<0.05) CCR2 and CCR1 expression on the CD16^pos monocyte subset as established previously (**Figure 6.18**).

6.10.4.2 Induction of Differential Chemokine Receptor Expression on Platelet-Activated Classical Monocytes

Following on from the flow-cytometric discrimination of monocyte subsets based on surface expression of CD14 and CD16, the classical monocyte subset was specifically isolated and incubated with washed, activated platelets. Blood from healthy volunteers (n=3) was collected into 3.2% trisodium citrate and centrifuged to separate PRP. From the PRP, washed platelets were prepared using a standard methodology (method section 3.2.2.3) and the remaining blood was carefully overlayed onto Lymphoprep™ to isolate PBMCs. From this cellular fraction, CD16^{pos} monocytes were positively selected and subsequently discarded leaving only the CD16^{neg} 'classical' monocyte subset (methods section 3.2.2.11). The isolated classical monocyte subset was then incubated with washed platelets (in a 250:1 stoichiometry) with and without activation with CRP-XL at a final concentration of 1.0µg/ml. Samples were incubated for 4 hours at 37°C on slow rotation and then analysed for the expression of surface chemokine receptors (**Figure 6.25**).

Analysis of the effect of platelet activation on the expression of chemokine receptors on classical subsets recapitulates the previous data. Classical monocyte subsets were characterised by high levels (>90%) of expression of CCR1, CCR2 and CXCR2. CCR1 expression fell upon platelet activation however this not reach statistical significance. The expression of CCR2 fell significantly with platelet activation ($p<0.05$) as did the median fluorescence intensity of CXCR2 ($p<0.05$). Conversely, the expression of CXCR1, CXCR3 and CXCR6 all increased with platelet activation ($p<0.05$).
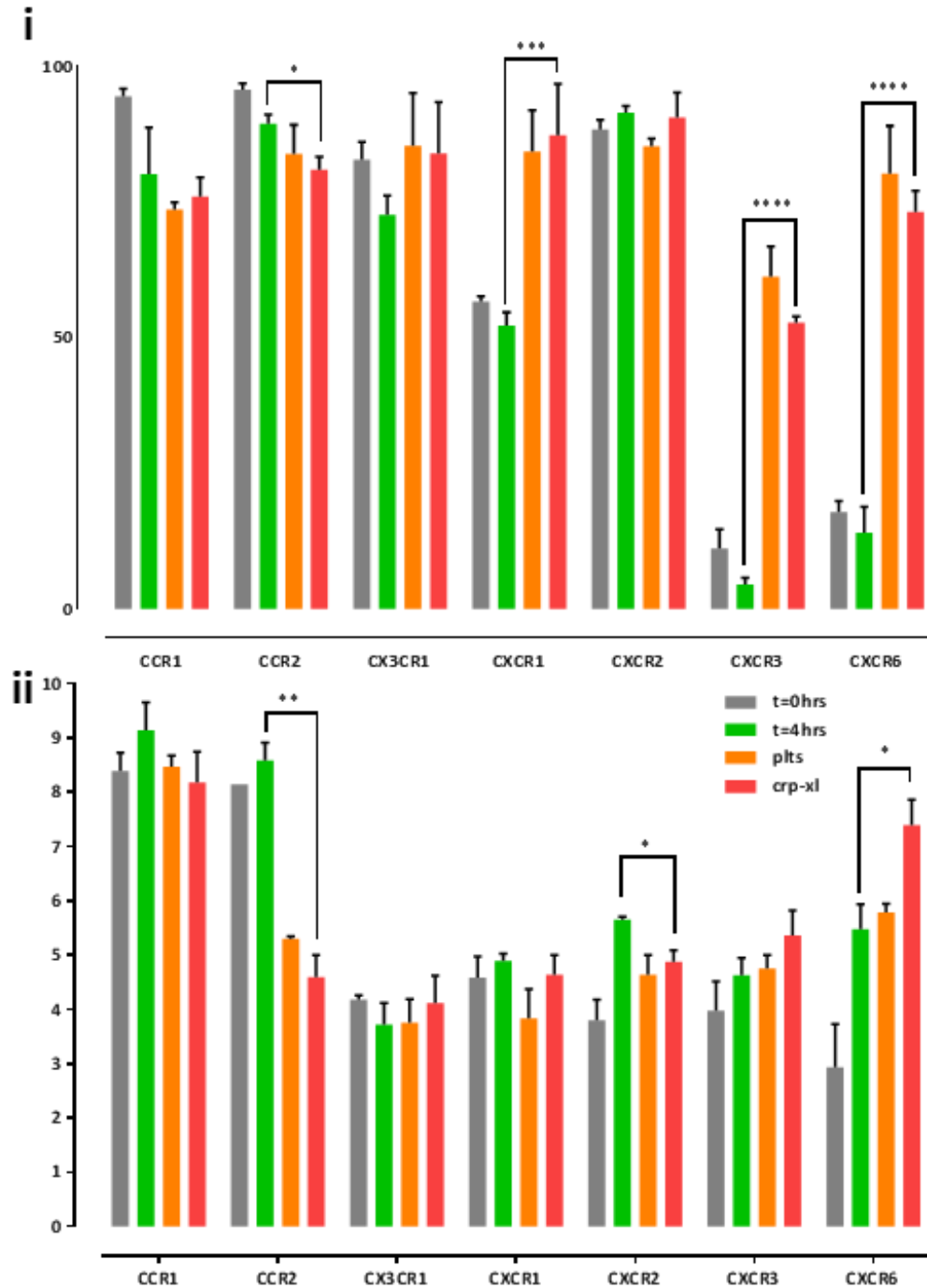
Figure 6.25: Expression of Chemokine Receptors on Platelet-Activated Classical Monocytes. Graphs show both the percentage expression (i) and median fluorescence intensity (ii) of chemokine receptor expression. Bars depict mean±SD of t=0hrs baseline classical monocytes (grey), following a 4hr incubation period without platelets (green), with non-activated platelets (orange) and CRP-activated platelets (red). CRP-activated classical monocytes show a significant increase in the expression of CXCR1, CXCR3 and CXCR6 with decreased expression of CCR2, CXCR3. '*'=p<0.05, '**'=p<0.01, '***'=p<0.001, '****'=p<0.0001.

6.10.5 Summary Data of Chemokine Receptor Expression

When the comparing the surface expression of chemokine receptors across different incubation conditions, there are some patterns that emerge and is shown in a summary heatmap (**Figure 6.26**). The baseline level of chemokine receptors on monocytes is largely mirrored by the levels on isolated CD16^{neg} monocytes. This is consistent with the fact that the majority (>80%) of all monocytes are classified as 'classical' and therefore are CD16^{neg} by definition. Isolated monocytes, when stimulated by platelets show a significant difference in expression of a range of chemokine receptors including CCR1, CCR2 and CX3CR1. The pattern of expression mirrors that seen in isolated CD16^{pos} cells. Furthermore, when CD16^{neg} are activated with platelets, the profile of chemokine receptor expression mirrors that of the CD16^{pos} monocyte. These results suggest that in addition to the effect of activated platelets on the transformation of a CD16^{neg} subset to one that is CD16^{pos} (see Section 6.5), they also promote a chemokine receptor expression profile that mirrors the pro-inflammatory CD16^{pos} subset.
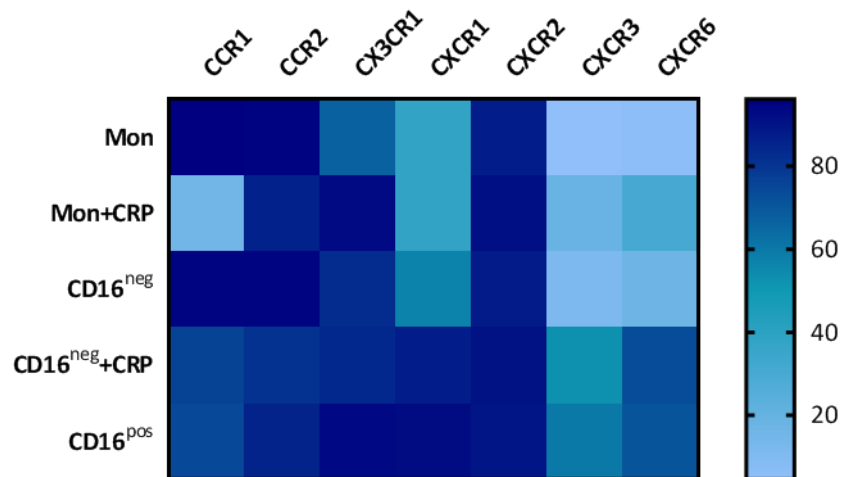
Figure 6.26: Heatmap Summary of Chemokine Receptor Expression. Plot shows the percentage surface expression of chemokine receptors (given along x-axis) on different isolated monocyte populations. 'Mon' refers to isolated monocytes, of all subsets, and 'Mon+CRP' shows data for platelet-activated monocytes. Shown also is chemokine expression on both CD16^{neg} and CD16^{pos} isolated monocyte subsets. Finally, data from CD16^{neg} monocytes incubated with activated platelets is shown (CD16^{neg}+CRP).

6.10.6 Release of Chemokine from Platelet-Activated Monocytes

In addition to the differential induction of chemokine receptor expression on the surface of monocytes by activated platelets, they may also induce the release of chemokines by monocytes and other leucocytes. In order to quantify the effect of platelets, the release of chemokines was measured by a semi-quantitative immunoblot assay.

Blood from healthy volunteers was collected and either separated into PRP or left as whole blood, both of which were incubated with CRP-XL for 4 hours to activate platelets. A control sample of whole blood was retained at t=0hrs to measure the baseline levels of chemokines as well as a 4-hour incubation of un-activated blood to record the effect of incubation alone on chemokine release. After the appropriate incubation periods, the samples were centrifuged to separate plasma which were then hybridised to a nitrocellulose membrane impregnated with antibodies directed against a range of chemokines. Mean pixel density was quantified (based on a HRP-Streptavidin system) to measure the relative expression of a range of chemokines. The chemokine profile from a resting blood sample and a 4hr un-activated sample was subtracted from the 4-hour activated to give the profile of a CRP-induced chemokine release. Furthermore, the profile from the isolated, activated PRP was also subtracted from the final 4-hour CRP-incubated whole blood to give the release of chemokines from monocytes and other leucocyte classes.

6.10.6.1 Method

18mls of whole blood was collected from healthy volunteers (n=5) into 3.2% trisodium citrate. For each donor, two 4.5ml tubes were set aside and centrifuged at either 600g for 20mins (see methods 3.2.2.2) and 160g for 20mins (see methods 3.2.2.1) to generate plasma and PRP respectively. The plasma was centrifuged for a further 5 mins at 13,000g to pellet microparticles. The supernatant was aspirated and filtered through a 0.22μm filter and stored at -80°C for future analysis as a t=0hr baseline sample. The remaining 2 tubes of whole blood and the isolated PRP sample were all incubated for 4 hours on gentle rotation at 37°C. Both the PRP and one tube of whole blood was incubated with 1.0μg/ml of CRP-XL with a HBS vehicle control for the 2nd tube of whole blood to act as a control. Following the incubation period, both the blood samples and PRP were centrifuged at 600g for 20mins and the supernatant was aspirated as plasma. As with the t=0hr sample, the plasma was centrifuged further at 13,000g for 5mins and the supernatant was passed through a 0.22μm filter (Acrodisc).

Quantification of chemokines within the plasma samples was performed using a Proteome Profiler™ Human Chemokine Array Kit (ARY017, R&D Systems). 200μl of plasma from each donor

was pooled together to give a 1ml pooled plasma sample for analysis. The pooled plasma sample was then incubated with a HRP-conjugated biotinylated antibody cocktails directed against a range of chemokines. A nitrocellulose membrane, impregnated with capture antibody (spotted in duplicate) directed against a range of chemokines was washed initially with a washing buffer and incubated overnight with the plasma/antibody mixture at 4°C (see **Figure 6.27**).
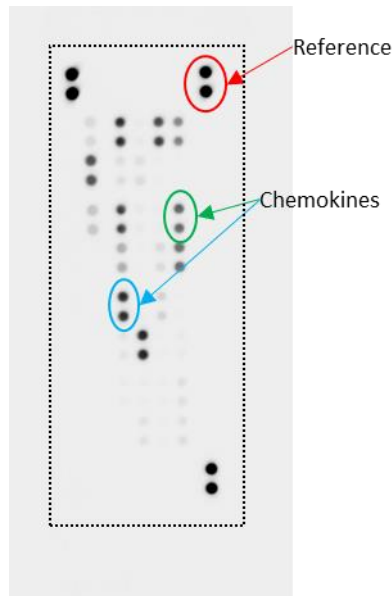
Figure 6.27: Example of Pre-incubated Nitrocellulose Membrane. Reference dots are shown with an example of chemokines spotted in duplicate (red and green circles). It can be visualised with the naked eye that that expression of the chemokine in the green circle is less than that circled in blue. The pixel density of all spots were quantified by an ImageQuant LAS 4000 (GE Healthcare)

After this incubation step, the membrane was washed repeatedly to leave the protein/detection antibody complex bound immobilised by its cognate receptor, The membrane was then incubated with a streptavidin fluorogenic substrate after which the membranes were carefully dried and placed with an Image Quant LAS 4000 (GE Healthcare). The signal intensity generated by the streptavidin conjugate is proportional to the amount of bound cytokine and this was quantified for each chemokine on the assay.

6.10.6.2   Results

A total of 34 proteins were analysed by the immunoblot technique of which 3 were endogenous protein positive controls (Fibrinogen, GP130, Transferrin R) and the remaining 31 were chemokines.

The pooled donor sample of plasma was used to analyse four different conditions. The first was a baseline control taken from plasma collected immediately after venepuncture to ascertain the basal levels of chemokines. The second was platelet-rich plasma (PRP) which was stimulated for

4hrs to ascertain the release of chemokines from platelet stores. The final 2 plasma samples were from whole blood incubated with either CRP-XL or a vehicle control for 4 hours which was used to quantify the release of chemokines from both platelet and non-platelet sources with and without platelet-activation. Subtraction of the pixel density at baseline from the control whole blood sample gave the induced release of chemokines (from both platelet and non-platelet sources) after the 4 hour incubation period (see **Table 6.2**). This value was then subtracted from the pixel densities quantified from the 4 hour activated sample to give the CRP-induced levels of chemokine release from both platelet and non-platelet sources. Finally, the chemokine pixel density quantified from the stimulated PRP sample was subtracted from the previous figure to give the chemokine release from non-platelet sources. As the chemokines were spotted on the membrane in duplicate, a mean value was calculated for each chemokine (see **Figure 6.28**) after which subsequent adjustments were performed.

Order	Chemokine	t=0hrs	Ctrl	CRPXL	PRP
1	Reference	18665.25	18877.5	18428.25	18704
2	Fibrinogen	941.93	1248.65	1164.81	1149.67
3	GP130	6754.045	8561	7960	7046
4	TransferrinR	1818.62	2213.785	2165.145	2164.31
5	Negative Ctrl	45.325	45.325	45.325	45.325
6	6Ckine	3259.625	4320.095	4891.525	3708.145
7	CCL28	21.03	39.555	44.18	22.025
8	Chemerin	6462	6915	9874	6874
9	CXCL16	5700	6159.715	5939.5	6120
10	ENA-78	97.55	126.99	685.2	164.675
11	Eotaxin-3	179.43	230.005	398.895	223.44
12	Fractalkine	499.825	527.73	576.74	751.495
13	GROα	515.3	510.745	299.645	742.575
14	HCC-1	6171.145	7064.5	7761.5	7434.5
15	I-309	102.68	151.695	157	111.07
16	IL-16	799.67	1485.26	1277.945	886.815
17	IL-8	124.955	2364.64	13162	184.82
18	IP-10	1074.385	1682.9	1087.42	1468.43
19	I-TAC	98.74	187.53	156.335	140.45
20	Lymphotaxin	131.855	207.325	270.785	211.14
21	MCP-1	86.98	139.26	140.055	141.02
22	MCP-3	222.09	344.185	355.56	228.895
23	MDC	784.055	837.81	1986.17	992.235
24	Midikine	246.97	299.75	429.51	312.59
25	MIG	62.085	96.735	97.39	125.16
26	MIP-1α/β	164.52	7702.5	11652.5	235.58
27	MIP-1δ	8040.5	9733.5	9901.5	9574
28	MIP-3α	128	8391.5	12977	240.96
29	MIP-3β	489.085	638.935	714.785	593.705
30	NAP-2	1181.065	5200.5	8665.5	5254
31	PARC	390.36	524.035	250.815	537.655
32	PF4	2543.5	5725.5	7355.42	7475.5
33	RANTES	2985.835	3671.5	6229.5	6403
34	SDF-1	8837	9089.5	9487	9095.5
35	TARC	452.44	641.565	3084.735	527.805
36	VCC-1	131.145	193	187.845	203.53

Table 6.2: Raw Pixel Density of Chemokine Assay. Table shows the chemokines against which antibodies were directed against (Chemokine column) with the corresponding position on the nitrocellulose membrane (Order column). The remaining columns show the pixel density, corresponding to each chemokine, from plasma samples at a baseline (t=0hrs), control plasma (Ctrl), a CRP-activated sample (CRPXL) and from platelet-rich plasma (PRP).
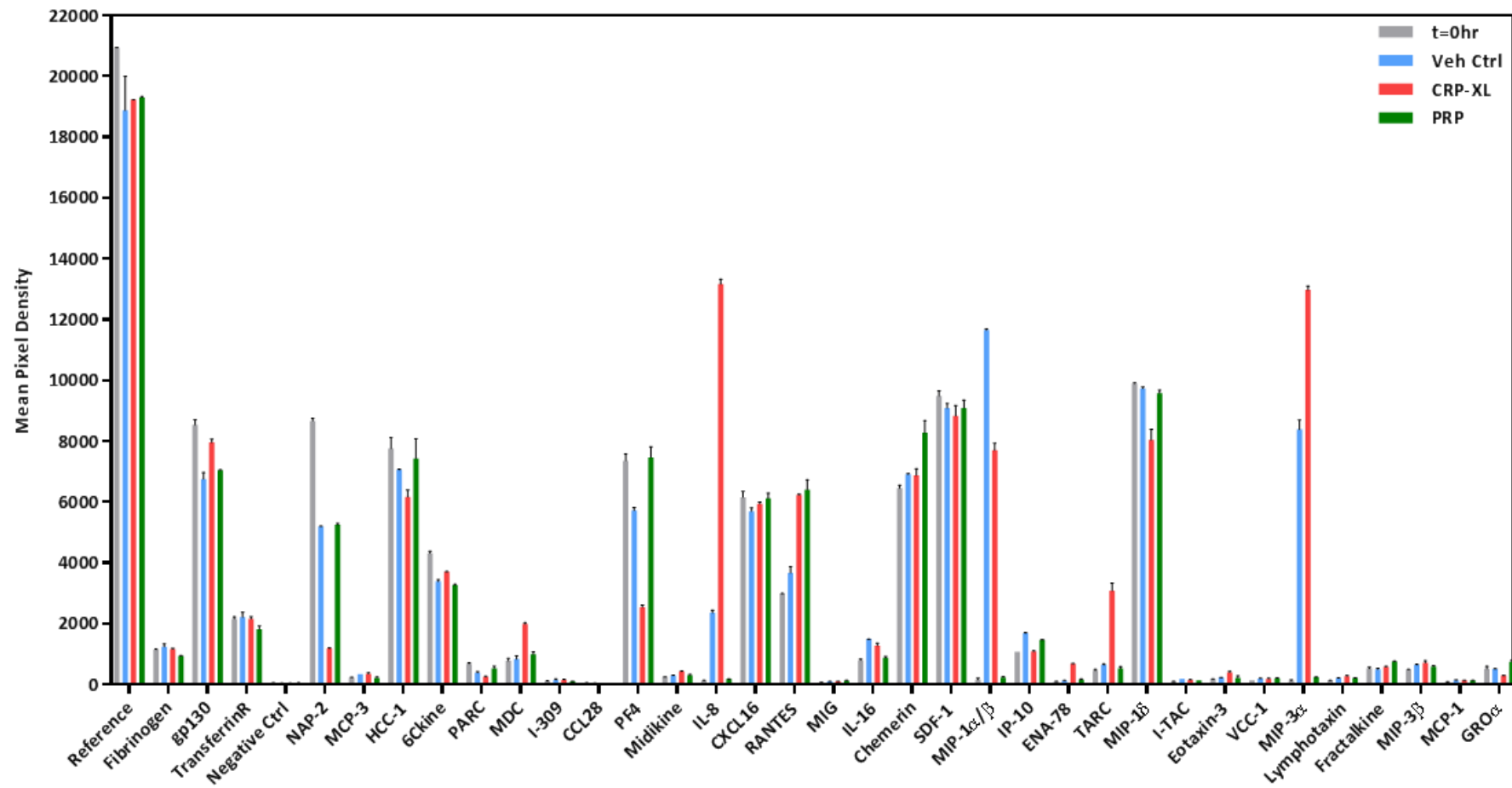
Figure 6.28: Raw Data of Mean Pixel Density. Immunoblot data of mean pixel density of each chemokine on the impregnated nitrocellulose membrane. Graph shows data for a 0hr baseline (grey bars), HBS vehicle control (blue bars), CRP-activated samples (red bars) and platelet-rich plasma (green bars). Bars show mean±SD of duplicate samples.
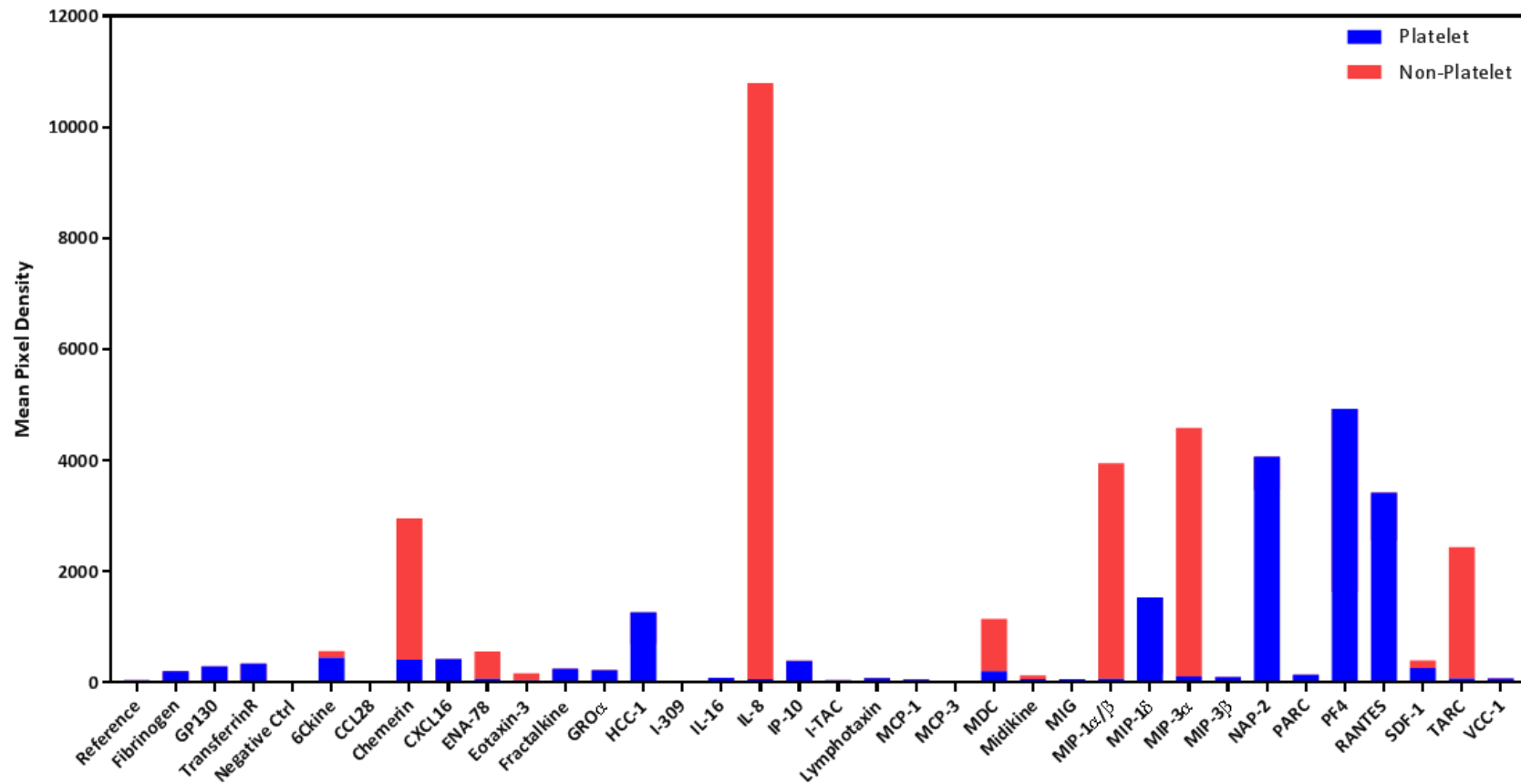
Figure 6.29: Chemokines Released from Platelet and Non-Platelet Sources with CRP activation. Graph shows adjusted (corrected for baseline chemokines in plasma) mean pixel density of chemokines showing the proportion of that chemokine released from platelet (blue bars) and non-platelet (red bars) sources. The chemokines IL-8, MIP-1α/β, MIP-3α, TARC and Chemerin were released predominantly from a non-platelet pool. MIP-1δ, NAP-2, PF4 and RANTES were released predominantly from platelets

Among the most highly induced chemokines released from platelet-activated monocytes were Chemerin, IL-8, MIP-1α/β, MIP-3α and TARC. Additionally, chemokines released at lower levels included ENA-78 and MDC which were released again predominantly from non-platelet sources. MIP-1δ, NAP-2, PF4, RANTES and smaller amounts of SDF-1 were predominantly released from platelets. The relative contribution of platelets and monocytes to the release of chemokines induced by CRP-XL activation is summarised in **Figure 6.29**.

6.11 <u>Summary</u>

Monocyte heterogeneity is a shared feature among the mammalian vertebrates. Both *in-vitro* studies of human monocytes and *in-vivo* studies of mouse monocytes show that these different subsets have different roles to play in sensing and responding to endothelial injury and this is particularly important with respect to atherosclerotic disease. The results within this chapter suggest that platelets might also influence monocyte biology through modification of monocyte subsets. One way in which this may occur is through the promotion of foam cell formation. It has been demonstrated that isolating and culturing monocytes based on their CD16 expression led to increased formation of foam cells from the CD16^{pos} subset (Section 6.1.1).

Activation with CRP-XL induces a robust and sustained platelet-activating response, including the formation of MPAs (Section 6.2). Furthermore, it has been demonstrated that the formation of MPAs is associated with the expression of surface CD16 on monocytes (Section 6.3.1) which is consistent with the evidence presented in the literature (**Passacquale et al.** *2011*). Whole Blood incubated for up to 24hrs showed the spontaneous formation of MPAs without the addition of an exogenous agonist *per se*. This phenomenon can be explained by the fact that platelets are known to undergo spontaneous aggregation, particularly in roller-mixed blood, which is largely dependent on the release of ADP from both platelets and erythrocytes (**Aursnes et al. 1981, Saniabadi *et al.* 1985**).

The demonstration of a causative relationship between platelet activation and the expression of surface CD16 on monocytes comes first from the finding that platelets, within a few minutes of activation, preferentially bind to the classical and intermediate subset (Section 6.4). These account for 90-95% of the circulating population and, by definition, express lower levels of CD16 than their non-classical counterparts. One caveat therefore is that when calculating the binding of platelets to the less abundant, non-classical subset, statistical variability is much greater and therefore results should be interpreted with caution. However, when using ICAM1 as a marker of monocyte activation, the binding of platelets to the classical subset led to higher levels of activation (Section 6.4.1). This assertion was supported by confirmatory *in-vitro* experiments where immuno-magnetically isolated CD16^{neg} monocytes were incubated with activated platelets. There was a clear increase in the expression of surface CD16 in response to platelet activation as well as a reduction in levels of CD14 (Section 6.5). Although not examined in this series of experiments, the reduction in surface CD14 might be due to the release of soluble CD14 (sCD14) from monocytes. This is a feature of activation and given that a fixed amount of CD14 antibody was used for the flow cytometric assay, sCD14 might in essence 'mop up' the excess antibody which leads to an overall reduced expression on monocytes.

The induced expression of CD16 on monocytes by activated platelets is *de-novo* and supported by two pieces of evidence. Firstly, there is increased expression of fcgr3 mRNA in response to platelet activation as demonstrated by RT-PCR (Section 6.7). Secondly, monocytes, even when activated by platelets, remain in a quiescent G_0, non-proliferative phase (Section 6.6) demonstrating that the increased numbers of intermediate monocytes are not due to proliferation of a pre-existing pool of intermediate (CD14^{pos}CD16^{pos}) monocytes.

Further immunophenotyping was used to delineate the nature of these platelet-activated monocytes using both CCR2 and Slan1 as additional markers (Section 6.9). A robust increase in the proportion of CD16^{pos}CCR2^{dim}Slan1^{neg} monocytes was found in response to platelet activation. The major caveat with identifying monocytes based on CD14 and CD16 fluorescence is that the segregation into the subsets depends largely on where one chooses to draw the gates on a flow cytometric plot. Use of 2 further antigens allows for disambiguation and shows that the increase in the intermediate subset, loosely analogous to the CD16^{pos}CCR2^{dim}Slan1^{neg} phenotype, is a legitimate finding.

Another interesting feature of the experimental work is that the change in monocyte subset in response to platelet activation is predominantly driven by direct cell-cell contact between platelets and monocytes. Inhibition of the P-selectin/PSGL1 dyad with the antibody 9E1 led to a significant and almost complete blunting of the platelet-induced increase in CD16 expression (Section 6.5). Whilst this does not rule out a role for soluble mediators in driving this phenotypic change, the effect of such agents must be, at best, marginal. However, the findings that direct cell-cell contact resulting in MPA formation, is crucial for this change in monocyte phenotype is consistent with the existing literature which demonstrates an association between MPA formation and CD16 expression on monocytes as well as their activation status.

Platelet-activated monocytes also induced a distinct expression of surface chemokine receptors when compared to un-activated monocytes. CCR2 and CXCR2 were reduced whereas CXCR3, CXCR6 and CXCR1 were increased on the surface of platelet-activated monocytes. There was also differential expression of chemokine receptors on CD16^{pos} and CD16^{neg} monocytes which may reflect differences in the behaviour of these subsets with respect to patrolling and response to endothelial damage. Importantly, platelets induced a pattern of surface chemokine receptors on CD16^{neg} monocytes that more closely resembles that on CD16^{pos} monocytes (**Figure 6.26**). Platelet also induce the release of chemokines from monocytes and include important pro-inflammatory mediators such as IL-8, MIP-1α and MDC. This is an important finding as platelets also induce the expression of receptors such a CXCR1, which binds to IL-8 (**Wu *et al.* 1996**) and

therefore promotes further inflammation. Platelets release their own chemokines from intracellular stores (**Figure 6.29**) which include PF4, RANTES and SDF-1. These have a number of actions including promoting inflammation, differentiation of macrophage subsets and promoting chemotaxis (all discussed in 2.5.5.2) which provide a further mechanism by which activated platelets promote a pro-inflammatory and pro-atherogenic monocyte phenotype.

Chapter 7: Foam Cell Formation in Myocardial Infarction (The FOAMI Study)

7.1 <u>Introduction</u>

Myocardial infarction is the necrosis of myocardial tissues often caused by rupture of a plaque within the coronary vasculature. It is a potent thrombotic stimulus leading to widespread activation of platelets. The *in-vitro* model employed in this thesis thus far, has used the platelet-specific agonist CRP-XL to give maximal activation of platelets permitting subsequent studies of monocyte phenotype. However, both the magnitude and nature of this platelet agonist is not necessarily reflective of platelet activation *in-vivo*, such as in the context of MI. In this chapter, platelet activation and monocyte phenotype are examined in patients within 24 hours of an MI event to see if this *in-vivo* platelet stimulus is sufficient to recapitulate the changes in monocyte phenotype observed *in-vitro.* Specifically, and in line with the data from previous chapters, it is hypothesised that MI will;

(1) Lead to platelet activation, formation of MPAs and monocyte activation

(2) Induce a change in monocyte phenotype to a pro-inflammatory CD16^{pos} subset

(3) Promote lipid droplet accumulation in circulating monocytes and promote the formation of foam cells in MDMs

These hypotheses will be addressed through a laboratory-based study of patients with MI.

7.1.1 Investigation of the Effects of Aspirin on the Formation of Foam Cells

Anti-platelet drugs are a widely used in the treatment of patients with MI. Preliminary experiments were conducted to ascertain if the use of anti-platelet drugs, in this case aspirin, has any significant effect on the primary end-point, namely foam cell formation in MDMs.

A stock concentration of aspirin was prepared by suspension of 30mg of Aspirin solute (Sigma-Aldrich) in 15mls of HBS. This was mixed gently by slow rolling until no particulate material was left to give a $1x10^{-2}$M stock solution. PRP was prepared from WB and then incubated with aspirin at a final concentration of either $8.3x10^{-5}$ M or $5.0x10^{-4}$M for 10mins at room temperature. These 2 doses were designated as 'low' and 'high' respectively which approximates to a maintenance dose of 300mg and 75mg once daily in a 70kg individual assuming 100% bioavailability. To confirm that these doses of aspirin were able to inhibit platelets, PRP was incubated with increasing concentrations of Arachidonic Acid (AA) to induce maximal platelet aggregation as assessed by light-transmission aggregometry. The selected dose of AA added to aspirin-incubated platelets and aggregation was followed for 10 mins. Aggregation was assessed by light-transmission aggregometry and degranulation was assessed by P-selectin expression by flow cytometry. Aspirin was found to inhibit the AA-induced aggregation of platelet at both the 'high' and 'low' doses however, there was no inhibition of P-selectin expression at either dose in line with previous data (**Chronos *et al.* 1994**). Aspirin at supra-maximal doses also inhibited the AA-induced aggregation of platelets but had no effect on the expression of surface P-selectin.

WB from healthy individuals (n=3), collected into 3.2% trisodium citrate (BD Vacutainer), was pre-incubated with aspirin for 10mins at a final concentration of either $8.3x10^{-5}$M or $5.0x10^{-4}$M equivalent to 'low' and 'high' doses respectively. Samples were then activated with 1.0µg/ml CRP-XL for 4hrs to maximally activate platelets. PBMCs were then separated by density-gradient centrifugation and monocytes were isolated by adherence. The isolated monocytes were re-suspended in serum-free medium and cultured for 3 days supplemented with 50ng/ml M-CSF. The formation of foam cells was quantified by both light microscopy and flow cytometry (**Figure 7.1**).
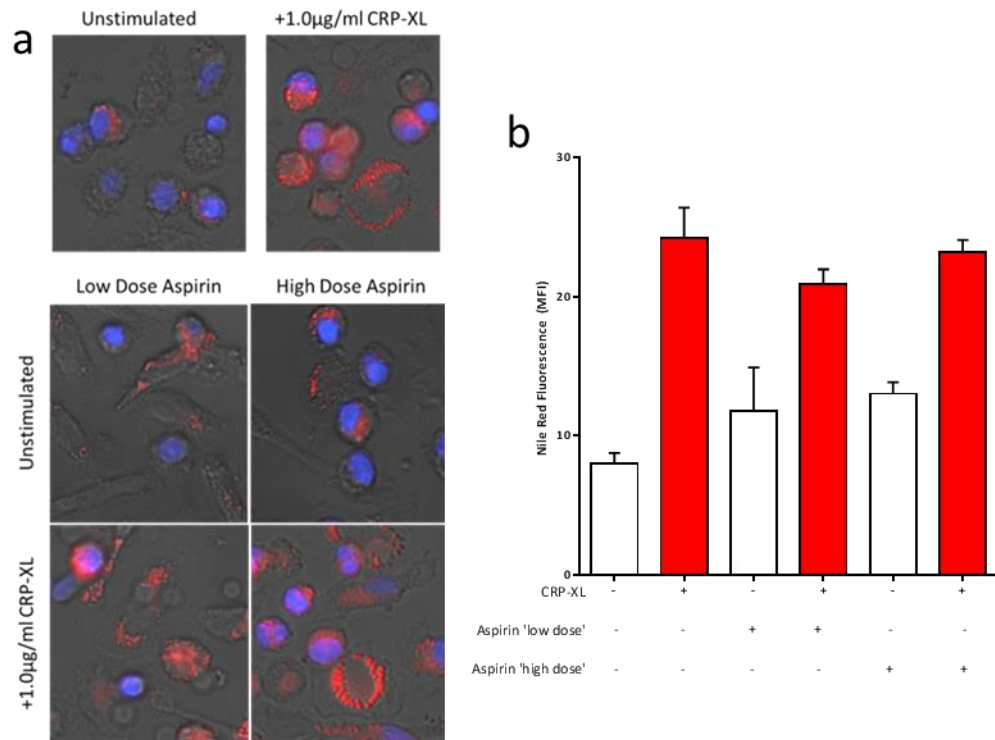
Figure 7.1: Effect of Aspirin on Foam Cell Formation in MDMs. Figure shows representative light-transmission microscopy images with superimposed fluorescence. Red depicts Nile Red and blue DAPI nuclear counterstain. Top row shows MDMs with and without CRP-XL activation. The middle and bottom rows shows cultured MDMs pre-incubated with aspirin with(out) CRP-XL stimulation. Bottom graph shows aggregate data (n=3) of Nile Red Fluorescence Intensity of MDMs as assessed by flow cytometry. Graph shows mean Nile Red fluorescence ±SD.

Consistent with previous experiments, activation of platelets with CRP-XL led to a significant increase (p>0.05) in the NR fluorescence intensity of MDMs. Furthermore, this experiment confirmed that pre-incubation with aspirin, either at 'high' or 'low' dose did not significantly inhibit (p>0.05) the effect of CRP-XL on monocyte NR fluorescence.

7.2   Outline of Study

FOAMI (**FO**am Cells in **A**cute **M**yocardial **I**nfarction) was a pilot, observation, laboratory-based study of patients presenting to the Glenfield Hospital with acute MI. Patients aged 18-70 with a diagnosis of non-ST Elevation Myocardial Infarction (NSTEMI) were enrolled and blood was sampled within 24hrs of clinical presentation followed by a further blood sample at a 3-month convalescent follow-up appointment (**Figure 7.2**). Blood was analysed for markers of platelet function as well as monocyte phenotype and activation to parallel the *in-vitro* work conducted previously. Blood samples from patients were compared to samples from healthy age-matched controls (aged 50-70yrs) obtained in a parallel study (FOAMI II). Data was also drawn from healthy volunteers (aged 20-30yrs) recruited from the department of cardiovascular sciences on which the assays were optimised, to present baseline values but were not included in the final analysis.
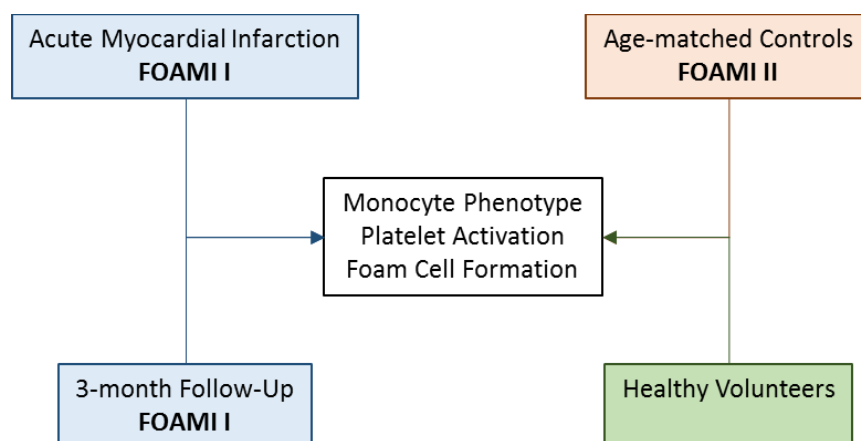

Figure 7.2: Outline of the FOAMI study. Blood was sampled from patients with MI both in the acute setting and at 3-month follow-up as part of the FOAMI I study (blue boxes). Age-matched controls were recruited as part of FOAMI II (orange box). Not included in the final analysis but used as a reference control was samples from healthy volunteers, aged 20-30yrs, which was used to initially optimise the laboratory assays (blue box). All samples were analysed in an identical manner for markers of monocyte phenotype, platelet activation and foam cell formation.

The formation of foam cells in MDMs was used as the primary end-point with secondary end-points including monocyte activation (e.g. ICAM1), the proportion of monocyte subsets (Classical/Intermediate/Non-Classical) and markers of platelet activation (P-selectin/MPA). Data from the acute phase of MI was compared to the convalescent phase, thereby acting as an internal control, and both of these data points were compared with age-matched controls.

7.3 <u>FOAMI</u>

FOAMI was designed to be an observational study of patients presenting to the coronary care unit (CCU) and clinical decisions unit (CDU) of the Glenfield Hospital (GGH) with a diagnosis of NSTEMI. Patients were screened for eligibility and suitable patients, fulfilling the pre-specified inclusion and exclusion criteria, were approached by the investigator within 24hrs of presentation to hospital. Consent for trial participation was sought and a blood sample was obtained in the acute phase of MI and processed within the adjacent university research lab. Participants were recalled for a 3-month follow-up visit where a second blood sample was obtained and the same analysis performed to enable comparison with the acute phase.

7.3.1   Inclusion Criteria

Participants must have met all of the following criteria in order to be eligible for recruitment into the study;

- Diagnosis of Acute Coronary Syndrome (ACS) requiring 2 features out of;
    (1) Typical anginal chest pain
    (2) Ischaemic and/or dynamic ECG abnormalities
    (3) Troponin I >50ng/ml
- Aged 18-70yrs at the time of recruitment
- Scheduled for in-patient coronary angiography ± percutaneous coronary intervention (PCI)
- Able to give informed consent

7.3.2   Exclusion Criteria

Potentially eligible participants who have fulfilled the inclusion criteria were excluded from the study if any of the following criteria were met;

1   History of thrombophilia
2   ST elevation on the presenting ECG
3   Unable to take anti-platelet medication
4   History of major gastro-intestinal bleeding
5   Abnormal blood counts or platelet response
6   Use of GPIIb/IIIa inhibitors
7   Bleeding diathesis
8   Use of Immunosuppressive therapy

| 9 | Anaemia (<8.0g/dL) |

9   Anaemia (<8.0g/dL)

10 Use of NSAIDs in the preceding week

11 Severe obesity (BMI>35kg/m^2)

12 Renal Dysfunction (CKD Stage IV/V or established RRT)

13 Hepatic Dysfunction (established cirrhosis, Albumin <25ng/ml, INR >1.4, Bilirubin >40μmol/L)

14 Pregnancy

15 Unable or unwilling to give informed consent

16 Inadequate understanding of written and spoken English

7.3.3 Outcome measures

The primary outcome measure for which the study was powered was the flow cytometric quantification of foam cell formation in MDMs. Other outcome measures for the study were as follows;

• Nile Red fluorescence intensity of circulating monocytes

• Proportions of monocyte subsets as characterised by surface expression of CD14, CD16, CCR2 and Slan1

• Cellular activation markers including surface expression of P-selectin, ICAM1, CD11b and MPA formation

• Relative expression of lipid-regulatory genes in monocytes and MDMs

7.3.4   Funding and Ethical Approval

Prior to the recruitment of the 1st patient into FOAMI, approval was sought from various regulatory bodies. This was done through the University of Leicester (UoL) who acted as sponsor and administered the online application through the Integrated Research Application System (IRAS) (https://www/myresearchproject.org.uk). In addition to the IRAS form, the following documentation was also submitted to UoL;

Study Protocol	A document which extensively detailed all study protocols and procedures
Case Record File (CRF)	A paper document in which the clinical and laboratory data obtained from each recruited patient was recorded. This serves as an ongoing physical record of their participation
Participant Documentation	This includes the Patient Information Sheet (PIS), Consent Forms and advertising material
Curriculum Vitae (CV)	The CV of the principal investigator and co-investigators
Peer Review	Two independent senior investigators within the UoL reviewed the study and assessed it for scientific merit and feasibility of study design. This report was submitted to UoL as part of the study documentation.
Schedule of Events	A document that chronicled all the anticipated tasks to be completed for the duration of the study
Feasibility Assessment	A detailed costing of the reagents and infrastructure required for the purposes of the study with an assessment of what proportion of the cost would be borne out by the funding body (BHF) and what proportion by University Hospitals of Leicester (UHL)

Following approval from UoL to act as the sponsor for the study, further approval from other regulatory bodies was obtained. The information on the IRAS form was passed on to various agencies involved in health research including the Human Tissue Authority (HTA), Department of Health (DoH) and National Institute for Health Research (NIHR). For the commencement of the study, the following approvals were sought[34];

Health Research Authority	The remit of the HRA is to ensure the appropriate procurement and storage of patient data
Research Ethics Committee	The study plan was submitted to the West Midlands Research Ethics Panel and a direct interview was conducted aimed at addressing potential ethical issues raised by the study (17/WM/0031)
University Hospitals of Leicester Feasibility Board	The study proposal was presented in brief to the UHL feasibility panel to ascertain if the clinical infrastructure was sufficient to support the study and if this study would be in direct competition others

---

[34] Approval letters from the HRA and REC are provided in Section 9.5 and Section 9.6 respectively

7.4 <u>Study Procedures</u>

7.4.1 Screening and Eligibility assessment

The screening process begun with the identification of all patients presenting to the hospital within the previous 24hrs with a diagnosis of NSTEMI. This was summarised in the admissions book where potentially eligible participants were identified, corroborated by the staff on both CCU and CDU. Once a potential participant was identified, consent was sought from the patient for the investigator to review their medical notes in order to screen for the stated inclusion and exclusion criteria. Any confusion or ambiguities about this were clarified with the attending medical staff or with the patient themselves if appropriate.

7.4.2 Informed Consent

Eligible patients were approached by the investigator within 24hrs of their presentation to hospital. The scope and purpose of the study was explained to the participants and supplementary information was provided in the form of a participant information sheet. This verbal and written information detailed; the exact nature of the study, the implications and constraints of the protocol and any risks involved in taking part. It was clearly stated that participants were free to withdraw from the study at any time and for any reason without prejudice to their clinical care. Participants were given a minimum of 1 hour to consider the information and decide if they would like to participate in the study. Written informed consent was then obtained by means of a participant-dated signature and countersigned by the person who obtained the consent. The person who obtained consent was suitably qualified, authorised to do so by the Principle Investigator and delegated to do so in the delegation log. The original form was retained at the study site within the Trial Master File (TMF), a copy with the patient and a copy within the medical notes. Consent was confirmed at the subsequent follow-up visit.

7.4.3 Blood Sampling

Following valid consent, blood was sampled by peripheral venepuncture using a 21G butterfly needle (BD Vacutainer) using the standard methodology (as described in section 3.2.1) to minimise iatrogenic platelet activation. Up to 50mls of blood was collected in the following order into the vacutainer tubes; 1 x 3.5ml EDTA, 1x4.5ml Hirudin and 9x4.5ml 3.2% Trisodium citrate tubes. The samples were processed within 30mins of acquisition.

7.4.4 Acquisition of Clinical & Demographic Data

Once recruited into the study, patients were interviewed, and their medical notes were reviewed to acquire the following information which was subsequently recorded in the CRF.

Demographic Information	Date of Birth
	Gender
	Smoking History
	Body Mass Index (BMI)
Co-Morbidities	Co-existent medical diagnoses
	Significant previous surgery
Medication	Prescribed and over the counter medication taken by patient
ECG	Rhythm
	Conduction Abnormalities
	Ischaemic Changes
Laboratory Tests	Full Blood Count
	Renal Function
	Liver Function Tests
	Troponin I
	HbA1c
Outcome	Percutaneous Coronary Intervention (PCI)
	Optimum Medical Therapy (OMT)
	Coronary Artery Bypass Grafting (CABG)

7.4.5 Follow-up visit

Follow-up was arranged for 3 months after their initial presentation to hospital. Patients were contacted following their discharge from hospital and a convenient appointment was arranged at the Leicester Biomedical Research Unit (BRU) at Glenfield Hospital. Participants were interviewed by the investigator to confirm consent and relevant clinical details followed by collection of a further 50ml blood sample, which was processed in a manner identical to the initial sample.

7.4.6 Discontinuation/Withdrawal of participants from study

It was explained to each participant that they had the right to withdraw from the study at any time and, in addition, the investigator may discontinue a participant from the study at any time if it is considered necessary for any reason including;

- Pregnancy
- Ineligibility (either arising during the study or retrospective having been previously overlooked at screening
- Significant protocol deviation

- Significant non-compliance with study requirements

- Adverse event resulting in an inability to continue with study procedure

- Withdrawal of consent

- Lost to follow-up

- Loss of capacity

The reason for withdrawal was recorded in the CRF and if the withdrawal was due to an adverse event, the investigator arranged follow-up visit or telephone calls until the adverse event has resolved or stabilised.

7.4.7   Laboratory Procedures

For the assessment of monocyte phenotype and platelet activation, a standard laboratory protocol, based on the preliminary *in-vitro* experiments, was used for all assessment as follows.

7.4.7.1 Cell Counting

10μl of blood collected into EDTA was analysed by automated cell counter (Act-T-Diff, Beckman-Coulter) to give a full blood count and differential. Platelet and leucocyte numbers were recorded for each sample.

7.4.7.2 Platelet Function Testing

Blood collected into hirudin anticoagulant was used to test platelet function using whole blood impedance aggregometry (Multiplate, Roche Diagnostics) as described in Section 3.2.8.1 . This assay was used primarily to check for the efficacy of anti-platelet medication. Additional measures of platelet function included the flow cytometric quantification of surface P-selectin on platelets (see methods section 3.2.5.1) and the quantification of MPAs (see methods section 3.2.5.2).

7.4.7.3 Monocyte Phenotype & Activation

Blood collected into 3.2% trisodium citrate was prepared (see methods section 3.2.5.7) and analysed by flow cytometry using a 5-colour flow cytometric assay to stratify monocytes into Classical ($CD14^{high}CD16^{neg}$), Intermediate ($CD14^{high}CD16^{pos}$) and Non-Classical ($CD14^{dim}$, $CD16^{pos}$) subsets as in Section 6.4 . The additional markers Slan1 and CCR2 were used to further stratify monocytes into either $CD14^{high}CCR2^{high}CD16^{neg}Slan1^{neg}$ (Classical or Mon1), $CD14^{high}CCR2^{high}CD16^{pos}Slan1^{neg}$ (Intermediate or Mon2) or $CD14^{dim}CCR2^{low}CD16^{pos}Slan1^{pos}$ (non-classical or Mon3) as in Section 6.8.1 . Activation of monocytes was quantified by recording the surface expression of both CD11b and ICAM1 as in section 4.4.2 .

7.4.7.4 Intracellular Lipid Droplets and Foam Cell Formation

Whole blood flow cytometry was used to quantify circulating monocytes with intracellular lipid droplets as described in the methods section 3.2.5.4 . As there was no isotype control available, samples from healthy volunteers were used to set the Nile Red Fluorescence (measured in the FL3 fluorescence channel) with the first log decade and so that 2% of events were positive for Nile Red. Samples from patients were run and the staining of Nile Red was quantified both as the percentage of monocytes and the median fluorescence intensity.

To measure the formation of foam cells, 36mls of whole blood, collected into 3.2% trisodium citrate, was used to isolate a pure population of monocytes (as described in the methods section 3.2.2.9) and cultured for 3 days to generate MDMs followed by analysis for the formation of foam cells by both flow cytometry (methods section 3.2.5.5) and by manual quantification using fluorescence microscopy (methods section 3.2.4.3). For fluorescent microscopy, foam cells were counted as those MDMs with >10 discernible intracellular lipid droplets and expressed as the proportion of all cells within a 40x field of zoom. For flow cytometry, no isotype control was available and therefore, the baseline fluorescence of Nile Red was set using isolated monocytes from healthy volunteers. The fluorescence of Nile Red was analysed in the FL3 channel and set within the first log decade and the 'positive' gate was set at the 2% level. Based on this, samples from patients and age-matched controls were analysed similarly and the formation of foam cells was quantified as the proportion of cells that were Nile Red positive and also the median fluorescence intensity of staining.

7.4.8 Statistical Processing of Data

7.4.8.1 Sample Size

The minimum number of patients required for the study was calculated *a-priori* based on assumptions derived from the *in-vitro* data of foam cell formation in MDMs. In the whole blood model of CRP-XL activation, cultured MDMs at Day 3 showed a mean difference in fluorescence intensity of 13.4±2.4 between CRP-activated and non-activated samples. It has been shown in previous studies that in patients with ACS, approximately 15% of platelets express the P-selectin surface antigen (**Stellos *et al.* 2010**) as compared with near 100% expression of P-selectin observed in the *in-vitro* model of CRP-XL activation. It was therefore assumed that a similar magnitude of difference would be observed with respect to median fluorescence intensity of Nile Red staining in MDMs when comparing patients to controls. The mean difference in MFI between CRP-activated and non-activated samples was 13.40 (see **Figure 5.1**) and there it was

determined that a difference of 2.68 (=15% of 13.40) would be biologically significant. Sample size was calculated using the following formula[35]:

$$n = f(\alpha, \beta) \cdot \frac{2s^2}{\delta^2}$$

In this formula, n denotes the sample size required for the study and was calculated as the product of a function of the significance level (α) and power (1-β) (

Table 7.1) and the standard deviation (s) as a proportion of the minimum difference deemed important (δ).

	β			
α	**0.05**	**0.1**	**0.2**	**0.5**
0.05	13.0	10.5	7.9	3.8
0.01	17.8	14.9	11.7	6.6

Table 7.1: Values of a Composite Function f(α,β) of Significance (α) and Power (1-β). The value of f(α,β) is 7.9 (shaded cell) based on a power of 80% (β=0.2) and significance of 5% (α=0.05).

Using this formula, it was calculated that to detect a difference of 2.68 in fluorescence intensity with 80% power at the 5% significance level, a minimum of 12 subjects was required for each arm of the study. Assuming a 10% attrition rate, a minimum of 14 subjects was required for each arm to satisfy the primary end-point.

7.4.8.2 Minimising Bias

Selection bias was minimised by recruiting consecutive, consenting patients who satisfied the pre-specified inclusion criteria. All data accrued from the clinical records were processed separately from laboratory analyses. Data from laboratory analyses were processed under a part-random identification code which could only be tracked back to the source patient data using the site file. Both clinical and laboratory data was analysed independently to further minimise bias.

7.4.8.3 Statistical Processing

Data from different laboratory parameters pertaining to monocyte and platelet phenotype and function were compared intra-participant, using paired t-tests, at baseline and at the 3-month follow-up period. Means for continuous outcomes (transformed logarithmically if required) was

---

[35] Taken from Designing Clinical Research, Second Edition; Lippincott Williams and Wilkins. Hulley SB, Cummings SR et al (2001); Chapter 6

compared using analysis of variance with adjustment for baseline values and with mathematical corrections made for multiple testing. Findings were reported as effect sizes with 95% confidence intervals with a p-value of <0.05 considered as statistically significant.

7.5 FOAMI II: Age-matched controls

The design of the FOAMI I study is such that the data from the 3-month follow up time point acts as a matched, resting control for samples acquired within the acute phase of MI. To provide an additional control of individuals without an index MI but matched in age, a parallel study was conducted that recruited healthy volunteers. Consent was sought from volunteers aged 50-70 years from within the Department of Cardiovascular Sciences (Glenfield Hospital, Leicester) without a prior history of MI. Up to 45mls of blood was collected at a single time point and processed in a manner identical to patient samples.

7.5.1 Ethical Approval

Ethical approval for FOAMI II was obtained from the Research Ethics Committee (REC) of the University of Leicester (see appendix 9.4). A brief outline of the study, characteristics of the study participants and what was required of them was submitted to UoL and considered by an appropriate panel within the University. Approval was given in writing prior to recruitment of the 1st participant.

7.5.2 Method

Potential participants within the department of Cardiovascular Sciences were approached and consent was sought. Basic information about the participant was gathered including age, history of CVD and modifiable risk factors for CAD. After consent was obtained, 45mls of blood was obtained and processed immediately (within 30mins) in the laboratory in a manner identical to samples obtained from FOAMI I. Volunteers were assigned a part-random ID number and all data pertinent to this was stored on a secure server.

7.6 Results

7.6.1   FOAMI I Patient Flow Chart

A total of 16 patients fulfilled the pre-specified inclusion and exclusion criteria and, after informed consent, were enrolled into the FOAMI I study. One patient (SR2887) was later deemed ineligible after information came to light that the patient had severe aortic stenosis and normal coronary arteries and that the clinical presentation was a result of left ventricular hypertrophy rather than CAD and plaque rupture *per se*. This patient's results were therefore excluded from final analysis (see **Table 7.3**). Therefore, a total of 15 patients were enrolled onto the study and recalled for follow up, of which 11 patients attended. Of those for whom follow-up data was not available, two patients refused follow-up, namely JT6069 who had plaque disease within the left circumflex artery deemed for medical management and AD9891 who had established three-vessel disease and went on to have coronary artery bypass grafting (CABG) complicated by pleural effusions and a prolonged hospital admission. Two patients were lost to follow-up; KW1948 had an NSTEMI in the context of left ventricular systolic dysfunction followed by a prolonged hospital admission, and AT4435 who refused coronary angiogram and did not attend their scheduled outpatient follow-up. The data obtained from their index MI was included in the final analysis and a total of n=11 patients completed the trial. All patients who completed the trial were on dual anti-platelet therapy except for LH3087 and DC2005 who were on a combination of a direct Factor X_a inhibitor (Rivaroxaban) and Aspirin for coronary ectasia and atrial fibrillation respectively.
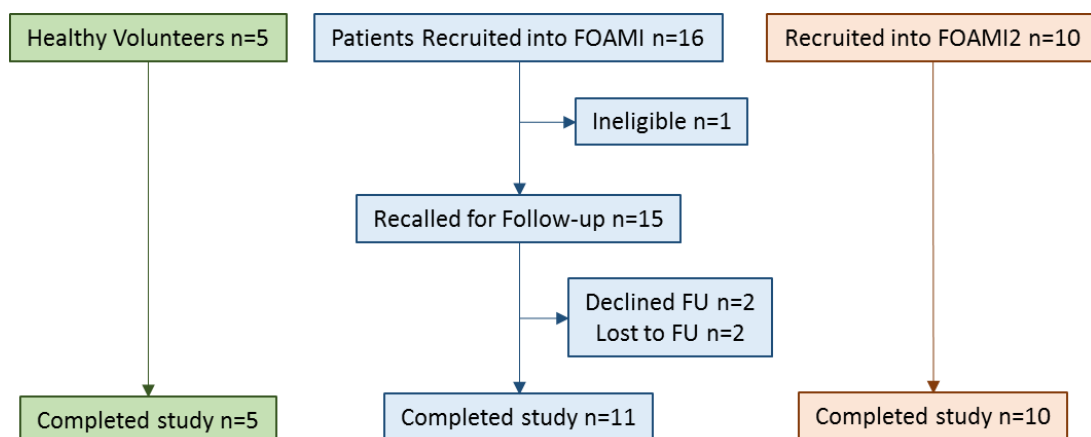
Figure 7.3: Flow Chart of Patients Recruited into FOAMI. The FOAMI I study (blue boxes) recruited 16 patients in total of which 1 was later deemed ineligible. A total of 15 patients had the first blood sample taken and 11 people attended and completed their follow-up appointment. Of those that did not complete the study, 2 declined and 2 were lost to follow-up. In parallel studies, n=10 age-matched healthy volunteers (FOAMI II) were recruited into the control arm (orange boxes) as well as 5 healthy volunteers (aged 20-30) to provide baseline data (green boxes).

7.6.2   Patient Characteristics

Of the 15 patients recruited into FOAMI, 13 were male (86.7%) with a mean age of 62.73±8.14 years and BMI of 30.09±5.45 kg/m^2. Patients recruited into the study exhibited relatively homogenous background characteristics with respect to the risk factors for CAD[36].
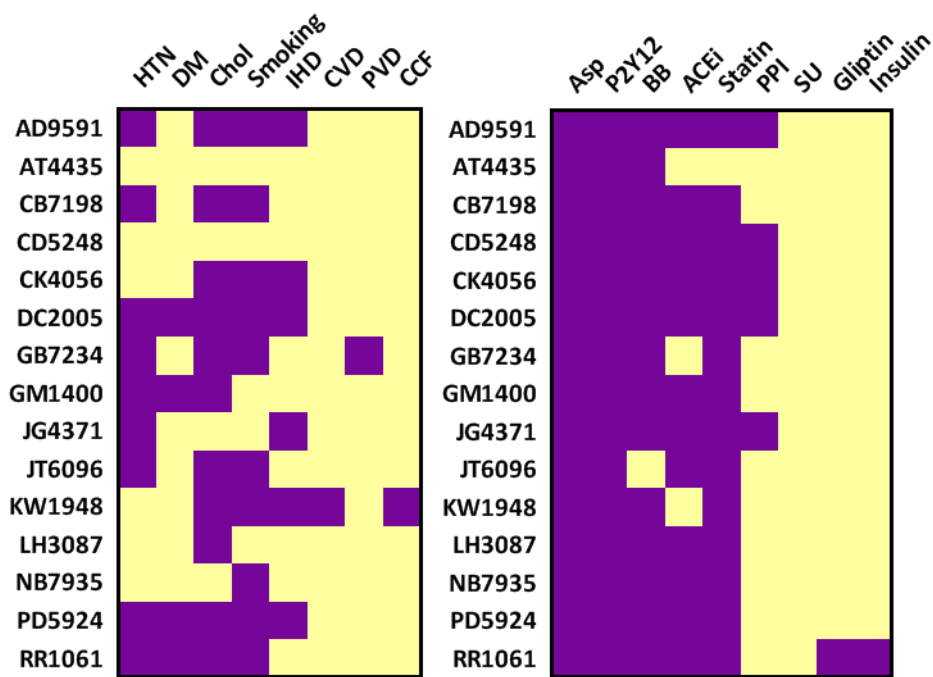
Figure 7.4: Clinical Data of Patients Recruited into FOAMI. Characteristics of patients recruited into FOAMI are shown in the categorical heart map (purple='yes', yellow='no'). HTN=hypertension, DM=diabetes mellitus, Chol=hypercholesterolaemia, CVD = cerebrovascular disease, PVD = peripheral vascular disease. Heat map also shows the drug treatment of patients recruited into FOAMI. Asp=Aspirin, P2Y12 = P2Y12 receptor antagonists, BB = Beta Blocker, ACEi = Angiotension Converting Enzyme Inhibitor, PPI = Proton Pump Inhibitor, SU = sulphonylurea.

The majority of patients (n=13) possessed at least one modifiable risk factor including Hypertension (HTN), Hypercholesterolaemia (Chol), Diabetes Mellitus (DM) and Smoking. Of these, the most prevalent risk factor was hypercholesterolaemia (n=11) followed by hypertension (n=9). Although blood pressure was not recorded on admission, mean blood pressure recorded at follow-up appointment was 142.5±33.5 mmHg systolic, 79.7±12.1 mmHg diastolic. A significant proportion of patients (n=10) also demonstrated a smoking history, either being ex-smokers or current smokers. Four of the patients recruited into the study were diabetic of which 3 had poor control with an HbA1c>7.5%. A significant minority of patients (n=6) gave a

[36] Originally described from the Framingham Heart Study (Mahmood, SS, D Levy, RS Vasan and TJ Wang. The Framingham Heart Study and the Epidemiology of Cardiovascular Disease: A Historical Perspective. *Lancet*.**2014**; **383: 999-1008**)

previous history of ischaemic heart disease (IHD), and one person with peripheral vascular disease (PVD). Upon recruitment into the study, 100% of patients were on dual anti-platelet therapy in the form of Aspirin and either Clopidogrel or Ticagrelor. The majority (73%; n=11) of patients were also on a combination of statin, ACE inhibitor and Beta-Blocker. Of the patients who attended the follow-up appointment, this proportion increased to 90%. Furthermore, 2 patients at follow up were placed on anticoagulant therapy (either Rivaroxaban or Warfarin), in addition to dual anti-platelet therapy, for a secondary indication.

Of the 15 patients recruited into the study, a total of 14 had invasive coronary angiography; one patient (AT4435) did not consent to PCI, and was subsequently lost to follow-up. Of those patients who had a diagnostic angiogram, 4 went on to have percutaneous coronary intervention to the index lesion on the same admission and 4 went on to have CABG on anatomic and prognostic grounds. The remaining 6 patients did not have a revascularisation procedure (either surgically or percutaneously) and were managed with optimum medical therapy (OMT). A total of 11 patients completed the study with a mean follow up period of 61.3±17.8 days.

	Patients	Age-Matched Controls	
Number	n=15	n=10	
Age (yrs±SD)	62.7±8.1	57.9±8.0	p=0.156
BMI (kg.m^2±SD)	30.1±5.5	25.0±2.9	**p=0.017**
Sex (%male)	87.6% (n=13)	90.0% (n=9)	p>0.05
Smokers (%smoker)	60.0%	0.0%	**p=0.0025**
Co-morbidities (%)	87.6% (n=13)	20.0% (n=2)	**p=0.0004**

Table 7.2: Summary Table of Demographic Data of Patients in the FOAMI Study. Values are shown (mean±SD) for both Patients and Age-Matched Controls. Given also are calculated p-values and statistically significant values are denoted in bold (p<0.05).

Age-matched controls (AMCs) recruited into the control arm (FOAMI II) had a mean age of 57.9±8.0yrs. This was marginally lower than patients (62.7±8.1yrs) but this difference was not statistically significant (p=0.156, t-test). The AMCs however exhibited a significantly lower body mass index (25.0±2.9 vs 30.1±5.5 kg.m^2, p=0.017) and possessed significantly fewer risk factors for CAD (20% as compared with 87.6% in the patient group, p<0.0004 Fishers Test). Furthermore, 60% of patients recruited into FOAMI declared either a current or previous smoking history as compared with no current smoking history in the AMCs (data summarised in **Table 7.2**).

Patient	Sex	Age (yrs)	BMI (kg/m²)	Smoking Status	Blood Pressure	ECG	Trop I (ng/L)	Hb (g/dL)	Mon (x10⁶/ml)	Plts (x10⁹/ml)	eGFR (ml/min)	Bilirubin (µmol/L)	ALT (IU/L)	Treatment
AD9591	M	65	NA	Y	NA	TWI	22.8	14.6	0.3	217	84	7	79	CABG
AT4435	F	72	NA	N	NA	N	35.9	14.1	0.3	200	73	5	23	OMT
CB7198	M	61	25.61	Y	121/78	N	239.4	16.1	0.4	245	90	NA		PCI
CD5248	M	69	33.50	N	199/67	TWI	1712	15.8	0.4	268	90	16	29	PCI
CK4056	M	67	28.90	Y	156/87	TWI	122	15.7	0.6	197	90	4	35	OMT
DC2005	F	70	37.06	X	93/67	RBBB	8160	9.3	0.5	195	56	10	26	OMT
GB7234	M	70	32.19	X	156/82	RBBB	30.3	15.5	0.6	233	90	8	18	PCI
GM1400	M	49	35.43	N	146/79	N	100.2	15.2	0.5	221	83	9	57	CABG
JG4371	M	62	30.23	N	187/106	Q	3743	14.4	0.4	187	90	25	45	PCI
JT6069	M	68	NA	Y	NA	N	76.1	14.6	0.7	170	88	10	14	OMT
KW1948	M	68	NA	X	NA	ST	29957	15.1	0.5	146	37	38	40	OMT
LH3087	M	45	21.80	N	105/66	RBBB	262.5	13.1	0.3	220	73	9	21	OMT
NB7935	M	56	27.28	Y	123/83	N	1104	16.9	0.6	218	88	NA		OMT
PD5924	M	65	22.23	X	134/78	TWI	2363	13.4	0.5	332	90	8	38	CABG
RR1061	M	60	36.73	Y	158/86	TWI	31	14.1	0.5	226	90	9	25	CABG

Table 7.3: Summary Table of Patient Characteristics. Patients are denoted using an anonymised code. BMI = Body Mass Index. For smoking status, Y= current smoker, N=never smoker, X=ex-smoker. For ECGs, TWI = T-wave inversion, N = normal, RBBB = Right Bundle Branch Block, Q = Q-waves, ST = ST segment depression. Hb Haemoglobin. Mon=Monocyte Count, Plts = Platelet Count. eGFR = estimated Glomerular Filtration Rate, ALT = Alanine Transaminase. For Treatment, CABG = Coronary Artery Bypass Grafting, OMT = Optimal Medical Therapy, PCI = Percutaneous Coronary Intervention. NA denotes data not available.

7.6.3 Platelet Function Testing

Patients recruited into the study has a mean platelet count of 218.3±11.2 x10^6/ml which was not significantly different to age-matched controls (232.8±33.0, p=0.3995, t-test) or indeed to healthy volunteers (282.2±92.1, p>0.05, t-test). The aggregatory responses of platelets in patients with MI and AMCs were quantified by impedance aggregometry by measurement of area under curve (AUC). Responses to TRAP (used as a positive control) was conserved across all participant groups and there was no overall significant difference in AUC in response to this agonist (p>0.05, ANOVA). Furthermore, there were no significant differences in platelet aggregatory responses to TRAP in patients both in the acute and convalescent phases of AMI (p=0.05, t-test). Arachidonic acid (AA) and Adenosine Diphosphate (ADP) produced differential effects on aggregation in both patients and age-matched controls. ADP led to significantly less (p<0.01, t-test) aggregation, as expressed by AUC, in patients following myocardial infarction as compared with age-match controls. This significant difference was maintained at a 3-month follow-up. Similar results were obtained with aggregatory responses to AA which was significantly less in patients than age-matched controls both in the acute and convalescent phases of AMI (p<0.001, t-test).

Platelet degranulation was measured by flow cytometry by the expression of surface P-selectin as shown in **Figure 7.5 (d)**. In healthy volunteers, 4.9±1.4% of platelets expressed surface P-selectin which was marginally higher in the age-matched controls (6.1±3.0%) but not statistically significant (p=0.38, t-test). In the acute phase of AMI, patients exhibited a mean P-selectin expression of 10.9±8.0 % which was significantly higher than that seen in the controls (p=0.0125, t-test). This fell back to the same level as in the control group by the 3-month follow-up (7.2±2.1%, p=0.0179, paired t-test).
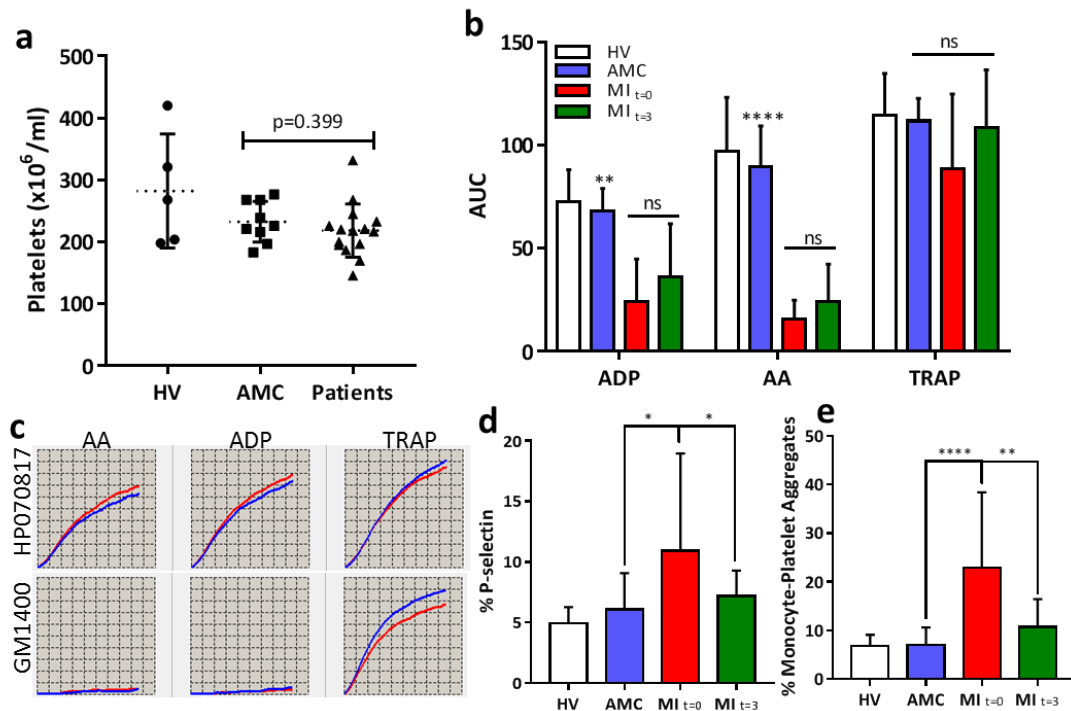
Figure 7.5: Laboratory Quantification of Platelet Function in FOAMI. (a) Platelet count in healthy volunteers (HV), age-matched controls (AMC) and patients with MI recruited into the FOAMI study (Patients). There was no significant difference in platelet count between patients and their age-matched controls (p=0.399). (b) Data from impedance aggregometry, shown as Area Under Curve (AUC), for HV (white), AMC (blue) and patients with MI both at the index event (red) and at 3-month follow-up (green). Data is shown for 3 agonists namely ADP, arachidonic acid (AA) and thrombin associated peptide (TRAP). In AMCs, there was significantly greater AUC in response to ADP and AA but not with TRAP. In patients with MI, there was no significant difference in platelet aggregatory responses across all three agonists. (c) Representative aggregometry images of AMC (HP070817) and a patient with myocardial infarction (GM1400) in response to AA, ADP and TRAP. The AMC shows a robust aggregatory response to all three agonists however the patient shows a markedly attenuated response to both ADP and AA but not to TRAP. (d) The expression of P-selectin on the surface of platelets. There was a significant increase in the expression of P-selectin in patients with MI as compared with AMC (p=0.0125) which was significantly reduced (p=0.0179) upon follow-up. (e) The proportion of monocytes with adherent platelets (MPAs). Patients with MI showed significantly more MPA formation than their age-matched controls (p<0.0001) which was significantly reduced at 3-month follow-up (p=0.0043). *=p<0.05, **=p<0.01, ***=p<0.001, ****=p<0.0001.

7.6.4 Activation of Monocytes

Patients which AMI had a mean monocyte count of 0.5±0.03 x10^6/ml upon recruitment which was significantly more than in age-matched control (0.3±0.04 x10^6/ml, p=0.001, t-test). There were also significant differences in the proportion of monocytes with adherent platelets (**Figure 7.5**, e). Both age-matched controls and healthy volunteers had comparable baseline levels of MPA formation (7.1±3.5% vs 6.9±2.3% respectively, p>0.05). In patients presenting within 24hours of MI, 22.9±15.5% of monocytes had adherent platelets, significantly more than age-matched controls (p<0.0001, t-test). At the 3-month follow up, levels of MPA formation fell in this group to 10.7±5.7% which was significantly lower than in the acute phase (p=0.001, t-test) but still higher than levels seen in the age-matched controls (p=0.02, t-test). MPA formation is therefore triggered by acute MI and decreased at 3-month although not back down to levels seen in the AMCs.

In addition to increased MPA formation, monocytes demonstrate an increased activation in patients with AMI. ICAM1 showed constitutive baseline expression levels in AMCs (70.6±9.1%) which was significantly less than in patients with acute MI (77.8±7.1%, p=0.018). Levels of ICAM1 expression remained high on monocytes from patients followed up at 3 months (81.0±6.3%, p>0.05). CD11b showed lower constitutive levels on AMCs (3.1±0.71%) which was significantly increased in patients with AMI (10.3±9.0%, p=0.003). At the 3-month follow up, CD11b expression halved to 5.1±2.9% (p=0.048), a level that was still significantly above that seen in AMCs (p=0.009). When comparing these values to healthy volunteers, there is constitutively greater expression of both CD11b (6.1±3.6% vs 3.1±0.7%, p=0.0015) and ICAM1 (81.8±5.0% vs 70.6±9.1%, p=0.003) when compared to age-matched controls. Overall, acute MI led to significant increases in the activation of monocytes (as measured by ICAM1 and CD11b expression) with elevated levels persisting at 3-months.
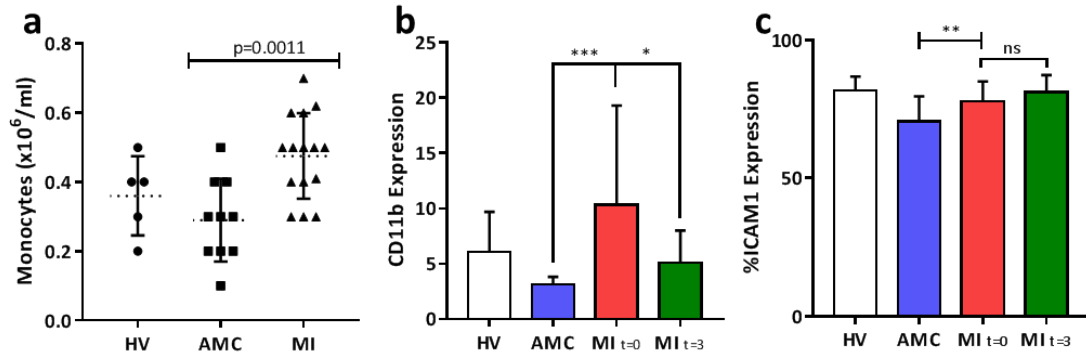
Figure 7.6: Counts and Activation Markers of Monocytes. (a) Monocyte counts in healthy volunteers (HV), age-matched controls (AMC) and patients with Myocardial Infarction (MI). Patients exhibited a significantly increased monocyte count (p=0.0011) than age-matched controls. (b) Surface expression of CD11b on monocytes which was significantly increased (p=0.0008) on monocytes during the acute phase of MI and was significantly reduced (p=0.0476) after 3-month follow-up. (c) The expression of ICAM1 on the surface of monocytes. There was a significant increase (p=0.0032) in ICAM1 expression between AMC and patients with MI with no significant change (p>0.05) at follow-up.

7.6.5   Studies of Monocyte Phenotype

Monocytes, as identified by the co-expression of the CD45 and CD14 antigens, were further stratified based on the expression of the CD16 antigen. As shown in **Figure 7.7**(a), there was a marginally greater proportion of CD16^{pos} monocytes in the AMC group than in healthy volunteers (11.4±1.1% vs 9.9±0.6%) but this was not statistically significant (p=0.41, t-test). Blood sampled from patients during the acute phase of MI showed a significantly greater (p=0.040, t-test) proportion of CD16^{pos} monocytes (14.3±0.9%). When patients were re-studied in the convalescent period, the proportion of CD16^{pos} monocytes remained at this higher level (p=0.85, t-test).

In addition to CD16, monocytes were stratified into 'classical', 'intermediate' and 'non-classical' monocyte subsets based on the expression of CD14, CD16, CCR2 and Slan-1 (as defined in section 6.8.1). In comparison to AMCs, patients with MI (MI$_{t=0}$) had significantly lower levels of the classical CD14^{high}CD16^{neg}CCR2^{high} monocyte subset (81.7±6.7% vs 86.7±5.4%, p=0.009) along with higher levels of the intermediate CD16^{pos}CCR2^{high}Slan1^{neg} subset (7.3±1.8% vs 12.6±5.2%, p<0.0001) as shown in **Figure 7.7**(b). When followed up at 3 months, levels of the classical subset were essentially unchanged (83.5±4.5%) when compared to the acute phase but still lower than that found in age-matched controls (p=0.043).
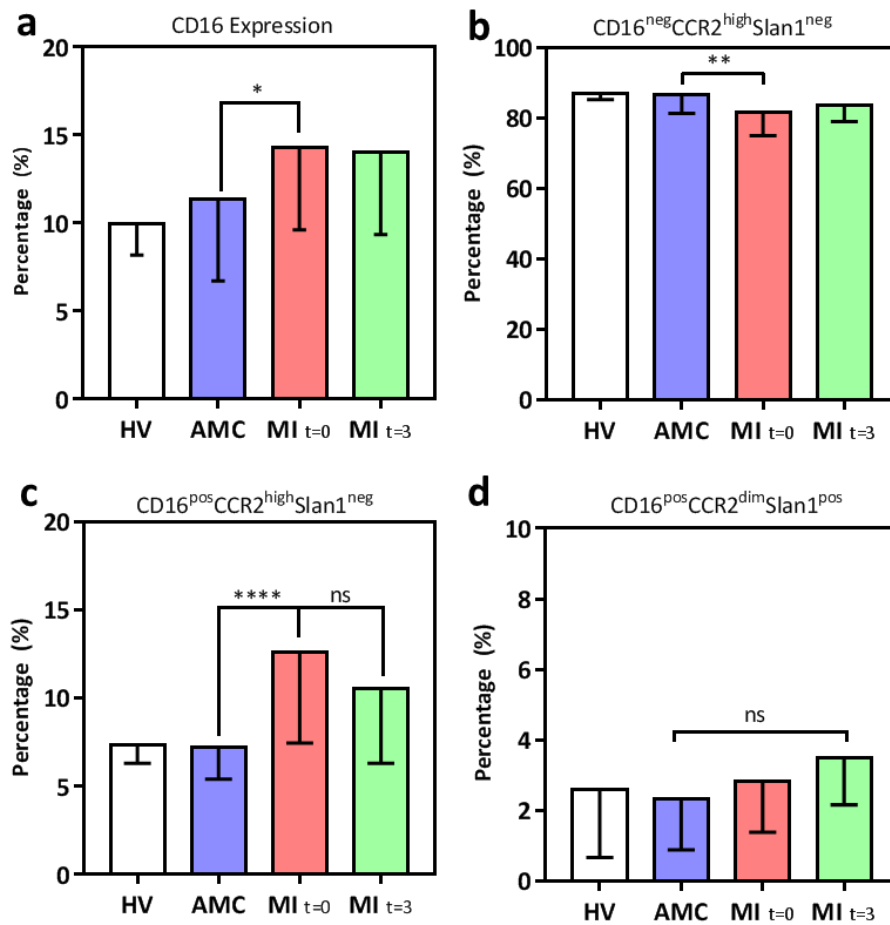
Figure 7.7: Monocyte Phenotype in FOAMI. (a) Overall expression of CD16 on monocytes in healthy volunteers (HV), age-matched controls (AMC) and patients with MI both in the acute ($MI_{t=0}$) and at 3-month follow-up ($MI_{t=3}$). The relative proportion of the monocytes subsets are shown for 'classical' ($CD16^{neg}CCR2^{high}Slan1^{neg}$), 'intermediate' ($CD16^{pos}CCR2^{high}Slan1^{neg}$) and 'non-classical' ($CD16^{pos}CCR2^{dim}Slan1^{pos}$) in (b), (c) and (d) respectively. CD16 expression is increased in patients with MI accompanied by increases in the levels of the intermediate subset and decreases in the classical subset. There was no overall significant difference in the non-classical subset across the groups. '*'=$p<0.05$, '**' = $p<0.01$, '****' = $p<0.0001$, 'ns'=non-significant.

The proportion of the intermediate subset, increased in the acute phase, was marginally reduced at 3-month follow up (10.6±4.2%) but this was not statistically significant as shown in **Figure 7.7**(c). However, when compared to the baseline AMCs, patients with MI followed up at 3 months had significantly higher levels of intermediate monocyte subsets (10.6±4.2 vs 7.2±1.8%, p=0.003). The non-classical $CD16^{pos}CCR2^{dim}Slan1^{pos}$ subset showed no overall significant difference across the different patient samples (p>0.05 multiple t-tests) despite there being an upward trend from 2.6±1.9% in AMCs to 3.5±1.3% in patients followed up at 3-month post-MI as shown in **Figure 7.7**(d).

7.6.6   Quantification of intracellular lipid droplets

Intracellular lipid droplets were quantified by flow cytometry both in circulating monocytes and monocyte-derived macrophages. Whole blood from healthy volunteers was used to set the baseline Nile Red fluorescence of 2% which was not significantly different from age-matched controls (p=0.34, t-test). In patients with AMI, the mean proportion of cells that were Nile Red positive was 14.72±8.47% which reduced to 0.88±0.64% in the convalescent phase. There was no statistically significant difference in the proportion of Nile Red positive monocytes between age-matched controls and patients with MI nor with the acute and convalescent phase of AMI.
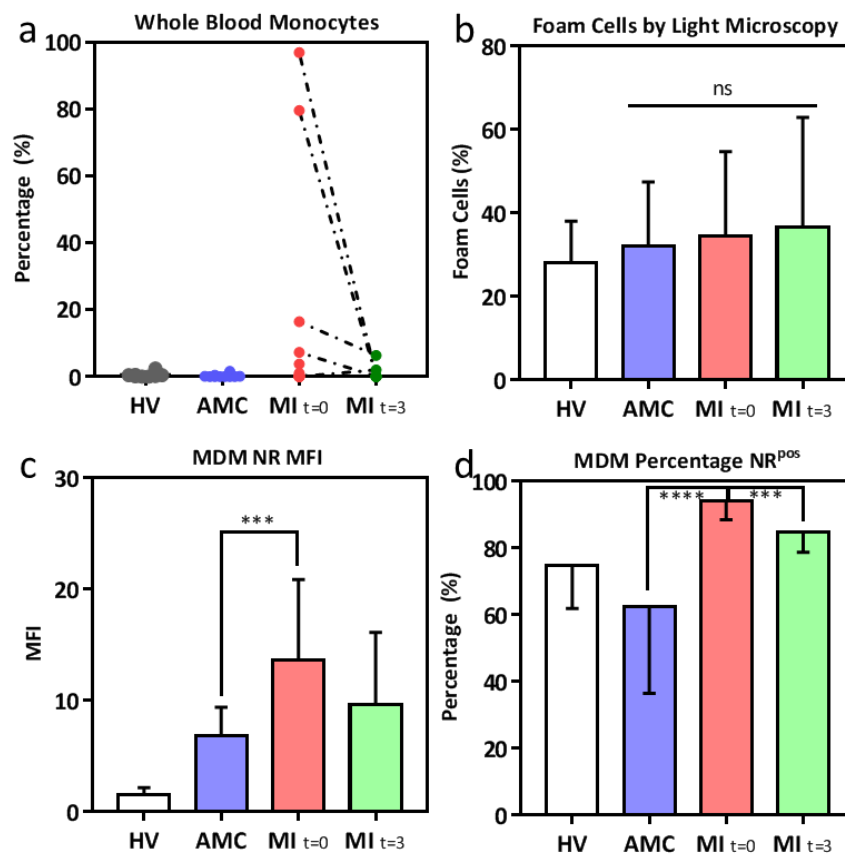
Figure 7.8: Quantification of Circulating Intracellular Lipid Droplets and Foam Cell Formation in FOAMI. (a)The proportion (%) of circulating monocytes that stain for Nile Red. Plot shows individual values from healthy volunteers (HV), age-matched controls (AMC) and in patients with MI within 24hrs of presentation ($MI_{t=0}$) and 3-month follow up ($MI_{t=3}$). Matched values are linked by the dotted line. Quantification of Foam Cells by light microscopy is shown for cultured MDMs in (b). Flow cytometric quantification of foam cells in MDMs is shown for both median fluorescence intensity (c) and percentage positivity (d). Patients with MI showed more lipid droplet formation in circulating monocytes (a) and foam cell formation (c and d) than AMCs. '***'=p<0.001, '****'=p<0.0001, 'ns'=non-significant.

In MDMs stained with Nile Red, the formation of foam cells was quantified by both direct fluorescent microscopy and flow cytometry. Overall, there was a trend towards a greater proportion of foam cells as quantified by fluorescent microscopy when comparing AMCs versus patients with AMI both in the acute and convalescent phase, but this was not statistically significant (p=0.82, ANOVA). When measuring foam cells by flow cytometry, 62.56±5.81% of MDMs were positive for Nile Red as compared with 94.06±1.08% in patients with AMI which was significantly different (p<0.001, t-test). The proportion of Nile Red positive MDMs fell to 84.8±1.4% at follow-up which was significantly less than during the acute phase of MI (p<0.001, t-test). This was still significantly higher than in AMCs (p=0.0011, t-test). Similar results were demonstrated when analysing median fluorescence intensity (MFI) of Nile Red staining in MDMs. Firstly, there was significantly greater (p<0.0001, t-test) staining of Nile red in MDMs of AMCs than in healthy volunteers (6.9±0.6 vs 1.6±0.2). This was further increased in patients with AMI during the acute phase of illness to 13.7±1.4 which was significantly different to AMCs (p=0.0002, t-test). There was a small drop (4.16±11.82) in median fluorescence intensity during the convalescent phase of AMI but this was not statistically significant.

7.7 Summary

FOAMI was a small, *in-vitro* observational study of patients with MI designed to ascertain if the changes in monocyte phenotype and foam cell formation seen *in-vitro,* were recapitulated *in-vivo* following a platelet-activating stimulus; specifically, plaque rupture.

Preliminary experiments were conducted to ascertain the effect of aspirin (as an example of a common anti-platelet agent) on the formation of foam cells. In aspirin-incubated samples, CRP-XL still led to a significant increase in the formation of foam cells despite the same concentration of aspirin having a significant inhibitory effect on AA-induced aggregation (Section 7.1.1). This is consistent with data from the published literature which shows that aspirin, although inhibiting AA-induce platelet activation, does not have a significant effect on P-selectin, activation of GPIIb-IIIa or degranulation in response to TRAP (**Taylor *et al.* 1998**). Therefore, many of the mechanisms demonstrated in previous chapters that induce foam cell formation are largely unaffected by anti-platelet agents.

Patients recruited into the FOAMI study displayed a relatively homogenous phenotype and in particular, the majority of patients had pre-established risk factors for CAD (Section 7.6.2) and therefore represents a 'typical' population of patients with MI. Patients with NSTEMI, as compared with STEMI, often tend to present with more diffuse and/or subacute vessel occlusion (**Sanchis-Gomar *et al.* 2016**) and is attested to in this study by the observation that a sizeable proportion went on to have CABG or OMT rather than single-vessel PCI. Furthermore, all patients recruited into the study exhibited a troponin rise which meant that, *a-priori*, they were more likely to have a plaque event leading to myocardial necrosis.

The use of pharmacotherapy was also relatively homogenous in the patient group. The majority of patients were on appropriate medications for secondary prevention as well as DAPT. This was reflected in the impedance aggregometry assay in which platelets had a markedly attenuated activation in response to both AA and ADP in patients with MI as compared with AMCs. This finding was preserved at 3-month follow-up indicating that patients were compliant with medication and that that the aggregatory function of their platelets continued to be inhibited, as one would expect to see in this cohort.

However, while patients were receiving appropriate DAPT, the expression of surface P-selectin was significantly greater in the patients at the time of their MI, accompanied by increased MPA formation (section 7.6.3). This means that although there is good inhibition of platelet aggregatory function in patients with MI, they continue to form complexes with monocytes and degranulate. This platelet activation was accompanied by increased activation of monocytes as

shown by increased ICAM and CD11b expression. When patients were followed up at 3-months, there was partial resolution of this increased activation state with reductions in monocyte CD11b expression, and platelet activation including MPA formation and P-selectin expression. However, these levels were still not comparable to those seen in the healthier, age-matched controls. These findings are consistent with the published literature describing plaque rupture and atherosclerosis as an acute on chronic inflammatory state (**Hansson *et al.* 2015, Tabas and Lichtman** *2017*).

In addition to increased monocyte activation, patients also exhibited a significantly greater proportion of the intermediate monocyte subset at the time of their MI accompanied by a decreased proportion of the Classical subset (Section 7.6.5). This pattern of monocyte subsets in acute MI recapitulates that seen with the *in-vitro* activation of platelets with CRP-XL. When these patients were followed up, there was a reduction in the intermediate subset although not down to levels seen in AMCs. This is also in keeping with data on monocyte and platelet activation which showed that all of these were elevated in the acute phase and less so in the convalescent phase.

The main outcome measure for which this study was powered was shown to be positive (Section 7.6.6). Monocytes isolated from patients with acute MI, more readily formed foam cells than either AMCs or at the 3-month follow up. Interestingly, the effect of MI on intracellular lipid droplet formation was observed within circulating monocytes themselves although this was not statistically significant. When taken together, these results once again mirror the *in-vitro* model wherein platelet activation with CRP-XL induces lipid droplet formation in monocytes and foam cell formation in MDMs. In this clinical study, the results suggest that plaque rupture, and by extension platelet activation, render monocytes pro-inflammatory and 'prime' them to accumulate lipids and become foam cells. The clinical implication of this may be that the effects of the thrombotic event persistent for some time afterwards and might increase the risk of developing further atherosclerotic events (**Dutta et al.** *2012*).

Chapter 8: General Discussion

In addition to their canonical role in haemostasis and thrombosis, platelets have an increasingly recognised role in the modulation of the immune system and the formation of atherosclerotic plaques (**Lievens and von Hundelshausen** *2011*). Evidence presented in this thesis, in summary, demonstrates that activated platelets, form complexes with monocytes and induce a pro-inflammatory phenotype which more readily form foam cells.

In Chapter 5, it was demonstrated that activated platelets promote a pro-atherogenic phenotype in cultured MDMs. Monocytes from WB incubated with the platelet-specific agonist CRP-XL, show an accelerated rate of foam cell formation when cultured into MDMs. This finding is consistent with the existing literature showing that platelets promote foam cell formation in MDMs when co-cultured (**Curtiss et al.** *1987*) however the model of WB activation with CRP-XL employed in this thesis provides a physiologically relevant stimulation of the *in-vivo* environment. Platelets are also more likely to be activated through GPVI *in-vivo* as collagen is a major component of the ruptured plaque. Activated platelets readily interact with monocytes in the circulation through both direct and indirect mechanisms (**Furman et al.** *1998,* **Stephen** *et al. 2013*) and, among many of its actions, promotes the diapedesis of monocytes across the endothelial border. However, when crossing this border, there is evidence to show that bound platelets are not translocated into the vessel media and that the process of monocyte migration drives the dissociation of MPAs (**van Gils et al.** *2008*). It is therefore argued that the co-culture of platelets and MDMs is not an adequate model of the *in-vivo* environment where platelets and MDMs do not come into direct contact. Post-mortem studies show some evidence to the contrary where platelets were found to be present within the plaque, but this is restricted to advanced plaques and as a result of either microhaemorrhage or intra-plaque rupture (**Kolodgie et al.** *2003*). This might also account for the localisation of platelet-derived chemokines (e.g. PF4) within the plaque (**Pitsilos et al.** *2003*) but is unlikely to be found in early lesions. The WB model employed in this thesis, even in the absence of endothelium, is therefore more representative of the *in-vivo* setting as it is the early interaction between platelets and monocytes that are reflected in the phenotype of MDMs. Furthermore, using the methods developed in Chapter 4, the vast majority of residual platelets were removed prior to culture thereby further recapitulating the *in-vivo* intra-plaque environment but does not exclude the possibility of contaminating platelet-derived microparticles. CRP-XL is a potent inducer of platelet activation through the GPVI collagen receptor (**Asselin et al.** *1997*). The formation of MPAs permitted the ingestion of platelets by circulating monocytes, as shown in Chapter 5, and allows for the passage of platelet material into a nascent plaque. The doses of CRP-XL used to activate platelets been optimised to induce maximal platelet aggregation, MPA formation and

P-selectin expression but with minimal formation of microparticles. However, the formation of this class of extracellular vesicles cannot be excluded from the analyses and may provide another mechanism by which platelets promote foam cell formation.

The presence of intracellular lipid droplets in circulating WB monocytes has been described in the early literature and were thought to be due to reverse transmigration events where foamy macrophages migrate out of the plaque and into the circulation (**Pachauri *et al.* 1976**). More recently, mouse models of atherosclerosis has shown that plaque stabilisation by cholesterol-lowering therapy led to regression of plaque macrophage content and the release of lipid-laden circulating mononuclear cells (**Potteaux *et al.* 2011**).

Notably, the model employed in the thesis was devoid of endothelium or plaque and it is therefore surmised that formation of intracellular lipid droplets in monocytes is *de-novo*. Part of the documented increase in monocyte NR fluorescence is due to platelet and/or microparticle phagocytosis but also the direct binding of platelets onto monocytes, which themselves stain for NR. Another mechanism might be the *de-novo* synthesis of intracellular lipid droplets which is hinted at in the transcriptomic data. Following a 4hr incubation period with activated platelets, some of the most highly upregulated genes in monocytes belong to the scavenger receptor family. OLR1 is the most notable example and is accompanied by increased surface expression of the OLR1-encoded protein, LOX-1, and would be in keeping with the traditional model of foam cell formation where the uptake of modified lipid species drives lipid accumulation (**Moore et al.** *2013*). It is important to note that in the model used in this thesis, there was no addition of exogenous lipid or oxidatively-modified species, but may arise from oxidative modification of LDL present in plasma when whole blood was used, and also from reactive oxygen species supplied by activated platelets (**Wachowicz *et al.* 2002**). Actinomycin D, used to inhibit gene transcription, effectively inhibited the accumulation of intracellular lipids in circulating monocytes which further supports the assertion that the platelet-induced transcriptome is an important driver of this process. Comparison of cholesterol-loaded macrophages from mouse models has shown that some of the most significant gene changes were those whose products were involved in lysosomal function and ER stress (**Berisha *et al.* 2013**). This is a homeostatic mechanism by which the transcriptomic response to cholesterol load in macrophages is the upregulation of mechanisms to deal with this increased load. Platelets induce a mix of both pro and anti-inflammatory/atherogenic gene expression in monocytes. On the one hand, there is upregulation of the scavenger receptors, native LDL receptors and downregulation of trafficking proteins (e.g. OSBPL5) which all suggest that platelets promote a phenotype in monocytes which promote lipid accumulation. Conversely, cholesterol efflux genes (e.g. ABCA1/ABCG1) and many

of the lysosomal trafficking genes are also upregulated in monocytes by platelets which suggests that these cells are 'primed' to deal with increased cholesterol loading as seen in macrophages. The experiments using inhibitors of cholesterol uptake and/or synthesis suggest that the 'overall' effect of platelet-induced gene transcription is to promote lipid uptake in monocytes. There are of course a number of caveats to making the assertion that the transcriptomic signature in monocytes is synonymous with increased atherosclerosis. It is assumed that this transcriptomic signature is preserved in macrophages and that the change at the mRNA is translated to protein with subsequent phenotypic change. Due to the complex nature of an atherosclerotic plaque with multiple growth and differentiation signals given to macrophages (**Moore et al.** *2013*), it is likely that in the *in-vivo* plaque setting, the effect of platelets is more modest than observed *in-vitro*. That is to say that although platelets induce early changes that set monocytes down a foam cell path, this might be modulated by the multitude of chemical and cellular signals in an atherosclerotic plaque that will mitigate the initial effects of platelets.

Further insights into the potential mechanisms of foam cell formation can be derived from the use of the inhibitors of cholesterol metabolism. Simvastatin, an inhibitor of HMG-CoA Reductase, attenuated the formation of foam cells in platelet-activated MDMs, suggesting that *de-novo* lipid synthesis is, in a large part, responsible for the formation of foam cells over uptake of platelets or platelet-derived MVs. This is supported by the platelet-activated monocyte transcriptome in which HMGCR is modestly elevated at 4 hours, and is supported by the observation that the intracellular location of platelet fragments did not necessarily co-localise with lipid droplets. Furthermore there is progressive increase in intracellular lipid formation in MDMs when cultured over 7 days which cannot be accounted for by platelet ingestion alone (as they were depleted from the culture system). However it cannot be discounted that ingested platelets fragments provide a source of lipid substrates from which cholesterol esters can be generated.

These results suggest an alternative mechanism by which foam cells are formed however the reality is likely to reflect a combination of different pathways. As discussed in the introduction, platelets release both pro and anti-foam cell cytokines (Section 2.5.5.2) but the overall effect seems to be the promotion of a foam-cell phenotype. This is done through an increased expression of scavenger receptors that promote the uptake of modified lipid species, and provide direct transfer of lipid through phagocytosis and uptake of microparticles. As only the effect of the platelet signal on foam cell formation in MDMs was examined, the interacting effects of the vascular endothelium, soluble mediators and other leucocytes are likely to provide both complimentary and competing signals to MDMs in atherosclerotic plaques.

Another mechanism by which platelets promote atherosclerosis is modulation of monocyte phenotype. It has been demonstrated that the incubation with activated platelets promote a change in monocytes from a classical CD16^{neg} subset to the pro-inflammatory intermediate (CD16^{pos}) subset. This is consistent with the evidence in the literature that, across a range of pro-inflammatory states, there are increased proportions of the intermediate monocyte subset (**Passacquale et al.** *2011,* **Poitou et al.** *2011,* **Rogacev** *et al. 2011*). Evidence presented in this thesis shows that not only is this relationship associative, but the CD16^{pos} phenotype arises from the CD16^{neg}, driven by activated platelets. The mouse model has often been used as an analogy to human monocyte subsets where the pro-inflammatory Ly6C^{high} subset is thought to derive from haematopoietic stores (**Jacquelin** *et al. 2013*). With a stimulus such as MI, splenic reserves of monocytes have been shown to be mobilised to the sites of damage to participate in wound healing where Ly6C^{high} cells digest damaged tissues and Ly6C^{low} promote wound healing (**Swirski** *et al. 2009*). It has also been demonstrated in a number of *in-vitro* mouse studies that Ly6C^{hi} monocytes convert to their Ly6C^{low} counterpart over time (**Varol et al.** *2009,* **Yona et al.** *2013*). In humans, the origin and temporal relationship between the monocyte subsets is less well understood (**Ziegler-Heitbrock** *2015*). In post-mortem studies, classical monocytes have been shown to accumulate in the peri-infarct border of MI with associated reduced numbers in the spleen (**van der Laan et al.** *2014*). Using an *in-vivo* deuterium-labelling of healthy volunteers, it has been shown that classical monocytes emerge first from the marrow with early release of this subset when experimental endotoxaemia was induced (**Patel** *et al. 2017*). However, it is yet to be demonstrated in the literature, to the author's knowledge, that human classical monocytes change their phenotype to either an intermediate or non-classical. The evidence presented in this thesis has demonstrated that the pro-inflammatory pool of monocytes can arise from the classical phenotype. This was supported by both flow-cytometric quantification of characteristic surface markers, increase expression of fcgr3 mRNA and a demonstration that this change did not arise from proliferation of the existing pool of CD16^{pos} monocytes. Furthermore, platelets induce differential expression of surface chemokine receptors from a pattern found on CD16^{neg} monocytes to one that more closely resembles CD16^{pos} monocytes. Differences in chemokine receptor expression on monocyte subsets have been described in the literature (**Sandblad** *et al. 2015,* **Gadd** *et al. 2016*) and though to account for the differences in migration and survival in atherosclerosis (**Gautier** *et al. 2009*). Although not demonstrated in this thesis, the increased expression of chemokines on the surface of platelet-activated cells (e.g. CX3CR1, CXCR2 and CXCR6) are likely to promote increased transmigration of the CD16^{pos} subset across the endothelial border which have a greater propensity towards foam cell formation than their CD16^{neg} counterpart (Section 6.1.1). In addition to the expression of surface chemokine

receptors, it has been demonstrated that platelets also release a number of chemokines (e.g. PF4 and RANTES), consistent with the literature (**von Hundelshausen** *et al. 2001,* **von Hundelshausen** *et al. 2005*), which in turn promote further release of pro-inflammatory chemokines such as IL-8 and CCL22 from monocytes.

The findings from this thesis is consistent with the hypothesis that function of platelets span not only the pro-thrombotic response, but also the pro-inflammatory immune response as is observed in a variety of animal models (**Semple and Freedman** *2010*). The upregulation of scavenger receptors for example as well as the increased phagocytosis by MDMs is an evolutionarily conserved mechanism activated in response to a PAMP stimulus (**Whelan** *et al. 2012*). This is likely to have evolved in higher-order mammals as a mechanism to mitigate against vascular injury. Often, traumatic injury is associated with both vascular damage and loss of skin integrity with pathogen exposure. The widespread activation of platelets not only provides a nidus for the formation of a haemostatic plug, but also, their effect on monocyte phenotype is part of an innate immune response enabling a more robust response to pathogen challenge. In the modern world, the risk factors for CAD share many of the same immunological features of pathogen exposure which would account for the ubiquitous role of platelets in mediating thrombosis but also promoting inflammation with the 'unforseen' consequence of promoting atherosclerosis.

8.1   <u>Clinical Implications and Therapeutics</u>

Myocardial infarction is an ubiquitous problem and results in not only the widespread activation of platelets, but also the activation of a number of neuro-humoral mechanisms, increased adrenergic drive and the widespread release of vasoactive amines that have effects on a range of cell types. Although the aggregatory function of platelets was inhibited by DAPT in patients with MI (as ascertained by whole blood impedance aggregometry), there are a number of other consequences of platelets activation including degranulation (as evidenced by expression of P-selectin) resulting in MPA formation, which persist despite the use of anti-platelet therapy (**Gremmel** *et al. 2009*). It has been demonstrated in this study and several others (**Berg et al.** *2012,* **Rogacev et al.** *2012*) that the formation of MPAs is important marker of cardiovascular disease and provide an avenue by which platelets are able to exert their effects on monocytes. Therefore, one assumes that despite appropriate anti-platelet therapy, platelets can continue to affect monocytes through the formation of MPAs.

This hypothesis is born out in the data from the patients with MI where the circulating monocytes are more activated as shown by increased levels of ICAM1 and CD11b. These monocytes are presumably more able to bind to and transmigrate across the endothelium (**da Costa Martins et al.** *2004*) to exert their pro-inflammatory effects on the arterial vasculature. It cannot be said from this study that this is entirely due to the effect of platelets as the aforementioned neuro-hormonal mediators and other cells types are likely to influence this phenomenon. However, the recapitulation of the *in-vitro* data suggests that platelets do indeed have a large role to play in the activation status of monocytes.

The surprising finding from the clinical data is that circulating monocytes show an increased formation of intracellular lipid droplets. Although this was not statistically significant, it is likely a reflection of the small numbers of patients recruited into the study and the fact that it was not designed to be powered for this secondary end-point. Also, although patients were recruited within 24hrs of presentation, the time after their event will vary considerably and may not necessarily correlate to within 24hrs of an index myocardial infarction. Furthermore, in contrast to the *in-vitro* model wherein a single stimulus was used, the platelet activation in MI tends to be more insidious in nature and therefore the magnitude of stimulus is a fraction of that seen with *in-vitro* activation. Intracellular lipid droplets were found despite these considerations and, as the levels of platelet activation is modest compared to the *in-vitro* model, is likely to represent an important result where the early changes of platelets phagocytosis and/or increased uptake of lipids is present in circulating monocytes themselves. This combined with the observation that there is increased ICAM1 on monocytes of patients with MI suggests that platelets do

indeed 'prime' monocytes following MI (**Zalai *et al.* 2001**) . This is complemented by the observation that when monocytes from patients with MI were cultured, they more avidly formed foam cells thus recapitulating the *in-vitro* data. Furthermore, the demonstration that were increased levels of the CD16^{pos}Slan1^{neg} monocyte subset in patients with MI further support not only the *in-vitro* work within this study, but also the literature which has shown increased levels of this subset in patients with MI (**Weber et al. 2016**). Once again, this likely reflects the increased inflammatory milieu as a result of both platelet activation and sympathetic nervous system activation.

The treatment of MI has undergone a revolution over the past 30 years. From the initial trials of aspirin (**Elwood *et al.* 1974**) which showed a significant reduction in mortality when administered to patients, to more recent trials of new anti-platelet agents such as Ticagrelor (**Wallentin *et al.* 2009**), the focus of therapy has been on the prevention of further thrombotic events as a result of plaque rupture. This has also led to the development of drugs such as statins which not only lower serum cholesterol, but also have a variety of off-target, anti-inflammatory effects including plaque stabilisation (**Libby and Aikawa *2003***). This approach to treating MI is entirely consistent with our understanding of atherosclerotic disease wherein progressive plaque formation at anatomically critical sites leads to stenosis with distal ischaemic combined with a catastrophic plaque rupture event which leads to necrosis.

In this thesis, evidence is provided that platelets might have more direct effects on monocytes so that they more likely form foam cells and by extension are more likely to form atherosclerotic plaques. This means that traditional anti-platelet agents, which inhibit the thrombotic sequelae of CAD, might not have a concomitant inhibitory effect on the pro-atherosclerotic effect. It has been demonstrated that aspirin, a known inhibitor of COX and subsequent inhibitor of platelet aggregation, does not have a significant effect on the formation of monocyte-derived foam cells. Platelets, pre-incubated with aspirin, and subsequently activated with a collagen peptide mimetic are still able to exert their pro-foam cell effects on MDMs. This is consistent with the literature which shows that inhibition with either aspirin or clopidogrel did not significantly affect the formation of MPAs when platelets were stimulated with either AA or ADP (**Gremmel et al. *2009***). Indeed, the expression of surface P-selectin is largely unaffected by inhibition of the ADP or AA pathways when stimulated with CRP-XL and therefore MPA formation can still occur. Once again, this is likely to reflect the evolutionary adaptation of platelets where inhibition of the thrombotic function with anti-platelets does not necessarily have a concomitant effect on its innate immune function with implications for the treatment of cardiovascular disease.

Up to 1 in 5 people with a history of MI will go on to have a further infarct within 1 year (**Jernberg** *et al. 2015*) and shows that one of the biggest risk factors for MI, is a history of previous MI. There is also evidence to show that in patients with risk factors for arterial disease, but without an index major thrombotic event, there are multiple micro-plaque ruptures and platelet activating events (**Stefanadis** *et al. 2017*). Therefore, a major thrombotic event is not a necessary requirement for the activation of platelets and subsequent modulation of monocyte phenotype. This phenomenon is important when thinking about methods to mitigate the risk of athero-thrombotic events in patients with risk factors for CVD. As an analogy, the management of rheumatological diseases has undergone a revolution in the last 20 years where the focus has gone away from inhibiting inflammation to actual modulation of disease phenotype. The prevention of MI should be viewed in the same light. It has long been recognised that atherosclerosis is a chronic inflammatory condition (**Ross** *1999*) and perhaps a focus should be towards modulation of platelet-monocyte interactions in addition to prevention/mitigation of thrombosis. This might involve administered agents to minimise MPA formation and thereby monocyte activation to high-risk patients with CAD. Furthermore, at the time of stenting for plaque events, stent struts may also be coated with pharmacological agents that prevent the formation of MPAs to further reduce the risk of re-rupture events or indeed remote ischaemic events. As yet, this has not been demonstrated as the trials of P-selectin inhibition have been disappointing. PSI-697 is a selective antagonist of P-selectin which has been shown to reduce platelet-monocyte aggregation in a canine model of thrombosis. However, when given to healthy volunteers as an oral preparation, there was no significant effect on MPA formation with blood was stimulated ex-vivo with TRAP (**Japp** *et al. 2013*). The inhibition of P-selectin might be potentially problematic as this surface receptor is involved in a number of cellular processes and most likely, inhibition will result in long-term effects on a variety of basic biological function (**Blann** *et al. 2003*). Although knockout mouse models of P-selectin have demonstrated decreased atherosclerosis (**Burger and Wagner** *2003*), it may be more prudent to inhibit the downstream effectors of the P-selectin/PSGL1 dyad involved in platelet-monocyte interactions. Platelet-monocyte interactions are also mediated through a range of cognate receptors which augment the interaction between these cell types. Inhibition of these other receptor dyads might modulate the inflammatory response (e.g. CD40/CD40L) and attenuate the effects of MPA formation. This would be predicted to affect not only the activation status of monocytes, but also their phenotype and therefore its effect on the vascular endothelium.

In addition to potential therapeutic avenues, the phenotype of activated platelets and their effect on monocytes might provide a prognostic tool in either patients with established CAD or

in primary prevention. Currently, the management of CV risk in either the primary or secondary prevention contexts is based on the aggressive control of modifiable risk factors based originally on the Framingham cohort (**Mahmood et al.** *2014*). There are of course a number of non-modifiable risk factors such as age and ethnicity which also contribute to a person's risk of coronary events. Identification of these moderate and high-risk individuals allows for treatment stratification ranging from lifestyle advice, to aggressive pharmacotherapy. MPAs are associated with a number of inflammatory conditions and both the *in-vitro* and clinical studies presented here have confirmed this (**Rogacev et al.** *2011*). This opens up the possibility of using the level of MPA formation, a surrogate marker of inflammation, as a tool to risk stratify patients at risk of further cardiovascular events.

8.2 <u>A Model</u>

Platelets are activated in the blood stream through a variety of mechanisms but most notable through (micro) rupture of atherosclerotic plaques. The exposure of the subendothelial matrix, rich in collagen, acts as a potent platelet-activating stimulus leading to their aggregation and also the formation of MPAs. Through both direct and paracrine mechanisms, both adherent and free activated platelets go on to activate monocytes and promote a pro-atherogenic phenotype. This is achieved through an increased expression of SRs, such as MARCO and LOX-1 (OLR1), as well as increased expression of CD16 and a shift into a pro-inflammatory phenotype including the release of chemokines/expression of chemokine receptors which promote diapedesis. Platelets are additionally phagocytosed by monocytes which also expressed increased levels of surface integrins thereby facilitating their diapedesis across the endothelial barrier. Once in the intima, the transcriptomic changes, in particular the upregulation of a number of key SRs and lipid regulating genes, initiated in circulating monocytes themselves take effect and allow for the accumulation of intracellular lipids and the uptake of oxidatively-modified lipid species. This combined with neolipogenesis and phagocytosis of platelets and platelet fragments accelerates the formation of foam cells which accumulate and form the necrotic lipid core characteristic of an advanced atherosclerotic lesion.
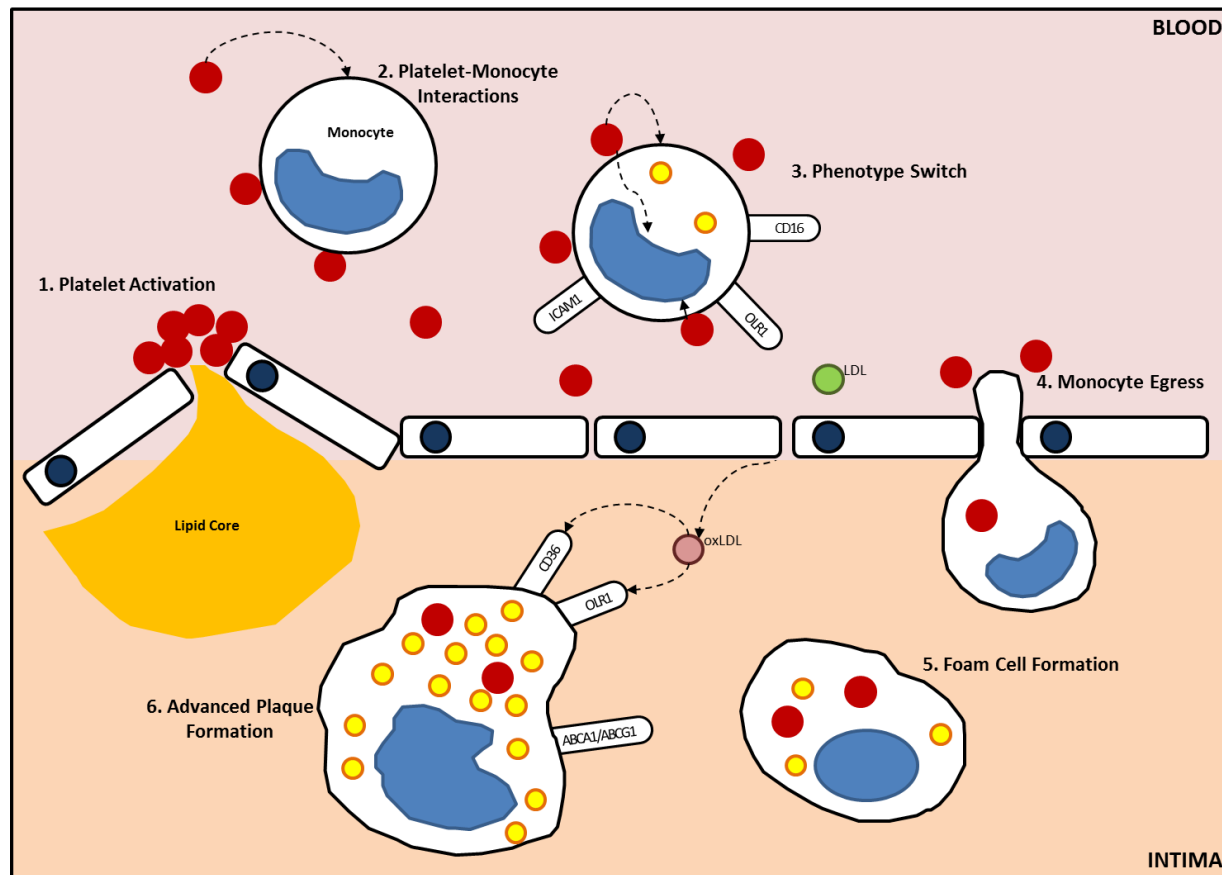
Figure 8.1: A Model of Platelet-Induced Foam Cell Formation. (1) Disruption of the endothelial layer and exposure of the subendothelial matrix and the prothrombotic lipid core of an advanced plaque induces the activation of platelets and the instigation of a primary haemostatic plug. (2) In addition to orchestration of thrombosis, platelet interact with monocytes in the circulation through both direct binding and paracrine signalling. (3) The interaction of platelets with monocytes induces a phenotypic change with an increased pro-inflammatory intermediate monocyte subset (CD16^{pos}) and increased expression of surface integrins. Additionally, platelets promote the formation of intracellular lipid droplets in circulating monocytes in addition to their ingestion. (4) The change in phenotype and the increased expression of integrins promote diapedesis of monocytes across the endothelial border. Platelets are left within the abluminal side, but ingested platelets are transported into the nascent plaque. (5) The differential expression of lipid-regulatory genes induced by platelets promotes further intracellular lipid accumulation. (6) The increased expression of scavenger receptors leads to increased accumulation of oxidised lipid species and the formation of advanced foam cells.

Pg. 236

8.3 <u>Future work</u>

The work conducted in this thesis acts as a stepping stone for a deeper understanding of the mechanisms of platelet-induced modulation of monocyte phenotype. One poorly explored avenue of enquiry arising from this thesis is the role of platelets in mediating oxidised lipid uptake into MDMs. Using the current model, quantification of oxidative stress using markers such as hydrogen peroxide, would allow for its manipulation using exogenous anti-oxidants such as glutathione, or indeed the addition of oxidatively-modified lipid species (e.g. oxLDL). Comparison with and without these oxidatively-active agents would allow for better delineation of the mechanism by which platelets promote foam cell formation. If indeed oxLDL does promote foam cell formation in this context, inhibitors of SRs, and particularly the oxLDLR, would allow for the translation of the transcriptomic signature into a demonstrable phenotype (**Stephen** *et al. 2010*).

The model, which cultured the MDMs in the absence of serum, also allows for a more detailed study of cholesterol influx/efflux into the platelet-activated MDMs. The ATP cassette-transporters have been shown to be important in the formation of foam cells and are upregulated in monocytes upon platelet activation. One poorly studied aspect in this work is the nature of the lipids that have accumulated in the cultured MDMs. The *in-vivo* growth of foam cells occurs in the milieu of cholesterol-rich and cholesterol-poor apolipoproteins which are circulated as part of reverse cholesterol transport (**Ohashi** *et al. 2005*). Radio-labelled H^3-cholesterol has been used in the quantification of cholesterol influx and efflux in J774 mouse macrophages and in a Fu5AH rat hepatoma cell line (**Weibel** *et al. 2014*). This radio-labelled cholesterol assay can be used in this isolated primary monocyte culture system so that the effect of platelet activation on cholesterol influx/efflux can be better described. The use of glibenclamide, as an example, accelerated the platelet-induced formation of foam cells, as quantified by Nile Red staining. Use of a radio-labelled cholesterol assay would be better able to describe if this phenomenon is indeed due to decreased efflux as predicted by the current model.

The inference from the experimental work to date is that the formation of MPAs is an important mechanism by which platelets accelerate foam cell formation in MDMs. Therefore, complementing the results of inhibition of the P-selectin/PSGL-1 dyad, two avenues of investigation are proposed. Firstly, to test the observation that the P-selectin/PSGL1 interaction mediates a pro-inflammatory effect on monocytes and MDMs, inhibitors of downstream signalling of PSGL1 (**Tinoco and Bradley** *2017*) or conversely PSGL1-activating antibodies can be used to study their subsequent effect on platelet-induced foam cell formation studied. The

second mechanism to test the veracity of the claim that MPA formation is responsible for the platelet-induced modulation of monocyte phenotype is to inhibit the range of the receptor dyads that mediate contact between these cell types. Once such example is the CD40-CD40L which has been shown to induce functional changes in monocytes (**Elgueta** *et al. 2009*). It is hypothesised that this, and other interactions may augment the signalling induced by MPA formation and provide another mechanism by which a pro-atherogenic phenotype is promoted and might provide therapeutic options.

The second mechanism by which platelet induce foam cell formation is the direct phagocytosis of platelets by monocytes and MDMs. The drawback of the present study is that the model did not include an endothelial barrier and it can only be postulated that the ingestion of platelets by monocytes provides a source of lipids in cultured MDMs. This could be explored in further experiments by use of a Boyden chamber (**Chen** *2005*). Platelets and monocytes can be co-incubated before being placed on an endothelial monolayer of either EaHy or HUVEC grown in a monoculture on a permeable membrane with a conditioned medium on the other side. Monocytes that pass through the endothelial layer can then be harvested and analysed for markers of platelets and foam cell formation. This would allow for measurements of the ability of platelet-activated monocytes to diapedeses across the endothelial border.

In addition to the *in-vitro* work, the functional relevance of the platelet-monocyte interaction in atherosclerotic disease can be better ascertained with a more robust clinical study. The preliminary data from the FOAMI study has shown that there is a fundamental difference in the activation status and phenotype of monocytes and is postulated to be secondary to platelet activation. The selection of different patient groups, from which to conduct functional studies of platelets and monocytes, will allow for the discrimination of the effects of systemic inflammation and platelet activation in the modulation of monocyte phenotype. Samples from patients with risk factors for CAD but without an index ischaemic event will provide evidence of the 'inflammatory' component of atherosclerotic risk. These patients often exhibit an increased inflammatory risk profile associated with widespread atherosclerotic lesions (**Ruparelia** *et al. 2017*) and may also be followed up to see if they go on to develop a plaque event and if this correlates with any of the markers of monocyte phenotype identified in FOAMI. Additionally, the recruitment of patients admitted for elective coronary angiography provides a stable group of patients with risk factors for CAD, where samples may be collected both before and after their elective PCI. Both platelet and monocyte responses may be measured in both of these groups of patients and correlated with carotid intimal thickness as a surrogate marker of atherosclerotic burden (**Darabian** *et al. 2013*).

Chapter 9: Appendix

9.1   Table of Chemokines

GROUP	NAME	GENE	OHER NAME(S)	RECEPTOR	UNIPROT
CC	CCL1	Scya1	I-309, TCA-3	CCR8	P22362
	CCL2	Scya2	MCP-1	CCR2	P13500
	CCL3	Scya3	MIP-1α	CCR1	P10147
	CCL4	Scya4	MIP-1β	CCR1, CCR5	P13236
	CCL5	Scya5	RANTES	CCR5	P13501
	CCL6	Scya6	C10, MRP-2	CCR1	P27784
	CCL7	Scya7	MARC, MCP-3	CCR2	P80098
	CCL8	Scya8	MCP-2	CCR1, CCR2B, CCR5	P80075
	CCL9/CCL10	Scya9	MRP-2, CCF18	CCR1	P51670
	CCL11	Scya11	Eotaxin	CCR2, CCR3, CCR5	P51671
	CCL12	Scya12	MCP-5	CCR2	Q62401
	CCL13	Scya13	MCP-4, NCC-1, Cκβ10	CCR2, CCR3, CCR5	Q99616
	CCL14	Scya14	HCC-1, MCIF, Cκβ1, NCC-2, CCL	CCR1	Q16627
	CCL15	Scya15	Leukotactin-1, MIP-5, HCC-2, NCC-3	CCR1, CCR3	Q16663
	CCL16	Scya16	LEC, NCC-4, LMC, Cκβ12	CCR1, CCR2, CCR5, CCR8	O15467
	CCL17	Scya17	TARC, dendrokine, ABCD-2	CCR4	Q92583
	CCL18	Scya18	PARC, DC-CK1, AMAC-1, Cκβ7, MIP-4	CCR8	P55774
	CCL19	Scya19	ELC, Exodus-3, Cκβ11	CCR7	Q99731
	CCL20	Scya20	LARC, Exodus-1, Cκβ4	CCR6	P8556
	CCL21	Scya21	SLC, 6Ckine, Exodus-2, Cκβ9, TCA-4	CCR7	O00585
	CCL22	Scya22	MDC, DC/β-CK	CCR4	P55773
	CCL23	Scya23	MIPF, Cκβ8, MIP-3, MPIF-1	CCR1	O00175
	CCL24	Scya24	Eotaxin-2, MPIF-2, Cκβ6	CCR3	O00175
	CCL25	Scya25	TECK, Cκβ15	CCR9	O15444
	CCL26	Scya26	Eotaxin-2, MIP-4a, IMAC, TSC-1	CCR3	Q9Y258
	CCL27	Scya27	CTACK, ILC, Eskine, PESKY, skinkine	CCR10	Q9Y4X3
	CCL28	Scya28	MEC	CCR3, CCR10	Q9NRJ3
CXC	CXCL1	Scyb1	Gro-α, GRO-1, NAP-3, KC	CXCR2	P09341
	CXCL2	Scyb2	Gro-β, GRO2, MIP-2α	CXCR2	P19875
	CXCL3	Scyb3	GRO3, MIP-2β	CXCR2	P19876
	CXCL4	Scyb4	PF-4	CXCR3B	P02776
	CXCL5	Scyb5	ENA-78	CXCR2	P42830
	CXCL6	Scyb6	GCP-2	CXCR1, CXCR2	P80162
	CXCL7	Scyb7	NAP-2, CTAPIII, β-Ta, PEP	GPR35/CXCR8	P02775

CXCL8	Scyb8	IL-8, NAP-1, MDNCF, GCP-1	CXCR1, CXCR2	P10145
CXCL9	Scyb9	MIG, CRG-10	CXCR3	P07325
CXCL10	Scyb10	IP-10, CRG-2	CXCR3	P02778
CXCL11	Scyb11	I-TAC, β-R1, IP-9	CXCR3, CXCR7	O14625
CXCL12	Scyb12	SDF-1, PBSF	CXCR4, CXCR7	P48061
CXCL13	Scyb13	BCA-1, BLC	CXCR5	O43927
CXCL14	Scyb14	BRAK, bolekine	*	O95715
CXCL15	Scyb15	Lungkine, WECHE	*	Q9WVL7
CXCL16	Scyb16	SRPSOX	CXCR6	Q9H2A7
CXCL17	VCC-1	DMC, VCC1	GPR35/CXCR8	Q6UXB2
XC XCL1	Scyc1	Lymphotactin α, SCM-1α, ATAC	XCR1	P47992
XCL2	Scyc2	Lymphotactin β, SCM-1β	XCR1	Q9UBD3
CX3C CX3CL1	Scyd1	Fractalkine, Neurotactin, ABCD-3	CX3CR1	P78423

Table 9.1: Summary of Chemokines. Table gives the list of known chemokines grouped according to their subfamilies. Given also are the alternative names for the chemokines, along with their cognate receptor and a corresponding Uniprot reference number. '*' refers to those chemokines for which a receptor has yet to be identified.

9.2 Table of Cytokines

CLASS	NAME	ORIGIN	TARGET	FUNCTION
Colony-Stimulating Factors	Granulocyte-Colony Stimulating Factor (G-CSF)	Endothelium, Macrophages	Neutrophil Progenitor Cells	Growth and differentiation of neutrophils
	Granulocyte Macrophage-Colony Stimulating Factor (GM-CSF)	T_H Cells	Progenitor Cells	Growth and differentiation of monocytes and dendritic cells
	Macrophage-Colony Stimulating Factor (M-CSF)	Thymic epithelial cells, chrondrocytes, mesangial cells, Endothelial cells	Macrophage lineage	Growth and differentiation of monocytes, chemotaxis and promotes phagocytic/cytotoxic activity of monocytes
Interleukins	IL-1	Monocytes, macrophages, B-cells, dendritic cells	T_H Cells	Costimulation
			B-cells	Maturation and proliferation
			NK cells	Activation
			Various	Inflammation, acute phase response
	IL-2	T_H1 cells	T, B and NK cells	Cell growth, proliferation, activation, antibody synthesis
	IL-3	T_H cells, NK cells	Stem cells, mast cells	Growth and differentiation, histamine release
	IL-4	T_H2 Cells		
	IL-5	T_H2		
	IL-6	Monocytes, macrophages, T_H2 cells		
	IL-7	Marrow stroma, thymus stroma	Stem cells	Differentiation into progenitor B and T-cells
	IL-8	Macrophages, endothelial cells	Neutrophils	Chemotaxis
	IL-10	T_H2 cells	Macrophages	Inhibition of function, cytokine production
			B-cells	Activation
	IL-12	Macrophages, B-cells	T-cells, NK cells	Activation

	MIP-1α	Macrophages	Monocyte, T-cells	Chemotaxis
	MIP-1β	Lymphocytes	Monocytes, T-cells	Chemotaxis
	TGF-β	T-cells, monocytes, platelets	Monocyte/macrophages, B-cells	Chemotaxis, IL-1 synthesis, IgA synthesis, proliferation
	TNF-α	Macrophages, mast cells, NK cells	Macrophages, tumour cells	Adhesion molecule and cytokine expression
	TNF-β	T_H1 cells	Phagocytes, B-cells	Phagocytosis, B-cell stimulation

Table 9.2: Table of Cytokines. Given is a table of the cytokines referred to in this thesis along with their predominant cell of origin, cell of effect and the priniciple function for which they are responsible for.

9.3 Cluster of Differentiation Antigens

Number	Name	Alternate Name(s)	Cell of Expression	Function
3	CD3	T3	T-cells	T-cell co-receptor, used as a marker of T-cells
4	CD4	Leu03, T4	T-helper cells, monocytes, macrophages, dendritic cells	Co-receptor for the T-cell receptor and acts to communicate with antigen-presenting cells
7	CD7	gp40, TP41	Thymocytes and mature T-cells	Interacts with PI3 Kinase
8	CD8	Leu2, T8, Lyt2,3	Cytotoxic T-cells, NK cells, thymocytes and Dendritic Cells	Marker of cytotoxic T-cells
11	CD11b	Integrin alpha M (ITGAM)	Monocytes, granulocytes, macrophages, NK cells	Forms heterodimers with $\alpha_M\beta_2$ integrin. Mediates leucocyte adhesion, migration, phagocytosis, chemotaxis and cell-mediated cytotoxicity
14	CD14	LPS Receptor	Monocytes	Co-receptor for bacterial LPS with TLR4
15	CD15	3-fucosyl-N-acetyl-lactosamine, Lewis x, SSEA-1	Neutrophils	Phagocytosis and chemotaxis. Markers of Hodkins Lymphoma (Reed-Sternberg Cell)
16	CD16	FcγRIII	NK cells, PML, Monocytes, Macrophages	Neutrophil degranulation, phagocytosis and oxidative burst
19	CD19	B-lymphocyte Surface Antigen B4, T-cell Surface Antigen Leu-12, CVID3	B-cells	Marker of B-cells
20	CD20	B1, Bp35	B-cells	B-cell marker
32	CD32	FCGR2A	B-cells	B-cell co-receptor
33	CD33	Siglex-3, gp67, p67	Myeloid Cells	ITIM receptor implicated in inhibition of cellular activity
34	CD34		Haematopoetic stem cell	Marker of haematopoetic stem cell
36	CD36	Platelet glycoprotein 4, Fatty Acid translocase, SCARB3	Multiple cell types	Scavenger receptor

41	CD41	GPIIb, Integrin αIIb, GPIIb, ITGA2B, HPA-3	Platelets	Cell adhesion, platelet aggregation
42	CD42	GP9	Platelets	Platelet adhesion
42	CD42b	GPIbα	Platelets	Platelet adhesion
45	CD45	Protein Tyrosine phosphatase receptor type C (PTPRC)	Leucocyte common antigen	Cell proliferation, B and T-cell receptor signalling
45	CD45RO		Common leucocyte antigen	Isoform of CD45
56	CD56	Neural cell adhesion molecule	Neurons, glia, NK cells	Marker of NK cells
61	CD61	Integrin β₃	Platelets	Forms part of platelet integrins participating in cell-cell adhesion and cell-surface signalling
62	CD62L	L-selectin	Lymphocytes	Acts as a homing receptor for lymphocytes
64	CD64	FcγRI	Monocyte/Macrophages	Used as a marker of Macrophage differentiation
123	CD123	IL3 receptor	Pluripotent progenitor cells	Marker for acute myeloid leukaemia
163	CD163	M130, GHI/61, RM3/1	Monocyte/Macrophages	High affinity scavenger receptor for haemoglobin-haptoglobin complex
235	CD235a	Glycophorin A	Erythrocytes	Major sialoglycoproteins of human erythrocyte membrane determining blood groups
335	CD335	Natural cytotoxicity triggering receptor 1	NK Cells	Involved in natural killer cell cytotoxicity

Table 9.3: Table of Cluster of Differentiation Antigens. Presents are the commonly used CD nomenclature for the antigens referred to in this thesis. Given are the alternative names, predominant cell of expression and their function.

9.4   Ethics Approval for Healthy Volunteers

University Ethics Sub-Committee for Medicine and Biological Sciences

31/08/2016

Ethics Reference: 8455-ahg5-cardiovascularsciences

TO:
Name of Researcher Applicant: Alison Goodall
Department: Cardiovascular Studies
Research Project Title: How do platelets induce foam cell formation

Dear Alison Goodall,

RE: Ethics review of Research Study application

The University Ethics Sub-Committee for Medicine and Biological Sciences has reviewed and discussed the above application.

1.   Ethical opinion

The Sub-Committee grants ethical approval to the above research project on the basis described in the application form and supporting documentation, subject to the conditions specified below.

2.   Summary of ethics review discussion

The Committee noted the following issues:
In the review process it was noted that this application is very similar to another (8545) that has recently been reviewed. The two should be considered separate from an ethical point of view and donors whose blood is used for both studies should be given the two sets of information sheets and sign the two consent forms.

3.   General conditions of the ethical approval

The ethics approval is subject to the following general conditions being met prior to the start of the project:

As the Principal Investigator, you are expected to deliver the research project in accordance with the University's policies and procedures, which includes the University's Research Code of Conduct and the University's Research Ethics Policy.

If relevant, management permission or approval (gate keeper role) must be obtained from host organisation prior to the start of the study at the site concerned.

4.   Reporting requirements after ethical approval

You are expected to notify the Sub-Committee about:
- Significant amendments to the project
- Serious breaches of the protocol
- Annual progress reports
- Notifying the end of the study

5.   Use of application information

Details from your ethics application will be stored on the University Ethics Online System. With your permission, the Sub-Committee may wish to use parts of the application in an anonymised format for training or sharing best practice. Please let me know if you do not want the application details to be used in this manner.

Best wishes for the success of this research project.

Yours sincerely,

Dr. Chris Talbot
Chair

9.5 HRA Approval

NHS
Health Research Authority

Professor Alison Goodall
University of Leicester
Groby Road
Leicester
LE3 9QP

Email: hra.approval@nhs.net

24 March 2017

Dear Professor Goodall

Letter of HRA Approval

Study title:	Investigation of the effect of Myocardial Infarction on Platelet-Induced Monocyte Phenotype and Foam Cell Formation (FOAMI Study)
IRAS project ID:	214176
Protocol number:	0600
REC reference:	17/WM/0031
Sponsor	University of Leicester

I am pleased to confirm that **HRA Approval** has been given for the above referenced study, on the basis described in the application form, protocol, supporting documentation and any clarifications noted in this letter.

Participation of NHS Organisations in England

The sponsor should now provide a copy of this letter to all participating NHS organisations in England.

Appendix B provides important information for sponsors and participating NHS organisations in England for arranging and confirming capacity and capability. Please read *Appendix B* carefully, in particular the following sections:

- *Participating NHS organisations in England* – this clarifies the types of participating organisations in the study and whether or not all organisations will be undertaking the same activities
- *Confirmation of capacity and capability* - this confirms whether or not each type of participating NHS organisation in England is expected to give formal confirmation of capacity and capability. Where formal confirmation is not expected, the section also provides details on the time limit given to participating organisations to opt out of the study, or request additional time, before their participation is assumed.
- *Allocation of responsibilities and rights are agreed and documented (4.1 of HRA assessment criteria)* - this provides detail on the form of agreement to be used in the study to confirm capacity and capability, where applicable.

Further information on funding, HR processes, and compliance with HRA criteria and standards is also provided.

Page 1 of 8

IRAS project ID	214176

It is critical that you involve both the research management function (e.g. R&D office) supporting each organisation and the local research team (where there is one) in setting up your study. Contact details and further information about working with the research management function for each organisation can be accessed from www.hra.nhs.uk/hra-approval.

Appendices

The HRA Approval letter contains the following appendices:

- A – List of documents reviewed during HRA assessment
- B – Summary of HRA assessment

After HRA Approval

The document *"After Ethical Review – guidance for sponsors and investigators"*, issued with your REC favourable opinion, gives detailed guidance on reporting expectations for studies, including:

- Registration of research
- Notifying amendments
- Notifying the end of the study

The HRA website also provides guidance on these topics, and is updated in the light of changes in reporting expectations or procedures.

In addition to the guidance in the above, please note the following:

- HRA Approval applies for the duration of your REC favourable opinion, unless otherwise notified in writing by the HRA.
- Substantial amendments should be submitted directly to the Research Ethics Committee, as detailed in the *After Ethical Review* document. Non-substantial amendments should be submitted for review by the HRA using the form provided on the HRA website, and emailed to hra.amendments@nhs.net.
- The HRA will categorise amendments (substantial and non-substantial) and issue confirmation of continued HRA Approval. Further details can be found on the HRA website.

Scope

HRA Approval provides an approval for research involving patients or staff in NHS organisations in England.

If your study involves NHS organisations in other countries in the UK, please contact the relevant national coordinating functions for support and advice. Further information can be found at http://www.hra.nhs.uk/resources/applying-for-reviews/nhs-hsc-rd-review/.

If there are participating non-NHS organisations, local agreement should be obtained in accordance with the procedures of the local participating non-NHS organisation.

User Feedback

The Health Research Authority is continually striving to provide a high quality service to all applicants and sponsors. You are invited to give your view of the service you have received and the application

IRAS project ID	214176

procedure. If you wish to make your views known please use the feedback form available on the HRA website: http://www.hra.nhs.uk/about-the-hra/governance/quality-assurance/.

HRA Training
We are pleased to welcome researchers and research management staff at our training days – see details at http://www.hra.nhs.uk/hra-training/

Your IRAS project ID is **214176**. Please quote this on all correspondence.

Yours sincerely

Michael Pate
Assessor

Email: hra.approval@nhs.net

Copy to: *Dr Diane Delahooke – University of Leicester – Sponsor contact*
Mrs Carolyn Maloney - University Hospitals of Leicester NHS Trust – Lead NHS R&D contact
Dr Sameer Kurmani – University of Leicester – PhD student.

IRAS project ID	214176

Appendix A - List of Documents

The final document set assessed and approved by HRA Approval is listed below.

Document	Version	Date
Contract/Study Agreement [Personal Indemnity Insurance]	v1.0	29 July 2016
Costing template (commercial projects) [Research Cost Estimate]	v1.0	21 November 2016
Covering letter on headed paper [Covering Letter]	v1.0	21 November 2016
Evidence of Sponsor insurance or indemnity (non NHS Sponsors only) [Clinical Trials Insurance]	v1.0	29 July 2016
GP/consultant information sheets or letters [Letter to GP]	v1.0	21 November 2016
Interview schedules or topic guides for participants [Case Record File]	v1.0	21 November 2016
IRAS Application Form [IRAS_Form_04012017]		04 January 2017
Letter from funder [BHF Award Confirmation]	v1.0	22 July 2014
Letter from sponsor [Confirmation of sponsorship]	v1.0	22 November 2016
Other [Recruitment Email]	v1.0	02 December 2016
Other [Recruitment Poster]	v1.0	02 December 2016
Other [Statement of Activities]	1	23 March 2017
Other [Schedule of Events]	1	23 March 2017
Participant consent form [Consent Form]	v2.0	30 January 2017
Participant information sheet (PIS) [Patient Information Sheet]	v2.0	30 January 2017
Referee's report or other scientific critique report [Peer Review-Prof McCann]	v1.0	25 October 2016
Referee's report or other scientific critique report [Peer Review-Prof Squire]	v1.0	24 October 2016
Research protocol or project proposal [Protocol]	v2.0	30 January 2017
Summary CV for Chief Investigator (CI) [Prof Goodall Short CV]	v1.0	26 October 2016
Summary CV for student [Kurmani CV]	N/A	29 November 2016

IRAS project ID	214176

Appendix B - Summary of HRA Assessment

This appendix provides assurance to you, the sponsor and the NHS in England that the study, as reviewed for HRA Approval, is compliant with relevant standards. It also provides information and clarification, where appropriate, to participating NHS organisations in England to assist in assessing and arranging capacity and capability.

For information on how the sponsor should be working with participating NHS organisations in England, please refer to the, *participating NHS organisations, capacity and capability* and *Allocation of responsibilities and rights are agreed and documented (4.1 of HRA assessment criteria)* sections in this appendix.

The following person is the sponsor contact for the purpose of addressing participating organisation questions relating to the study:

Name: Dr Diane Delahooke
Tel: 0116 258 4099
Email: uolsponsor@le.ac.uk

HRA assessment criteria

Section	HRA Assessment Criteria	Compliant with Standards	Comments
1.1	IRAS application completed correctly	Yes	No comments
2.1	Participant information/consent documents and consent process	Yes	Dr Kurmani agreed that verbal consent would be taken by the referring clinician for him to access the participant notes to screen for eligibility. Dr Kurmani would then approach eligible patients, following screening, and take consent. A record of the verbal consent should be placed in the medical notes.
3.1	Protocol assessment	Yes	Clinical staff will have been primed by use of the poster and email as to the criteria for study involvement. The poster will be placed on messages boards in the Coronary Care Unit and Clinical Decisions Unit.
4.1	Allocation of responsibilities	Yes	A Statement of Activities will form the

IRAS project ID	214176

Section	HRA Assessment Criteria	Compliant with Standards	Comments
	and rights are agreed and documented		agreement between the Sponsor and participating site.
4.2	Insurance/indemnity arrangements assessed	Yes	Where applicable, independent contractors (e.g. General Practitioners) should ensure that the professional indemnity provided by their medical defence organisation covers the activities expected of them for this research study
4.3	Financial arrangements assessed	Yes	The study is funded by a BHF fellowship award to Dr Kurmani. There are no funds to the participating site.
5.1	Compliance with the Data Protection Act and data security issues assessed	Yes	No comments
5.2	CTIMPS – Arrangements for compliance with the Clinical Trials Regulations assessed	Not Applicable	No comments
5.3	Compliance with any applicable laws or regulations	Yes	No comments
6.1	NHS Research Ethics Committee favourable opinion received for applicable studies	Yes	No comments
6.2	CTIMPS – Clinical Trials Authorisation (CTA) letter received	Not Applicable	No comments
6.3	Devices – MHRA notice of no objection received	Not Applicable	No comments
6.4	Other regulatory approvals and authorisations received	Yes	Samples will be put into long-term storage in the licensed tissue bank at Glenfield Hospital with licence number 11011.

IRAS project ID	214176

Participating NHS Organisations in England

This provides detail on the types of participating NHS organisations in the study and a statement as to whether the activities at all organisations are the same or different.

This is a single site study where that site is conducting all activities as per the protocol; therefore, one site type.

The Chief Investigator or sponsor should share relevant study documents with participating NHS organisations in England in order to put arrangements in place to deliver the study. The documents should be sent to both the local study team, where applicable, and the office providing the research management function at the participating organisation. For NIHR CRN Portfolio studies, the Local LCRN contact should also be copied into this correspondence. For further guidance on working with participating NHS organisations please see the HRA website.

If chief investigators, sponsors or principal investigators are asked to complete site level forms for participating NHS organisations in England which are not provided in IRAS or on the HRA website, the chief investigator, sponsor or principal investigator should notify the HRA immediately at hra.approval@nhs.net. The HRA will work with these organisations to achieve a consistent approach to information provision.

Confirmation of Capacity and Capability

This describes whether formal confirmation of capacity and capability is expected from participating NHS organisations in England.

Participating NHS organisations in England will be expected to formally confirm their capacity and capability to host this research.

- Following issue of this letter, participating NHS organisations in England may now confirm to the sponsor their capacity and capability to host this research, when ready to do so. How capacity and capacity will be confirmed is detailed in the *Allocation of responsibilities and rights are agreed and documented (4.1 of HRA assessment criteria)* section of this appendix.
- The Assessing, Arranging, and Confirming document on the HRA website provides further information for the sponsor and NHS organisations on assessing, arranging and confirming capacity and capability.

IRAS project ID	214176

Principal Investigator Suitability

This confirms whether the sponsor position on whether a PI, LC or neither should be in place is correct for each type of participating NHS organisation in England and the minimum expectations for education, training and experience that PIs should meet (where applicable).

A local Principal Investigator should be in place at the participating site.

The Sponsor expects the Principal Investigator to have up-to-date GCP training.

GCP training is not a generic training expectation, in line with the HRA statement on training expectations.

HR Good Practice Resource Pack Expectations

This confirms the HR Good Practice Resource Pack expectations for the study and the pre-engagement checks that should and should not be undertaken

All research activity will be conducted by researchers who hold a contract with the single participating site. Therefore, no other contracts are required.

Other Information to Aid Study Set-up

This details any other information that may be helpful to sponsors and participating NHS organisations in England to aid study set-up.

- The applicant has indicated that they do not intend to apply for inclusion on the NIHR CRN Portfolio.

9.6 Research Ethics Committee Approval

REISSUE 22.02.2017

NHS
Health Research Authority

West Midlands - Edgbaston Research Ethics Committee
The Old Chapel
Royal Standard Place
Nottingham
NG1 6FS

> **Please note:** This is the favourable opinion of the REC only and does not allow you to start your study at NHS sites in England until you receive HRA Approval

14 February 2017

Professor Alison Goodall
University of Leicester
Groby Road
Leicester
LE3 9QP

Dear Professor Goodall

Study title:	Investigation of the effect of Myocardial Infarction on Platelet-Induced Monocyte Phenotype and Foam Cell Formation (FOAMI Study)
REC reference:	17/WM/0031
Protocol number:	0600
IRAS project ID:	214176

Thank you for your letter of 9 February 2017, responding to the Committee's request for further information on the above research and submitting revised documentation.

The further information has been considered on behalf of the Committee by the Chair.

We plan to publish your research summary wording for the above study on the HRA website, together with your contact details. Publication will be no earlier than three months from the date of this opinion letter. Should you wish to provide a substitute contact point, require further information, or wish to make a request to postpone publication, please contact hra.studyregistration@nhs.net outlining the reasons for your request.

Confirmation of ethical opinion

REISSUE 22.02.2017

On behalf of the Committee, I am pleased to confirm a favourable ethical opinion for the above research on the basis described in the application form, protocol and supporting documentation as revised, subject to the conditions specified below.

Conditions of the favourable opinion

The REC favourable opinion is subject to the following conditions being met prior to the start of the study.

Management permission must be obtained from each host organisation prior to the start of the study at the site concerned.

Management permission should be sought from all NHS organisations involved in the study in accordance with NHS research governance arrangements. Each NHS organisation must confirm through the signing of agreements and/or other documents that it has given permission for the research to proceed (except where explicitly specified otherwise).

Guidance on applying for NHS permission for research is available in the Integrated Research Application System, www.hra.nhs.uk or at http://www.rdforum.nhs.uk.

Where a NHS organisation's role in the study is limited to identifying and referring potential participants to research sites ("participant identification centre"), guidance should be sought from the R&D office on the information it requires to give permission for this activity.

For non-NHS sites, site management permission should be obtained in accordance with the procedures of the relevant host organisation.

Sponsors are not required to notify the Committee of management permissions from host organisations

Registration of Clinical Trials

All clinical trials (defined as the first four categories on the IRAS filter page) must be registered on a publically accessible database within 6 weeks of recruitment of the first participant (for medical device studies, within the timeline determined by the current registration and publication trees).

There is no requirement to separately notify the REC but you should do so at the earliest opportunity e.g. when submitting an amendment. We will audit the registration details as part of the annual progress reporting process.

To ensure transparency in research, we strongly recommend that all research is registered but for non-clinical trials this is not currently mandatory.

If a sponsor wishes to request a deferral for study registration within the required timeframe, they should contact hra.studyregistration@nhs.net. The expectation is that all clinical trials will be registered, however, in exceptional circumstances non registration may be permissible with prior agreement from the HRA. Guidance on where to register is provided on the HRA website.

REISSUE 22.02.2017

It is the responsibility of the sponsor to ensure that all the conditions are complied with before the start of the study or its initiation at a particular site (as applicable).

Ethical review of research sites

NHS sites

The favourable opinion applies to all NHS sites taking part in the study, subject to management permission being obtained from the NHS/HSC R&D office prior to the start of the study (see "Conditions of the favourable opinion" below).

Approved documents

The final list of documents reviewed and approved by the Committee is as follows:

Document	Version	Date
Contract/Study Agreement [Personal Indemnity Insurance]	v1.0	29 July 2016
Covering letter on headed paper [Covering Letter]	v1.0	21 November 2016
Evidence of Sponsor insurance or indemnity (non NHS Sponsors only) [Clinical Trials Insurance]	v1.0	29 July 2016
GP/consultant information sheets or letters [Letter to GP]	v1.0	21 November 2016
Interview schedules or topic guides for participants [Case Record File]	v1.0	21 November 2016
IRAS Application Form [IRAS_Form_04012017]		04 January 2017
Letter from funder [BHF Award Confirmation]	v1.0	22 July 2014
Letter from sponsor [Confirmation of sponsorship]	v1.0	22 November 2016
Other [Recruitment Email]	v1.0	02 December 2016
Other [Recruitment Poster]	v1.0	02 December 2016
Participant consent form [Consent Form]	v2.0	30 January 2017
Participant information sheet (PIS) [Patient Information Sheet]	v2.0	30 January 2017
Referee's report or other scientific critique report [Peer Review-Prof McCann]	v1.0	25 October 2016
Referee's report or other scientific critique report [Peer Review-Prof Squire]	v1.0	24 October 2016
Research protocol or project proposal [Protocol]	v2.0	30 January 2017
Summary CV for Chief Investigator (CI) [Prof Goodall Short CV]	v1.0	26 October 2016
Summary CV for student [Kurmani CV]	N/A	29 November 2016

Statement of compliance

The Committee is constituted in accordance with the Governance Arrangements for Research Ethics Committees and complies fully with the Standard Operating Procedures for Research Ethics Committees in the UK.

After ethical review

Reporting requirements

The attached document *"After ethical review – guidance for researchers"* gives detailed guidance on reporting requirements for studies with a favourable opinion, including:

REISSUE 22.02.2017

- Notifying substantial amendments
- Adding new sites and investigators
- Notification of serious breaches of the protocol
- Progress and safety reports
- Notifying the end of the study

The HRA website also provides guidance on these topics, which is updated in the light of changes in reporting requirements or procedures.

User Feedback

The Health Research Authority is continually striving to provide a high quality service to all applicants and sponsors. You are invited to give your view of the service you have received and the application procedure. If you wish to make your views known please use the feedback form available on the HRA website:
http://www.hra.nhs.uk/about-the-hra/governance/quality-assurance/

HRA Training

We are pleased to welcome researchers and R&D staff at our training days – see details at
http://www.hra.nhs.uk/hra-training/

17/WM/0031	Please quote this number on all correspondence

With the Committee's best wishes for the success of this project.

Yours sincerely

pp. S. O'Neil

Mr Paul Hamilton
Chair

Email:NRESCommittee.WestMidlands-Edgbaston@nhs.net

Copy to: *Dr Diane Delahooke*
            Mrs Carolyn Maloney, University Hospitals of Leicester NHS Trust

Chapter 10:   References

Adorni, MP, F Zimetti, JT Billheimer, N Wang, DJ Rader, MC Phillips and GH Rothblat. The Roles of Different Pathways in the Release of Cholesterol from Macrophages. *J Lipid Res*.**2007**; **48: 2453-2462**

Ahnadi, CE, E Sabrinah Chapman, M Lepine, D Okrongly, N Pujol-Moix, A Hernandez, . . . AM Grant. Assessment of Platelet Activation in Several Different Anticoagulants by the Advia 120 Hematology System, Fluorescence Flow Cytometry, and Electron Microscopy. *Thromb Haemost*.**2003**; **90: 940-948**

Ahuja, V, SE Miller and DN Howell. Identification of Two Subpopulations of Rat Monocytes Expressing Disparate Molecular Forms and Quantities of Cd43. *Cell Immunol*.**1995**; **163: 59-69**

Aiello, RJ, PA Bourassa, S Lindsey, W Weng, E Natoli, BJ Rollins and PM Milos. Monocyte Chemoattractant Protein-1 Accelerates Atherosclerosis in Apolipoprotein E-Deficient Mice. *Arterioscler Thromb Vasc Biol*.**1999**; **19: 1518-1525**

Akbiyik, F, DM Ray, KF Gettings, N Blumberg, CW Francis and RP Phipps. Human Bone Marrow Megakaryocytes and Platelets Express Ppargamma, and Ppargamma Agonists Blunt Platelet Release of Cd40 Ligand and Thromboxanes. *Blood*.**2004**; **104: 1361-1368**

Ali, FY, SJ Davidson, LA Moraes, SL Traves, M Paul-Clark, D Bishop-Bailey, . . . JA Mitchell. Role of Nuclear Receptor Signaling in Platelets: Antithrombotic Effects of Pparbeta. *FASEB J*.**2006**; **20: 326-328**

Allender, S, C Foster, L Hutchinson and C Arambepola. Quantification of Urbanization in Relation to Chronic Diseases in Developing Countries: A Systematic Review. *J Urban Health*.**2008**; **85: 938-951**

Alon, R, RC Fuhlbrigge, EB Finger and TA Springer. Interactions through L-Selectin between Leukocytes and Adherent Leukocytes Nucleate Rolling Adhesions on Selectins and Vcam-1 in Shear Flow. *J Cell Biol*.**1996**; **135: 849-865**

Alonso-Lebrero, JL, JM Serrador, C Dominguez-Jimenez, O Barreiro, A Luque, MA del Pozo, . . . F Sanchez-Madrid. Polarization and Interaction of Adhesion Molecules P-Selectin Glycoprotein Ligand 1 and Intercellular Adhesion Molecule 3 with Moesin and Ezrin in Myeloid Cells. *Blood*.**2000**; **95: 2413-2419**

An, D, F Hao, F Zhang, W Kong, J Chun, X Xu and MZ Cui. Cd14 Is a Key Mediator of Both Lysophosphatidic Acid and Lipopolysaccharide Induction of Foam Cell Formation. *J Biol Chem*.**2017**; **292: 14391-14400**

An, G, H Wang, R Tang, T Yago, JM McDaniel, S McGee, . . . L Xia. P-Selectin Glycoprotein Ligand-1 Is Highly Expressed on Ly-6chi Monocytes and a Major Determinant for Ly-6chi Monocyte Recruitment to Sites of Atherosclerosis in Mice. *Circulation*.**2008**; **117: 3227-3237**

Ancuta, P, KY Liu, V Misra, VS Wacleche, A Gosselin, X Zhou and D Gabuzda. Transcriptional Profiling Reveals Developmental Relationship and Distinct Biological Functions of Cd16+ and Cd16- Monocyte Subsets. *BMC Genomics*.**2009**; **10: 403**

Ancuta, P, R Rao, A Moses, A Mehle, SK Shaw, FW Luscinskas and D Gabuzda. Fractalkine Preferentially Mediates Arrest and Migration of Cd16+ Monocytes. *J Exp Med*.**2003**; **197: 1701-1707**

Andreesen, R, W Brugger, C Scheibenbogen, M Kreutz, HG Leser, A Rehm and GW Lohr. Surface Phenotype Analysis of Human Monocyte to Macrophage Maturation. *J Leukoc Biol*.**1990**; **47: 490-497**

Argmann, CA, CH Van Den Diepstraten, CG Sawyez, JY Edwards, RA Hegele, BM Wolfe and MW Huff. Transforming Growth Factor-Beta1 Inhibits Macrophage Cholesteryl Ester Accumulation Induced by Native and Oxidized Vldl Remnants. *Arterioscler Thromb Vasc Biol*.**2001**; **21: 2011-2018**

Arya, M, JA Lopez, GM Romo, MA Cruz, A Kasirer-Friede, SJ Shattil and B Anvari. Glycoprotein Ib-Ix-Mediated Activation of Integrin Alpha(Iib)Beta(3): Effects of Receptor Clustering and Von Willebrand Factor Adhesion. *J Thromb Haemost*.**2003**; **1: 1150-1157**

Ashraf, MT and RH Khan. Mitogenic Lectins. *Med Sci Monit*.**2003**; **9: RA265-269**

Asselin, J, JM Gibbins, M Achison, YH Lee, LF Morton, RW Farndale, . . . SP Watson. A Collagen-Like Peptide Stimulates Tyrosine Phosphorylation of Syk and Phospholipase C Gamma2 in Platelets Independent of the Integrin Alpha2beta1. *Blood*.**1997**; **89: 1235-1242**

Auffray, C, D Fogg, M Garfa, G Elain, O Join-Lambert, S Kayal, . . . F Geissmann. Monitoring of Blood Vessels and Tissues by a Population of Monocytes with Patrolling Behavior. *Science*.**2007**; **317: 666-670**

Auffray, C, MH Sieweke and F Geissmann. Blood Monocytes: Development, Heterogeneity, and Relationship with Dendritic Cells. *Annu Rev Immunol*.**2009**; **27: 669-692**

Aursnes, I, K Gjesdal and U Abildgaard. Platelet Aggregation Induced by Adp from Unsheared Erythrocytes at Physiological Ca++-Concentration. *Br J Haematol*.**1981**; **47: 149-152**

Badrnya, S, WC Schrottmaier, JB Kral, KC Yaiw, I Volf, G Schabbauer, . . . A Assinger. Platelets Mediate Oxidized Low-Density Lipoprotein-Induced Monocyte Extravasation and Foam Cell Formation. *Arterioscler Thromb Vasc Biol*.**2014**; **34: 571-580**

Barczyk, M, S Carracedo and D Gullberg. Integrins. *Cell Tissue Res*.**2010**; **339: 269-280**

Barreiro, O, M Yanez-Mo, JM Serrador, MC Montoya, M Vicente-Manzanares, R Tejedor, . . . F Sanchez-Madrid. Dynamic Interaction of Vcam-1 and Icam-1 with Moesin and Ezrin in a Novel Endothelial Docking Structure for Adherent Leukocytes. *J Cell Biol*.**2002**; **157: 1233-1245**

Battinelli, EM, BA Markens and JE Italiano, Jr. Release of Angiogenesis Regulatory Proteins from Platelet Alpha Granules: Modulation of Physiologic and Pathologic Angiogenesis. *Blood*.**2011**; **118: 1359-1369**

Bazil, V and JL Strominger. Shedding as a Mechanism of Down-Modulation of Cd14 on Stimulated Human Monocytes. *J Immunol*.**1991**; **147: 1567-1574**

Belge, KU, F Dayyani, A Horelt, M Siedlar, M Frankenberger, B Frankenberger, . . . L Ziegler-Heitbrock. The Proinflammatory Cd14+Cd16+Dr++ Monocytes Are a Major Source of Tnf. *J Immunol*.**2002**; **168: 3536-3542**

Bennett, MR, S Sinha and GK Owens. Vascular Smooth Muscle Cells in Atherosclerosis. *Circ Res*.**2016**; **118: 692-702**

Bennett, S, SB Por, ER Stanley and SN Breit. Monocyte Proliferation in a Cytokine-Free, Serum-Free System. *J Immunol Methods*.**1992**; **153: 201-212**

Bennett, WE and ZA Cohn. The Isolation and Selected Properties of Blood Monocytes. *J Exp Med*.**1966**; **123: 145-160**

Berg, KE, I Ljungcrantz, L Andersson, C Bryngelsson, B Hedblad, GN Fredrikson, . . . H Bjorkbacka. Elevated Cd14++Cd16- Monocytes Predict Cardiovascular Events. *Circ Cardiovasc Genet*.**2012**; **5: 122-131**

Bergmeier, W, CL Piffath, T Goerge, SM Cifuni, ZM Ruggeri, J Ware and DD Wagner. The Role of Platelet Adhesion Receptor Gpibalpha Far Exceeds That of Its Main Ligand, Von Willebrand Factor, in Arterial Thrombosis. *Proc Natl Acad Sci U S A*.**2006**; **103: 16900-16905**

Berisha, SZ, J Hsu, P Robinet and JD Smith. Transcriptome Analysis of Genes Regulated by Cholesterol Loading in Two Strains of Mouse Macrophages Associates Lysosome Pathway and Er Stress Response with Atherosclerosis Susceptibility. *PLoS One*.**2013**; **8: e65003**

Blann, AD, SK Nadar and GY Lip. The Adhesion Molecule P-Selectin and Cardiovascular Disease. *Eur Heart J*.**2003**; **24: 2166-2179**

Boring, L, J Gosling, M Cleary and IF Charo. Decreased Lesion Formation in Ccr2-/- Mice Reveals a Role for Chemokines in the Initiation of Atherosclerosis. *Nature*.**1998**; **394: 894-897**

Bottalico, LA, RE Wager, LB Agellon, RK Assoian and I Tabas. Transforming Growth Factor-Beta 1 Inhibits Scavenger Receptor Activity in Thp-1 Human Macrophages. *J Biol Chem*.**1991**; **266: 22866-22871**

Boudjeltia, KZ, D Brohee, P Piro, V Nuyens, J Ducobu, M Kherkofs, . . . M Vanhaeverbeek. Monocyte-Platelet Complexes on Cd14/Cd16 Monocyte Subsets: Relationship with Apoa-I Levels. A Preliminary Study. *Cardiovasc Pathol*.**2008**; **17: 285-288**

Boyette, LB, C Macedo, K Hadi, BD Elinoff, JT Walters, B Ramaswami, . . . DM Metes. Phenotype, Function, and Differentiation Potential of Human Monocyte Subsets. *PLoS One*.**2017**; **12: e0176460**

Boyle, JJ. Heme and Haemoglobin Direct Macrophage Mhem Phenotype and Counter Foam Cell Formation in Areas of Intraplaque Haemorrhage. *Curr Opin Lipidol*.**2012**; **23: 453-461**

Boyum, A. Isolation of Mononuclear Cells and Granulocytes from Human Blood. Isolation of Monuclear Cells by One Centrifugation, and of Granulocytes by Combining Centrifugation and Sedimentation at 1 G. *Scand J Clin Lab Invest Suppl*.**1968**; **97: 77-89**

Boyum, A. Isolation of Human Blood Monocytes with Nycodenz, a New Non-Ionic Iodinated Gradient Medium. *Scand J Immunol*.**1983**; **17: 429-436**

Bozza, FA, AM Shah, AS Weyrich and GA Zimmerman. Amicus or Adversary: Platelets in Lung Biology, Acute Injury, and Inflammation. *Am J Respir Cell Mol Biol*.**2009**; **40: 123-134**

Brach, MA, R Henschler, RH Mertelsmann and F Herrmann. Regulation of M-Csf Expression by M-Csf: Role of Protein Kinase C and Transcription Factor Nf Kappa B. *Pathobiology*.**1991**; **59: 284-288**

Bradfield, PF, C Scheiermann, S Nourshargh, C Ody, FW Luscinskas, GE Rainger, . . . BA Imhof. Jam-C Regulates Unidirectional Monocyte Transendothelial Migration in Inflammation. *Blood*.**2007**; **110: 2545-2555**

Brambilla, M, M Camera, D Colnago, G Marenzi, M De Metrio, PL Giesen, . . . E Tremoli. Tissue Factor in Patients with Acute Coronary Syndromes: Expression in Platelets, Leukocytes, and Platelet-Leukocyte Aggregates. *Arterioscler Thromb Vasc Biol*.**2008**; **28: 947-953**

Brandt, E, A Ludwig, F Petersen and HD Flad. Platelet-Derived Cxc Chemokines: Old Players in New Games. *Immunol Rev*.**2000**; **177: 204-216**

Brunham, LR, RR Singaraja, M Duong, JM Timmins, C Fievet, N Bissada, . . . MR Hayden. Tissue-Specific Roles of Abca1 Influence Susceptibility to Atherosclerosis. *Arterioscler Thromb Vasc Biol*.**2009**; **29: 548-554**

Burger, PC and DD Wagner. Platelet P-Selectin Facilitates Atherosclerotic Lesion Development. *Blood*.**2003**; **101: 2661-2666**

Burgess, B, K Naus, J Chan, V Hirsch-Reinshagen, G Tansley, L Matzke, . . . C Wellington. Overexpression of Human Abcg1 Does Not Affect Atherosclerosis in Fat-Fed Apoe-Deficient Mice. *Arterioscler Thromb Vasc Biol*.**2008**; **28: 1731-1737**

Burleigh, ME, VR Babaev, JA Oates, RC Harris, S Gautam, D Riendeau, . . . MF Linton. Cyclooxygenase-2 Promotes Early Atherosclerotic Lesion Formation in Ldl Receptor-Deficient Mice. *Circulation*.**2002**; **105: 1816-1823**

Calkin, AC and P Tontonoz. Transcriptional Integration of Metabolism by the Nuclear Sterol-Activated Receptors Lxr and Fxr. *Nat Rev Mol Cell Biol*.**2012**; **13: 213-224**

Carlin, LM, C Auffray and F Geissmann. Measuring Intravascular Migration of Mouse Ly6c(Low) Monocytes in Vivo Using Intravital Microscopy. *Curr Protoc Immunol*.**2013**; **Chapter 14: Unit 14 33 11-16**

Chamorro, S, C Revilla, B Alvarez, F Alonso, A Ezquerra and J Dominguez. Phenotypic and Functional Heterogeneity of Porcine Blood Monocytes and Its Relation with Maturation. *Immunology*.**2005**; **114: 63-71**

Chandler, AB and RA Hand. Phagocytized Platelets: A Source of Lipids in Human Thrombi and Atherosclerotic Plaques. *Science*.**1961**; **134: 946-947**

Chao, LC, E Soto, C Hong, A Ito, L Pei, A Chawla, . . . P Tontonoz. Bone Marrow Nr4a Expression Is Not a Dominant Factor in the Development of Atherosclerosis or Macrophage Polarization in Mice. *J Lipid Res*.**2013**; **54: 806-815**

Chawla, A, WA Boisvert, CH Lee, BA Laffitte, Y Barak, SB Joseph, . . . P Tontonoz. A Ppar Gamma-Lxr-Abca1 Pathway in Macrophages Is Involved in Cholesterol Efflux and Atherogenesis. *Mol Cell*.**2001**; **7: 161-171**

Chen, HC. Boyden Chamber Assay. *Methods Mol Biol*.**2005**; **294: 15-22**

Chen, M, M Kakutani, T Naruko, M Ueda, S Narumiya, T Masaki and T Sawamura. Activation-Dependent Surface Expression of Lox-1 in Human Platelets. *Biochem Biophys Res Commun*.**2001**; **282: 153-158**

Chen, M, W Li, N Wang, Y Zhu and X Wang. Ros and Nf-Kappab but Not Lxr Mediate Il-1beta Signaling for the Downregulation of Atp-Binding Cassette Transporter A1. *Am J Physiol Cell Physiol*.**2007**; **292: C1493-1501**

Chinetti-Gbaguidi, G, S Colin and B Staels. Macrophage Subsets in Atherosclerosis. *Nat Rev Cardiol*.**2015**; **12: 10-17**

Chinetti, G, S Lestavel, V Bocher, AT Remaley, B Neve, IP Torra, . . . B Staels. Ppar-Alpha and Ppar-Gamma Activators Induce Cholesterol Removal from Human Macrophage Foam Cells through Stimulation of the Abca1 Pathway. *Nat Med*.**2001**; **7: 53-58**

Chistiakov, DA, AA Melnichenko, VA Myasoedova, AV Grechko and AN Orekhov. Mechanisms of Foam Cell Formation in Atherosclerosis. *J Mol Med (Berl)*.**2017**; **95: 1153-1165**

Chronos, NA, DJ Wilson, SL Janes, RA Hutton, NP Buller and AH Goodall. Aspirin Does Not Affect the Flow Cytometric Detection of Fibrinogen Binding to, or Release of Alpha-Granules or Lysosomes from, Human Platelets. *Clin Sci (Lond)*.**1994**; **87: 575-580**

Collins, RG, R Velji, NV Guevara, MJ Hicks, L Chan and AL Beaudet. P-Selectin or Intercellular Adhesion Molecule (Icam)-1 Deficiency Substantially Protects against Atherosclerosis in Apolipoprotein E-Deficient Mice. *J Exp Med*.**2000**; **191: 189-194**

Conde-Vancells, J, E Rodriguez-Suarez, N Embade, D Gil, R Matthiesen, M Valle, . . . JM Falcon-Perez. Characterization and Comprehensive Proteome Profiling of Exosomes Secreted by Hepatocytes. *J Proteome Res*.**2008**; **7: 5157-5166**

Cros, J, N Cagnard, K Woollard, N Patey, SY Zhang, B Senechal, . . . F Geissmann. Human Cd14dim Monocytes Patrol and Sense Nucleic Acids and Viruses Via Tlr7 and Tlr8 Receptors. *Immunity*.**2010**; **33: 375-386**

Curtiss, LK, AS Black, Y Takagi and EF Plow. New Mechanism for Foam Cell Generation in Atherosclerotic Lesions. *J Clin Invest*.**1987**; **80: 367-373**

da Costa Martins, P, N van den Berk, LH Ulfman, L Koenderman, PL Hordijk and JJ Zwaginga. Platelet-Monocyte Complexes Support Monocyte Adhesion to Endothelium by Enhancing Secondary Tethering and Cluster Formation. *Arterioscler Thromb Vasc Biol*.**2004**; **24: 193-199**

Darabian, S, M Hormuz, MA Latif, S Pahlevan and MJ Budoff. The Role of Carotid Intimal Thickness Testing and Risk Prediction in the Development of Coronary Atherosclerosis. *Curr Atheroscler Rep*.**2013**; **15: 306**

Daub, K, H Langer, P Seizer, K Stellos, AE May, P Goyal, . . . M Gawaz. Platelets Induce Differentiation of Human Cd34+ Progenitor Cells into Foam Cells and Endothelial Cells. *FASEB J*.**2006**; **20: 2559-2561**

Davies, JQ and S Gordon. Isolation and Culture of Human Macrophages. *Methods Mol Biol*.**2005**; **290: 105-116**

de Almeida, MC, AC Silva, A Barral and M Barral Netto. A Simple Method for Human Peripheral Blood Monocyte Isolation. *Mem Inst Oswaldo Cruz*.**2000**; **95: 221-223**

de Baey, A, I Mende, G Riethmueller and PA Baeuerle. Phenotype and Function of Human Dendritic Cells Derived from M-Dc8(+) Monocytes. *Eur J Immunol*.**2001**; **31: 1646-1655**

de Bruijne-Admiraal, LG, PW Modderman, AE Von dem Borne and A Sonnenberg. P-Selectin Mediates Ca(2+)-Dependent Adhesion of Activated Platelets to Many Different Types of Leukocytes: Detection by Flow Cytometry. *Blood*.**1992**; **80: 134-142**

de Lemos, JA, DA Morrow, MA Blazing, P Jarolim, SD Wiviott, MS Sabatine, . . . E Braunwald. Serial Measurement of Monocyte Chemoattractant Protein-1 after Acute Coronary Syndromes: Results from the a to Z Trial. *J Am Coll Cardiol*.**2007**; **50: 2117-2124**

De Meyer, GR, DM De Cleen, S Cooper, MW Knaapen, DM Jans, W Martinet, . . . MM Kockx. Platelet Phagocytosis and Processing of Beta-Amyloid Precursor Protein as a Mechanism of Macrophage Activation in Atherosclerosis. *Circ Res*.**2002**; **90: 1197-1204**

Dean, M, Y Hamon and G Chimini. The Human Atp-Binding Cassette (Abc) Transporter Superfamily. *J Lipid Res*.**2001**; **42: 1007-1017**

Denis, C, N Methia, PS Frenette, H Rayburn, M Ullman-Cullere, RO Hynes and DD Wagner. A Mouse Model of Severe Von Willebrand Disease: Defects in Hemostasis and Thrombosis. *Proc Natl Acad Sci U S A*.**1998**; **95: 9524-9529**

Devlin, CM, G Kuriakose, E Hirsch and I Tabas. Genetic Alterations of Il-1 Receptor Antagonist in Mice Affect Plasma Cholesterol Level and Foam Cell Lesion Size. *Proc Natl Acad Sci U S A*.**2002**; **99: 6280-6285**

Dodge, JT, Jr., BG Brown, EL Bolson and HT Dodge. Lumen Diameter of Normal Human Coronary Arteries. Influence of Age, Sex, Anatomic Variation, and Left Ventricular Hypertrophy or Dilation. *Circulation*.**1992**; **86: 232-246**

Dong, ZM, AA Brown and DD Wagner. Prominent Role of P-Selectin in the Development of Advanced Atherosclerosis in Apoe-Deficient Mice. *Circulation*.**2000**; **101: 2290-2295**

Draude, G and RL Lorenz. Tgf-Beta1 Downregulates Cd36 and Scavenger Receptor a but Upregulates Lox-1 in Human Macrophages. *Am J Physiol Heart Circ Physiol*.**2000**; **278: H1042-1048**

Du, X, J Kumar, C Ferguson, TA Schulz, YS Ong, W Hong, . . . H Yang. A Role for Oxysterol-Binding Protein-Related Protein 5 in Endosomal Cholesterol Trafficking. *J Cell Biol*.**2011**; **192: 121-135**

Dubland, JA and GA Francis. So Much Cholesterol: The Unrecognized Importance of Smooth Muscle Cells in Atherosclerotic Foam Cell Formation. *Curr Opin Lipidol*.**2016**; **27: 155-161**

Dutta, P, G Courties, Y Wei, F Leuschner, R Gorbatov, CS Robbins, . . . M Nahrendorf. Myocardial Infarction Accelerates Atherosclerosis. *Nature*.**2012**; **487: 325-329**

Elgueta, R, MJ Benson, VC de Vries, A Wasiuk, Y Guo and RJ Noelle. Molecular Mechanism and Function of Cd40/Cd40l Engagement in the Immune System. *Immunol Rev*.**2009**; **229: 152-172**

Elwood, PC, AL Cochrane, ML Burr, PM Sweetnam, G Williams, E Welsby, . . . R Renton. A Randomized Controlled Trial of Acetyl Salicylic Acid in the Secondary Prevention of Mortality from Myocardial Infarction. *Br Med J*.**1974**; **1: 436-440**

Engelmann, B, C Kogl, R Kulschar and B Schaipp. Transfer of Phosphatidylcholine, Phosphatidylethanolamine and Sphingomyelin from Low- and High-Density Lipoprotein to Human Platelets. *Biochem J*.**1996**; **315 (Pt 3): 781-789**

Epple, LM, SG Griffiths, AM Dechkovskaia, NL Dusto, J White, RJ Ouellette, . . . MW Graner. Medulloblastoma Exosome Proteomics Yield Functional Roles for Extracellular Vesicles. *PLoS One*.**2012**; **7: e42064**

Escolar, G and JG White. The Platelet Open Canalicular System: A Final Common Pathway. *Blood Cells*.**1991**; **17: 467-485; discussion 486-495**

Farfan, P, J Lee, J Larios, P Sotelo, G Bu and MP Marzolo. A Sorting Nexin 17-Binding Domain within the Lrp1 Cytoplasmic Tail Mediates Receptor Recycling through the Basolateral Sorting Endosome. *Traffic*.**2013**; **14: 823-838**

Fazio, S, AS Major, LL Swift, LA Gleaves, M Accad, MF Linton and RV Farese, Jr. Increased Atherosclerosis in Ldl Receptor-Null Mice Lacking Acat1 in Macrophages. *J Clin Invest*.**2001**; **107: 163-171**

Feng, B, PM Yao, Y Li, CM Devlin, D Zhang, HP Harding, . . . I Tabas. The Endoplasmic Reticulum Is the Site of Cholesterol-Induced Cytotoxicity in Macrophages. *Nat Cell Biol*.**2003**; **5: 781-792**

Fernandes, LS, ID Conde, C Wayne Smith, GS Kansas, KR Snapp, N Bennet, . . . NS Kleiman. Platelet-Monocyte Complex Formation: Effect of Blocking Psgl-1 Alone, and in Combination with Alphaiibbeta3 and Alphambeta2, in Coronary Stenting. *Thromb Res*.**2003**; **111: 171-177**

Ferroni, P, FM Pulcinelli, L Lenti and PP Gazzaniga. Is Soluble P-Selectin Determination a More Reliable Marker of in Vivo Platelet Activation Than Cd62p Flow Cytometric Analysis? *Thromb Haemost*.**1999**; **81: 472-473**

Frangogiannis, NG. The Immune System and Cardiac Repair. *Pharmacol Res*.**2008**; **58: 88-111**

Fricke, I, D Mitchell, F Petersen, A Bohle, S Bulfone-Paus and S Brandau. Platelet Factor 4 in Conjunction with Il-4 Directs Differentiation of Human Monocytes into Specialized Antigen-Presenting Cells. *FASEB J*.**2004**; **18: 1588-1590**

Furman, MI, SE Benoit, MR Barnard, CR Valeri, ML Borbone, RC Becker, . . . AD Michelson. Increased Platelet Reactivity and Circulating Monocyte-Platelet Aggregates in Patients with Stable Coronary Artery Disease. *J Am Coll Cardiol*.**1998**; **31: 352-358**

Gadd, VL, PJ Patel, S Jose, L Horsfall, EE Powell and KM Irvine. Altered Peripheral Blood Monocyte Phenotype and Function in Chronic Liver Disease: Implications for Hepatic Recruitment and Systemic Inflammation. *PLoS One*.**2016**; **11: e0157771**

Garcia, BA, DM Smalley, H Cho, J Shabanowitz, K Ley and DF Hunt. The Platelet Microparticle Proteome. *J Proteome Res*.**2005**; **4: 1516-1521**

Gautier, EL, C Jakubzick and GJ Randolph. Regulation of the Migration and Survival of Monocyte Subsets by Chemokine Receptors and Its Relevance to Atherosclerosis. *Arterioscler Thromb Vasc Biol*.**2009**; **29: 1412-1418**

Gawaz, M, H Langer and AE May. Platelets in Inflammation and Atherogenesis. *J Clin Invest*.**2005**; **115: 3378-3384**

Gawaz, MP, JC Loftus, ML Bajt, MM Frojmovic, EF Plow and MH Ginsberg. Ligand Bridging Mediates Integrin Alpha Iib Beta 3 (Platelet Gpiib-Iiia) Dependent Homotypic and Heterotypic Cell-Cell Interactions. *J Clin Invest*.**1991**; **88: 1128-1134**

Geissmann, F, S Jung and DR Littman. Blood Monocytes Consist of Two Principal Subsets with Distinct Migratory Properties. *Immunity*.**2003**; **19: 71-82**

Gerszten, RE, EA Garcia-Zepeda, YC Lim, M Yoshida, HA Ding, MA Gimbrone, Jr., . . . A Rosenzweig. Mcp-1 and Il-8 Trigger Firm Adhesion of Monocytes to Vascular Endothelium under Flow Conditions. *Nature*.**1999**; **398: 718-723**

Ghosh, S and M Karin. Missing Pieces in the Nf-Kappab Puzzle. *Cell*.**2002**; **109 Suppl: S81-96**

Ghosh, S, RW St Clair and LL Rudel. Mobilization of Cytoplasmic Ce Droplets by Overexpression of Human Macrophage Cholesteryl Ester Hydrolase. *J Lipid Res*.**2003**; **44: 1833-1840**

Gkaliagkousi, E, V Corrigall, S Becker, P de Winter, A Shah, C Zamboulis, . . . A Ferro. Decreased Platelet Nitric Oxide Contributes to Increased Circulating Monocyte-Platelet Aggregates in Hypertension. *Eur Heart J*.**2009**; **30: 3048-3054**

Gleissner, CA, I Shaked, C Erbel, D Bockler, HA Katus and K Ley. Cxcl4 Downregulates the Atheroprotective Hemoglobin Receptor Cd163 in Human Macrophages. *Circ Res*.**2010**; **106: 203-211**

Gleissner, CA, I Shaked, KM Little and K Ley. Cxc Chemokine Ligand 4 Induces a Unique Transcriptome in Monocyte-Derived Macrophages. *J Immunol*.**2010**; **184: 4810-4818**

Goff, WL, WC Johnson, CR Wyatt and CW Cluff. Assessment of Bovine Mononuclear Phagocytes and Neutrophils for Induced L-Arginine-Dependent Nitric Oxide Production. *Vet Immunol Immunopathol*.**1996**; **55: 45-62**

Gremmel, T, CW Kopp, D Seidinger, GA Giurgea, R Koppensteiner, S Steiner and S Panzer. The Formation of Monocyte-Platelet Aggregates Is Independent of on-Treatment Residual Agonists'-Inducible Platelet Reactivity. *Atherosclerosis*.**2009**; **207: 608-613**

Grey, D, WN Erber, KM Saunders and JA Lown. Monocyte Activation in Platelet Concentrates. *Vox Sang*.**1998**; **75: 110-114**

Griffith, JW, CL Sokol and AD Luster. Chemokines and Chemokine Receptors: Positioning Cells for Host Defense and Immunity. *Annu Rev Immunol*.**2014**; **32: 659-702**

Han, J, DP Hajjar, JM Tauras, J Feng, AM Gotto, Jr. and AC Nicholson. Transforming Growth Factor-Beta1 (Tgf-Beta1) and Tgf-Beta2 Decrease Expression of Cd36, the Type B Scavenger Receptor, through Mitogen-Activated Protein Kinase Phosphorylation of Peroxisome Proliferator-Activated Receptor-Gamma. *J Biol Chem*.**2000**; **275: 1241-1246**

Hanna, RN, LM Carlin, HG Hubbeling, D Nackiewicz, AM Green, JA Punt, . . . CC Hedrick. The Transcription Factor Nr4a1 (Nur77) Controls Bone Marrow Differentiation and the Survival of Ly6c- Monocytes. *Nat Immunol*.**2011**; **12: 778-785**

Hanna, RN, I Shaked, HG Hubbeling, JA Punt, R Wu, E Herrley, . . . CC Hedrick. Nr4a1 (Nur77) Deletion Polarizes Macrophages toward an Inflammatory Phenotype and Increases Atherosclerosis. *Circ Res*.**2012**; **110: 416-427**

Hansson, GK, P Libby and I Tabas. Inflammation and Plaque Vulnerability. *J Intern Med*.**2015**; **278: 483-493**

Harder, T and K Simons. Clusters of Glycolipid and Glycosylphosphatidylinositol-Anchored Proteins in Lymphoid Cells: Accumulation of Actin Regulated by Local Tyrosine Phosphorylation. *Eur J Immunol*.**1999**; **29: 556-562**

Harding, SA, AJ Sommerfield, J Sarma, PJ Twomey, DE Newby, BM Frier and KA Fox. Increased Cd40 Ligand and Platelet-Monocyte Aggregates in Patients with Type 1 Diabetes Mellitus. *Atherosclerosis*.**2004**; **176: 321-325**

Haselmayer, P, L Grosse-Hovest, P von Landenberg, H Schild and MP Radsak. Trem-1 Ligand Expression on Platelets Enhances Neutrophil Activation. *Blood*.**2007**; **110: 1029-1035**

Hasko, G, EA Deitch, ZH Nemeth, DG Kuhel and C Szabo. Inhibitors of Atp-Binding Cassette Transporters Suppress Interleukin-12 P40 Production and Major Histocompatibility Complex Ii up-Regulation in Macrophages. *J Pharmacol Exp Ther*.**2002**; **301: 103-110**

Hayashida, K, N Kume, M Minami, H Kataoka, M Morimoto and T Kita. Peroxisome Proliferator-Activated Receptor a Ligands Increase Lectin-Like Oxidized Low Density Lipoprotein Receptor-1 Expression in Vascular Endothelial Cells. *Ann N Y Acad Sci*.**2001**; **947: 370-372**

Heidt, T, HB Sager, G Courties, P Dutta, Y Iwamoto, A Zaltsman, . . . M Nahrendorf. Chronic Variable Stress Activates Hematopoietic Stem Cells. *Nat Med*.**2014**; **20: 754-758**

Heijnen, HF, AE Schiel, R Fijnheer, HJ Geuze and JJ Sixma. Activated Platelets Release Two Types of Membrane Vesicles: Microvesicles by Surface Shedding and Exosomes Derived from Exocytosis of Multivesicular Bodies and Alpha-Granules. *Blood*.**1999**; **94: 3791-3799**

Hettinger, J, DM Richards, J Hansson, MM Barra, AC Joschko, J Krijgsveld and M Feuerer. Origin of Monocytes and Macrophages in a Committed Progenitor. *Nat Immunol*.**2013**; **14: 821-830**

Hidalgo, A, AJ Peired, MK Wild, D Vestweber and PS Frenette. Complete Identification of E-Selectin Ligands on Neutrophils Reveals Distinct Functions of Psgl-1, Esl-1, and Cd44. *Immunity*.**2007**; **26: 477-489**

Hidari, KI, AS Weyrich, GA Zimmerman and RP McEver. Engagement of P-Selectin Glycoprotein Ligand-1 Enhances Tyrosine Phosphorylation and Activates Mitogen-Activated Protein Kinases in Human Neutrophils. *J Biol Chem*.**1997**; **272: 28750-28756**

Hollopeter, G, HM Jantzen, D Vincent, G Li, L England, V Ramakrishnan, . . . PB Conley. Identification of the Platelet Adp Receptor Targeted by Antithrombotic Drugs. *Nature*.**2001**; **409: 202-207**

Horne, BD, JL Anderson, JM John, A Weaver, TL Bair, KR Jensen, . . . G Intermountain Heart Collaborative Study. Which White Blood Cell Subtypes Predict Increased Cardiovascular Risk? *J Am Coll Cardiol*.**2005**; **45: 1638-1643**

Hristov, M, W Erl and PC Weber. Endothelial Progenitor Cells: Isolation and Characterization. *Trends Cardiovasc Med*.**2003**; **13: 201-206**

Huang, JS, SK Ramamurthy, X Lin and GC Le Breton. Cell Signalling through Thromboxane A2 Receptors. *Cell Signal*.**2004**; **16: 521-533**

Huo, Y, A Schober, SB Forlow, DF Smith, MC Hyman, S Jung, . . . K Ley. Circulating Activated Platelets Exacerbate Atherosclerosis in Mice Deficient in Apolipoprotein E. *Nat Med*.**2003**; **9: 61-67**

Ibeas, E, L Fuentes, R Martin, M Hernandez and ML Nieto. Secreted Phospholipase A2 Type Iia as a Mediator Connecting Innate and Adaptive Immunity: New Role in Atherosclerosis. *Cardiovasc Res*.**2009**; **81: 54-63**

Ingersoll, MA, R Spanbroek, C Lottaz, EL Gautier, M Frankenberger, R Hoffmann, . . . GJ Randolph. Comparison of Gene Expression Profiles between Human and Mouse Monocyte Subsets. *Blood*.**2010**; **115: e10-19**

Irvine, KM, MR Andrews, MA Fernandez-Rojo, K Schroder, CJ Burns, S Su, . . . MJ Sweet. Colony-Stimulating Factor-1 (Csf-1) Delivers a Proatherogenic Signal to Human Macrophages. *J Leukoc Biol*.**2009**; **85: 278-288**

Jacoby, RC, JT Owings, J Holmes, FD Battistella, RC Gosselin and TG Paglieroni. Platelet Activation and Function after Trauma. *J Trauma*.**2001**; **51: 639-647**

Jacquelin, S, F Licata, K Dorgham, P Hermand, L Poupel, E Guyon, . . . A Boissonnas. Cx3cr1 Reduces Ly6chigh-Monocyte Motility within and Release from the Bone Marrow after Chemotherapy in Mice. *Blood*.**2013**; **122: 674-683**

Jaiswal, R, F Luk, J Gong, JM Mathys, GE Grau and M Bebawy. Microparticle Conferred Microrna Profiles--Implications in the Transfer and Dominance of Cancer Traits. *Mol Cancer*.**2012**; **11: 37**

Jakubzick, C, EL Gautier, SL Gibbings, DK Sojka, A Schlitzer, TE Johnson, . . . GJ Randolph. Minimal Differentiation of Classical Monocytes as They Survey Steady-State Tissues and Transport Antigen to Lymph Nodes. *Immunity*.**2013**; **39: 599-610**

Jandrot-Perrus, M, S Busfield, AH Lagrue, X Xiong, N Debili, T Chickering, . . . JL Villeval. Cloning, Characterization, and Functional Studies of Human and Mouse Glycoprotein Vi: A Platelet-Specific Collagen Receptor from the Immunoglobulin Superfamily. *Blood*.**2000**; **96: 1798-1807**

Janeway, CA, Jr. and R Medzhitov. Innate Immune Recognition. *Annu Rev Immunol*.**2002**; **20: 197-216**

Japp, AG, R Chelliah, L Tattersall, NN Lang, X Meng, K Weisel, . . . DE Newby. Effect of Psi-697, a Novel P-Selectin Inhibitor, on Platelet-Monocyte Aggregate Formation in Humans. *J Am Heart Assoc*.**2013**; **2: e006007**

Jenkins, SJ, D Ruckerl, PC Cook, LH Jones, FD Finkelman, N van Rooijen, . . . JE Allen. Local Macrophage Proliferation, Rather Than Recruitment from the Blood, Is a Signature of Th2 Inflammation. *Science*.**2011**; **332: 1284-1288**

Jernberg, T, P Hasvold, M Henriksson, H Hjelm, M Thuresson and M Janzon. Cardiovascular Risk in Post-Myocardial Infarction Patients: Nationwide Real World Data Demonstrate the Importance of a Long-Term Perspective. *Eur Heart J*.**2015**; **36: 1163-1170**

Jin, J, JL Daniel and SP Kunapuli. Molecular Basis for Adp-Induced Platelet Activation. Ii. The P2y1 Receptor Mediates Adp-Induced Intracellular Calcium Mobilization and Shape Change in Platelets. *J Biol Chem*.**1998**; **273: 2030-2034**

Jin, M, G Drwal, T Bourgeois, J Saltz and HM Wu. Distinct Proteome Features of Plasma Microparticles. *Proteomics*.**2005**; **5: 1940-1952**

Jung, U, KE Norman, K Scharffetter-Kochanek, AL Beaudet and K Ley. Transit Time of Leukocytes Rolling through Venules Controls Cytokine-Induced Inflammatory Cell Recruitment in Vivo. *J Clin Invest*.**1998**; **102: 1526-1533**

Junt, T, H Schulze, Z Chen, S Massberg, T Goerge, A Krueger, . . . UH von Andrian. Dynamic Visualization of Thrombopoiesis within Bone Marrow. *Science*.**2007**; **317: 1767-1770**

Kaplan, JE and TM Saba. Platelet Removal from the Circulation by the Liver and Spleen. *Am J Physiol*.**1978**; **235: H314-320**

Karnovsky, ML. Metchnikoff in Messina: A Century of Studies on Phagocytosis. *N Engl J Med*.**1981**; **304: 1178-1180**

Keating, FK, HL Dauerman, DA Whitaker, BE Sobel and DJ Schneider. Increased Expression of Platelet P-Selectin and Formation of Platelet-Leukocyte Aggregates in Blood from Patients Treated with Unfractionated Heparin Plus Eptifibatide Compared with Bivalirudin. *Thromb Res*.**2006**; **118: 361-369**

Keating, FK, MK Fung and DJ Schneider. Induction of Platelet White Blood Cell (Wbc) Aggregate Formation by Platelets and Wbcs in Red Blood Cell Units. *Transfusion*.**2008**; **48: 1099-1105**

Khallou-Laschet, J, A Varthaman, G Fornasa, C Compain, AT Gaston, M Clement, . . . G Caligiuri. Macrophage Plasticity in Experimental Atherosclerosis. *PLoS One*.**2010**; **5: e8852**

Kim, WK, Y Sun, H Do, P Autissier, EF Halpern, M Piatak, Jr., . . . K Williams. Monocyte Heterogeneity Underlying Phenotypic Changes in Monocytes According to Siv Disease Stage. *J Leukoc Biol*.**2010**; **87: 557-567**

Kirkland, TN and S Viriyakosol. Structure-Function Analysis of Soluble and Membrane-Bound Cd14. *Prog Clin Biol Res*.**1998**; **397: 79-87**

Kisucka, J, AK Chauhan, BQ Zhao, IS Patten, A Yesilaltay, M Krieger and DD Wagner. Elevated Levels of Soluble P-Selectin in Mice Alter Blood-Brain Barrier Function, Exacerbate Stroke, and Promote Atherosclerosis. *Blood*.**2009**; **113: 6015-6022**

Koivusalo, M, C Welch, H Hayashi, CC Scott, M Kim, T Alexander, . . . S Grinstein. Amiloride Inhibits Macropinocytosis by Lowering Submembranous Ph and Preventing Rac1 and Cdc42 Signaling. *J Cell Biol*.**2010**; **188: 547-563**

Koller, CA, GW King, PE Hurtubise, AL Sagone and AF LoBuglio. Characterization of Glass Adherent Human Mononuclear Cells. *J Immunol*.**1973**; **111: 1610-1612**

Kolodgie, FD, HK Gold, AP Burke, DR Fowler, HS Kruth, DK Weber, . . . R Virmani. Intraplaque Hemorrhage and Progression of Coronary Atheroma. *N Engl J Med*.**2003**; **349: 2316-2325**

Kruth, HS. Platelet-Mediated Cholesterol Accumulation in Cultured Aortic Smooth Muscle Cells. *Science*.**1985**; **227: 1243-1245**

Kubota, K, J Okazaki, O Louie, KC Kent and B Liu. Tgf-Beta Stimulates Collagen (I) in Vascular Smooth Muscle Cells Via a Short Element in the Proximal Collagen Promoter. *J Surg Res*.**2003**; **109: 43-50**

Kume, N, MI Cybulsky and MA Gimbrone, Jr. Lysophosphatidylcholine, a Component of Atherogenic Lipoproteins, Induces Mononuclear Leukocyte Adhesion Molecules in Cultured Human and Rabbit Arterial Endothelial Cells. *J Clin Invest*.**1992**; **90: 1138-1144**

Kunjathoor, VV, M Febbraio, EA Podrez, KJ Moore, L Andersson, S Koehn, . . . MW Freeman. Scavenger Receptors Class a-I/Ii and Cd36 Are the Principal Receptors Responsible for the Uptake of Modified Low Density Lipoprotein Leading to Lipid Loading in Macrophages. *J Biol Chem*.**2002**; **277: 49982-49988**

Landry, P, I Plante, DL Ouellet, MP Perron, G Rousseau and P Provost. Existence of a Microrna Pathway in Anucleate Platelets. *Nat Struct Mol Biol*.**2009**; **16: 961-966**

Landsman, L, L Bar-On, A Zernecke, KW Kim, R Krauthgamer, E Shagdarsuren, . . . S Jung. Cx3cr1 Is Required for Monocyte Homeostasis and Atherogenesis by Promoting Cell Survival. *Blood*.**2009**; **113: 963-972**

Larsen, E, T Palabrica, S Sajer, GE Gilbert, DD Wagner, BC Furie and B Furie. Padgem-Dependent Adhesion of Platelets to Monocytes and Neutrophils Is Mediated by a Lineage-Specific Carbohydrate, Lnf Iii (Cd15). *Cell*.**1990**; **63: 467-474**

Lee, CH, A Chawla, N Urbiztondo, D Liao, WA Boisvert, RM Evans and LK Curtiss. Transcriptional Repression of Atherogenic Inflammation: Modulation by Ppardelta. *Science*.**2003**; **302: 453-457**

Ley, K, C Laudanna, MI Cybulsky and S Nourshargh. Getting to the Site of Inflammation: The Leukocyte Adhesion Cascade Updated. *Nat Rev Immunol*.**2007**; **7: 678-689**

Li, AC, CJ Binder, A Gutierrez, KK Brown, CR Plotkin, JW Pattison, . . . CK Glass. Differential Inhibition of Macrophage Foam-Cell Formation and Atherosclerosis in Mice by Pparalpha, Beta/Delta, and Gamma. *J Clin Invest*.**2004**; **114: 1564-1576**

Li, G, C Chen, SD Laing, C Ballard, KC Biju, RL Reddick, . . . S Li. Hematopoietic Knockdown of Ppardelta Reduces Atherosclerosis in Ldlr-/- Mice. *Gene Ther*.**2016**; **23: 78-85**

Li, G, JM Sanders, MH Bevard, Z Sun, JW Chumley, EV Galkina, . . . IJ Sarembock. Cd40 Ligand Promotes Mac-1 Expression, Leukocyte Recruitment, and Neointima Formation after Vascular Injury. *Am J Pathol*.**2008**; **172: 1141-1152**

Libby, P and M Aikawa. Mechanisms of Plaque Stabilization with Statins. *Am J Cardiol*.**2003**; **91: 4B-8B**

Lievens, D and P von Hundelshausen. Platelets in Atherosclerosis. *Thromb Haemost*.**2011**; **106: 827-838**

Lindmark, E, T Tenno and A Siegbahn. Role of Platelet P-Selectin and Cd40 Ligand in the Induction of Monocytic Tissue Factor Expression. *Arterioscler Thromb Vasc Biol*.**2000**; **20: 2322-2328**

Lozano, R, M Naghavi, K Foreman, S Lim, K Shibuya, V Aboyans, . . . CJ Murray. Global and Regional Mortality from 235 Causes of Death for 20 Age Groups in 1990 and 2010: A Systematic Analysis for the Global Burden of Disease Study 2010. *Lancet*.**2013**; **380: 2095-2128**

Lusis, AJ. Atherosclerosis. *Nature*.**2000**; **407: 233-241**

Mahmood, SS, D Levy, RS Vasan and TJ Wang. The Framingham Heart Study and the Epidemiology of Cardiovascular Disease: A Historical Perspective. *Lancet*.**2014**; **383: 999-1008**

Makowski, L, JB Boord, K Maeda, VR Babaev, KT Uysal, MA Morgan, . . . MF Linton. Lack of Macrophage Fatty-Acid-Binding Protein Ap2 Protects Mice Deficient in Apolipoprotein E against Atherosclerosis. *Nat Med*.**2001**; **7: 699-705**

Manyonda, IT, AJ Soltys and FC Hay. A Critical Evaluation of the Magnetic Cell Sorter and Its Use in the Positive and Negative Selection of Cd45ro+ Cells. *J Immunol Methods*.**1992**; **149: 1-10**

Marcus, AJ, ST Silk, LB Safier and HL Ullman. Superoxide Production and Reducing Activity in Human Platelets. *J Clin Invest*.**1977**; **59: 149-158**

Martinez, FO, S Gordon, M Locati and A Mantovani. Transcriptional Profiling of the Human Monocyte-to-Macrophage Differentiation and Polarization: New Molecules and Patterns of Gene Expression. *J Immunol*.**2006**; **177: 7303-7311**

Maschberger, P, M Bauer, J Baumann-Siemons, KJ Zangl, EV Negrescu, AJ Reininger and W Siess. Mildly Oxidized Low Density Lipoprotein Rapidly Stimulates Via Activation of the Lysophosphatidic Acid Receptor Src Family and Syk Tyrosine Kinases and Ca2+ Influx in Human Platelets. *J Biol Chem*.**2000**; **275: 19159-19166**

Massberg, S, K Brand, S Gruner, S Page, E Muller, I Muller, . . . M Gawaz. A Critical Role of Platelet Adhesion in the Initiation of Atherosclerotic Lesion Formation. *J Exp Med*.**2002**; **196: 887-896**

Mathers, CD and D Loncar. Projections of Global Mortality and Burden of Disease from 2002 to 2030. *PLoS Med*.**2006**; **3: e442**

McEver, RP. Selectins: Initiators of Leucocyte Adhesion and Signalling at the Vascular Wall. *Cardiovasc Res*.**2015**; **107: 331-339**

Metcalfe, P, LM Williamson, CP Reutelingsperger, I Swann, WH Ouwehand and AH Goodall. Activation During Preparation of Therapeutic Platelets Affects Deterioration During Storage: A Comparative Flow Cytometric Study of Different Production Methods. *Br J Haematol*.**1997**; **98: 86-95**

Methe, H, JO Kim, S Kofler, M Weis, M Nabauer and J Koglin. Expansion of Circulating Toll-Like Receptor 4-Positive Monocytes in Patients with Acute Coronary Syndrome. *Circulation*.**2005**; **111: 2654-2661**

Michelsen, KS, MH Wong, PK Shah, W Zhang, J Yano, TM Doherty, . . . M Arditi. Lack of Toll-Like Receptor 4 or Myeloid Differentiation Factor 88 Reduces Atherosclerosis and Alters Plaque Phenotype in Mice Deficient in Apolipoprotein E. *Proc Natl Acad Sci U S A*.**2004**; **101: 10679-10684**

Michelson, AD, MR Barnard, HB Hechtman, H MacGregor, RJ Connolly, J Loscalzo and CR Valeri. In Vivo Tracking of Platelets: Circulating Degranulated Platelets Rapidly Lose Surface P-Selectin but Continue to Circulate and Function. *Proc Natl Acad Sci U S A*.**1996**; **93: 11877-11882**

Miller, YI, SH Choi, P Wiesner, L Fang, R Harkewicz, K Hartvigsen, . . . JL Witztum. Oxidation-Specific Epitopes Are Danger-Associated Molecular Patterns Recognized by Pattern Recognition Receptors of Innate Immunity. *Circ Res*.**2011**; **108: 235-248**

Misharin, AV, CM Cuda, R Saber, JD Turner, AK Gierut, GK Haines, 3rd, . . . H Perlman. Nonclassical Ly6c(-) Monocytes Drive the Development of Inflammatory Arthritis in Mice. *Cell Rep*.**2014**; **9: 591-604**

Mobley, JL, M Leininger, S Madore, TJ Baginski and R Renkiewicz. Genetic Evidence of a Functional Monocyte Dichotomy. *Inflammation*.**2007**; **30: 189-197**

Mody, M, AH Lazarus, JW Semple and J Freedman. Preanalytical Requirements for Flow Cytometric Evaluation of Platelet Activation: Choice of Anticoagulant. *Transfus Med*.**1999**; **9: 147-154**

Moore, KJ, FJ Sheedy and EA Fisher. Macrophages in Atherosclerosis: A Dynamic Balance. *Nat Rev Immunol*.**2013**; **13: 709-721**

Morabito, F, EF Prasthofer, NE Dunlap, CE Grossi and AB Tilden. Expression of Myelomonocytic Antigens on Chronic Lymphocytic Leukemia B Cells Correlates with Their Ability to Produce Interleukin 1. *Blood*.**1987**; **70: 1750-1757**

Muller, WA, SA Weigl, X Deng and DM Phillips. Pecam-1 Is Required for Transendothelial Migration of Leukocytes. *J Exp Med*.**1993**; **178: 449-460**

Neumann, FJ, D Zohlnhofer, L Fakhoury, I Ott, M Gawaz and A Schomig. Effect of Glycoprotein Iib/Iiia Receptor Blockade on Platelet-Leukocyte Interaction and Surface Expression of the Leukocyte Integrin Mac-1 in Acute Myocardial Infarction. *J Am Coll Cardiol*.**1999**; **34: 1420-1426**

Newby, AC and AB Zaltsman. Fibrous Cap Formation or Destruction--the Critical Importance of Vascular Smooth Muscle Cell Proliferation, Migration and Matrix Formation. *Cardiovasc Res*.**1999**; **41: 345-360**

Nielsen, H. Isolation and Functional Activity of Human Blood Monocytes after Adherence to Plastic Surfaces: Comparison of Different Detachment Methods. *Acta Pathol Microbiol Immunol Scand C*.**1987**; **95: 81-84**

Nieswandt, B, C Brakebusch, W Bergmeier, V Schulte, D Bouvard, R Mokhtari-Nejad, . . . R Fassler. Glycoprotein Vi but Not Alpha2beta1 Integrin Is Essential for Platelet Interaction with Collagen. *EMBO J*.**2001**; **20: 2120-2130**

O'Brien, KD, MD Allen, TO McDonald, A Chait, JM Harlan, D Fishbein, . . . et al. Vascular Cell Adhesion Molecule-1 Is Expressed in Human Coronary Atherosclerotic Plaques. Implications for the Mode of Progression of Advanced Coronary Atherosclerosis. *J Clin Invest*.**1993**; **92: 945-951**

Ohashi, R, H Mu, X Wang, Q Yao and C Chen. Reverse Cholesterol Transport and Cholesterol Efflux in Atherosclerosis. *QJM*.**2005**; **98: 845-856**

Osborn, L, C Hession, R Tizard, C Vassallo, S Luhowskyj, G Chi-Rosso and R Lobb. Direct Expression Cloning of Vascular Cell Adhesion Molecule 1, a Cytokine-Induced Endothelial Protein That Binds to Lymphocytes. *Cell*.**1989**; **59: 1203-1211**

Ouimet, M, V Franklin, E Mak, X Liao, I Tabas and YL Marcel. Autophagy Regulates Cholesterol Efflux from Macrophage Foam Cells Via Lysosomal Acid Lipase. *Cell Metab*.**2011**; **13: 655-667**

Pachauri, SP, B Jacotot and JL Beaumont. Circulating Lipophages and Aortic Foam Cells in Experimental Atherosclerosis of Rabbits under Altered Reticuloendothelial Activity. *Nutr Metab*.**1976**; **20: 14-26**

Pahl, HL. Activators and Target Genes of Rel/Nf-Kappab Transcription Factors. *Oncogene*.**1999**; **18: 6853-6866**

Panousis, CG, G Evans and SH Zuckerman. Tgf-Beta Increases Cholesterol Efflux and Abc-1 Expression in Macrophage-Derived Foam Cells: Opposing the Effects of Ifn-Gamma. *J Lipid Res*.**2001**; **42: 856-863**

Park, BS, DH Song, HM Kim, BS Choi, H Lee and JO Lee. The Structural Basis of Lipopolysaccharide Recognition by the Tlr4-Md-2 Complex. *Nature*.**2009**; **458: 1191-1195**

Passacquale, G, P Vamadevan, L Pereira, C Hamid, V Corrigall and A Ferro. Monocyte-Platelet Interaction Induces a Pro-Inflammatory Phenotype in Circulating Monocytes. *PLoS One*.**2011**; **6: e25595**

Passlick, B, D Flieger and HW Ziegler-Heitbrock. Identification and Characterization of a Novel Monocyte Subpopulation in Human Peripheral Blood. *Blood*.**1989**; **74: 2527-2534**

Patel-Hett, S, JL Richardson, H Schulze, K Drabek, NA Isaac, K Hoffmeister, . . . JE Italiano, Jr. Visualization of Microtubule Growth in Living Platelets Reveals a Dynamic Marginal Band with Multiple Microtubules. *Blood*.**2008**; **111: 4605-4616**

Patel, AA, Y Zhang, JN Fullerton, L Boelen, A Rongvaux, AA Maini, . . . S Yona. The Fate and Lifespan of Human Monocyte Subsets in Steady State and Systemic Inflammation. *J Exp Med*.**2017**; **214: 1913-1923**

Paulson, KE, SN Zhu, M Chen, S Nurmohamed, J Jongstra-Bilen and MI Cybulsky. Resident Intimal Dendritic Cells Accumulate Lipid and Contribute to the Initiation of Atherosclerosis. *Circ Res*.**2010**; **106: 383-390**

Persson, J, J Nilsson and MW Lindholm. Interleukin-1beta and Tumour Necrosis Factor-Alpha Impede Neutral Lipid Turnover in Macrophage-Derived Foam Cells. *BMC Immunol*.**2008**; **9: 70**

Pertoft, H, TC Laurent, T Laas and L Kagedal. Density Gradients Prepared from Colloidal Silica Particles Coated by Polyvinylpyrrolidone (Percoll). *Anal Biochem*.**1978**; **88: 271-282**

Phillips, JH, CW Chang and LL Lanier. Platelet-Induced Expression of Fc Gamma Riii (Cd16) on Human Monocytes. *Eur J Immunol*.**1991**; **21: 895-899**

Pitsilos, S, J Hunt, ER Mohler, AM Prabhakar, M Poncz, J Dawicki, . . . BS Sachais. Platelet Factor 4 Localization in Carotid Atherosclerotic Plaques: Correlation with Clinical Parameters. *Thromb Haemost*.**2003**; **90: 1112-1120**

Plouffe, BD, SK Murthy and LH Lewis. Fundamentals and Application of Magnetic Particles in Cell Isolation and Enrichment: A Review. *Rep Prog Phys*.**2015**; **78: 016601**

Podrez, EA, TV Byzova, M Febbraio, RG Salomon, Y Ma, M Valiyaveettil, . . . SL Hazen. Platelet Cd36 Links Hyperlipidemia, Oxidant Stress and a Prothrombotic Phenotype. *Nat Med*.**2007**; **13: 1086-1095**

Podrez, EA, M Febbraio, N Sheibani, D Schmitt, RL Silverstein, DP Hajjar, . . . SL Hazen. Macrophage Scavenger Receptor Cd36 Is the Major Receptor for Ldl Modified by Monocyte-Generated Reactive Nitrogen Species. *J Clin Invest*.**2000**; **105: 1095-1108**

Podrez, EA, D Schmitt, HF Hoff and SL Hazen. Myeloperoxidase-Generated Reactive Nitrogen Species Convert Ldl into an Atherogenic Form in Vitro. *J Clin Invest*.**1999**; **103: 1547-1560**

Poitou, C, E Dalmas, M Renovato, V Benhamo, F Hajduch, M Abdennour, . . . I Cremer. Cd14dimcd16+ and Cd14+Cd16+ Monocytes in Obesity and During Weight Loss: Relationships with Fat Mass and Subclinical Atherosclerosis. *Arterioscler Thromb Vasc Biol*.**2011**; **31: 2322-2330**

Poltorak, A, X He, I Smirnova, MY Liu, C Van Huffel, X Du, . . . B Beutler. Defective Lps Signaling in C3h/Hej and C57bl/10sccr Mice: Mutations in Tlr4 Gene. *Science*.**1998**; **282: 2085-2088**

Poole, JC. Phagocytosis of Platelets by Monocytes in Organizing Arterial Thrombi. An Electron Microscopical Study. *Q J Exp Physiol Cogn Med Sci*.**1966**; **51: 54-59**

Potteaux, S, EL Gautier, SB Hutchison, N van Rooijen, DJ Rader, MJ Thomas, . . . GJ Randolph. Suppressed Monocyte Recruitment Drives Macrophage Removal from Atherosclerotic Plaques of Apoe-/- Mice During Disease Regression. *J Clin Invest*.**2011**; **121: 2025-2036**

Pugin, J, ID Heumann, A Tomasz, VV Kravchenko, Y Akamatsu, M Nishijima, . . . RJ Ulevitch. Cd14 Is a Pattern Recognition Receptor. *Immunity*.**1994**; **1: 509-516**

Quinn, JF, T Patel, D Wong, S Das, JE Freedman, LC Laurent, . . . JA Saugstad. Extracellular Rnas: Development as Biomarkers of Human Disease. *J Extracell Vesicles*.**2015**; **4: 27495**

Ramos, CL, Y Huo, U Jung, S Ghosh, DR Manka, IJ Sarembock and K Ley. Direct Demonstration of P-Selectin- and Vcam-1-Dependent Mononuclear Cell Rolling in Early Atherosclerotic Lesions of Apolipoprotein E-Deficient Mice. *Circ Res*.**1999**; **84: 1237-1244**

Randolph, GJ, G Sanchez-Schmitz, RM Liebman and K Schakel. The Cd16(+) (Fcgammariii(+)) Subset of Human Monocytes Preferentially Becomes Migratory Dendritic Cells in a Model Tissue Setting. *J Exp Med*.**2002**; **196: 517-527**

Rawat, KA, JR Bhamore, RK Singhal and SK Kailasa. Microwave Assisted Synthesis of Tyrosine Protected Gold Nanoparticles for Dual (Colorimetric and Fluorimetric) Detection of Spermine and Spermidine in Biological Samples. *Biosens Bioelectron*.**2017**; **88: 71-77**

Ray, DM, SL Spinelli, SJ Pollock, TI Murant, JJ O'Brien, N Blumberg, . . . RP Phipps. Peroxisome Proliferator-Activated Receptor Gamma and Retinoid X Receptor Transcription Factors Are Released from Activated Human Platelets and Shed in Microparticles. *Thromb Haemost*.**2008**; **99: 86-95**

Ribatti, D and E Crivellato. Giulio Bizzozero and the Discovery of Platelets. *Leuk Res*.**2007**; **31: 1339-1341**

Ribes, S, S Ebert, T Regen, A Agarwal, SC Tauber, D Czesnik, . . . R Nau. Toll-Like Receptor Stimulation Enhances Phagocytosis and Intracellular Killing of Nonencapsulated and Encapsulated Streptococcus Pneumoniae by Murine Microglia. *Infect Immun*.**2010**; **78: 865-871**

Ridker, PM, JE Buring and N Rifai. Soluble P-Selectin and the Risk of Future Cardiovascular Events. *Circulation*.**2001**; **103: 491-495**

Rios, FJ, M Gidlund and S Jancar. Pivotal Role for Platelet-Activating Factor Receptor in Cd36 Expression and Oxldl Uptake by Human Monocytes/Macrophages. *Cell Physiol Biochem*.**2011**; **27: 363-372**

Robbins, CS, A Chudnovskiy, PJ Rauch, JL Figueiredo, Y Iwamoto, R Gorbatov, . . . FK Swirski. Extramedullary Hematopoiesis Generates Ly-6c(High) Monocytes That Infiltrate Atherosclerotic Lesions. *Circulation*.**2012**; **125: 364-374**

Rogacev, KS, B Cremers, AM Zawada, S Seiler, N Binder, P Ege, . . . GH Heine. Cd14++Cd16+ Monocytes Independently Predict Cardiovascular Events: A Cohort Study of 951 Patients Referred for Elective Coronary Angiography. *J Am Coll Cardiol*.**2012**; **60: 1512-1520**

Rogacev, KS, S Seiler, AM Zawada, B Reichart, E Herath, D Roth, . . . GH Heine. Cd14++Cd16+ Monocytes and Cardiovascular Outcome in Patients with Chronic Kidney Disease. *Eur Heart J*.**2011**; **32: 84-92**

Rogacev, KS, C Ulrich, L Blomer, F Hornof, K Oster, M Ziegelin, . . . GH Heine. Monocyte Heterogeneity in Obesity and Subclinical Atherosclerosis. *Eur Heart J*.**2010**; **31: 369-376**

Rokita, E and EJ Menzel. Characteristics of Cd14 Shedding from Human Monocytes. Evidence for the Competition of Soluble Cd14 (Scd14) with Cd14 Receptors for Lipopolysaccharide (Lps) Binding. *APMIS*.**1997**; **105: 510-518**

Rong, MY, CH Wang, ZB Wu, W Zeng, ZH Zheng, Q Han, . . . P Zhu. Platelets Induce a Proinflammatory Phenotype in Monocytes Via the Cd147 Pathway in Rheumatoid Arthritis. *Arthritis Res Ther*.**2014**; **16: 478**

Ross, R. Atherosclerosis--an Inflammatory Disease. *N Engl J Med*.**1999**; **340: 115-126**

Ross, R and JA Glomset. The Pathogenesis of Atherosclerosis (First of Two Parts). *N Engl J Med*.**1976**; **295: 369-377**

Rossol, M, S Kraus, M Pierer, C Baerwald and U Wagner. The Cd14(Bright) Cd16+ Monocyte Subset Is Expanded in Rheumatoid Arthritis and Promotes Expansion of the Th17 Cell Population. *Arthritis Rheum*.**2012**; **64: 671-677**

Rothe, G, H Gabriel, E Kovacs, J Klucken, J Stohr, W Kindermann and G Schmitz. Peripheral Blood Mononuclear Phagocyte Subpopulations as Cellular Markers in Hypercholesterolemia. *Arterioscler Thromb Vasc Biol*.**1996**; **16: 1437-1447**

Ruggeri, ZM. Platelets in Atherothrombosis. *Nat Med*.**2002**; **8: 1227-1234**

Ruparelia, N, JT Chai, EA Fisher and RP Choudhury. Inflammatory Processes in Cardiovascular Disease: A Route to Targeted Therapies. *Nat Rev Cardiol*.**2017**; **14: 314**

Sachais, BS, A Kuo, T Nassar, J Morgan, K Kariko, KJ Williams, . . . AA Higazi. Platelet Factor 4 Binds to Low-Density Lipoprotein Receptors and Disrupts the Endocytic Machinery, Resulting in Retention of Low-Density Lipoprotein on the Cell Surface. *Blood*.**2002**; **99: 3613-3622**

Sachais, BS, T Turrentine, JM Dawicki McKenna, AH Rux, D Rader and MA Kowalska. Elimination of Platelet Factor 4 (Pf4) from Platelets Reduces Atherosclerosis in C57bl/6 and Apoe-/- Mice. *Thromb Haemost*.**2007**; **98: 1108-1113**

Sanchis-Gomar, F, C Perez-Quilis, R Leischik and A Lucia. Epidemiology of Coronary Heart Disease and Acute Coronary Syndrome. *Ann Transl Med*.**2016**; **4: 256**

Sandblad, KG, P Jones, MJ Kostalla, L Linton, H Glise and O Winqvist. Chemokine Receptor Expression on Monocytes from Healthy Individuals. *Clin Immunol*.**2015**; **161: 348-353**

Sandgren, KJ, J Wilkinson, M Miranda-Saksena, GM McInerney, K Byth-Wilson, PJ Robinson and AL Cunningham. A Differential Role for Macropinocytosis in Mediating Entry of the Two Forms of Vaccinia Virus into Dendritic Cells. *PLoS Pathog*.**2010**; **6: e1000866**

Saniabadi, AR, GD Lowe, JC Barbenel and CD Forbes. Further Studies on the Role of Red Blood Cells in Spontaneous Platelet Aggregation. *Thromb Res*.**1985**; **38: 225-232**

Santoso, S, UJ Sachs, H Kroll, M Linder, A Ruf, KT Preissner and T Chavakis. The Junctional Adhesion Molecule 3 (Jam-3) on Human Platelets Is a Counterreceptor for the Leukocyte Integrin Mac-1. *J Exp Med*.**2002**; **196: 679-691**

Schakel, K, R Kannagi, B Kniep, Y Goto, C Mitsuoka, J Zwirner, . . . E Rieber. 6-Sulfo Lacnac, a Novel Carbohydrate Modification of Psgl-1, Defines an Inflammatory Type of Human Dendritic Cells. *Immunity*.**2002**; **17: 289-301**

Schakel, K, E Mayer, C Federle, M Schmitz, G Riethmuller and EP Rieber. A Novel Dendritic Cell Population in Human Blood: One-Step Immunomagnetic Isolation by a Specific Mab (M-Dc8) and in Vitro Priming of Cytotoxic T Lymphocytes. *Eur J Immunol*.**1998**; **28: 4084-4093**

Schakel, K, M von Kietzell, A Hansel, A Ebling, L Schulze, M Haase, . . . EP Rieber. Human 6-Sulfo Lacnac-Expressing Dendritic Cells Are Principal Producers of Early Interleukin-12 and Are Controlled by Erythrocytes. *Immunity*.**2006**; **24: 767-777**

Scheuerer, B, M Ernst, I Durrbaum-Landmann, J Fleischer, E Grage-Griebenow, E Brandt, . . . F Petersen. The Cxc-Chemokine Platelet Factor 4 Promotes Monocyte Survival and Induces Monocyte Differentiation into Macrophages. *Blood*.**2000**; **95: 1158-1166**

Schimke, J, J Mathison, J Morgiewicz and RJ Ulevitch. Anti-Cd14 Mab Treatment Provides Therapeutic Benefit after in Vivo Exposure to Endotoxin. *Proc Natl Acad Sci U S A*.**1998**; **95: 13875-13880**

Schwarz, H, M Schmittner, A Duschl and J Horejs-Hoeck. Residual Endotoxin Contaminations in Recombinant Proteins Are Sufficient to Activate Human Cd1c+ Dendritic Cells. *PLoS One*.**2014**; **9: e113840**

Seizer, P, S Schiemann, T Merz, K Daub, B Bigalke, K Stellos, . . . AE May. Cd36 and Macrophage Scavenger Receptor a Modulate Foam Cell Formation Via Inhibition of Lipid-Laden Platelet Phagocytosis. *Semin Thromb Hemost*.**2010**; **36: 157-162**

Semple, JW and J Freedman. Platelets and Innate Immunity. *Cell Mol Life Sci*.**2010**; **67: 499-511**

Senzel, L, DV Gnatenko and WF Bahou. The Platelet Proteome. *Curr Opin Hematol*.**2009**; **16: 329-333**

Serbina, NV and EG Pamer. Monocyte Emigration from Bone Marrow During Bacterial Infection Requires Signals Mediated by Chemokine Receptor Ccr2. *Nat Immunol*.**2006**; **7: 311-317**

Shaw, RJ, DE Doherty, AG Ritter, SH Benedict and RA Clark. Adherence-Dependent Increase in Human Monocyte Pdgf(B) Mrna Is Associated with Increases in C-Fos, C-Jun, and Egr2 Mrna. *J Cell Biol*.**1990**; **111: 2139-2148**

Shen, HH, MA Talle, G Goldstein and L Chess. Functional Subsets of Human Monocytes Defined by Monoclonal Antibodies: A Distinct Subset of Monocytes Contains the Cells Capable of Inducing the Autologous Mixed Lymphocyte Culture. *J Immunol*.**1983**; **130: 698-705**

Shi, C and EG Pamer. Monocyte Recruitment During Infection and Inflammation. *Nat Rev Immunol*.**2011**; **11: 762-774**

Silverstein, RL, AS Asch and RL Nachman. Glycoprotein Iv Mediates Thrombospondin-Dependent Platelet-Monocyte and Platelet-U937 Cell Adhesion. *J Clin Invest*.**1989**; **84: 546-552**

Simon, DI, Z Chen, H Xu, CQ Li, J Dong, LV McIntire, . . . JA Lopez. Platelet Glycoprotein Ibalpha Is a Counterreceptor for the Leukocyte Integrin Mac-1 (Cd11b/Cd18). *J Exp Med*.**2000**; **192: 193-204**

Sirpal, S. Myeloperoxidase-Mediated Lipoprotein Carbamylation as a Mechanistic Pathway for Atherosclerotic Vascular Disease. *Clin Sci (Lond)*.**2009**; **116: 681-695**

Smethurst, PA, DJ Onley, GE Jarvis, MN O'Connor, CG Knight, AB Herr, . . . RW Farndale. Structural Basis for the Platelet-Collagen Interaction: The Smallest Motif within Collagen That Recognizes and Activates Platelet Glycoprotein Vi Contains Two Glycine-Proline-Hydroxyproline Triplets. *J Biol Chem*.**2007**; **282: 1296-1304**

Smith, JD, E Trogan, M Ginsberg, C Grigaux, J Tian and M Miyata. Decreased Atherosclerosis in Mice Deficient in Both Macrophage Colony-Stimulating Factor (Op) and Apolipoprotein E. *Proc Natl Acad Sci U S A*.**1995**; **92: 8264-8268**

Snapp, KR, CE Heitzig and GS Kansas. Attachment of the Psgl-1 Cytoplasmic Domain to the Actin Cytoskeleton Is Essential for Leukocyte Rolling on P-Selectin. *Blood*.**2002**; **99: 4494-4502**

Stancu, C and A Sima. Statins: Mechanism of Action and Effects. *J Cell Mol Med*.**2001**; **5: 378-387**

Stefanadis, C, CK Antoniou, D Tsiachris and P Pietri. Coronary Atherosclerotic Vulnerable Plaque: Current Perspectives. *J Am Heart Assoc*.**2017**; **6**

Stellos, K, B Bigalke, D Stakos, N Henkelmann and M Gawaz. Platelet-Bound P-Selectin Expression in Patients with Coronary Artery Disease: Impact on Clinical Presentation and Myocardial Necrosis, and Effect of Diabetes Mellitus and Anti-Platelet Medication. *J Thromb Haemost*.**2010**; **8: 205-207**

Stephen, J, B Emerson, KA Fox and I Dransfield. The Uncoupling of Monocyte-Platelet Interactions from the Induction of Proinflammatory Signaling in Monocytes. *J Immunol*.**2013**; **191: 5677-5683**

Stephen, SL, K Freestone, S Dunn, MW Twigg, S Homer-Vanniasinkam, JH Walker, . . . S Ponnambalam. Scavenger Receptors and Their Potential as Therapeutic Targets in the Treatment of Cardiovascular Disease. *Int J Hypertens*.**2010**; **2010: 646929**

Stoger, JL, MJ Gijbels, S van der Velden, M Manca, CM van der Loos, EA Biessen, . . . MP de Winther. Distribution of Macrophage Polarization Markers in Human Atherosclerosis. *Atherosclerosis*.**2012**; **225: 461-468**

Stoorvogel, W, MJ Kleijmeer, HJ Geuze and G Raposo. The Biogenesis and Functions of Exosomes. *Traffic*.**2002**; **3: 321-330**

Swertfeger, DK, G Bu and DY Hui. Low Density Lipoprotein Receptor-Related Protein Mediates Apolipoprotein E Inhibition of Smooth Muscle Cell Migration. *J Biol Chem*.**2002**; **277: 4141-4146**

Swirski, FK, P Libby, E Aikawa, P Alcaide, FW Luscinskas, R Weissleder and MJ Pittet. Ly-6chi Monocytes Dominate Hypercholesterolemia-Associated Monocytosis and Give Rise to Macrophages in Atheromata. *J Clin Invest*.**2007**; **117: 195-205**

Swirski, FK, M Nahrendorf, M Etzrodt, M Wildgruber, V Cortez-Retamozo, P Panizzi, . . . MJ Pittet. Identification of Splenic Reservoir Monocytes and Their Deployment to Inflammatory Sites. *Science*.**2009**; **325: 612-616**

Tabas, I. Consequences of Cellular Cholesterol Accumulation: Basic Concepts and Physiological Implications. *J Clin Invest*.**2002**; **110: 905-911**

Tabas, I and AH Lichtman. Monocyte-Macrophages and T Cells in Atherosclerosis. *Immunity*.**2017**; **47: 621-634**

Tacke, F, D Alvarez, TJ Kaplan, C Jakubzick, R Spanbroek, J Llodra, . . . GJ Randolph. Monocyte Subsets Differentially Employ Ccr2, Ccr5, and Cx3cr1 to Accumulate within Atherosclerotic Plaques. *J Clin Invest*.**2007**; **117: 185-194**

Tapp, LD, E Shantsila, BJ Wrigley, B Pamukcu and GY Lip. The Cd14++Cd16+ Monocyte Subset and Monocyte-Platelet Interactions in Patients with St-Elevation Myocardial Infarction. *J Thromb Haemost*.**2012**; **10: 1231-1241**

Taylor, JM, F Borthwick, C Bartholomew and A Graham. Overexpression of Steroidogenic Acute Regulatory Protein Increases Macrophage Cholesterol Efflux to Apolipoprotein Ai. *Cardiovasc Res*.**2010**; **86: 526-534**

Taylor, ML, MK Ilton, NL Misso, DN Watkins, J Hung and PJ Thompson. The Effect of Aspirin on Thrombin Stimulated Platelet Adhesion Receptor Expression and the Role of Neutrophils. *Br J Clin Pharmacol*.**1998**; **46: 139-145**

Ting-Beall, HP, AS Lee and RM Hochmuth. Effect of Cytochalasin D on the Mechanical Properties and Morphology of Passive Human Neutrophils. *Ann Biomed Eng*.**1995**; **23: 666-671**

Tinoco, R and LM Bradley. Targeting the Psgl-1 Pathway for Immune Modulation. *Immunotherapy*.**2017**; **9: 785-788**

Tontonoz, P, L Nagy, JG Alvarez, VA Thomazy and RM Evans. Ppargamma Promotes Monocyte/Macrophage Differentiation and Uptake of Oxidized Ldl. *Cell*.**1998**; **93: 241-252**

Tordjman, K, C Bernal-Mizrachi, L Zemany, S Weng, C Feng, F Zhang, . . . CF Semenkovich. Pparalpha Deficiency Reduces Insulin Resistance and Atherosclerosis in Apoe-Null Mice. *J Clin Invest*.**2001**; **107: 1025-1034**

Trigatti, B, H Rayburn, M Vinals, A Braun, H Miettinen, M Penman, . . . M Krieger. Influence of the High Density Lipoprotein Receptor Sr-Bi on Reproductive and Cardiovascular Pathophysiology. *Proc Natl Acad Sci U S A*.**1999**; **96: 9322-9327**

Truss, NJ, PC Armstrong, E Liverani, I Vojnovic and TD Warner. Heparin but Not Citrate Anticoagulation of Blood Preserves Platelet Function for Prolonged Periods. *J Thromb Haemost*.**2009**; **7: 1897-1905**

Tsuchiya, S, M Yamabe, Y Yamaguchi, Y Kobayashi, T Konno and K Tada. Establishment and Characterization of a Human Acute Monocytic Leukemia Cell Line (Thp-1). *Int J Cancer*.**1980**; **26: 171-176**

Tucker, SB, RV Pierre and RE Jordon. Rapid Identification of Monocytes in a Mixed Mononuclear Cell Preparation. *J Immunol Methods*.**1977**; **14: 267-269**

van den Besselaar, AM, J Meeuwisse-Braun, R Jansen-Gruter and RM Bertina. Monitoring Heparin Therapy by the Activated Partial Thromboplastin Time--the Effect of Pre-Analytical Conditions. *Thromb Haemost*.**1987**; **57: 226-231**

van der Laan, AM, EN Ter Horst, R Delewi, MP Begieneman, PA Krijnen, A Hirsch, . . . JJ Piek. Monocyte Subset Accumulation in the Human Heart Following Acute Myocardial Infarction and the Role of the Spleen as Monocyte Reservoir. *Eur Heart J*.**2014**; **35: 376-385**

van Furth, R and ZA Cohn. The Origin and Kinetics of Mononuclear Phagocytes. *J Exp Med*.**1968**; **128: 415-435**

Van Furth, R, MC Diesselhoff-den Dulk and H Mattie. Quantitative Study on the Production and Kinetics of Mononuclear Phagocytes During an Acute Inflammatory Reaction. *J Exp Med*.**1973**; **138: 1314-1330**

van Gils, JM, PA da Costa Martins, A Mol, PL Hordijk and JJ Zwaginga. Transendothelial Migration Drives Dissociation of Plateletmonocyte Complexes. *Thromb Haemost*.**2008**; **100: 271-279**

van Gils, JM, JJ Zwaginga and PL Hordijk. Molecular and Functional Interactions among Monocytes, Platelets, and Endothelial Cells and Their Relevance for Cardiovascular Diseases. *J Leukoc Biol*.**2009**; **85: 195-204**

Varol, C, A Vallon-Eberhard, E Elinav, T Aychek, Y Shapira, H Luche, . . . S Jung. Intestinal Lamina Propria Dendritic Cell Subsets Have Different Origin and Functions. *Immunity*.**2009**; **31: 502-512**

Vasconcelos, EM, GR Degasperi, HC de Oliveira, AE Vercesi, EC de Faria and LN Castilho. Reactive Oxygen Species Generation in Peripheral Blood Monocytes and Oxidized Ldl Are Increased in Hyperlipidemic Patients. *Clin Biochem*.**2009**; **42: 1222-1227**

Virmani, R, FD Kolodgie, AP Burke, A Farb and SM Schwartz. Lessons from Sudden Coronary Death: A Comprehensive Morphological Classification Scheme for Atherosclerotic Lesions. *Arterioscler Thromb Vasc Biol*.**2000**; **20: 1262-1275**

Vogel, SN, PY Perera, MM Hogan and JA Majde. Use of Serum-Free, Compositionally Defined Medium for Analysis of Macrophage Differentiation in Vitro. *J Leukoc Biol*.**1988**; **44: 136-142**

Volf, I, T Moeslinger, J Cooper, W Schmid and E Koller. Human Platelets Exclusively Bind Oxidized Low Density Lipoprotein Showing No Specificity for Acetylated Low Density Lipoprotein. *FEBS Lett*.**1999**; **449: 141-145**

von Hundelshausen, P, RR Koenen, M Sack, SF Mause, W Adriaens, AE Proudfoot, . . . C Weber. Heterophilic Interactions of Platelet Factor 4 and Rantes Promote Monocyte Arrest on Endothelium. *Blood*.**2005**; **105: 924-930**

von Hundelshausen, P, KS Weber, Y Huo, AE Proudfoot, PJ Nelson, K Ley and C Weber. Rantes Deposition by Platelets Triggers Monocyte Arrest on Inflamed and Atherosclerotic Endothelium. *Circulation*.**2001**; **103: 1772-1777**

Wachowicz, B, B Olas, HM Zbikowska and A Buczynski. Generation of Reactive Oxygen Species in Blood Platelets. *Platelets*.**2002**; **13: 175-182**

Wallentin, L, RC Becker, A Budaj, CP Cannon, H Emanuelsson, C Held, . . . M Thorsen. Ticagrelor Versus Clopidogrel in Patients with Acute Coronary Syndromes. *N Engl J Med*.**2009**; **361: 1045-1057**

Wang, JX, AM Bair, SL King, R Shnayder, YF Huang, CC Shieh, . . . PA Nigrovic. Ly6g Ligation Blocks Recruitment of Neutrophils Via a Beta2-Integrin-Dependent Mechanism. *Blood*.**2012**; **120: 1489-1498**

Weber, C, E Shantsila, M Hristov, G Caligiuri, T Guzik, GH Heine, . . . GY Lip. Role and Analysis of Monocyte Subsets in Cardiovascular Disease. Joint Consensus Document of the European Society of Cardiology (Esc) Working Groups "Atherosclerosis & Vascular Biology" and "Thrombosis". *Thromb Haemost*.**2016**; **116: 626-637**

Weibel, GL, D Drazul-Schrader, DK Shivers, AN Wade, GH Rothblat, MP Reilly and M de la Llera-Moya. Importance of Evaluating Cell Cholesterol Influx with Efflux in Determining the Impact of Human Serum on Cholesterol Metabolism and Atherosclerosis. *Arterioscler Thromb Vasc Biol*.**2014**; **34: 17-25**

Weyrich, AS, MR Elstad, RP McEver, TM McIntyre, KL Moore, JH Morrissey, . . . GA Zimmerman. Activated Platelets Signal Chemokine Synthesis by Human Monocytes. *J Clin Invest*.**1996**; **97: 1525-1534**

Weyrich, AS, TM McIntyre, RP McEver, SM Prescott and GA Zimmerman. Monocyte Tethering by P-Selectin Regulates Monocyte Chemotactic Protein-1 and Tumor Necrosis Factor-Alpha Secretion. Signal Integration and Nf-Kappa B Translocation. *J Clin Invest*.**1995**; **95: 2297-2303**

Whelan, FJ, CJ Meehan, GB Golding, BJ McConkey and DM Bowdish. The Evolution of the Class a Scavenger Receptors. *BMC Evol Biol*.**2012**; **12: 227**

Williams, KJ and I Tabas. The Response-to-Retention Hypothesis of Early Atherogenesis. *Arterioscler Thromb Vasc Biol*.**1995**; **15: 551-561**

Wong, KL, JJ Tai, WC Wong, H Han, X Sem, WH Yeap, . . . SC Wong. Gene Expression Profiling Reveals the Defining Features of the Classical, Intermediate, and Nonclassical Human Monocyte Subsets. *Blood*.**2011**; **118: e16-31**

Wong, KL, WH Yeap, JJ Tai, SM Ong, TM Dang and SC Wong. The Three Human Monocyte Subsets: Implications for Health and Disease. *Immunol Res*.**2012**; **53: 41-57**

Woollard, KJ and F Geissmann. Monocytes in Atherosclerosis: Subsets and Functions. *Nat Rev Cardiol*.**2010**; **7: 77-86**

Wright, SD, RA Ramos, PS Tobias, RJ Ulevitch and JC Mathison. Cd14, a Receptor for Complexes of Lipopolysaccharide (Lps) and Lps Binding Protein. *Science*.**1990**; **249: 1431-1433**

Wu, L, N Ruffing, X Shi, W Newman, D Soler, CR Mackay and S Qin. Discrete Steps in Binding and Signaling of Interleukin-8 with Its Receptor. *J Biol Chem*.**1996**; **271: 31202-31209**

Xu, Q. The Impact of Progenitor Cells in Atherosclerosis. *Nat Clin Pract Cardiovasc Med*.**2006**; **3: 94-101**

Xu, S, S Ogura, J Chen, PJ Little, J Moss and P Liu. Lox-1 in Atherosclerosis: Biological Functions and Pharmacological Modifiers. *Cell Mol Life Sci*.**2013**; **70: 2859-2872**

Yanez-Mo, M, PR Siljander, Z Andreu, AB Zavec, FE Borras, EI Buzas, . . . O De Wever. Biological Properties of Extracellular Vesicles and Their Physiological Functions. *J Extracell Vesicles*.**2015**; **4: 27066**

Yeap, WH, KL Wong, N Shimasaki, EC Teo, JK Quek, HX Yong, . . . SC Wong. Cd16 Is Indispensable for Antibody-Dependent Cellular Cytotoxicity by Human Monocytes. *Sci Rep*.**2016**; **6: 34310**

Yla-Herttuala, S, JF Bentzon, M Daemen, E Falk, HM Garcia-Garcia, J Herrmann, . . . B Vascular. Stabilization of Atherosclerotic Plaques: An Update. *Eur Heart J*.**2013**; **34: 3251-3258**

Yona, S, KW Kim, Y Wolf, A Mildner, D Varol, M Breker, . . . S Jung. Fate Mapping Reveals Origins and Dynamics of Monocytes and Tissue Macrophages under Homeostasis. *Immunity*.**2013**; **38: 79-91**

Yoshida, M, T Sawada, H Ishii, RE Gerszten, A Rosenzweig, MA Gimbrone, Jr., . . . F Numano. Hmg-Coa Reductase Inhibitor Modulates Monocyte-Endothelial Cell Interaction under Physiological Flow Conditions in Vitro: Involvement of Rho Gtpase-Dependent Mechanism. *Arterioscler Thromb Vasc Biol*.**2001**; **21: 1165-1171**

Yvan-Charvet, L, M Ranalletta, N Wang, S Han, N Terasaka, R Li, . . . AR Tall. Combined Deficiency of Abca1 and Abcg1 Promotes Foam Cell Accumulation and Accelerates Atherosclerosis in Mice. *J Clin Invest*.**2007**; **117: 3900-3908**

Yvan-Charvet, L, N Wang and AR Tall. Role of Hdl, Abca1, and Abcg1 Transporters in Cholesterol Efflux and Immune Responses. *Arterioscler Thromb Vasc Biol*.**2010**; **30: 139-143**

Zalai, CV, MD Kolodziejczyk, L Pilarski, A Christov, PN Nation, M Lundstrom-Hobman, . . . A Lucas. Increased Circulating Monocyte Activation in Patients with Unstable Coronary Syndromes. *J Am Coll Cardiol*.**2001**; **38: 1340-1347**

Zani, IA, SL Stephen, NA Mughal, D Russell, S Homer-Vanniasinkam, SB Wheatcroft and S Ponnambalam. Scavenger Receptor Structure and Function in Health and Disease. *Cells*.**2015**; **4: 178-201**

Zawada, AM, LH Fell, K Untersteller, S Seiler, KS Rogacev, D Fliser, . . . GH Heine. Comparison of Two Different Strategies for Human Monocyte Subsets Gating within the Large-Scale Prospective Care for Home Study. *Cytometry A*.**2015**; **87: 750-758**

Zawada, AM, KS Rogacev, B Rotter, P Winter, RR Marell, D Fliser and GH Heine. Supersage Evidence for Cd14++Cd16+ Monocytes as a Third Monocyte Subset. *Blood*.**2011**; **118: e50-61**

Zhang, W, SP Neo, J Gunaratne, A Poulsen, L Boping, EH Ong, . . . SM Cohen. Feedback Regulation on Pten/Akt Pathway by the Er Stress Kinase Perk Mediated by Interaction with the Vault Complex. *Cell Signal*.**2015**; **27: 436-442**

Zhao, Y, M Pennings, CL Vrins, L Calpe-Berdiel, M Hoekstra, JK Kruijt, . . . M Van Eck. Hypocholesterolemia, Foam Cell Accumulation, but No Atherosclerosis in Mice Lacking Abc-Transporter A1 and Scavenger Receptor Bi. *Atherosclerosis*.**2011**; **218: 314-322**

Zhao, Y, PM Vanhoutte and SW Leung. Vascular Nitric Oxide: Beyond Enos. *J Pharmacol Sci*.**2015**; **129: 83-94**

Zhou, C, N King, KY Chen and JL Breslow. Activation of Pxr Induces Hypercholesterolemia in Wild-Type and Accelerates Atherosclerosis in Apoe Deficient Mice. *J Lipid Res*.**2009**; **50: 2004-2013**

Zhou, L, R Somasundaram, RF Nederhof, G Dijkstra, KN Faber, MP Peppelenbosch and GM Fuhler. Impact of Human Granulocyte and Monocyte Isolation Procedures on Functional Studies. *Clin Vaccine Immunol*.**2012**; **19: 1065-1074**

Zhu, X, JS Owen, MD Wilson, H Li, GL Griffiths, MJ Thomas, . . . JS Parks. Macrophage Abca1 Reduces Myd88-Dependent Toll-Like Receptor Trafficking to Lipid Rafts by Reduction of Lipid Raft Cholesterol. *J Lipid Res*.**2010**; **51: 3196-3206**

Ziegler-Heitbrock, HW. Molecular Mechanism in Tolerance to Lipopolysaccharide. *J Inflamm*.**1995**; **45: 13-26**

Ziegler-Heitbrock, L. Blood Monocytes and Their Subsets: Established Features and Open Questions. *Front Immunol*.**2015**; **6: 423**

Ziegler-Heitbrock, L, P Ancuta, S Crowe, M Dalod, V Grau, DN Hart, . . . MB Lutz. Nomenclature of Monocytes and Dendritic Cells in Blood. *Blood*.**2010**; **116: e74-80**

Zouggari, Y, H Ait-Oufella, P Bonnin, T Simon, AP Sage, C Guerin, . . . Z Mallat. B Lymphocytes Trigger Monocyte Mobilization and Impair Heart Function after Acute Myocardial Infarction. *Nat Med*.**2013**; **19: 1273-1280**